Conformational studies of crowded and non-crowded merocyanine dyes
by John Joseph Monson

A thesis submitted in partial fulfillment of the requirements for the degree of Doctor of Philosophy in Chemistry
Montana State University

Abstract:
Our interest in the effect on allopolar isomerism of molecular electron distribution and intramolecular van der Waals interaction has led to the preparation and solution of the crystal structures of several merocyanine and chain-methyl merocyanine dyes derived from various heterocyclic nuclei. Bond lengths and torsion angle comparisons for the merocyanine dyes completely confirm qualitative predictions based on the Brooker deviation, an experimentally determined electron attracting/donating scale, and recent molecular orbital calculations by Bowler. Chain-methyl crowded merocyanine dyes have not behaved as expected. Crystallographic evidence has shown that crowding by a methyl group isn't sufficient to cause the molecule to twist its end groups out of the plane of each other. Unexpectedly, the chain carbon-carbon bond lengths increase to relieve van der Waal interactions. We-have also shown that this must be true in the solution state.

Chain-methyl and uncrowded merocyanines are expected to remain planar in the solution state because their wavelengths differ by approximately five nanometers and they retain their epsilon values. NMR spectroscopy also suggested that this is true. Modern techniques have provided the means for the first rigorous assignment of these dye systems. Brooker deviations and chain carbon-carbon bond lengthening were observed by proton chemical shift information.

CONFORMATIONAL STUDIES OF CROWDED AND NON-CROWDED MEROCYANINE DYES

by

John Joseph Monson

A thesis submitted in partial fulfillment of the requirements for the degree

of

Doctor of Philosophy

in

Chemistry

MONTANA STATE UNIVERSITY
Bozeman, Montana

December 1989

APPROVAL

of a thesis submitted by

John Joseph Monson

This thesis has been read by each member of the thesis committee and has been found to be satisfactory regarding content, English usage, format, citations, bibliographic style, and consistency, and is ready for submission to the College of Graduate Studies.

Dec. 16 1989
Date

Arnold C. Craig
Chairperson, Graduate Committee

Approved for the Major Department

Dec 18 1989
Date

Edwin H. Abbott
Head, Major Department

Approved for the College of Graduate Studies

December 26, 1989
Date

Henry J. Parsons
Graduate Dean

STATEMENT OF PERMISSION TO USE

In presenting this thesis in partial fulfillment of the requirements for a doctoral degree at Montana State University, I agree that the Library shall make it available to borrowers under the rules of the Library. I further agree that copying of this thesis is allowed only for scholarly purposes, consistent with "fair use" as prescribed in the U.S. Copyright Law. Requests for extensive copying or reproduction of this thesis should be referred to University Microfilms International, 300 North Zeeb Road, Ann Arbor, Michigan 48106, to whom I have granted "the exclusive right to reproduce and distribute copies of the dissertation in and from microfilm and the right to reproduce and distribute by abstract in any format."

Signature John O'Morgan

Date 21 December 1989

TABLE OF CONTENTS

LIST OF TABLES

LIST OF TABLES (continued)

LIST OF TABLES (continued)

LIST OF TABLES (continued)

LIST OF TABLES (continued)

LIST OF TABLES (continued)

LIST OF FIGURES

LIST OF FIGURES (continued)

LIST OF FIGURES (continued)

ABSTRACT

Our interest in the effect on allopolar isomerism of molecular electron distribution and intramolecular van der Waals interaction has led to the preparation and solution of the crystal structures of several merocyanine and chain-methyl merocyanine dyes derived from various heterocyclic nuclei. Bond lengths and torsion angle comparisons for the merocyanine dyes completely confirm qualitative predictions based on the Brooker deviation, an experimentally determined electron attracting/donating scale, and recent molecular orbital calculations by Bowler. Chain-methyl crowded merocyanine dyes have not behaved as expected. Crystallographic evidence has shown that crowding by a methyl group isn't sufficient to cause the molecule to twist its end groups out of the plane of each other. Unexpectedly, the chain carbon-carbon bond lengths increase to relieve van der Waal interactions. We have also shown that this must be true in the solution state.

Chain-methyl and uncrowded merocyanines are expected to remain planar in the solution state because their wavelengths differ by approximately five nanometers and they retain their epsilon values. NMR spectroscopy also suggested that this is true. Modern techniques have provided the means for the first rigorous assignment of these dye systems. Brooker deviations and chain carbon-carbon bond lengthening were observed by proton chemical shift information.

HISTORY

Cyanines are a large family of dyes used almost exclusively as spectral sensitizers for color and high speed photographic films. The first cyanine was discovered by Williams in 1856 (1). He discovered this class of compounds while working on the synthesis of new types of textile dyes. Some cyanines were useful in the textile industry but for the most part cyanines were not found to be valuable for this type of application. It wasn't until the early 1870's that the importance of the compounds was realized. At this time cyanines were introduced into the photographic field and became one of the most important class of compounds used in the industry.

The first undyed photographic materials were only sensitive to invisible ultra-violet and blue light. In 1873 A. W. Vogel discovered that a photographic plate dipped in a cyanine dye solution was sensitive to green light. Homolka later synthesized another cyanine, pinacyanol, which sensitized photographic plates in the red area of the visible spectrum (2). These compounds are shown in Figure 1.

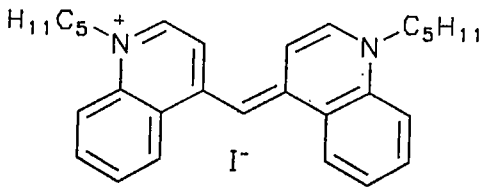

Williams' Cyanine (1856)

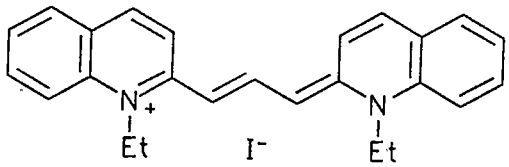

Pinacyanol (1904)

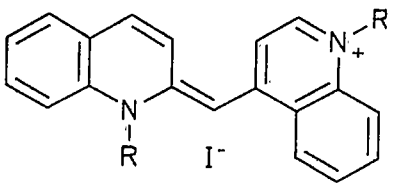

Isocyanine (1902)

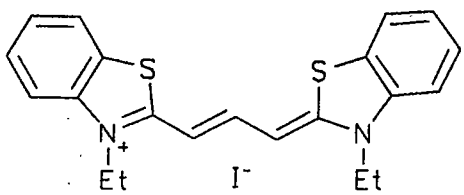

Thiacarbocyanine (1887)

Figure 1. Early cyanine dyes.

These early sensitizers were used for green and red light. A big drawback was that these dyes would fog photographic medium if present in greater than one part of dye in five million parts of emulsion. This forced researchers to find other sensitizers that were as good as the first cyanines but alleviated fogging. E. Koenig solved this problem with his synthesis of isocyanines (3). Isocyanines gave the same sensitivities but didn't fog the emulsion.

The main application of these sensitizers was during the development of sound motion pictures. The dyes allowed higher speed films to be used, making filament lighting possible for filming instead of the noisy arc lamps previously used (4).

The motion picture industry was one of the main reasons for further work with these dye systems. Major developments in cyanine dyes can be classified into three areas; pioneering, standardization, and design.

The pioneering days in the research and development of cyanines were from the 1920's into the 1950's. Four major discoveries mark this time period. The first is the incorporation by Koening of orthoesters and vinylogs into the synthesis of symmetric dyes. This procedure allowed the dye chain length to vary depending upon the type of orthoester or vinylog used. The technique also allowed cyanines to have extended chain lengths of up to seven methine carbons (5).

A second major development, by Piggott and Rodd at ICI Ltd., entailed the evolution of reagents for unsymmetric dyes. These intermediates are acetanilidovinyl heterocyclic compounds called ICI intermediates and are shown in Figure 2. Other types of intermediates important in unsymmetric dye synthesis were keto methylene compounds developed by Dains (6).

Third was the discovery of merocyanines in the 1930's. These unsymmetrical dyes were developed independently by the United States, England, and Japan (7). World wide interest like this showed how important this class of compounds were at the time. Merocyanines are not only unsymmetric, but were

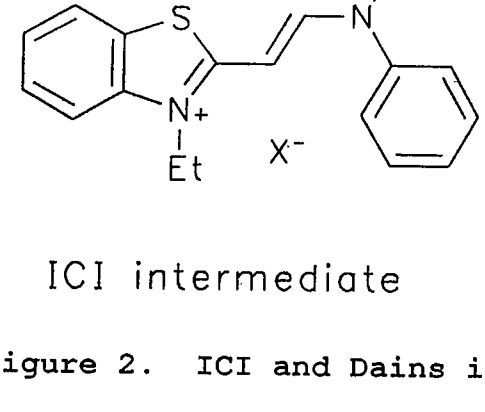

ICI intermediate

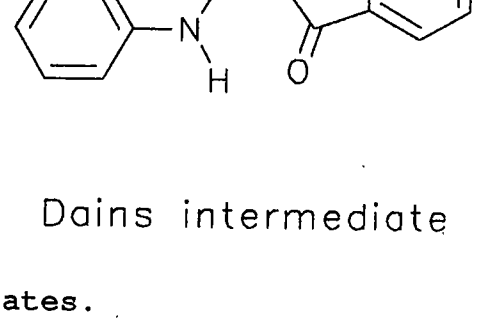

Dains intermediate

Figure 2. ICI and Dains intermediates.

the first neutral dyes of this type. They could also be used as building blocks for more complex dye systems. Some of these dyes are also very strong sensitizers.

The final research of importance was the development of extended chain quaternary salts which include the ICI and Dains intermediates. These salts are used for synthesizing unsymmetric dyes. This allowed researchers to understand color and constitution by broadening the types of dyes available.

The period from the 1950's to the late 1960's generalized the synthesis of cyanines and oxonols (8). For the first time a large variety of heterocycles could be easily incorporated into different types of dyes. This allowed dyes to be targeted for various wavelengths or solubility and improved color sensitization.

Since the 1960's information on and applications of cyanines have mushroomed. The photographic industry is still the primary user of cyanines. Targeted molecules can now be designed by computers (9) to predict a dye that has certain properties desired by a particular researcher's application problem. Other areas of interest have been uses in the medical field. An example of these are biological tracers (10) or in cell membrane studies (11).

In laser research some of these dyes are useful as mode lockers or Q-switchers (12-13). The most recent interest has been in the development of photo-electrodes for solar cells (14-15) and in optical recording technology (16-17). Representative examples for each have been cited. No area has been subject to complete review.

Comprehensive references for the synthesis of these compounds have been prepared by Hamer (18), Brooker (19-20), Ficken (21), Kipranov (22-25), and Sturmer (26). A good source for the applications of cyanines can be found in "The Theory of the Photographic Process, fourth edition," edited by James (27). Even with the wealth of studies done to date further research is needed to achieve a better understanding of the solid, solution, and surface properties of these compounds.

TYPES OF CYANINES

In general, cyanines are unsaturated molecules made up of two heterocyclic end groups linked by one or more methine carbon atoms. The number of methine or chain carbons for a normal cyanine is always an odd number (see Figure 3). One methine carbon in the chain linking two heterocycles is called a simple cyanine. A three carbon chain is a carbocyanine, and five carbons in a chain is a dicarbocyanine. Longer chain lengths are possible and the nomenclature follows the same pattern, however longer chain dyes are typically more difficult to synthesize.

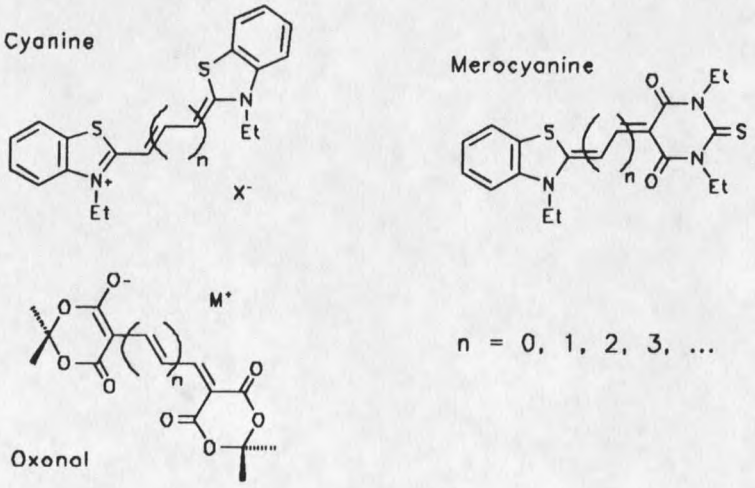

Figure 3. Examples of three dye systems.

The cyanine dye chromophore is an amidinium ion where the positive charge resonates between two nitrogen atoms through the conjugated carbon chain as shown in Figure 4. The wavelength where the dye absorbs is dependent upon the length of the chromophore and type of heterocyclic groups incorporated into the dye molecule. Solubilities can be altered by changing the alkyl group attached to nitrogen or around the heterocyclic ring systems.

The chromophores for cyanines are said to be non-convergent (28). For a dye to be non converging the following condition must be met. Each time the chain length is increased by two methine carbons the wavelength of the dye will increase by approximately the same amount no matter how long the chain length was originally. This increase for cyanines is on the order of 100 nm for every two methine carbons added as shown in Table 1.

Oxonols are similar to cyanines; however, their chromophores are based on a carboxyl ion system. The negative charge resonates between two oxygen atoms through the conjugated carbon chain. Oxonols are also non-converging dyes.

Merocyanines are made from the combination of a carbocyanine and an oxonol, as shown in Figure 5. This combination forms an unsymmetric dye with an even methine

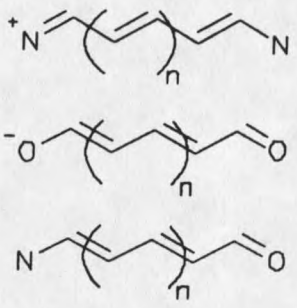

amidinium ion

carboxyl ion

dipolar amidic

Figure 4. Different dye chromophores.

Table 1. Convergence of cyanine dyes.

DYE	λ_{max} in nm			
	n = 0	1	2	3
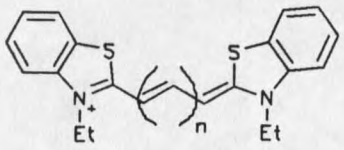	423	557	650	758
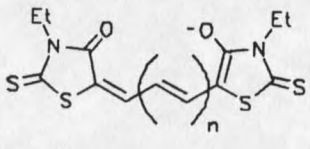	542	613	714	---
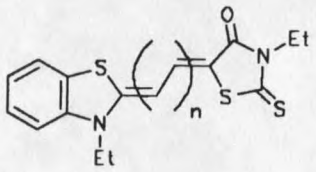	432	528	605	635

chain length. The chromophore is a dipolar amidic system and the molecule is neutral. These dyes are converging. Each time the chain is lengthened the wavelength increases; however, the more the chain is lengthened the smaller the increase in wavelength.

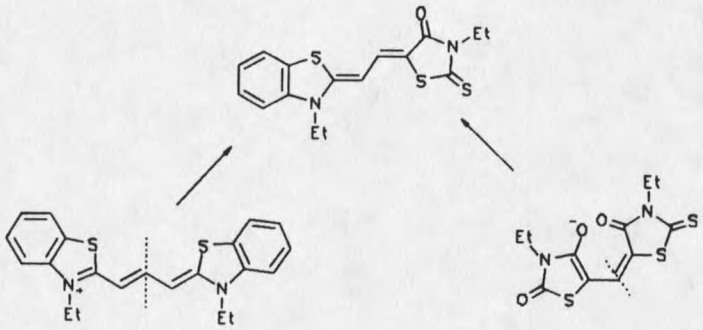

Figure 5. Composition of a merocyanine dye.

Merocyanines have two distinct resonance structures. The relative importance of the two structures is determined by the electron donating/withdrawing abilities of the two heterocycles incorporated into the dye. This donating/ withdrawing measure will be discussed later. For now, let us consider a dye with strong electron donating and withdrawing groups. The ground state resonance for this dye can be thought to resemble the charge separated structure shown in Figure 6. In a non-polar solvent, this dye would have an absorption ($\lambda_{max.}$) resulting from an energy difference between the ground state and the first excited state which would resemble the neutral resonance structure. When the same dye

dye is dissolved in a polar solvent the wavelength would be shorter. When this occurs the dye is said to be a "blue shifter."

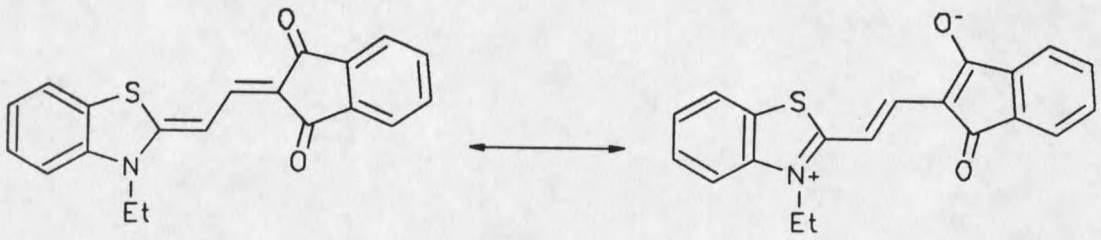

Figure 6. Resonance structures for a merocyanine dye.

This is thought to happen because the polar solvent interacts with the dye so that the energy needed to reach the neutral first excited state of the merocyanine is increased (29). Dyes that are neutral in the ground state would be charge separated in the excited state and are called "red shifters." When they are dissolved in a non-polar solvent the first excited state will have a larger energy difference from the ground state compared to when the dye is dissolved in a polar solvent.

The last class of dye in the cyanine family we will address is a combination dye consolidating merocyanine and carbocyanine components. Cyanines of this type are known as allopolar dyes. These dyes are made up of two basic heterocycles that are often identical and an acidic

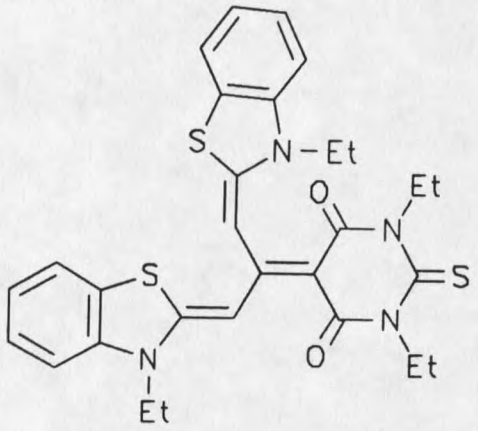

Figure 7. An allopolar dye.

heterocycle. An allopolar dye can also be made with one electron donating group and two electron accepting groups. These are linked with methine carbon chains (see Figure 7). Two solution conformations are observed. In non-polar solvents the meropolar or neutral conformation is favored and in polar solvents the holopolar or charge separated conformation is favored.

These conformations have been postulated from UV/VIS spectroscopy (30). In a polar solvent the holopolar conformer would dominate. This conformation has the same chromophore as a cyanine. An example of this can be seen in Figure 8. The same can be said for the meropolar conformation. Its wavelength is the same as the parent merocyanine dye that the meropolar conformation represents.

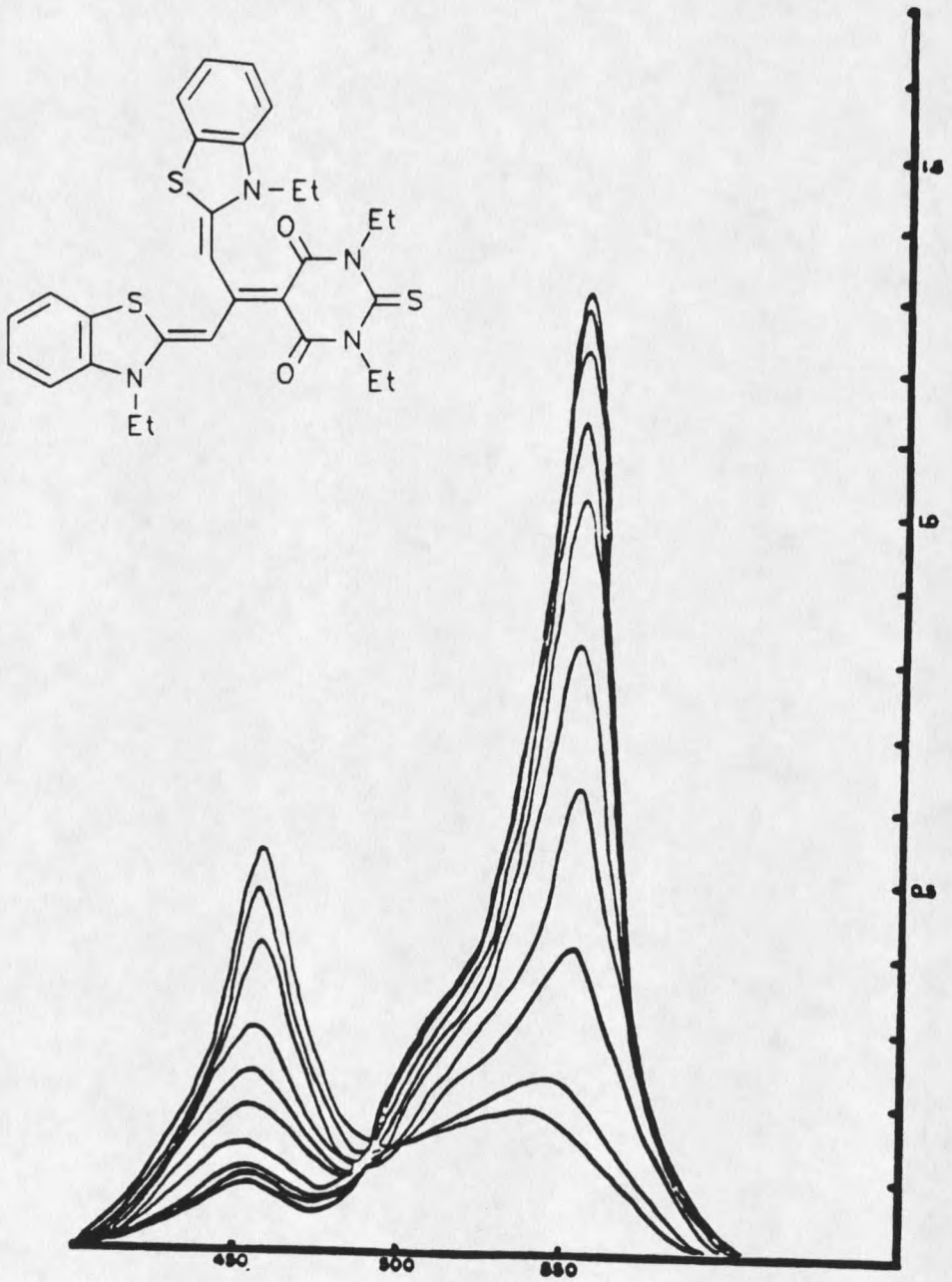

Figure 8. UV/VIS spectra of an allopolar dye (31).

AREA OF INTEREST

The objective of this thesis concerns conformational studies and π electron distributions of allopolar and related dye systems. An allopolar dye has been thought by Brooker to have conformations in which two heterocycles are in the plane with respect to one another and the other heterocycle perpendicular to this plane (32). We plan on studying this conformational ideal. A basis for modeling parent dye molecules needs to be made before the allopolar dyes can be studied. This foundation can then be expanded to make competent predictions for conformations of allopolar dyes. The groundwork will encompass merocyanines that model the meropolar conformation, and methyl crowded merocyanines to promote twisting due to steric interactions. The methyl crowded dyes can even be thought of as very simple allopolar dyes as shown in Figure 9.

During the development of simple merocyanines it was noted by Brooker (33) that some dyes absorbed at shorter wavelengths than predicted. He believed that a merocyanine should absorb at the mean wavelength of the two parent dyes from which the merocyanine was derived. These are the oxonol

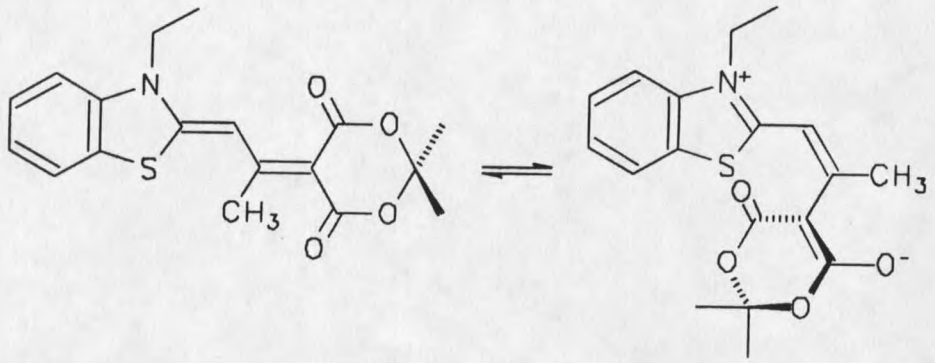

Meropolar conformation Holopolar conformation

Figure 9. Two conformations of a methyl crowded merocyanine.

and carbocyanine dyes discussed earlier and shown in Figure 3. This relationship was observed in a majority of the merocyanines studied. Some dyes absorbed at or near their predicted values but others were markedly different. Brooker made a series of dyes that would help understand this phenomena and to ultimately predict the wavelength of targeted merocyanines.

The reference dye used for this study was Michler's hydrol blue (see Figure 10). This dye's electron donating group is weakly basic (p-di-methylaminophenyl) and shouldn't donate a lot of electron density into the chromophore (34). If the nitrogen did donate electron density, the aromatic ring would be perturbed. Because of this non-contributing heterocycle, the resulting change in the expected wavelength of a dye when this heterocycle was incorporated would be due

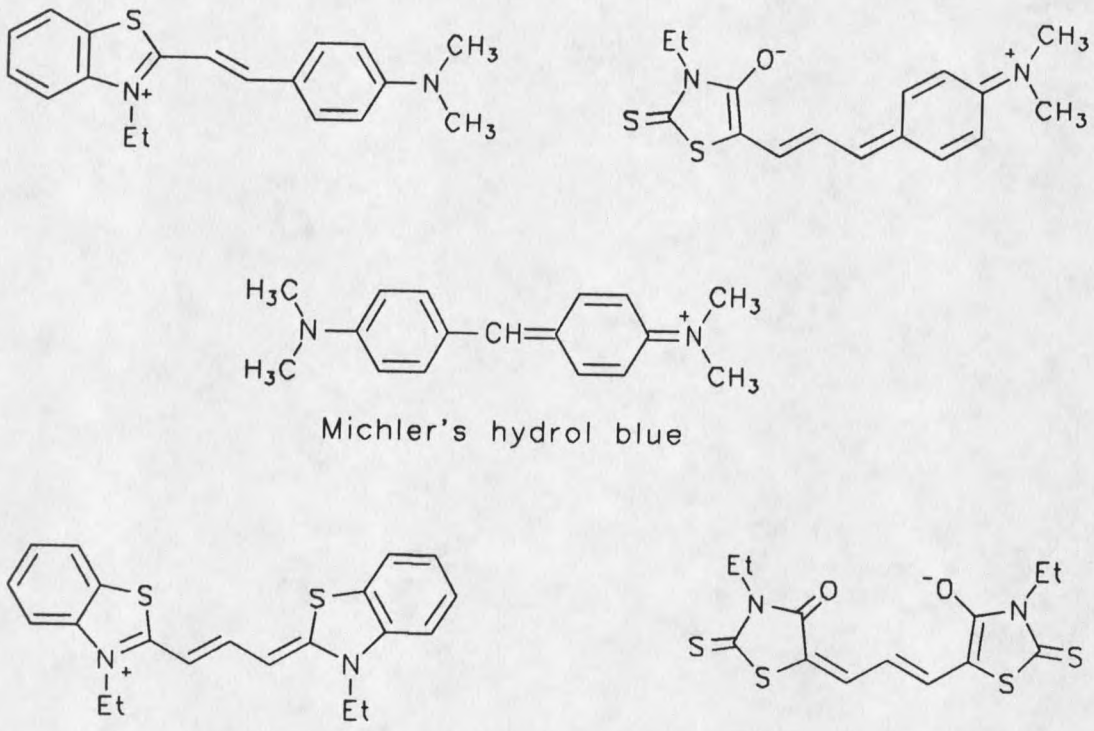

Figure 10. Dyes derived from Michler's hydrol blue.

primarily to the electron donating or basicity of the other heterocycle used in the dye. These groups are shown in Table 2.

$$\text{Deviation} = \Delta\lambda = \lambda_1 - \lambda_{obs}$$

Equation 1

The term **deviation** was derived from these data. The deviation of a compound is defined in Equation 1 (36). A heterocycle's deviation is the mean wavelength expected from

Table 2. Heterocycles and deviations. **A**. Basic heterocycles and **B**. Acidic heterocycles (35).

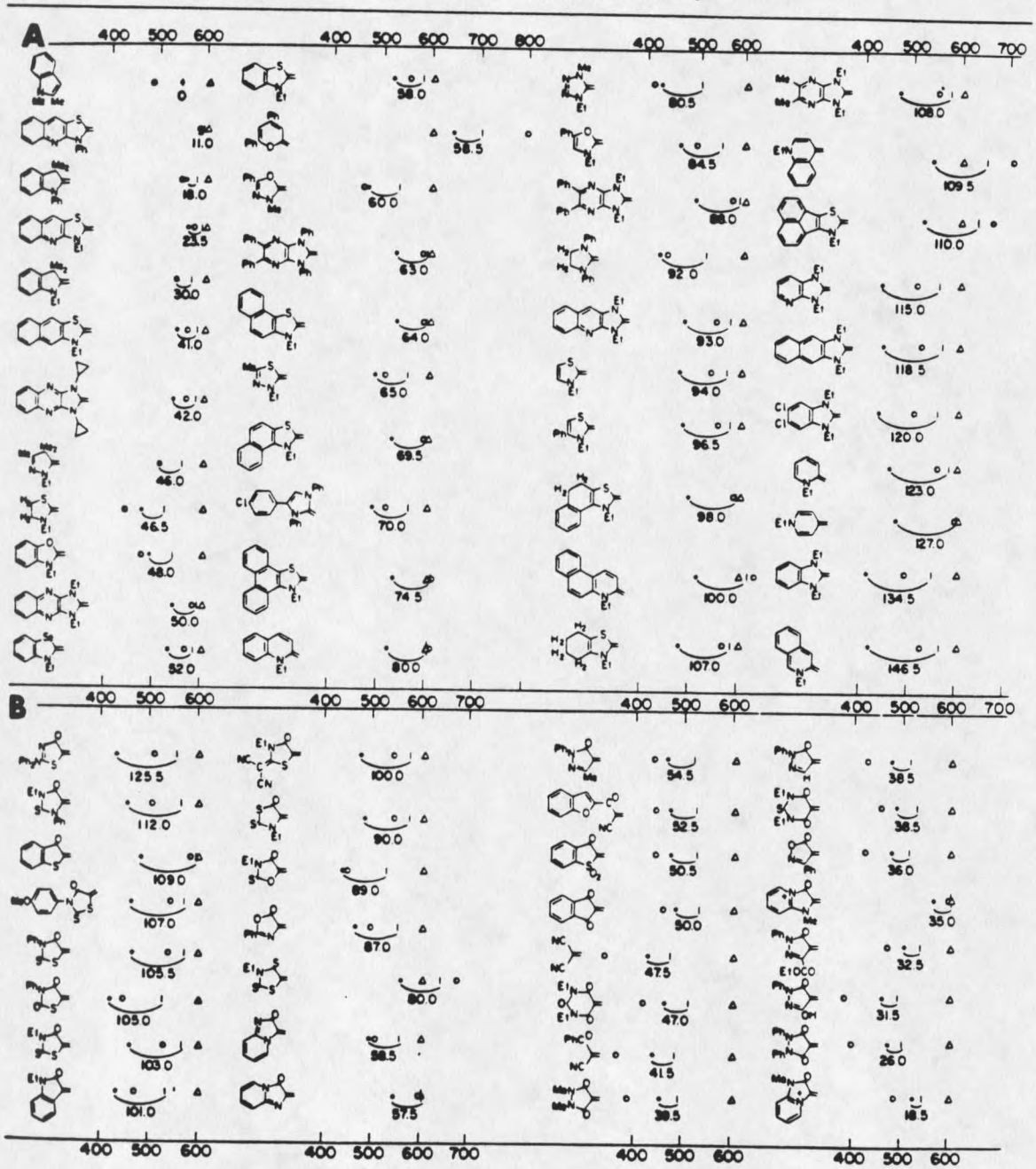

Symbols for absorption maxima: Δ = symmetrical *bis*(*p*-dimethylaminophenyl) cyonine;
O = symmetrical carbocyanine (methine oxonol) from nucleus shown
● = (experimental) unsymmetrical styryl (benzylidene)
I = mean wavelength λ_I

the dye's parent compounds minus the actual wavelength observed. From these experiments Brooker deduced that the greater the electron donating ability of a heterocycle the larger the observed deviation. This work was also independently developed by Kiprianov in the Soviet Union (37).

This same procedure was carried out for acidic heterocycles. It has been shown that nonpolar dyes have characteristics similar to polyenes (38). This type of dye absorbs much lower than the calculated mean values. Using this idea as a basis for his work, Brooker showed that a good electron withdrawing group would make a dye that resembled the charge separated resonance structure and should absorb closer to the mean value of its parent dyes. For these reasons a good electron withdrawing group will have a small deviation whereas a poor withdrawing group has a larger deviation.

We believe that if the observations by Brooker are true then an experiment can be designed to show this. A merocyanine with poor donating and poor withdrawing groups should have chain carbon-carbon bond lengths similar to the neutral resonance structure in Figure 6. Likewise we should be able to see the charge separated resonance dominate for dyes with strong donating and accepting groups. We expect to be able to observe this by x-ray crystallography and nuclear magnetic resonance (NMR) spectroscopy. The crystallographic

data will give exact bond lengths and angles for single crystals of the desired compounds. NMR data can be used to show the polarity of a molecule using chemical shift arguments.

The three dyes chosen to study non-crowded merocyanines are shown in Figure 11. The first dye, 2-[2-(3-ethyl-2-benzothiazolinylidene)ethylidene]-1,3-indandione, has a good electron donating group (benzothiazole) and a good electron withdrawing group (indandione) and is represented as BTHIND. This dye is the most polar of the three and should show single-double-single bond character through the chain carbon bonds.

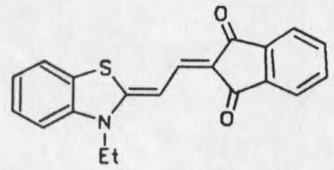

2-[2-(3-ethyl-2-benzothiazolinylidene)-ethylidene]-1,3-indandione (BTHIND)

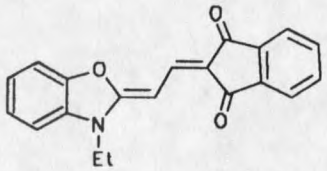

2-[2-(3-ethyl-2-benzothiazolinylidene)-ethylidene]-1,3-indandione (BOXIND)

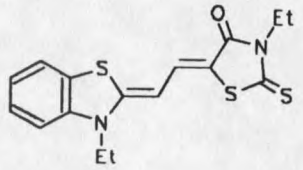

3-ethyl-5-[2-(3-ehtyl-2-benzothiazolinylidene)-ethylidene]rhodanine (BTHRHO)

Figure 11. Selected non-crowded merocyanines.

2-[2-(3-Ethyl-2-benzoxazolinylidene)ethylidene]-1,3-indandione (BOXIND) has a weaker donating group (benzoxazole) and indandione. Using Brooker's theory we think that this dye won't be as polar as BTHIND but more polar than dye three. This third dye, 3-ethyl-5-[2-(3-ethyl-2-benzothiazolinylidene)ethylidene]rhodanine, has a good donating group (benzothiazole) but a very poor withdrawing group (rhodanine). This dye is thought to be nonpolar and is represented as BTHRHO. Table 3 lists the deviations of these heterocycles.

The chain methyl merocyanines have a methyl group on a chain carbon atom (shown in Figure 12) to promote twisting. In crowded and non-crowded merocyanines where the acidic heterocycle contained a six membered ring, different solvent systems showed that the chromophore could be in the meropolar conformation (VIS region) or holopolar conformation (UV region). These conformations have been shown previously in Figure 9. It was suggested that these dyes would show some twisting when going from one conformation to another.

The first attempt to look at these dyes was computing work by Ann Bowler (39). Bowler used various molecular modeling approaches to calculate the ground state conformation of similar dyes. The computer program used was

Table 3. Deviation of selected basic and acidic heterocyclic end groups.

A) Basic Heterocycles

	Δλ		Range
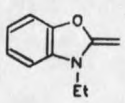	48	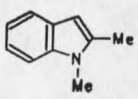	0
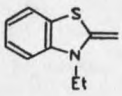	58		
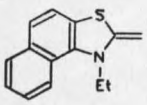	69.5	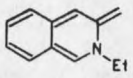	146.5

B) Acidic Heterocycles.

	Δλ		Range
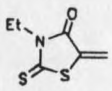	103.0	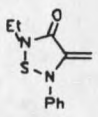	112
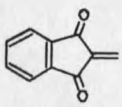	50.0	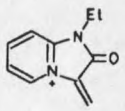	18.5
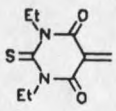	38.5		

Gaussian 80 (an *ab initio* computing package). Merocyanines were too large for the computation so simpler model molecules were used to get an idea of the chain geometry as well as electron distribution.

The program was very sensitive to steric interactions. The calculations predicted some bond lengthening was occurring for crowded merocyanines. The calculation tended to bend the

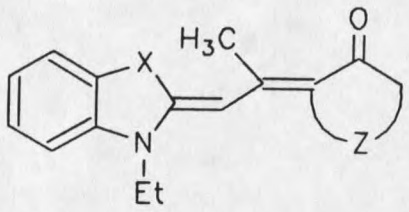

X = O or S
Z completes a rhodanine, barbituric acid, indandione, or similar heterocyclic ring system.

Figure 12. Representative chain methyl merocyanines.

molecules instead of twist them, as required to go from one conformation to another. The computational chain bending made the chain methyl bearing carbon more sp^3 than sp^2.

Force field modeling using AlchemyII twists a merocyanine dye when a methyl group is incorporated. The twist is very small (2-3 degrees) in some dyes and larger (10-15 degrees) in others. The program also tends to bend the molecules (similar to the bending seen by Bowler) into a "banana" as shown in Figure 13.

Three dimensional models (Corey-Pauling-Koltun type) were also used for modeling studies. The models have exact Van der Waals radii so that a molecule can be made as close to the real compound as possible. The chain methyl merocyanines did not give a planar conformation with these models.

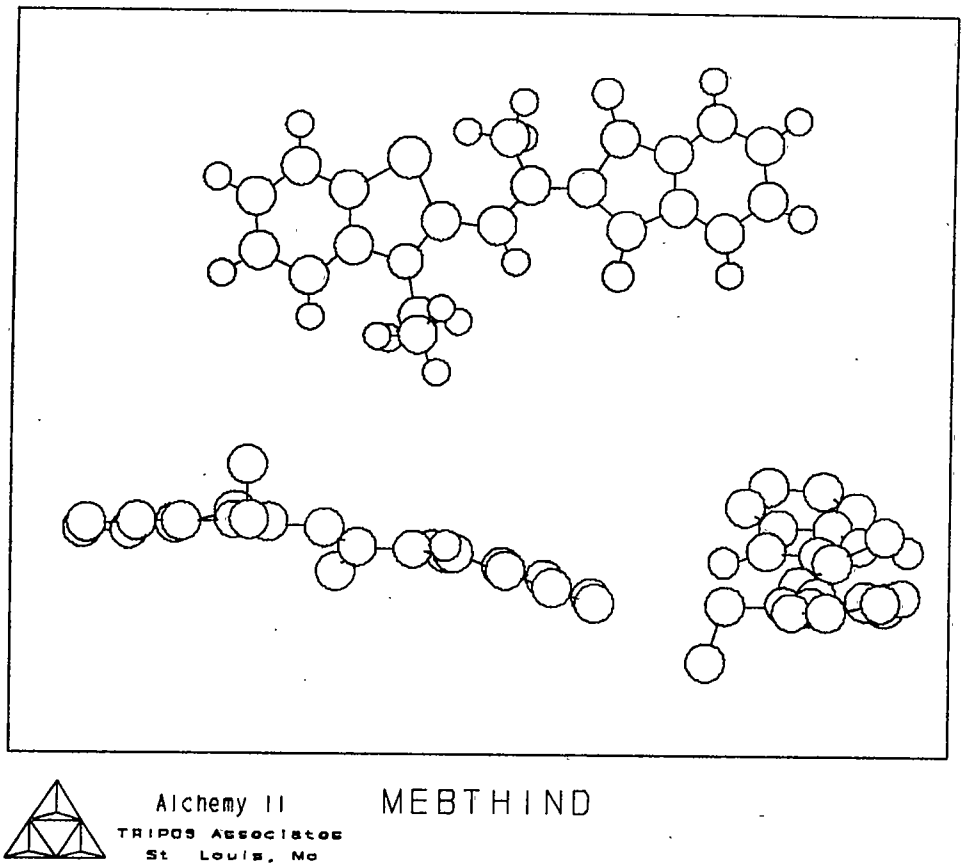

Figure 13. Three views of a chain methyl merocyanine using Alchemy II.

We decided to use three dyes for our study of chain methyl merocyanines. 3-Ethyl-5-[2-(3-ethyl-2-benzothiazol-inylidene)-1-methylethylidene]rhodanine (MEBTHRHO) was chosen because of two conformations that are possible when the methyl group is in the chain. The first is the Z conformation that would be observed if the methyl group had no effect on the dye's planarity (see Figure 14). If there was an effect one would expect either the dye to twist out of the plane or at

least form the E conformation. The E conformation is more likely than the Z because the carbonyl is 180° from the methyl group where no crowding by the carbonyl oxygen atom can occur.

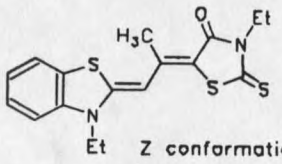

Z conformation

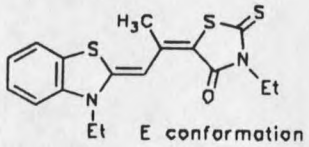

E conformation

3-ethyl-5-[2-(3-ethyl-2-benzothiazolinylidene)-1-methylethylidene]rhodanine
MEBTHRHO

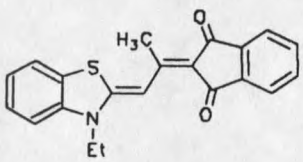

2-[2-(3-ethyl-2-benzothiazolinylidene)-
1-methylethylidene]-1,3-indandione
MEBTHIND

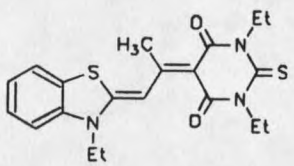

2-[2-(3-ethyl-2-benzothiazolinylidene)-
1-methylethylidene]-2-thiobarbituric acid
MEBTHTBA

Figure 14. Chain methyl merocyanines studied.

2-[2-(3-Ethyl-2-benzothiazolinylidene)-1-methyl-ethylidene]-1,3-indandione (MEBTHIND) was the next dye to be considered in the study. We chose this dye because it has two carbonyl groups that eliminate the possibility for the molecule to twist the carbonyl group into an E conformation. In fact only one planar conformation is expected. This should allow us to see if the methyl group is large enough to twist the molecule out of the plane.

The last methyl crowded merocyanine to be studied was 1,3-diethyl-5-[2-(3-ethyl-2-benzothiazolinylidene)-1-methyl-ethylidene]-2-thiobarbituric acid (MEBTHTBA). This dye should be more crowded than the other two because the acidic heterocycle is a six membered ring while the other dyes contain five membered rings. This will force a carbonyl group to be closer to the methyl group on the ring. Thiobarbituric acid is also symmetric with respect to the carbonyl groups so only one planar conformation is expected.

SYNTHESIS

Merocyanine Dyes

Synthesis of the targeted straight chain merocyanines was accomplished using modifications of reactions developed by Brooker and coworkers (40). The synthesis begins with the alkylation of 2-methyl-benzothiazole (or benzoxazole), with an alkylating agent, to give the 3-ethyl-2-methyl-benzothiazolium salt (**1**) shown in Figure 15. Iodoethane was used as the reagent of choice. Ethyl p-toluenesulfonate and ethyl triflouromethanesulfonate were also used and alkylated well. An ethyl alkylation was chosen because dyes with this group tend to be more soluble than their methyl counterparts. The problem with using an ethyl group was that the methyl quaternary salts were reportedly more reactive intermediates for dye synthesis.

The quaternary salt (**2**) was condensed with diphenyl-formamidine and acetic anhydride to form 2-[2-acetanilido-vinyl]-3-ethylbenzothiazolium iodide (**3**, an ICI intermediate). This ICI intermediate was then condensed with 1,3-indandione (**5**, or any of the other heterocycles discussed previously) in

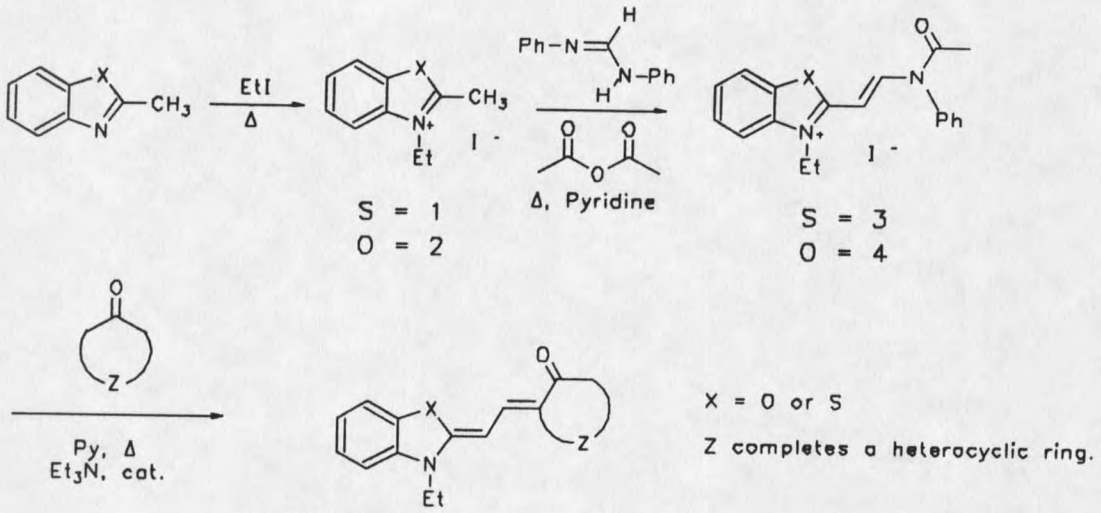

Figure 15. Synthesis of non-crowded merocyanines.

pyridine with triethylamine added as a catalyst. The resulting dyes precipitated from solution upon addition of cold methanol.

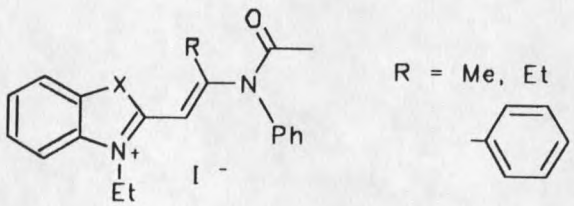

Figure 16. ICI intermediates that could be used for crowded merocyanines.

Chain methyl merocyanines are more difficult to prepare. Procedures for the formation of an acetanilidovinyl salt with an alkyl group on the olefinic carbon have been used (41). An intermediate of this type (shown in Figure 16) could make the synthesis of chain methyl merocyanines straight forward by using reaction conditions similar to the non crowded merocyanine dye synthesis. These intermediates are reported to be obtained in low yields and difficult to isolate. We wanted to maximize the overall yield in the total synthesis and felt that the reported intermediates wouldn't be suitable. For these reasons other synthetic routes were attempted.

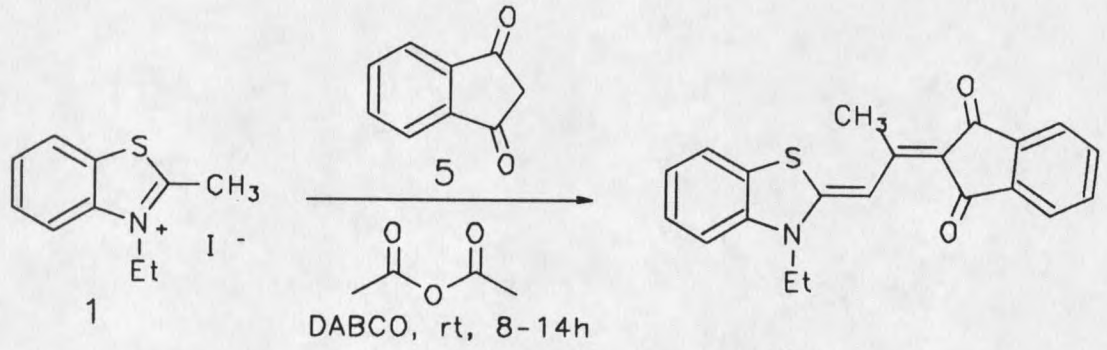

		Yields
MEBTHMEL	2,2-Dimethyl-1,3-dioxone-4,6-dione	45.9%
MEBTHIND	1,3-Indandione	31.6%
MEBTHTBA	1,3-Diethyl-2-thiobarbituric Acid	25.9%
MEBTHRHO	3-Ethylrhodanine	11.9%
	1,3-Cyclopentanedione	0%

Figure 17. Synthesis of methyl crowded merocyanines.

The only other reference for a chain methyl merocyanine dye synthesis was reported in a paper by Dieter Shelz (42). He developed a condensation reaction that worked well for benzothiazoles. The reaction conditions are shown in Figure 17. MEBTHIND was synthesized by reacting 3-ethyl-2-methyl-benzothiazolium iodide (**1**) with 1,3-indandione (**5**) and 1,4-diazabicyclo[2.2.2]octane (DABCO) in acetic anhydride. The reaction conditions were improved by increasing reaction times and the amount of acetic anhydride used. The synthesis was used to make the other dyes discussed in this study; MEBTHMEL, MEBTHRHO, and MEBTHTBA.

The reaction conditions were tried for benzoxazoles, imidazoles, quinolines, and indoles. None of the desired dyes were isolated. The base was changed to triethylamine or pyridine for each case. Temperature was varied from an ice bath to reflux and acetyl chloride substituted for acetic anhydride. The desired dyes still were not isolated. Another synthetic pathway is needed that would be more general than the one developed by Shelz.

We decided to look at various approaches to 2-[2-(3-ethyl-2-benzoxazolinylidene)-1-methylethylidene]-1,3-indandione (MEBOXIND). This target dye was chosen because it

could also be tied into the non-crowded merocyanine study. Retro-synthetic ideas led us to try different synthetic pathways. The first of these pathways is shown in Figure 18.

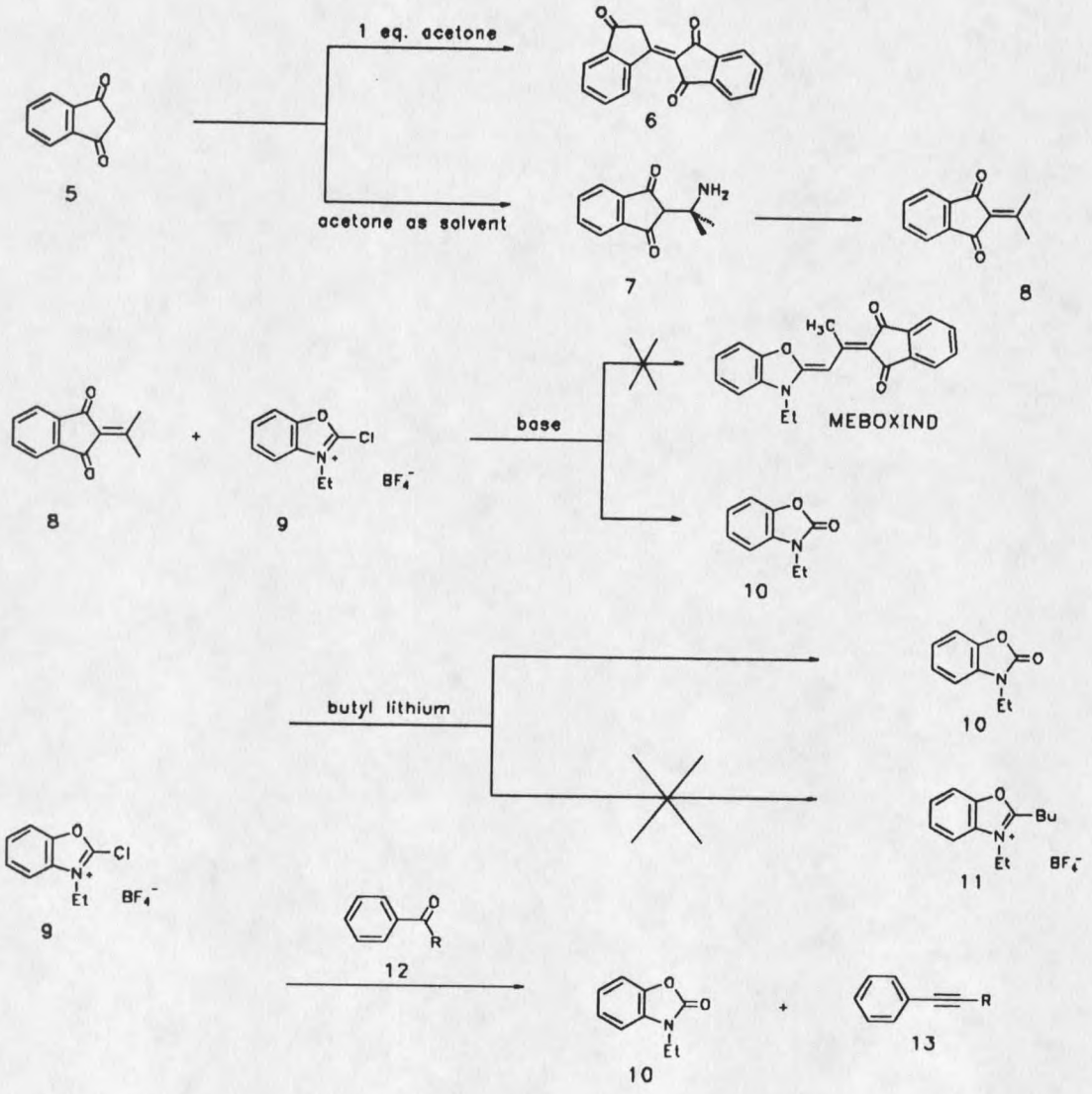

Figure 18. Synthetic approach for MEBOXIND starting from 1,3-indandione.

The literature led us to believe that a benzoxazole could be made with a leaving group in the (-2-) position. In fact the chlorine intermediate substituted in this position is available from chemical retailers as the tetrafluoroborate salt (**9**). 2-Isopropenyl-1,3-indandione (**8**) was the only other intermediate needed to be made. Our first attempt yielded the condensation of two 1,3-indandione molecules (**6**).

The undesired condensation occurred when 1,3-indandione (**5**) was condensed with one equivalent of acetone in chloroform with triethylamine added as a catalyst. Stirring at room temperature yielded the dimer, which was identified by mass spectrometry. The desired isopropenyl intermediate (**8**) was obtained using the method described by Junek (43).

1,3-Indandione (**5**) was dissolved in acetone and concentrated ammonium hydroxide slowly added to the reaction mixture. From these conditions an amine (**7**) was supposed to be isolated that would later evolve ammonia yielding the desired intermediate (**8**). The reported intermediate was not found which we believe was due to the reaction time allowed. Mass spectrometry showed that the isolated product was the isopropenyl indandione (**8**).

The isopropenyl indandione (**8**) was combined with the benzoxazolium salt (**9**) in pyridine and triethylamine and heated. There was no dye precipitation after the addition of

methanol. Observation of the reaction mixture by mass spectrometry showed that there was 3-ethyl-2-benzoxazolinone (10) present in the reaction mixture. This lead us to believe that the benzoxazolium salt (9) incorporates oxygen better than alkylation by the indandione intermediate (8). We attempted to alkylate the quaternary salt (9) using butyllithium in freshly distilled solvents and an inert atmosphere but the only isolated compound was the benzoxazolinone (10). The literature shows (44) that (9) has been used primarily for dehydration of arylketones (12) to alkynes (13). For these reasons, another pathway was pursued.

The Schelz reaction scheme applying to this crowded merocyanine, MEBOXIND, resulted only in the isolation of starting materials for these conditions, as shown by ^{1}H-NMR and mass spectrometry. This synthetic pathway was not pursued.

The reaction scheme shown in Figure 19 incorporates an idea similar to that used in the non-crowded merocyanine dye synthesis. Condensation was attempted using a Dains' type intermediate approach as opposed to the ICI intermediate employed in the previous dye synthesis. We believed that if a leaving group could be used on an indandione intermediate (14) the 3-ethyl-2-methylbenzoxazolium salt (2) could be used

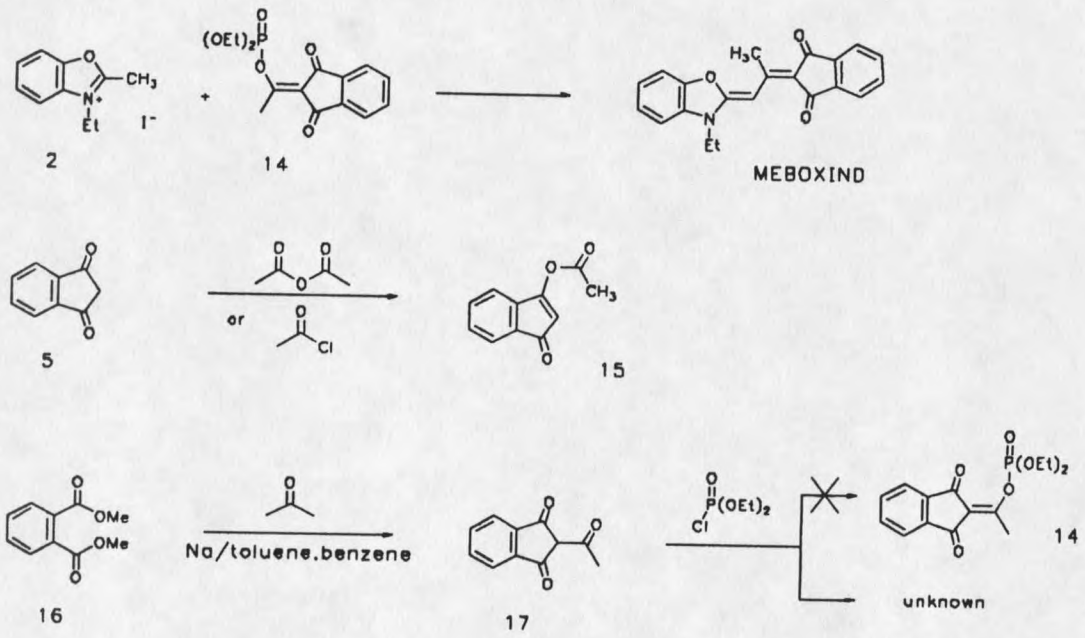

Figure 19. Attempt at MEBOXIND from a pathway similar to the Dains' intermediates.

as a nucleophile in the dye formation via a push-pull mechanism. To get this intermediate, 2-acetyl-1,3-indandione (**17**) was first synthesized.

1,3-indandione (**5**) was added to acetyl chloride or acetic anhydride in pyridine (tetrahydrofuran or chloroform) with triethylamine and heated. The desired intermediate (**17**) didn't form as shown by mass spectrometry. The fragmentation pattern suggested that alkylation occurred on the oxygen atom

to form an α,β unsaturated ester (**15**) which could be converted to the desired compound. The intermediate we wanted was finally synthesized more efficiently using a Michael addition described by Kilgore (45).

Methyl phthalate (**16**) was dissolved in a benzene/toluene mixture along with dry acetone and sodium metal. This mixture was heated for twenty four hours and the mixture extracted with water and the organic layer saved. This layer was evaporated to an oil and 2-acetyl-1,3-indandione (**17**) crystallized from cold methanol.

The acetyl indandione (**17**) was then reacted with diethyl chlorophosphate. Conditions were varied but the desired intermediate (**14**) never formed. This was determined by mass spectrometry. There was no parent ion or any of the predicted fragmentation ions for the intermediate (**14**). The isolated compounds from the reaction were mainly starting materials. There were also complex products whose structure could not be determined. This was suggested because of a fragment ion at 263 (among others). Fragment patterns ruled out the desired indandione intermediate (**14**). These types of losses make no chemical sense. The parent ion could not be determined so the compound obtained cannot be logically formulated.

Our final attempt at the chain methyl benzoxazole dye is shown in Figure 20. This synthesis incorporates a leaving group on the olefinic carbon similar to an ICI intermediate but the leaving group is now a chlorine atom (**18**). Compounds of this type have been obtained in the benzothiazole series. The 2-chloro-(3-ethyl-2-benzothiazolinylidene)propenes (**22**) are made by chlorinating 1-[3-ethyl-2-benzothiazolinylidene]-2-propenone (**21**) using phosgene as the chlorinating reagent (46). This was the basis for our synthetic approach.

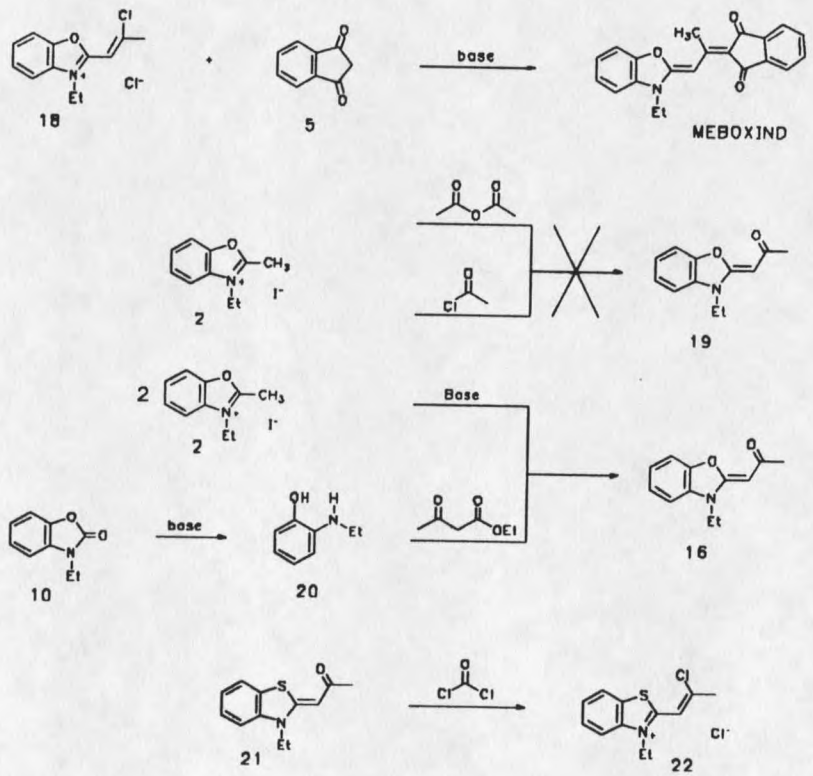

Figure 20. Synthetic approach to MEBOXIND using ICI intermediate ideals.

The first step was the alkylation of the benzoxazolium salt (**2**) to form the propenone intermediate (**19**). Our synthesis ended at this step when the benzoxazole quaternary salt proved to be unreactive. Condensation reactions were run using acetic anhydride, and acetyl chloride as reagents. Different solvents, bases, reaction times, and temperatures were tried. The only isolated product was the starting salt (**2**). The intermediate preparation (**16**) has been shown in the literature by Oliveros and Wahl (47). These reactions were tried many times with no successful results.

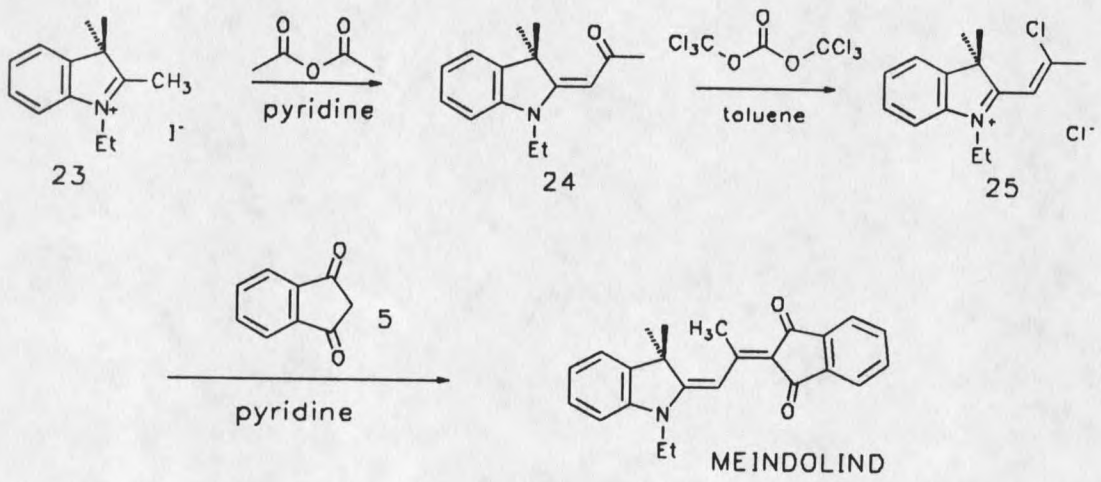

Figure 21. New synthesis of chain methyl merocyanines.

A promising point was that this synthetic pathway was successful for indoles. This synthesis is shown in Figure 21. The corresponding indole salt (**23**) was alkylated with acetic anhydride to form the 2-propanone intermediate (**24**). This

conjugated amide was then treated with triphosgene to form the chloride salt (**25**). To this salt, indandione (**5**) was added in pyridine. The reaction mixture yielded 2-[2-(3,3-dimethyl-1-ethyl-2-indolinylidene)-1-methylethylidene]-1,3-indandione (MEINDOLIND) upon the addition of methanol. This shows that different chain methyl dyes can be obtained by this pathway.

Allopolar Dyes

An BAA allopolar was inadvertently formed while making intermediates for the crowding study. Another chain crowding group, phenyl, was considered in place of the methyl group. Benzoyl chloride (**26**) was condensed with 3-ethyl-2-methyl-benzothiazolium iodide (**1**) to make 2-(3-ethyl-2-benzothiazolylidene)-1,3-diphenyl-1,3-propanedione (**28**) shown in Figure 22. Another intermediate (**27**) was expected from these conditions. Mass spectrometry data showed that this was not the case. The parent ion suggested that two benzoylchloride molecules had condensed with each benzothiazole molecule. X-ray crystallography confirmed this to be true. Benzoyl chloride did condense to form the allopolar-like dye (**28**).

Symmetric BBA allopolar dyes are formed by an unsymmetric approach. 1-Ethyl-2-methyl-β-naphthothiazolium iodide (**29**) was condensed with acetic anhydride to give the 2-propenone

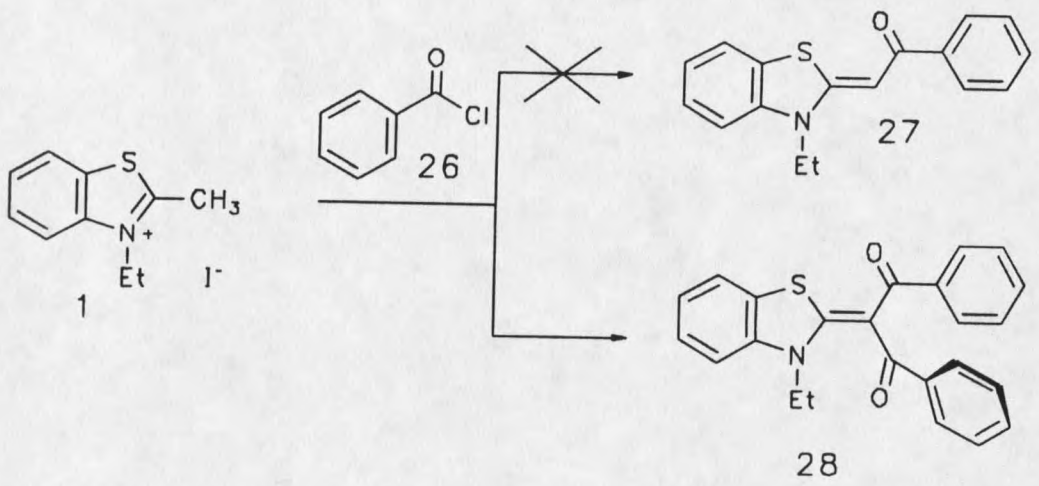

Figure 22. Formation of BAA allopolar like dye.

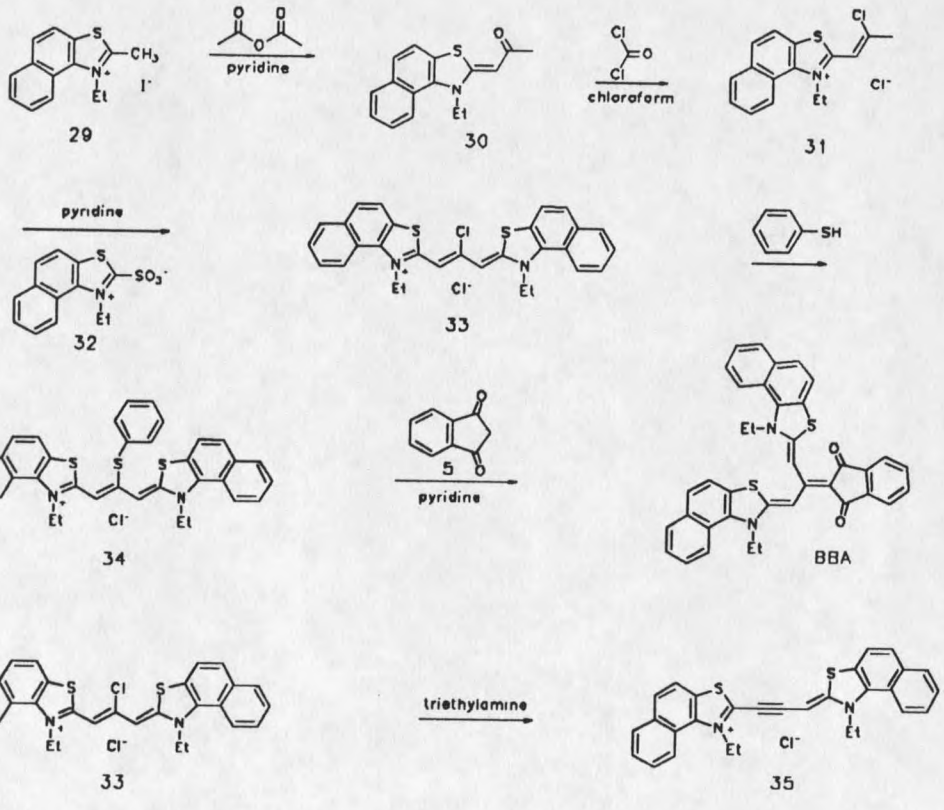

Figure 23. Allopolar dye synthesis.

intermediate (**30**) shown in Figure 23. This was chlorinated with phosgene using the procedure by Sveshnikov (48). The chloride intermediate (**31**) was then used as a nucleophile to displace the sulfite group (other leaving groups were also used) on 3-ethyl-2-sulfobetanaphthathiazole (**32**) in a weak base (pyridine). This formed a salt (**33**) that has a chlorine leaving group on the chain carbon however the yields are very low. Stronger bases like triethylamine reportedly dehydrohalogenated the intermediates (**33**) which gives the alkyne carbocyanine dyes (**35**). The reactive intermediate (**33**) was precipitated from solution by displacing the chloride with a thiophenyl group. The thiophenyl intermediate (**34**) was then condensed with 1,3-indandione (**5**) to give 2-[1,3-(bis-1-ethyl-2-naphtho[1,2-d]thiazolenylidene)isopropylidene]-1,3-indandione. This compound was determined by fast atom bombardment mass spectrometry.

CRYSTALLOGRAPHY

Twinning

Structural determination of cyanines by x-ray crystallography has been very limited (49-53). There are a relatively low number of structures solved with this technique compared to the known number of cyanines and merocyanines. This was puzzling because of the apparent ease of crystallization when our dyes were purified. The merocyanines readily formed long needles upon recrystallization from ethanol. It was later found that these dyes tended to twin when larger crystals were grown.

To be able to solve a structure using x-ray crystallography we needed a single crystal of the pure merocyanine. These crystals had to be large enough so that they reflected enough observable intensities for data collection. The larger data set allows a better structure refinement. Many crystals appeared to be single but were determined not to be upon closer observation. Most twinning problems can be seen by viewing the crystal by polarizing light. When light was polarized in the correct direction relative to the orientation of a single crystal, the entire

crystal would extinguish (darken) simultaneously. If the crystal isn't single the light may extinguish from one end of the crystal to the other or from side to side. The crystal may not extinguish polarized light at all. These polarized light observations are typical of twinned crystals. There are many different types of twinning. We will discuss the types found in our crystals.

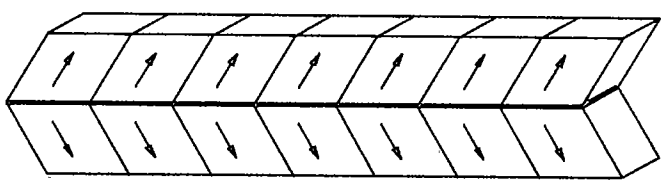

Arrows represent the orientation of the molecules in the unit cell.

Figure 24. Twinning along a common axis.

When a crystal extinguishes on one side and not the other it is usually due to two crystals fused together along a common axis as shown in Figure 24. This is a very common form of macro twinning which was observed in crystals that were more rapidly grown. In most cases slow diffusion of methanol into a pyridine solution that was saturated with a dye yielded long single crystals that had to be cut before they could be used for data collection. The maximum length that could be

used was 1.5 mm. Crystals longer than this have parts that stick out of the x-ray beam and will cause problems with the continuity of observed reflections.

Crystals that were longer than the maximum length were cut with a razor blade. This caused some crystals to split along the long axis. This splitting wasn't always obvious to the naked eye but could be shown by observing the peak shapes while the crystal was rotated in the x-ray beam. When the crystal was split we observed two peaks or broadened peaks. Normal peaks resemble a Gaussian curve.

One benefit from cutting crystals was that a macro twinned crystal which extinguished under polarized light was discovered when it was cut. Instead of two pieces the crystal fanned out when pressure was asserted by the edge of the razor. This was due to a large number of crystals that were all growing along the long axis. Pressure from the razor forced the crystals apart.

Another twinning problem observed was when the unit cells for a chain methyl merocyanine stacked in two different orientations as shown in Figure 25. This was discovered when the crystallographic data suggested that the unit cell was orthorhombic. The problem with this cell was that there were systematic absences of reflections that should be observed for an orthorhombic cell due to symmetry. The computer believed

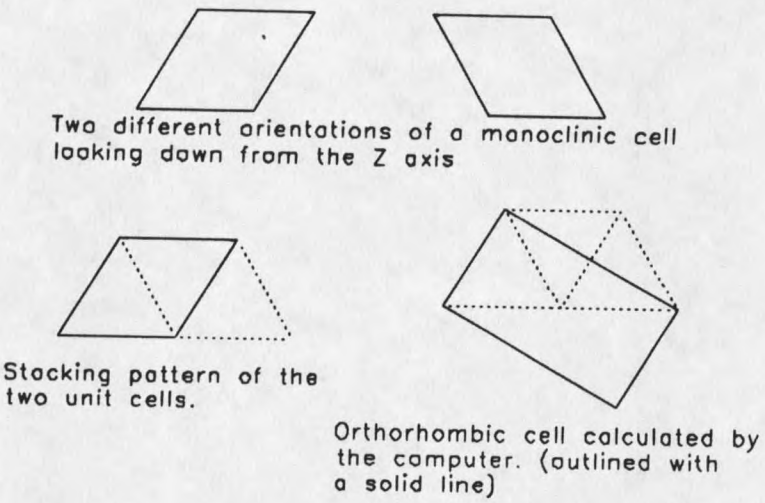

Figure 25. Twinning caused by stacking problems.

the unit cell was orthorhombic but further analysis suggests the unit cell is actually monoclinic in two orientations. This type of problem cannot be modeled due to the overlap of reflections which made the data set for this dye meaningless.

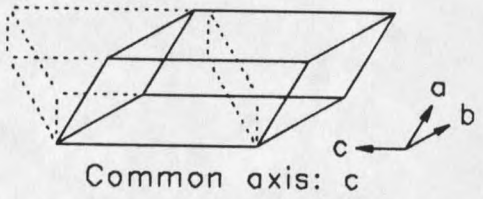

Figure 26. Twinning caused by two different unit cell orientations partially superimposed in a crystal.

Another type of twinned crystal was solved by Larsen and Ellerd (54). They solved the structure for a cyanine which crystallized with a unit cell that couldn't be readily determined. This was due to the crystal being micro-twinned as shown in Figure 26. The crystal had two different unit

cell orientations that were partially superimposed on one another. Structures of this type are very difficult to solve. The cell orientations had to be determined by photography. Once the two unit cell orientations were found data was taken on each. The crystal structure was then solved for each cell.

We have shown by our work and previous work that the lack of structural information for cyanines and merocyanines could be due to twinning problems. Very slow growth and careful sizing have given single crystals which can be studied to give insights to the bonding of the merocyanines. We have obtained a series of crystal structures that have allowed us to look at the bonding of merocyanines through experimental rather than indirect evidence.

Brooker's idea of deviation should be most easily observed in the dye chromophore. Any evidence of the charge separated or neutral ground state resonances can be easily observed by studying these bond lengths. For this reason we will focus on the chain carbon-carbon bond characteristics. The structures have been numbered so that the chain carbons are easily found in the structure tables. Only selected data from the structure refinements have been presented in this section. Complete structural information for each dye is tabulated in Appendices A-J. Refinement results for all of the merocyanines are listed in Table 4.

Table 4. Refinement data for all merocyanines determined by x-ray crystallography.

Dye	Total number unique data	Number obs / σ (I)	Number param.	R/Rw	Goodness of fit	Largest difference map peak (final)
BTHIND(H_2O)	3881	1291>2 1/2	242	.049/.045	1.29	0.19 e/A^3 0.5 A from H2
BOXIND	3551	1519 > 3	218	.049/.051	1.39	0.13 e/A^3 1.5 A from C2&H2
BTHRHO	4044	1892>2 1/2	202	.044/.045	1.18	0.25 e/A^3 between S2 & C4
BTHIND*	6895	2832 > 3	218	.047/.050	1.38	0.33 e/A^3 between C1 & S1
MEBTHRHO**	7689	4651 > 3	212	.046/.053	1.72	0.63 e/A^3 0.8 A from C17 1.5 A from C16
MEBTHIND***	5328	2255 > 3	227	.059/.064	1.60	0.73 e/A^3 1 A from C20&C21
ABMF****	2617	2168 > 3	254	.042/.047	1.87	0.23 e/A^3 1.38 A from S1
INTERMED*****	5687	3645 > 3	179	.045/.050	1.25	0.44 e/A^3 0.8 A from CL^-

* Three reflections showing strong extinction were excluded from the data set.

** Absorption correction by Gaussian integration μ(Mo Kα) = 4.1 cm^{-1}; transmission factor range = 0.79 to 0.91.

*** Five reflections showing strong extinction were excluded from the data set.

**** Cu Kα data; empirical absorption correction based on ψ scan data μ(Cu Kα) = 16.0 cm^{-1}; Transmission factor range = 0.57 to 0.91.

*****Ten reflections showing strong extinction were excluded from the data set.

Non Crowded Merocyanines

BTHIND, BOXIND, and BTHRHO were the first merocyanines solved by x-ray crystallography. Reduced thermal ellipsoid (50%) plots are shown in Figure 27. The first structure determined was BTHIND. The dye was refined to a R of 0.049 and a Rw of 0.048. There were 1291 observed reflections greater than two and one half times the standard deviation. This resulted in a goodness of fit equal to 1.29 for 242 parameters.

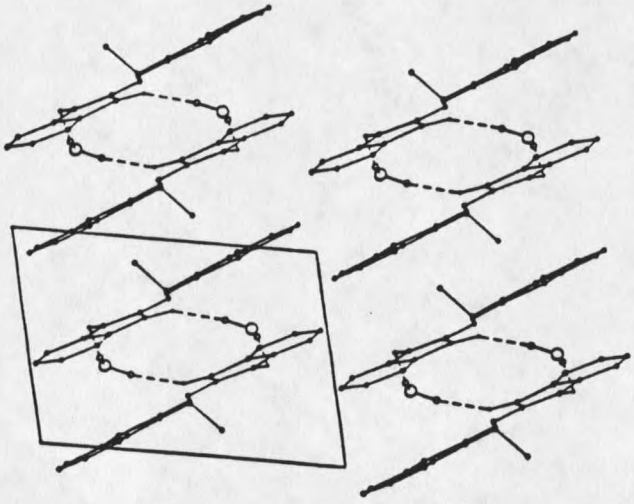

Figure 28. Packing diagram for BTHIND with disordered water. (oxygen and hydrogen bonded atoms enlarged for clarity)

The data revealed that the dye had crystallized with water in the unit cell. This water showed hydrogen bonding for one proton to the carbonyl oxygen on the indandione ring

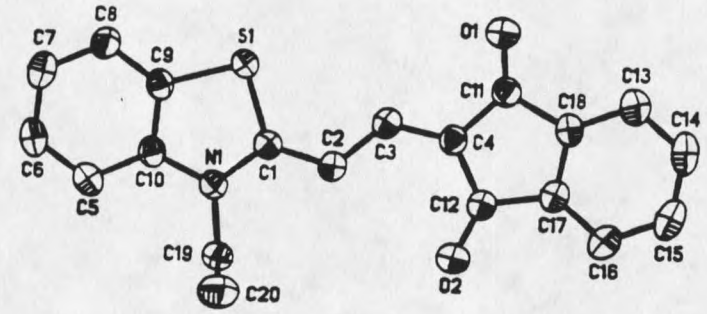

BTHIND

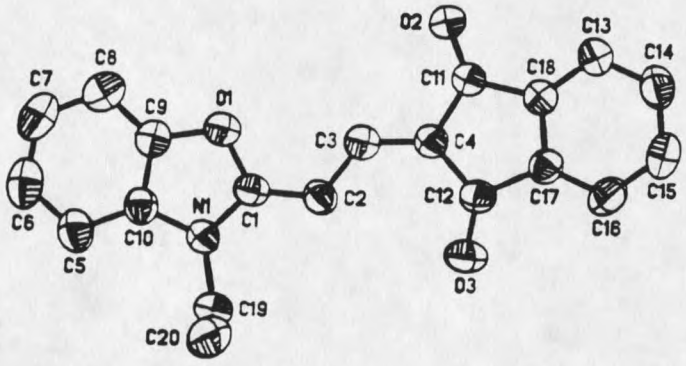

BOXIND

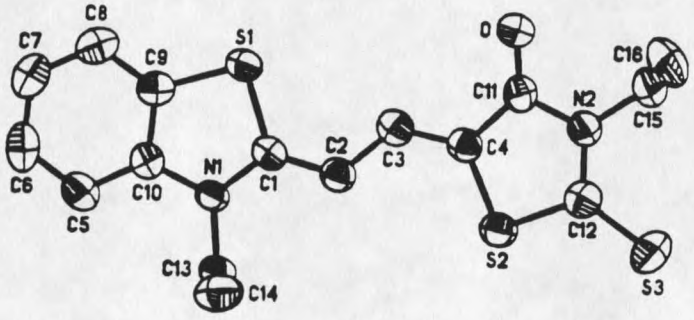

BTHRHO

Figure 27. Thermal ellipsoid plots for non-crowded merocyanines.

for one dye. The other proton was hydrogen bonded to another dye in similar fashion. An interesting observation was that two water molecules hold two dye molecules together like a sandwich (see Figure 28). This suggests that the dye may dimerize in solution before crystallization.

The oxygen atom for the water molecules showed some disorder. This means the oxygen can occupy more than one position in the unit cell. These positions were modeled and improved the structure refinement. Hydrogen bonding was the first indication of the polar nature of BTHIND. This was encouraging because we thought BTHIND would exhibit the most charge separated character of the dyes considered.

Table 5. Bond lengths (Å) for non-crowded merocyanines.

DYE	N_1-C_1	C_1-C_2	C_2-C_3	C_3-C_4	C_4-C_{11}
BTHIND (H_2O)	1.349 (5)	1.400 (6)	1.372 (6)	1.386 (6)	1.459 (6)
BOXIND	1.343 (3)	1.375 (4)	1.382 (4)	1.385 (4)	1.451 (4)
BTHRHO	1.362 (4)	1.371 (5)	1.404 (5)	1.367 (5)	1.442 (5)
BTHIND	1.365 (3)	1.386 (3)	1.384 (3)	1.388 (3)	1.452 (3)

Bond lengths (Table 5) show that the dye does have the expected bond lengths for a polar molecule. The C_1-C_2 and C_3-C_4 bond lengths are both longer than the C_2-C_3 bond. This was expected when the ground state of a merocyanine resembles the charge separated versus the neutral resonance structure.

BOXIND was expected to be slightly less polar than BTHIND. This dye refined to a R value of 0.049 and Rw of 0.050. There were 1519 observed reflections greater than three times the standard deviation. This resulted in a goodness of fit equal to 1.39 for 218 parameters.

Carbon-carbon bond lengths showed BOXIND to be less polar than the BTHIND structure with disordered water. Bond distances are nearly equal throughout the chain with the C_1-C_2 bond slightly shorter.

The last noncrowded merocyanine determined by x-ray crystallography was BTHRHO. This structure was also determined by Bai (55). The dye was predicted to be the least polar of any of the previous dyes due to the very poor electron withdrawing/accepting potential of the rhodanine heterocycle. The dye was refined to a R value of 0.044 and Rw of 0.045. There were 1892 reflections greater than two and one half times the standard deviation. This resulted in a goodness of fit equal to 1.18 for 202 parameters.

The chain carbon bond distances confirm our prediction for the ground state of the dye. Bond distances show that BTHRHO resembles the nonpolar resonance structure. The C_1-C_2 and C_3-C_4 bonds show more double bonded character and C_2-C_3 shows more single bonded character.

We felt that the BTHIND structure could be biased due to the hydrogen bonding from the water molecules. This bonding would help stabilize the charge separated resonance and therefore perturb the chain carbon-carbon bond lengths. The dye was recrystallized from 100% ethanol which limited the availability of water to come in contact with the dye. Single crystals without water were obtained after growing for a year in a stoppered vial at room temperature.

The BTHIND dye without water refined to a R value of 0.047 and a Rw of 0.050. There were 2832 reflections greater than three times the standard deviation. This resulted in a goodness of fit equal to 1.38.

After the structure was solved we found the bond lengths to be nearly identical throughout the chromophore. The lengths still suggest that the molecule has more of the polar ground state character. This wasn't as large as when water was in the crystal lattice but still suggests more polar characteristics than the BOXIND dye.

Methyl Crowded Merocyanines

For the methyl crowded merocyanines, we first look at the structure of MEBTHRHO. This dye has two possible planar conformations discussed earlier. When the dye was formed it should be in a conformation where the carbonyl is anti to the methyl group. If this isn't enough to release steric interactions (ie. the methyl group is still crowded by the sulfur atom) then we would expect the molecule to twist out of the plane. The structure for MEBTHRHO refined to a R value of 0.046 and a Rw of 0.053. There were 4651 reflections greater than three times the standard deviation. This resulted in a goodness of fit of 1.72 for 212 parameters.

Figure 29 shows that the expected E conformation was seen in the crystal structure. The molecule does prefer this conformation over the Z conformation when observed in the solid state. Additional out of plane twisting was not seen (Table 6). The planarity of the dye was found to be comparable to BTHRHO.

The next type of methyl crowded dye we looked at was MEBTHIND which was refined to an R value of 0.59 and a Rw of 0.64. There were 1591 reflections observed greater than three times the standard deviation. This resulted in a goodness of fit equal to 1.39 for 218 parameters.

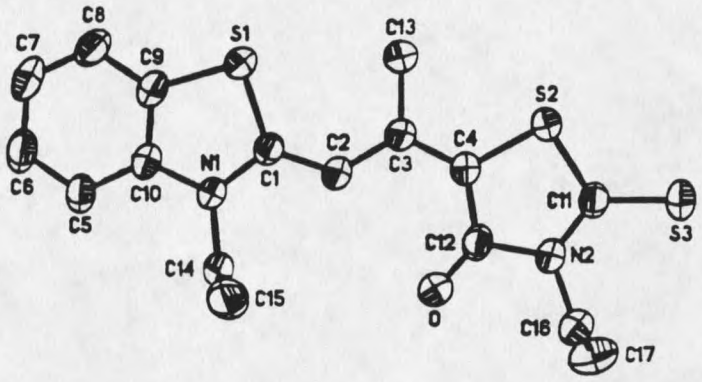

MEBTHRHO

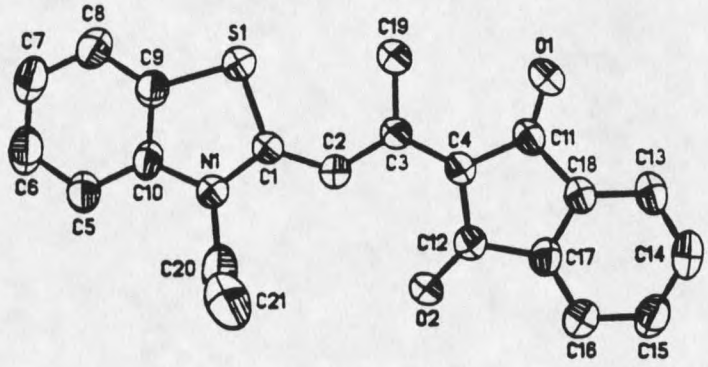

MEBTHIND

Figure 29. Thermal ellipsoid plots for methyl crowded merocyanines.

Both of the planar conformations for this merocyanine are equivalent because of the symmetry of the indandione heterocycle. The steric interactions should have been relieved by twisting. This wasn't observed. The molecule was as planar (if not more so) as the non crowded dye, BTHIND,

Table 6. Torsion angles (°) for merocyanines.

DYE	$N_1C_1C_2C_3$	$S_1C_1C_2C_3$	$C_1C_2C_3C_4$	$C_2C_3C_4C_{11}$	$C_3C_4C_{11}O_1$
BTHIND (H_2O)	174.4 (.4)	-7.1 (.7)	179.1 (.5)	178.6 (.5)	1.2 (.8)
BTHIND	173.0 (.2)	-9.1 (.3)	178.7 (.2)	178.4 (.2)	-2.7 (.3)
BTHRHO	179.4 (.3)	-1.3 (.5)	-179.9 (.3)	-179.9 (.3)	1.0 (.6)
		$O_1C_1C_2C_3$			$C_3C_4C_{11}O_2$
BOXIND	176.6 (.3)	-3.9 (.5)	-178.9 (.3)	179.0 (.3)	-0.5 (.5)
				$C_2C_3C_4C_{12}$	$C_3C_4C_{12}O_1$
MEBTHRHO	178.7 (.2)	-2.1 (.3)	178.3 (.2)	0.8 (.3)	1.2 (.3)
MEBTHIND	179.3 (.4)	-0.4 (.6)	179.5 (.3)	-179.6 (.3)	-0.2 (.6)

DYE	$C_1C_2C_3Me$	$MeC_3C_4C_{11}$
MEBTHRHO	-1.2 (.3)	-179.8 (.2)
MEBTHIND	-0.4 (.6)	0.3 (.5)

which can be seen from the torsion angle data. If there was crowding by the methyl group it had to be released in some other fashion. We discovered what was happening by looking at the bond distances (see Table 7).

Table 7. Bond lengths (Å) for selected merocyanines.

DYE	N_1-C_1	C_1-C_2	C_2-C_3	C_3-C_4	C_4-C_{11}
MEBTHRHO	1.374 (2)	1.383 (2)	1.412 (2)	1.389 (2)	1.447 (3)
MEBTHIND	1.370 (4)	1.387 (4)	1.389 (4)	1.411 (4)	1.464 (4)
BTHRHO	1.362 (4)	1.371 (5)	1.404 (5)	1.367 (5)	1.442 (5)
BTHIND	1.365 (3)	1.386 (3)	1.384 (3)	1.388 (3)	1.452 (3)

Bond distances showed that Brooker's deviation arguments still hold true. The more polar dye, MEBTHIND, has chain carbon bond lengths that resemble the charge separated resonance structure. What wasn't expected was that the bonds all lengthened. The C_3-C_4 bond distance increased the most when compared to BTHIND. The same type of lengthening was also observed for MEBTHRHO when compared to BTHRHO. The methyl crowded dyes are decreasing steric interactions by increasing bond lengths. This must involve a smaller energy change as opposed to twisting which impairs the conjugation of the chromophore.

Allopolar Dyes

Studies of allopolar dye systems have yet to be done. We haven't been able to grow a large enough crystal to solve by x-ray crystallography. Some ground work has been accomplished by looking at the structure of an "allopolar like" molecule. The compound used was 2-(3-ethyl-2-benzothiazolylidene)-1,3-diphenyl-1,3-propanedione (ABMF) which resembles a BAA allopolar dye. This structure was refined to a R value of 0.042 and Rw of 0.047. There were 2168 observed reflections greater than three times the standard deviation. This resulted in a goodness of fit equal to 1.87 for 254 parameters.

Table 8. Selected torsion angles (°) for BAA allopolar dye.

$S_1C_1C_2C_3$	$N_1C_1C_2C_3$	$N_1C_1C_2C_5$	$C_1C_2C_3O_1$	$C_1C_2C_5O_2$	$C_1C_2C_3C_4$
-7.1 (.3)	170.7 (.2)	-17.9 (.4)	-1.4 (.4)	-61.4 (.4)	177.6 (.2)

The chromophore doesn't have a large contribution from the phenyl rings. The carbonyl groups are more conjugated with the benzothiazole ring because the resonance is the same as the dipolar amidic chromophore in merocyanines but with fewer carbon atoms. One of the carbonyls was found in the plane of the benzothiazole ring (see Table 8). The other carbonyl had a torsion angle sixty degrees from the plane of the benzothiazole ring. A reduced thermal ellipsoid plot for this molecule is shown in Figure 30.

The molecule shows that it would prefer the planar conformation similar to a merocyanine. The out of plane carbonyl does show deviation from the expected perpendicular conformation. We believe this was due to the crowding from the phenyl group attached to the second carbonyl group. True allopolar dyes are two carbons longer in the meropolar conformation and also have an additional carbon before the out of plane carbonyl. Since the allopolar dyes have less steric

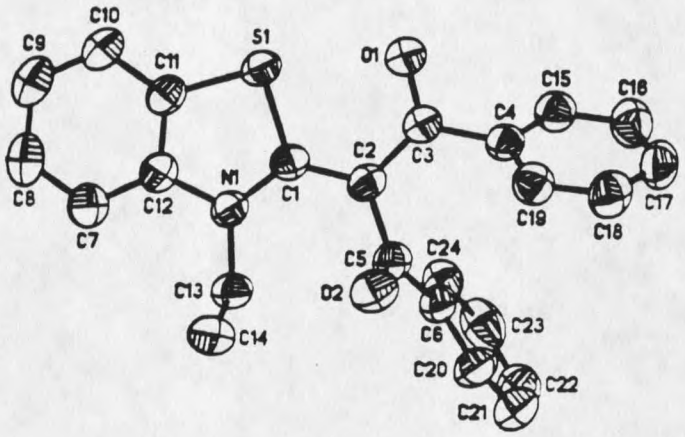

Figure 30. Thermal ellipsoid plot for BAA dye (ABMF).

interactions than this compound, we believe the out of plane ring system for the allopolar dye could still be perpendicular to the plane of the chromophore.

Basicity of Dye Intermediates

Calculations by Bowler suggest that for 1-(3-ethyl-2-benzothiazolinylidene)-2-propanone would be more basic when the carbonyl group was in the syn versus the anti conformation with respect to the sulfur atom. We studied this by forming the intermediate using 3-ethyl-2-methyl-benzothiazolium iodide and acetyl chloride in chloroform and triethylamine. We refined the structure to a R value of 0.045 and a Rw of 0.050.

There were 3645 reflections greater than three times the standard deviation. This resulted in a goodness of fit equal to 1.25 for 179 parameters.

The intermediate was found to be in the syn conformation, but there was a twist. The intermediate was so basic that it abstracted a proton, chlorine atom, and adventitious water from the reaction mixture (see Figure 31). The crystal structure shows that the propanone intermediate was protonated on the carbonyl oxygen. This proton was hydrogen bonded to a water molecule which in turn was hydrogen bonded to chlorine and another water molecule.

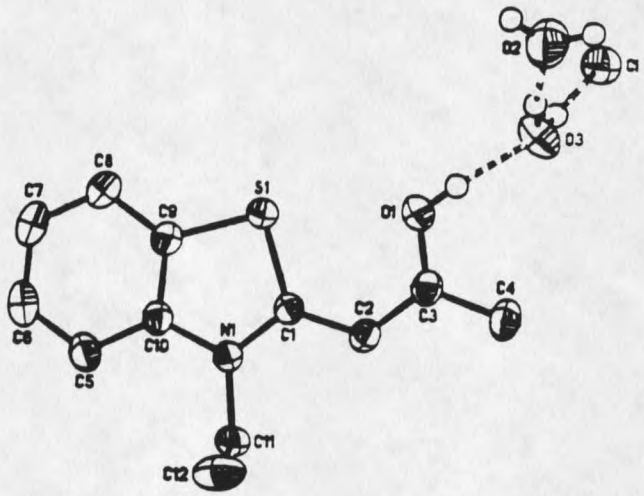

Figure 31. Thermal ellipsoid plot of basic intermediate.

NMR SPECTROSCOPY

Nuclear Magnetic Resonance (NMR) spectroscopy of cyanines has been extremely limited in the past (56-60). This was because these dye systems tend to be very insoluble in common NMR solvent systems. For example, in chloroform the solubility for BTHRHO is on the order of 10^{-6} mols/L. For this reason, early structural assignment work was confined to the proton spectra. With the advent of Fourier transform instruments, the carbon spectra of some dyes became available (61-64). This allowed more structural interpretation but assignments could only be based on chemical shift arguments. However, in the last ten years, better magnets and a larger variety of probes have made instruments more powerful and very sensitive so that NMR experiments are easier and more reliable. This along with new sophisticated pulsing techniques, allows extensive investigation of these dye systems. We plan to rigorously assign a model system using these techniques. The model will then be expanded to the other merocyanine dyes in our study.

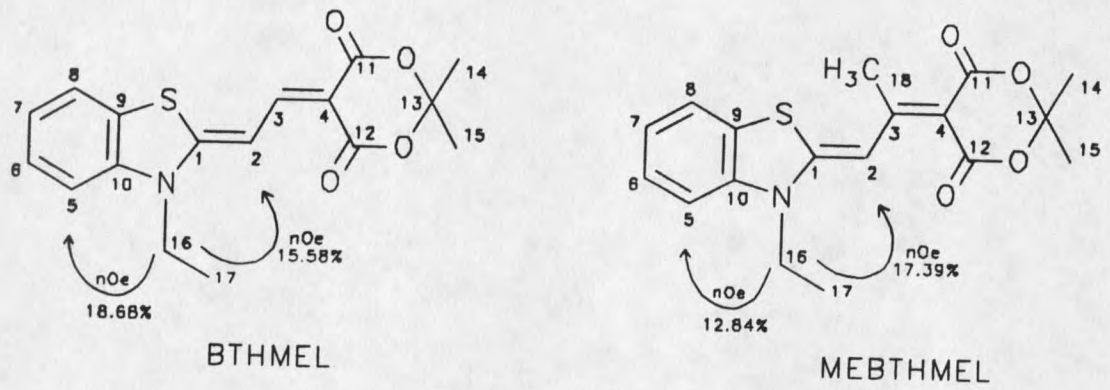

Figure 32. NMR model dyes.

2,2-Dimethyl-5-[2-(3-ethyl-2-benzothiazolinylidene)-ethylidene]-1,3-dioxane-4,6-dione (BTHMEL) and 2,2-dimethyl-5-[2-(3-ethyl-2-benzothiazolinylidene)-1-methylethylidene]-1,3-dioxane-4,6-dione (MEBTHMEL) were chosen as the model dyes for our NMR study (shown in Figure 32). These two merocyanine dyes have many structural similarities, including identical electron donating/withdrawing ring groups and the same methine carbon chain length. These dyes are also more soluble than the merocyanines discussed previously. This makes them more desirable for NMR studies because less time is required per experiment when more compound is dissolved.

The reason we want more compound in solution is because fewer scans are needed for a spectrum. If one wanted to double the signal to noise then one would have to take four times the number of scans. This is because the signal-to-noise ratio increases by the square root of the number of times the signal increases (65). As an example, to double the signal to noise of a two hour experiment, it would take eight hours.

Once these dyes (BTHMEL and MEBTHMEL) have been rigorously assigned by a series of NMR experiments we can use this information to assign chemical shifts to the less soluble merocyanines in our study. This should be possible because of the similarities between BTHMEL and the non crowded merocyanines in our discussion while MEBTHMEL would resemble the chain methyl merocyanines. It would also be the first rigorous assignment done on these types of compounds.

The easiest assignment of the two dyes in the proton NMR are the ethyl and methyl groups. The proton and COSY (correlation spectroscopy) spectra are shown in Figure 33 for BTHMEL and Figure 34 for MEBTHMEL. The COSY experiment shows proton-proton coupling by observing a proton while pulsing the whole proton region (66-67). The experiment is done for each chemical shift and then all of them are stacked together. The resulting contour map is a slice through all of these

Figure 33. Proton and COSY spectra of BTHMEL.

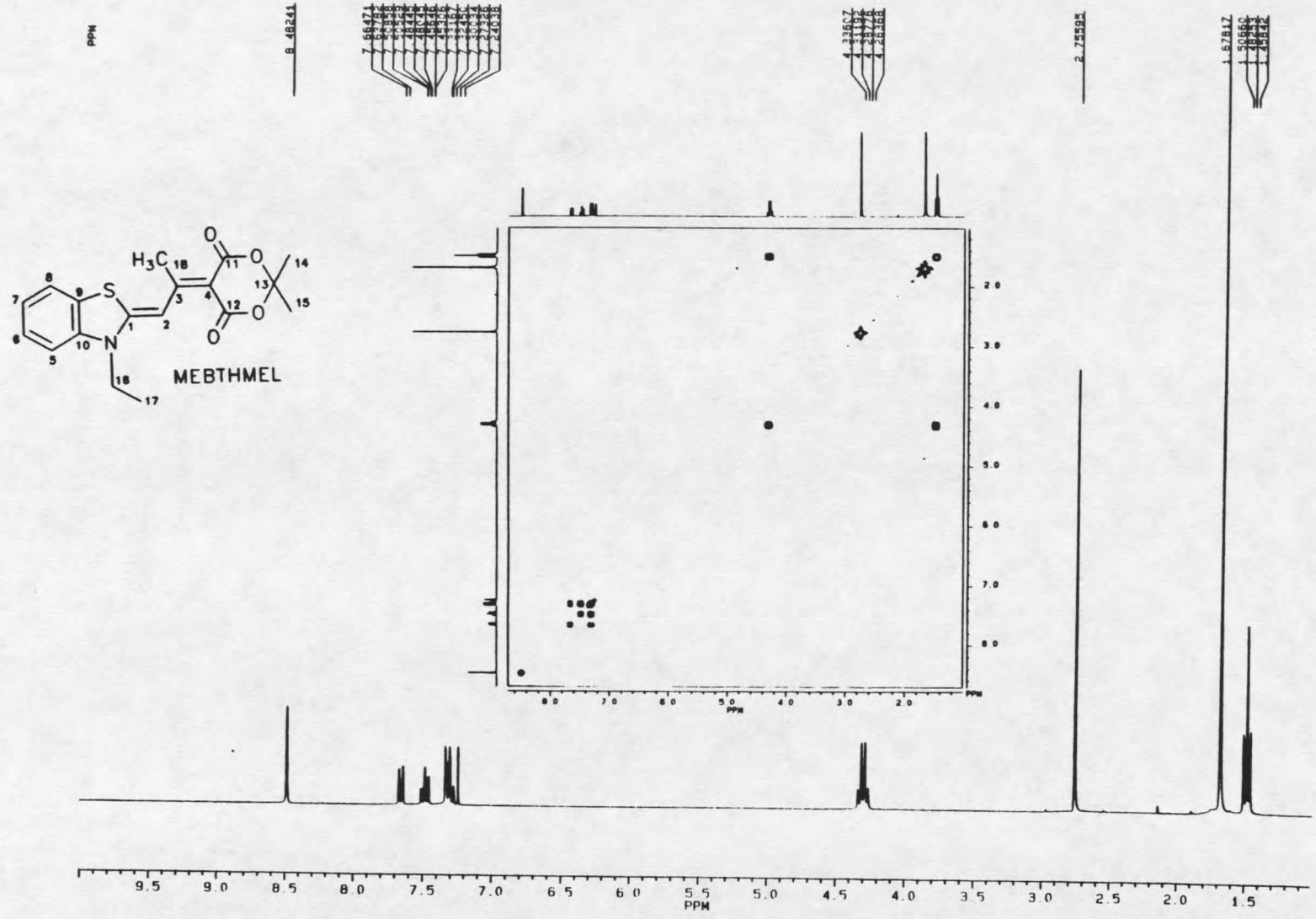

Figure 34. Proton and COSY spectra of MEBTHMEL.

plots (above most of the noise spikes). If there is coupling, it shows up in this two dimensional contour map. Proton connections are assigned by finding a signal in the spectrum (off of the diagonal) and tracing vertically to one proton, and horizontally to the other. The COSY is outlined in a box in both of the proton spectra.

In the proton spectra, the strong singlet at approximately δ 1.68 represents the two terminal methyl group protons on the lactone ring (C14 and C15). The triplet around δ 1.47 is due to the methyl protons (C17) of the ethyl group in both spectra. The quartets at δ 4.30 and δ 4.26 are methylene protons of the ethyl group (C16) pulled down field by the heterocyclic ring nitrogen for BTHMEL and MEBTHMEL respectively. In the case of MEBTHMEL the chain methyl (C18) proton signal is a singlet at δ 2.76 as a result of the methyl group on the olefinic carbon (C3). There are so many overlapping proton signals in the aromatic region of the spectrum (δ 5-9) that special techniques are needed to distinguish them.

The first protons we want to assign in the aromatic region are the chain protons on C2 and C3. These should be easy to identify because in the BTHMEL dye they would both be doublets and in the MEBTHMEL the C2 proton would be a singlet. This is indeed the case. BTHMEL chain protons are doublets

at δ 7.41 and δ 8.28 with coupling constants of 13.7 Hz. This is typical of trans olefinic coupling (full range 12-18 Hz, typical range 14-17 Hz) and cannot be confused with the benzothiazole ring protons because the coupling is too large (full range 0-12 Hz, typical range 7-10 Hz) (68). The C2 proton of MEBTHMEL is a singlet at δ 8.48.

At this point one would be tempted to assign the C2 proton on BTHMEL. The logic for this is that the methyl group replaces one proton allowing the other to collapse into a singlet. Since the two molecules are nearly identical in conformation and electronic structure, the assignment for the proton would be δ 8.26. Two subsequent experiments have shown that is not the case.

The first of these was the nuclear Overhauser effect (nOe) experiment (69-70). An nOe experiment indirectly measures dipolar coupling (or through space direct magnetic coupling) between two nuclei, in this case two protons, if close enough to one another. An nOe can be measured by saturating one signal and observing any differences at another signal. This is thought to occur while the system tries to regain (or stay at) equilibrium and can increase or decrease the intensity of the observed signal.

An nOe is reported as the intensity of a signal (i) observed while another is being saturated (s) minus the observed signal (had there been no perturbations) divided by the observed signal (see the Equation 2). This number is multiplied by 100 to make the figure a percentage. From this equation, one would expect that an nOe could be infinite. However, Equation 2 is used as the conventional way of reporting nOe data.

$$\eta_i(s) = \frac{(I - I_o)}{I_o} \qquad \% \text{ nOe} = \eta_i(s) \times 100$$

Equation 2.

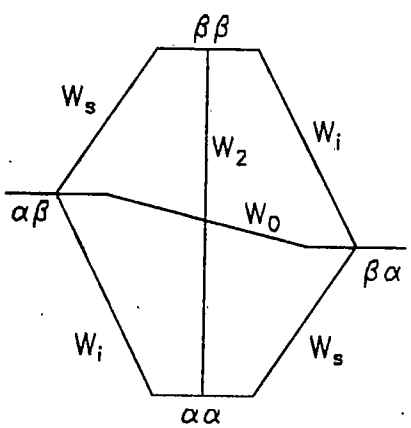

$$\eta_i(s) = \frac{W_2 - W_0}{2W_1 + W_2 + W_0}$$

Equation 3.

$$\eta_i(s) = \frac{(12 - 2)\tau_c/r^6}{(6 + 12 + 2)\tau_c/r^6} = \frac{1}{2}$$

Equation 4.

Figure 35. Transition states for a dipolar coupled system.

Theoretically, the largest positive nOe that can be observed for homonuclear dipolar coupling is 50 % (71). This can be shown by looking at the different transitions the

system uses to remain at equilibrium (Figure 35). Equation 3 relates these rates to an nOe . This assumes a two spin system that relaxes exclusively via dipolar coupling. W_2 and W_0 are both cross relaxation rates. W_1 is the normal relaxation rate for an observed transition. If extreme narrowing is assumed the rates can be expressed by Equation 4. The derivation of this expression is shown by Chandrakumar (72). Similar arguments were discussed by Freeman (73). Literature values can range from 2 to 35% but are typically 5-20%.

The type of experiment used in this study was the difference nOe experiment. Examples of these are seen in Figure 36 for BTHMEL and Figure 37 for MEBTHMEL. The methylene protons (C16) were thought to be close to the C2 proton and should generate a nOe. To perform the nOe experiment we first acquired a normal proton spectrum using a reference pulse away from any signal. A second spectrum was then taken with a pulse saturating the methylene proton signal of the ethyl group. These two spectra were then subtracted from one another. The resulting spectrum shows the observed nOe. These experiments were unoptimized and the values may vary.

The percentage was found by comparing the area of the methylene signal with the nOe signal. The methylene signal should have an area that is equal to two protons. This is

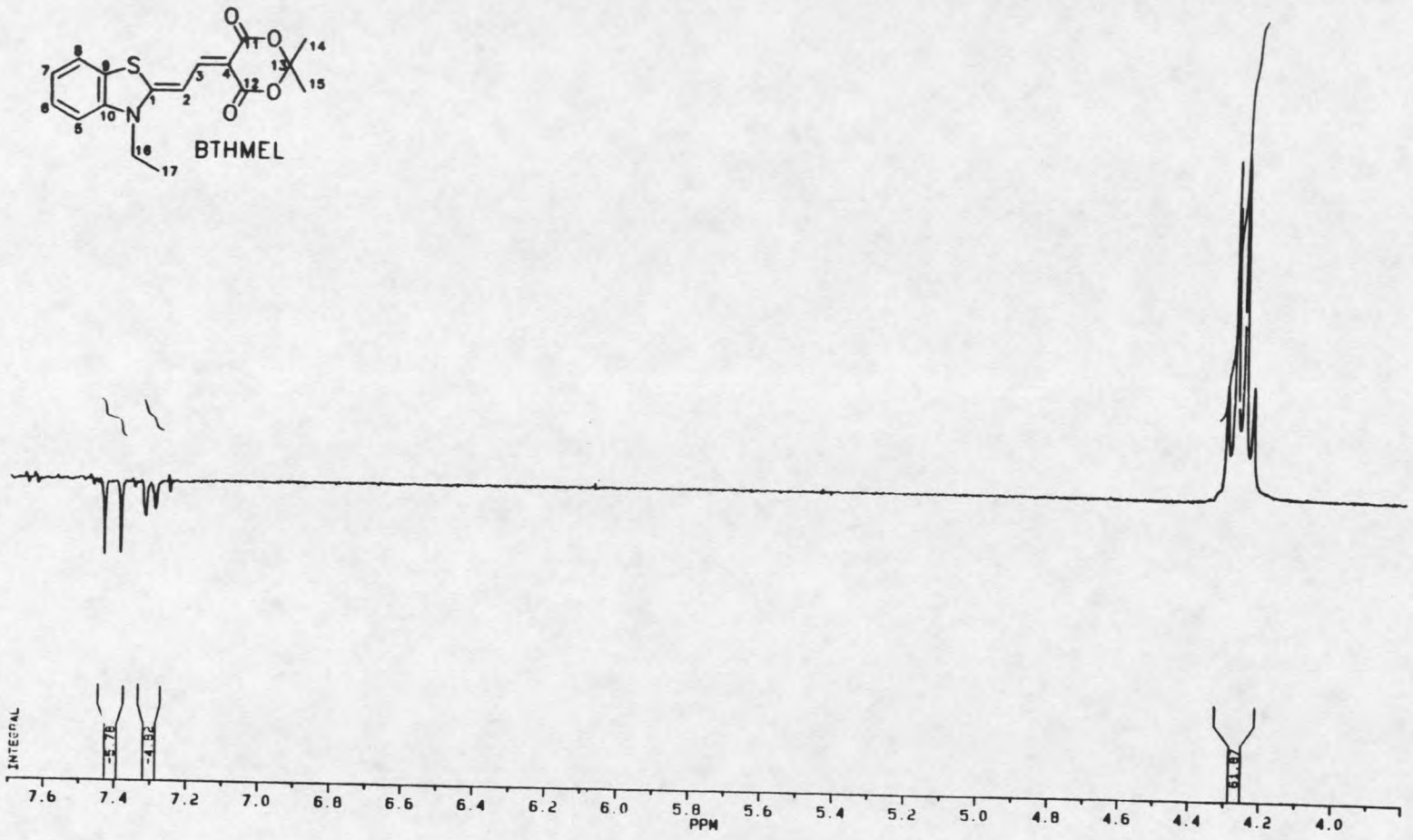

Figure 36. nOe spectrum of BTHMEL.

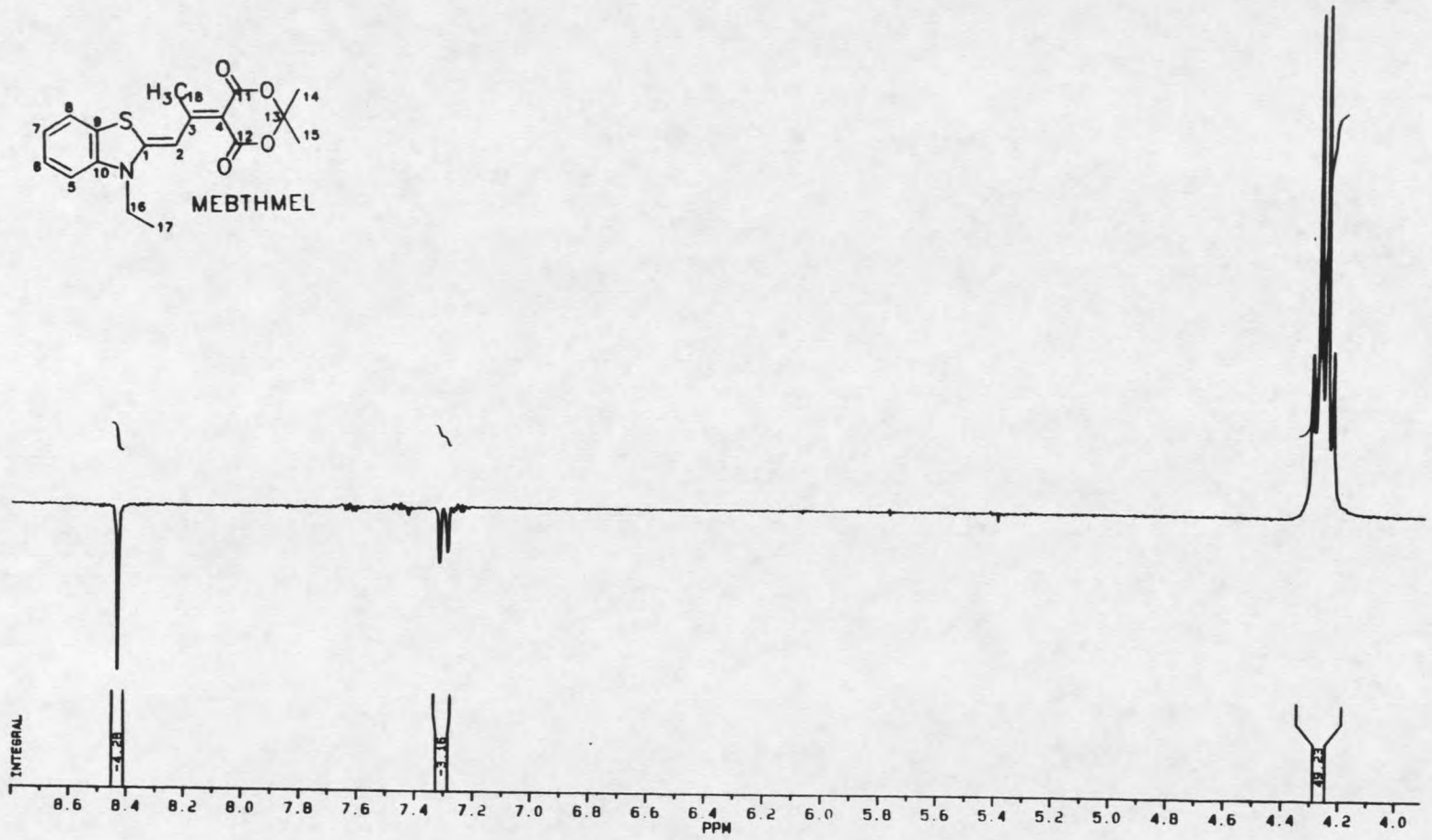

Figure 37. nOe spectrum of MEBTHMEL.

true because the saturating pulse should allow no signal to be observed for the methylene protons. Subtracting the two spectra should cause no change in the intensity of this signal. Since the observed nOe is due to one proton, we divide the area of the nOe by the area of the methylene proton signal (which represents two protons) and then multiply by two. This makes the number of protons equivalent. The result is then multiplied by 100 to give a percentage. In the case of MEBTHMEL the δ 8.48 singlet (C2) had an nOe of 17.4%. BTHMEL showed an nOe of 15.58% for the proton at δ 7.41 and not δ 8.28! Therefore the signal at δ 7.41 is due to the C2 proton of BTHMEL.

Another proof can be shown by a heteronuclear shift correlated 2-D NMR experiment (HETCORR or XHCORR). This experiment gives correlations from protons to their parent carbon atoms (74-75). Exact chemical shift assignments were then given using the proton spectra shown earlier and the carbon spectra shown in Figures 38 and 39. A XHCORR experiment is accomplished by pulsing the proton region and observing the coupling (J_{CH}) in the carbon spectrum. This is done using a dual probe where the carbon coils are nearer to the sample than the proton coils.

Quaternary carbons will not have this coupling so the experiment's sensitivity can be increased by using a spectral

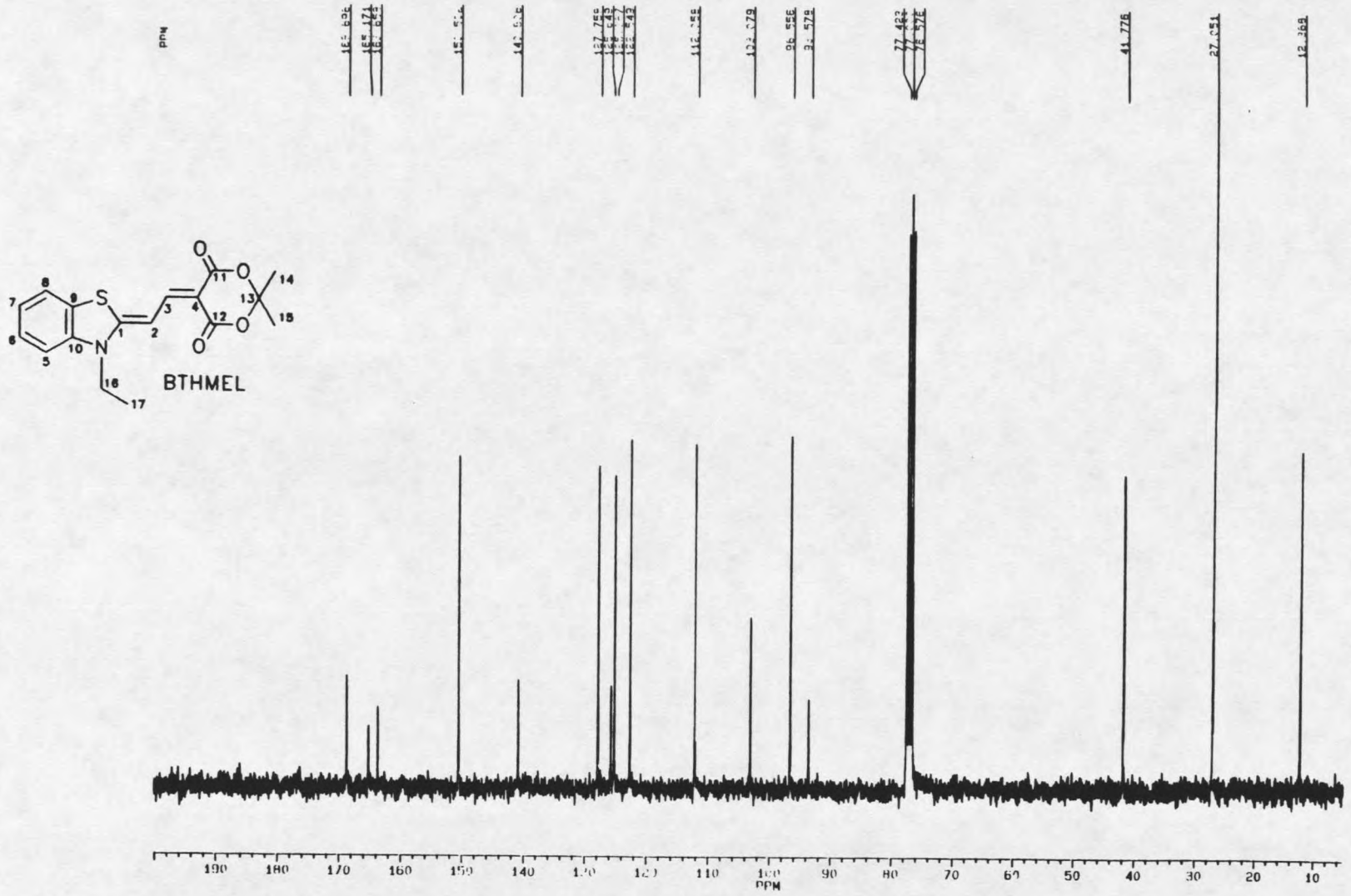

Figure 38. Carbon spectrum of BTHMEL.

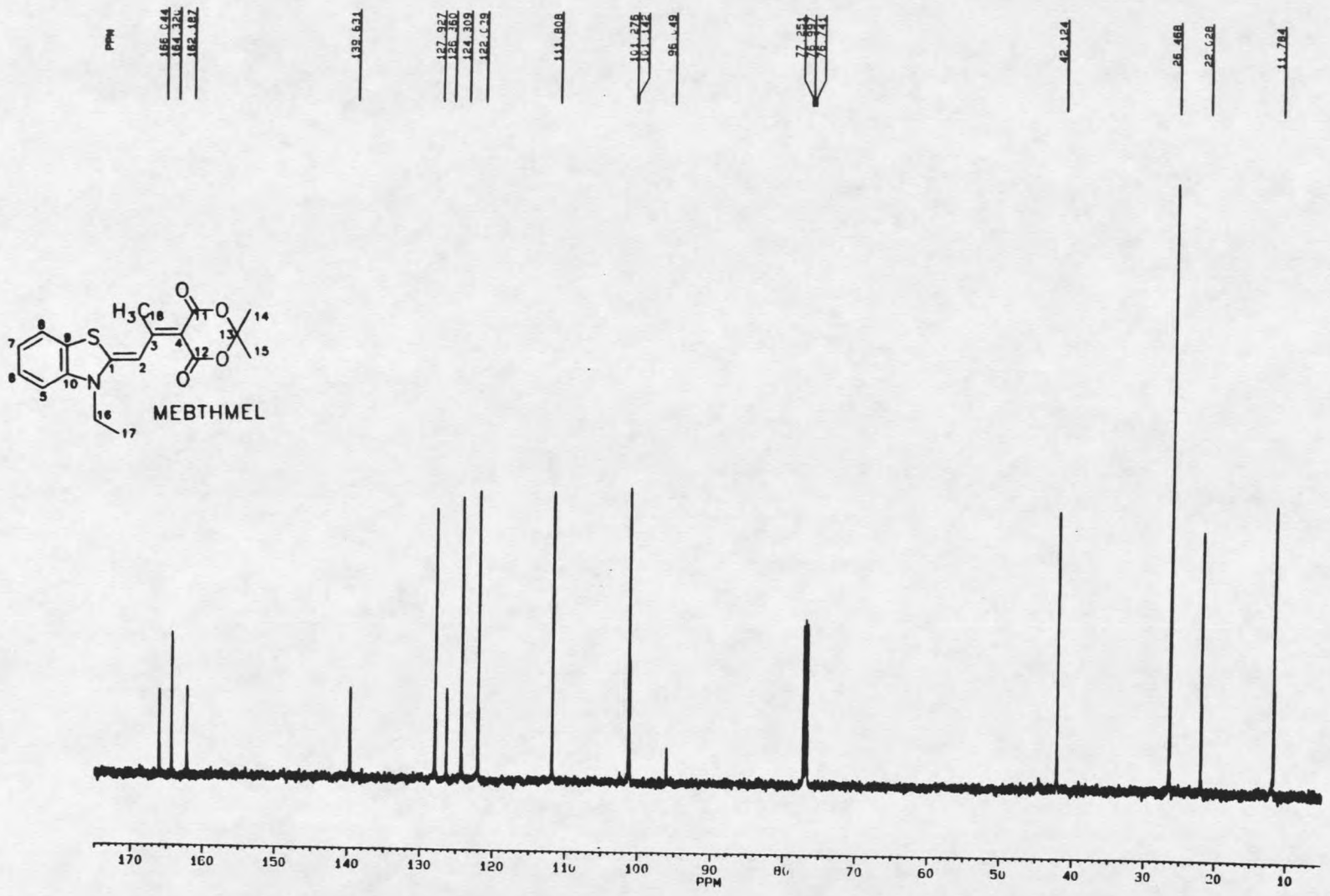

Figure 39. Carbon spectrum of MEBTHMEL.

width that includes only proton bearing carbons in the carbon spectrum when acquiring data. These correlations are shown in Figures 40 (BTHMEL) and 41 (MEBTHMEL). Figure 40 shows only the expanded region for the aromatic region of BTHMEL. This is done for clarity. The upfield signals that are shown for MEBTHMEL have nearly identical chemical shifts for BTHMEL.

The aromatic region of MEBTHMEL shown in (Figure 41) shows the proton responsible for the singlet at δ 8.48 is attached to a carbon at δ 101.0. This signal is assigned to C2 because the signal at δ 8.48 is from the C2 proton discussed earlier. In the BTHMEL spectrum the proton at δ 7.41 can be traced horizontally to a signal. This can then be traced vertically to give a carbon assignment of δ 96.5. Similarly, the proton at δ 8.28 was traced to the carbon at δ 150.5.

Since the C2 of MEBTHMEL has been shown to be at δ 101.0 we will tentatively assign δ 96.5 of BTHMEL to be C2. If this were true, C3 of the BTHMEL molecule has to be at δ 150.5. This can be concluded because of the coupling, electronic, and structural arguments made earlier. There is no evidence that a carbon signal will shift so dramatically in such similar structures (ie. from 100 to 150 ppm). In fact the chemical shifts in carbon spectra on similar compounds vary only a couple of ppm (76).

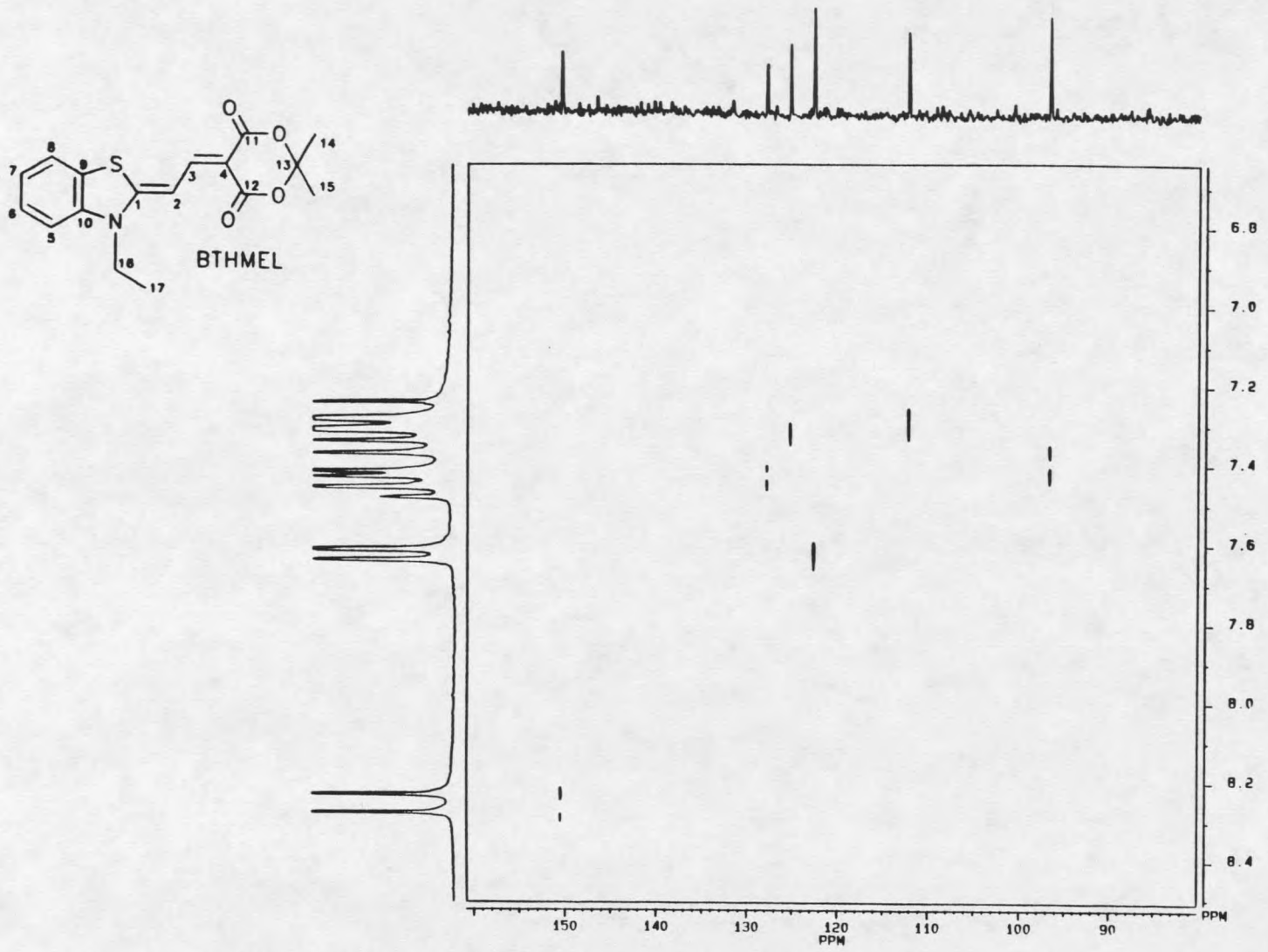

Figure 40. Aromatic region of a XHCORR spectrum of BTHMEL.

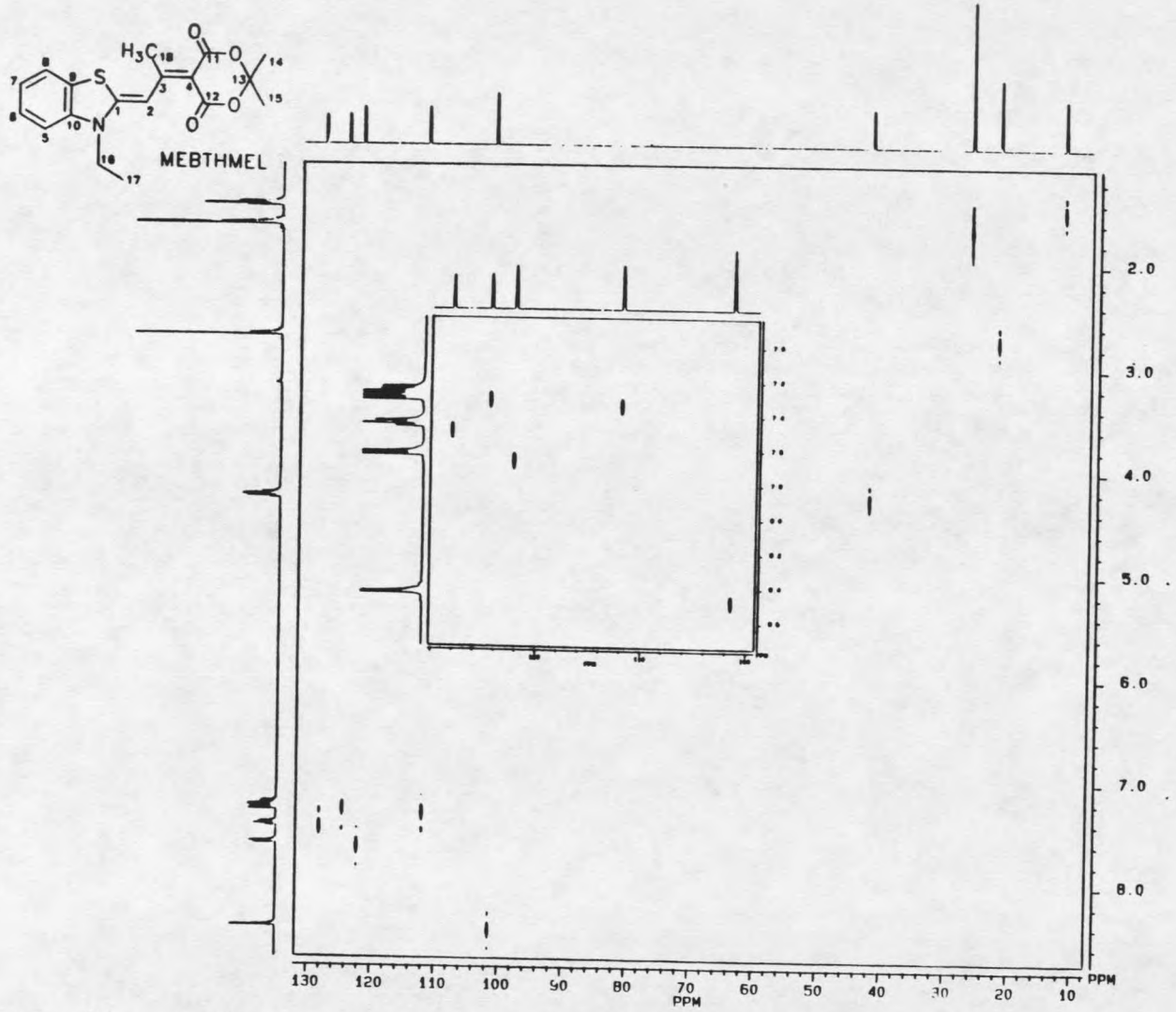

Figure 41. XHCORR spectrum of MEBTHMEL.

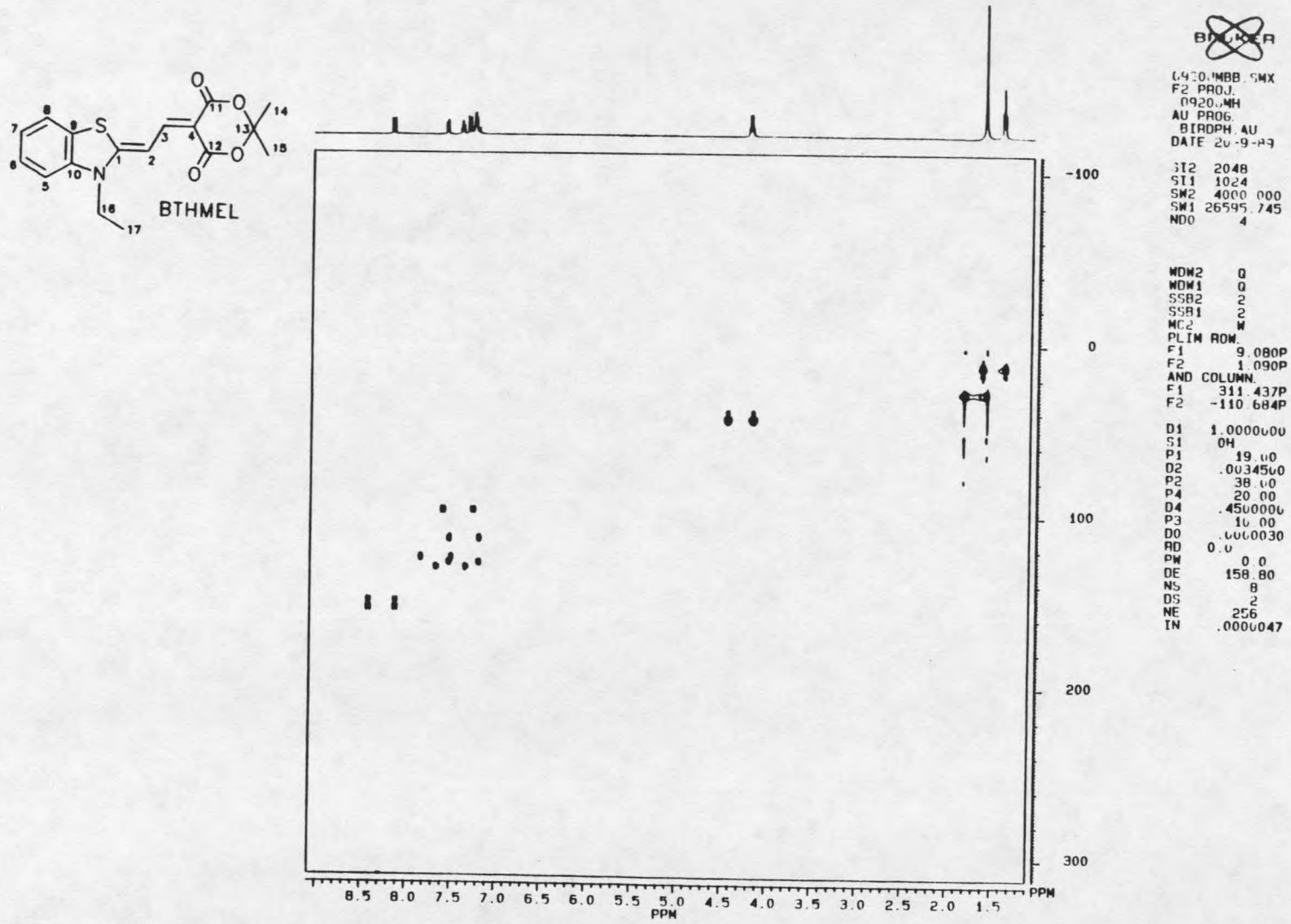

Figure 42. BIRDPH spectrum of BTHMEL.

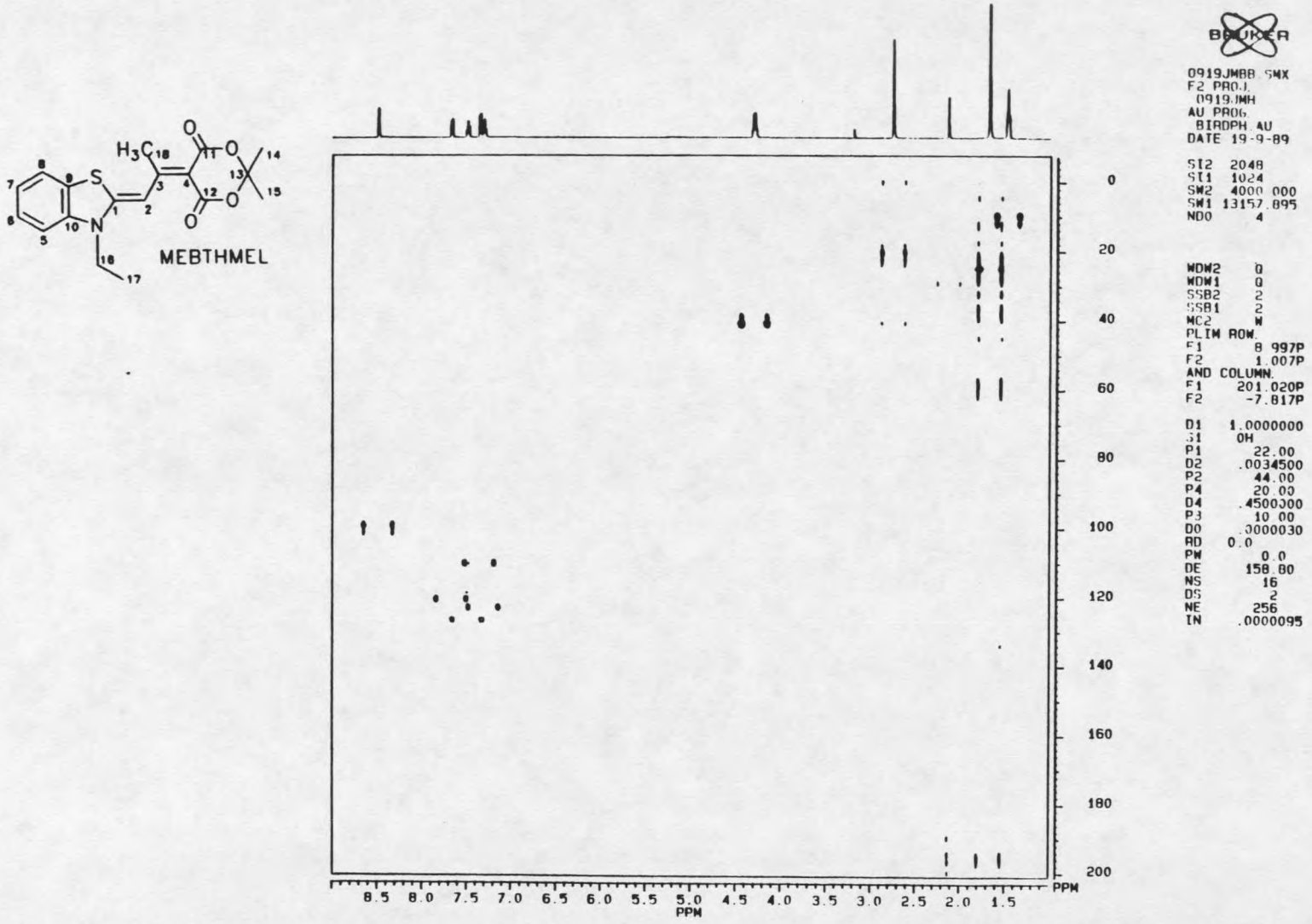

Figure 43. BIRDPH spectrum of MEBTHMEL.

Another experiment that gives the same connectivity information is the BIRDPH (77). This technique is three to four times more sensitive because the proton coils are now inside the carbon coils in an inverse probe. Interpretation of the data is nearly the same as the XHCORR experiment. The only difference is that the carbon atoms are pulsed and coupling (J_{CH}) is measured through the proton atoms. This results in doublets due to the two phases of the ^{13}C spin states and can be seen in Figures 42 for BTHMEL and 43 for MEBTHMEL.

When the BIRDPH, nOe, and XHCORR experiments are combined there can be no doubt that the assignments for C2 and C3 are correct. Since this is true, why does the proton on C2 shift from δ 7.41 in the BTHMEL dye to δ 8.48 in the MEBTHMEL dye? This can be argued by anisotropic shielding from the C12 carbonyl's oxygen electrons.

Bond distances when a methyl group is incorporated into the dye are longer than the non-crowded dyes. This has been shown earlier in the solid state (by crystallography of similar compounds) and is also thought to occur in solution. We believe this is true because the wavelength and ε values are nearly identical for the two dyes. These values are shown in Table 9. If this is true then we can argue that when there is no chain methyl group, the oxygen electrons from the

Table 9. UV/VIS data for selected merocyanines.

DYE	ABSORPTION OF MEROCYANINES	
	$\lambda_{max.}$ (nm)	ε values
BTHRHO	525	8.77×10^4
BOXIND	468	1.36×10^5
BTHMEL	456	1.67×10^4
BTHIND	504	1.27×10^5
BTHTBA	495	1.20×10^5
MEBTHRHO	530	1.00×10^5
MEBTHMEL	454	7.15×10^4
MEBTHIND	496	1.40×10^5
MEBTHTBA	492	3.29×10^4

carbonyl (C12) can shield the proton at C2. This causes the signal to be further upfield. When the methyl group is added to the C3 carbon this causes the chain carbons to lengthen their bonds and therefore move the shielding oxygen away from the proton at C2. Since it is no longer shielded (or not shielded as highly), the relatively unperturbed chemical shift is observed.

Another more common type of shielding was considered but rejected. This was shielding from the cone of anisotropy above the plane of the carbonyl. If the dye was twisted in solution, this type of shielding might occur. When looking

at Van der Waals models the proton on C2 doesn't appear to be in this region at any time for either of the dyes. This supports a nearly planar solution conformation postulated earlier.

Assigning the benzothiazole ring leads to another problem. We now need to assign the ring atoms. The assignment can be made if we can determine which carbon or proton is nearer the nitrogen or sulfur atom.

For MEBTHMEL the proton and COSY spectra were used to show the connectivity of the protons around the ring with respect to each other. That way the doublet from C2 in the BTHMEL dye is avoided and the spectrum simplified. Figure 44 shows the expanded proton and COSY spectra for MEBTHMEL. The doublet at δ 7.65 is coupled to the triplet at δ 7.30. This can be determined by using the COSY spectra. Find the signal corresponding to δ 7.65 and go horizontally until another signal is found. From this signal trace a line vertically to the proton spectra to see the corresponding signal. This is the proton at δ 7.30. Coupling constants can also be used however broadening of the signals by long range coupling makes this unreliable. Further study shows that the signal at δ 7.30 is coupled to δ 7.65 and δ 7.48. δ 7.48 is coupled to δ 7.30 and δ 7.32. The signal at δ 7.32 is only coupled to δ 7.48.

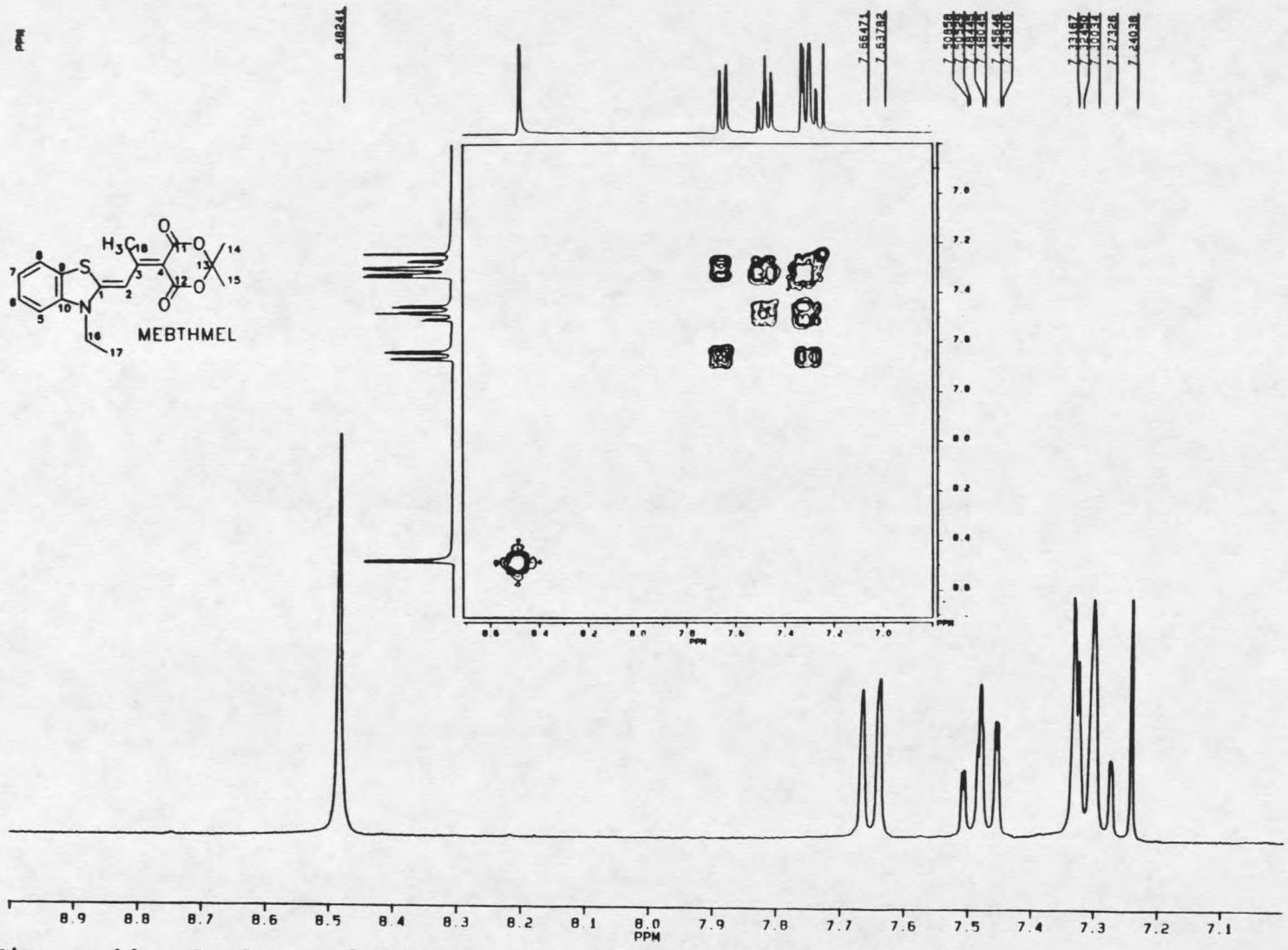

Figure 44. Proton and COSY spectra of MEBTHMEL showing the aromatic region.

We now know how the protons are connected in MEBTHMEL but have not determined how they are positioned on the benzothiazole ring. This was determined by an nOe experiment. The methylene protons of the ethyl group on nitrogen were saturated and a nOe (12.8%, shown previously in Figure 37) was observed for the proton at δ 7.32. This tells us that the proton on C5 has to be at δ 7.32. Combined with previous assignments the proton assignment is as follows; C6 is at δ 7.48, C7 is at δ 7.30, and C8 is at δ 7.65. BTHMEL was assigned in the same manner and the chemical shifts are comparable.

We assigned carbon atoms for MEBTHMEL using the XHCORR and BIRDPH data shown previously in Figures 41 and 43 respectively. The C5 carbon is at δ 111.8, C6 at δ 127.9, C7 at δ 124.3, and C8 at δ 122.0. These assignments were made by tracing horizontally from a proton until a signal is found (XHCORR). A trace is then made vertically to find the carbon position. The BIRDPH proton chemical shift is in the center of the doublet.

The final chemical shifts that need to be assigned for BTHMEL are the seven quaternary carbons C1, C4, C9, C10, C11, C12, and C13. In the case of MEBTHMEL, C3 is also a quaternary carbon. These can be assigned by two different experiments that give information for long range J_{CH} coupling

observed from β,δ, and λ carbon atoms. Direct proton coupling to α carbons is suppressed so that the long range coupling can be resolved. This coupling is on the order of 10 Hz. Since the coupling is similar for each of these carbons, observed signals can be stronger for remote carbon atoms. The experiments used are the COLOC (78-79) and long range inverse (INVDR2LP) experiments (80). The first to be considered is the COLOC.

This experiment correlates protons to β, δ, and γ carbons depending on optimized coupling constants determined by the pulse sequence. The α (or the carbon which the proton is connected) coupling is suppressed. Since the coupling constants vary the experiment was run at different optimized conditions to be able to assign each carbon. BTHMEL is the only COLOC experiment that will be shown (Figure 45). It details the aromatic region to make interpretation easier. The COLOC experiment is interpreted the same as the XHCORR earlier. The easiest quaternary carbon to determine is C13 (not shown in the expanded spectrum). It is strongly coupled to the protons on C14 and C15. The COLOC experiment showed correlations for the protons at δ 1.69 coupled to the carbons at δ 27.1 and δ 103.1. XHCORR, BIRDPH, GATE, and INVGATE experiments combined have shown that the carbon signal at

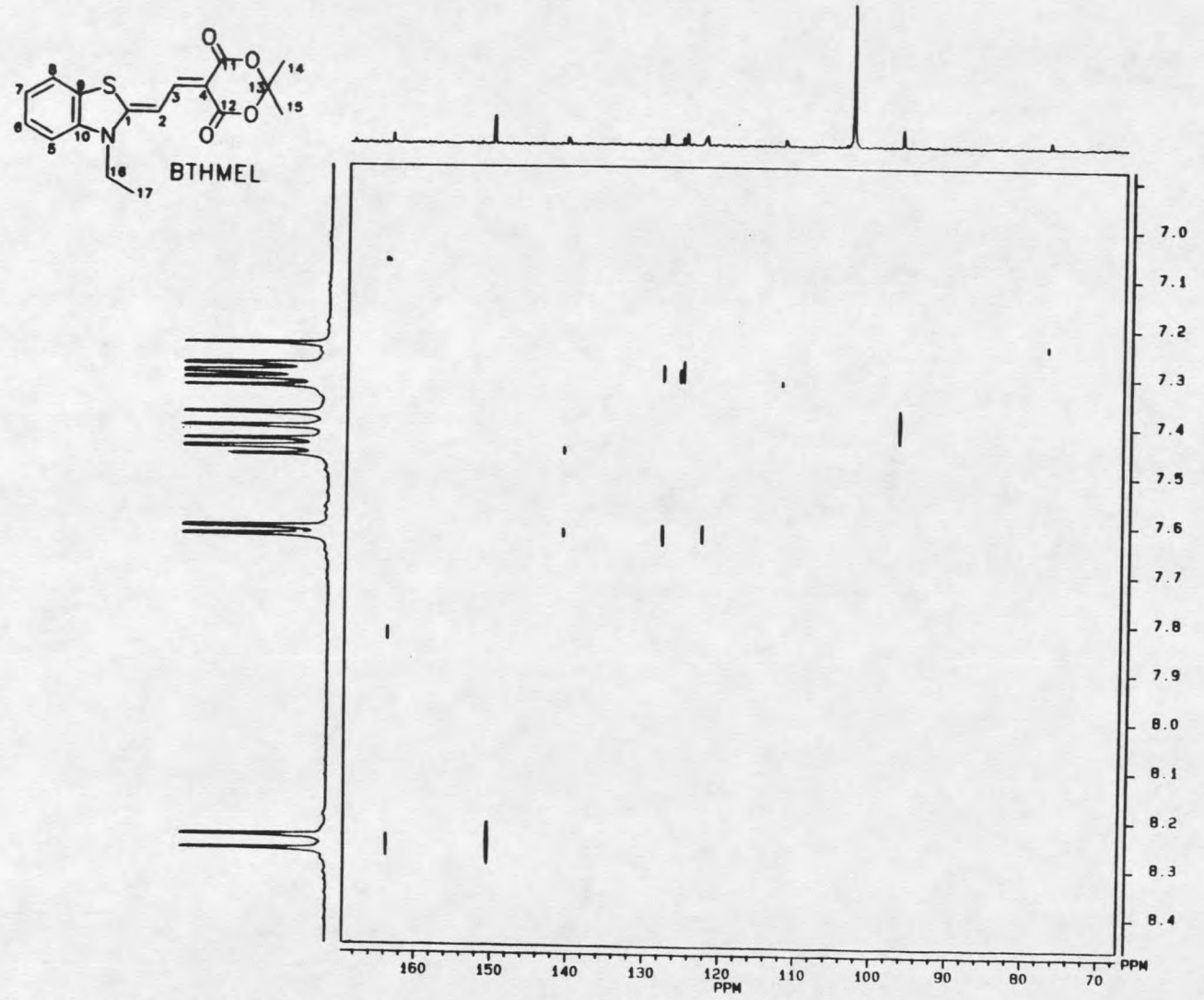

0522JMXH.SMX
F1 PROJ.
0522JMH.001
F2 PROJ.
INTERNAL
AU PROG.
COLOC AU
DATE 22-5-89

SI2 4096
SI1 1024
SW2 21739.130
SW1 1850.481
NDO 2

WDW2 0
WDW1 0
SSB2 4
SSB1 2
MC2 M
PLIM ROW.
F1 169.528P
F2 67.313P
AND COLUMN.
F1 8.466P
F2 6.876P

D1 2.0000000
S1 0H
P1 11.50
D2 .0500000
D0 .0000030
P2 23.00
P4 14.00
P3 7.00
D3 .0250000
S2 20H
RD 0.0
PW 0.0
DE 31.30
NS 24
DS 2
P9 123.00
NE 256
IN .0001351

Figure 45. COLOC spectrum of BTHMEL showing the aromatic region.

δ 27.1 is due to C14 and C15. C13 has to then be at δ 103.1. The chemical shift down field is due to the two lactone ring oxygen bonds.

The proton at C5 shows correlations to δ 127.8, 125.0, and 125.6. Earlier we showed that δ 127.8 is carbon C6 and δ 125.0 is carbon C7. From the GATE experiment the carbon at δ 125.6 is quaternary and the above evidence leads us to believe it is due to the C10 carbon. The proton at δ 7.63 correlates to the carbon signals at δ 140.8, 127.8, and 122.5. Again, XHCORR and BIRDPH were used to show that δ 127.8 is from C6 and δ 122.5 is from C8 itself. The δ 140.8 correlation should to be due to C9. C11 and C12 are expected to be nearly identical due to the structure of the molecules. These carbonyl signals in the BTHMEL dye are at δ 167.0 and δ 165.0 and cannot be rigorously assigned. MEBTHMEL signals (C11 and C12) are both at δ 164.3.

C4 was assigned for BTHMEL by evaluating the correlations generated by the proton on C3. These signals are at δ 163.7 and δ 150.5. C3 was already shown to be at δ 150.5 and C2 was earlier assigned at δ 96.5 so δ 163 should be due to C4. This leaves C1. It could not be determined experimentally by the COLOC experiment, however by the process of elimination this carbon signal is tentatively assigned to δ 93.6.

The inverse long range experiments were done to support the data given by the COLOC. This experiment is more sensitive and has the advantage of showing α carbon coupling (the carbon connected to the proton observed) as a doublet (the same as a BIRDPH) when not totally suppressed. Long range couplings are represented as singlets. Interpretation is still the same as the other two dimensional experiments. Two major benefits of this experiment are the substantial decrease in the time needed per experiment (1/5 to 1/6 the time) and more complete information is observed.

The first correlation that was considered for MEBTHMEL was the coupling shown for the proton at δ 8.48. This proton has coupling from it's connected carbon atom (the doublet at δ 101.3) and four other carbon atoms. Three of these long range couplings are shown in Figure 46. In the region shown, there are two weak couplings to δ 162.2 and δ 166.0 and a stronger coupling to δ 96.0. This seems to support the XHCORR data discussed previously when we tentatively assigned C1 to ~δ 96.0 and C4 to ~δ 162.2. The shifts at δ 166.0 and δ 22.0 (not shown in this figure) are due to C3 and C18 respectively. Similar assignments are made from the expanded BTHMEL spectrum shown in Figure 47.

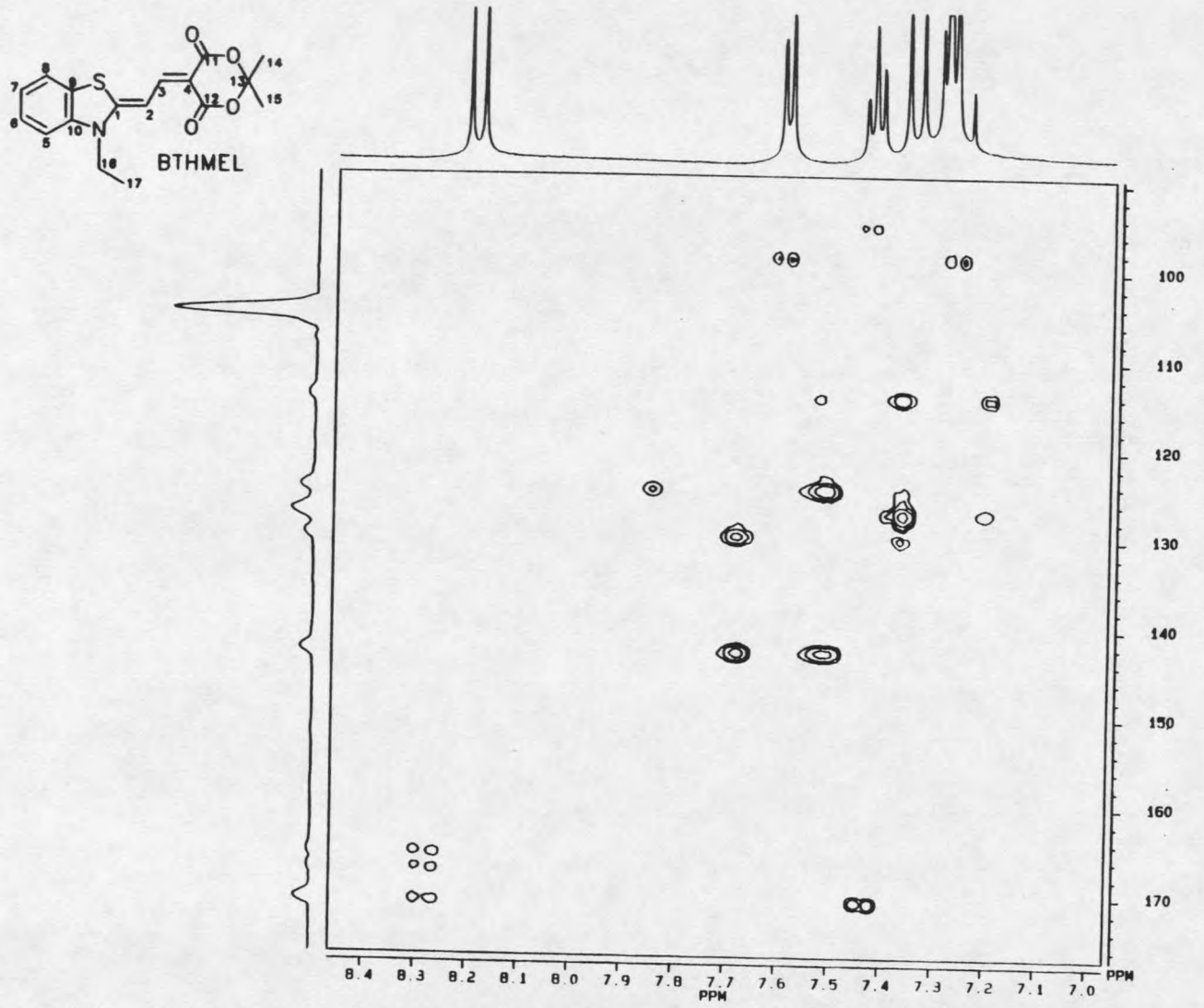

Figure 46. Long range inverse detection spectrum showing the aromatic region of BTHMEL.

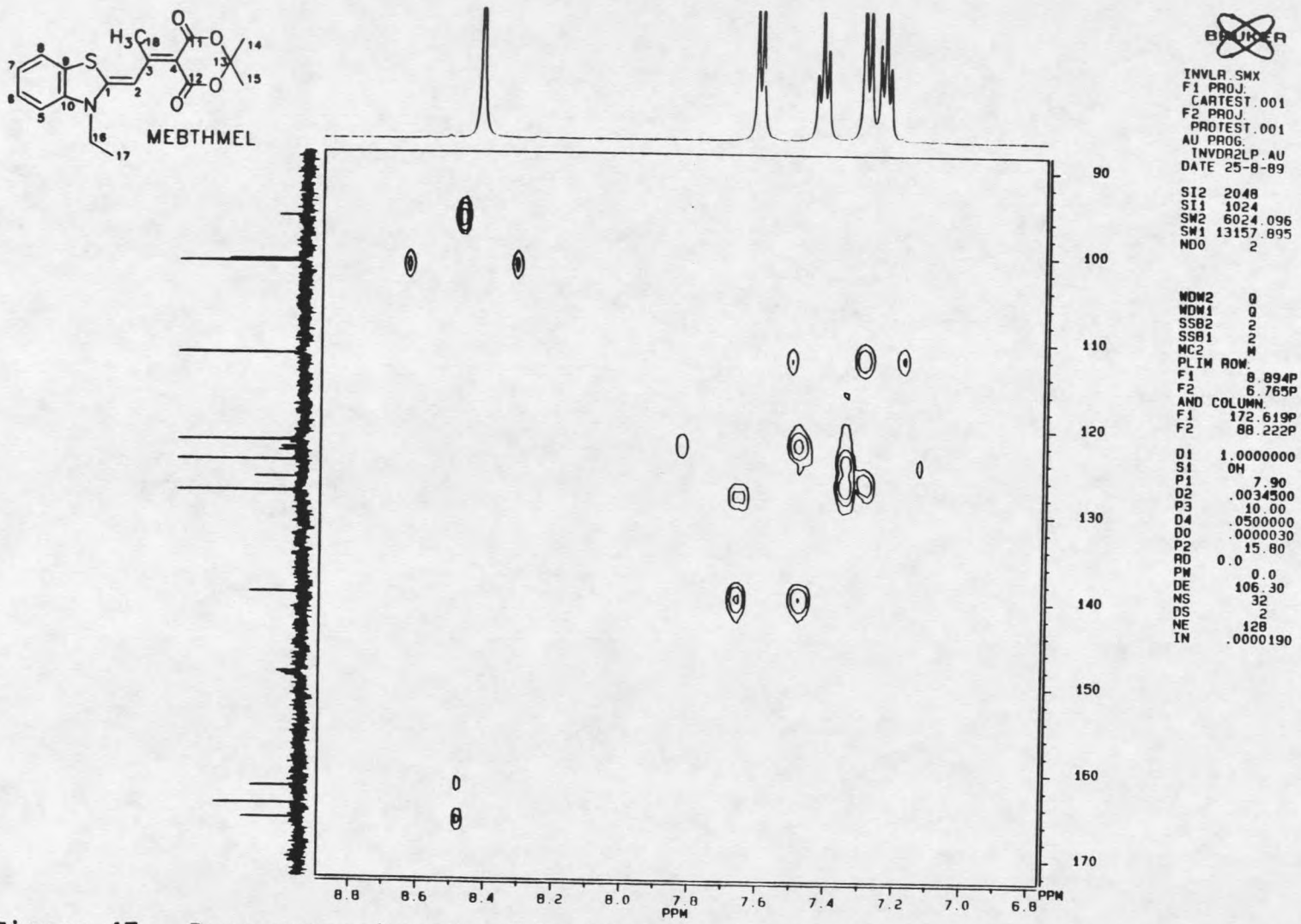

Figure 47. Long range inverse detection spectrum showing the aromatic region of MEBTHMEL.

Ring assignments can also be supported from the long range MEBTHMEL data. The proton at C8 is coupled to its parent carbon (the doublet at δ 122.0) and to C6 (δ 124.3) and C9 (our tentatively assigned δ 139.6 carbon atom). The first suggestion of a problem when trying to support the COLOC assignments may be noted here. There doesn't seem to be any coupling to C7 (δ 124.3). We continued to assign long range information and other apparent flaws developed. This was made clear upon interpretation of the methylene of the ethyl group shown in Figure 48 for BTHMEL and Figure 49 for MEBTHMEL.

There are some T_1 (relaxation delay) noise problems upfield. Upon close examination, this noise poses no hinderance in the interpretation of the spectra. The important section to consider is the long range coupling of the methylene protons of the ethyl group at δ 4.30 for MEBTHMEL (the same coupling is shown for BTHMEL). We expected to see the α doublet at δ 42.1 and long range coupling to the methyl carbon (C17) at δ 22.0. What was not seen in the COLOC but observed in this experiment is the through nitrogen coupling at δ 139.6 and δ 162.2. This type of coupling is common and shows that we incorrectly assigned C1, C4, C9, and C10.

The proton on C16 should not have coupling to a carbon atom five atoms away. This has been shown to occur however very rarely and only in saturated systems (the record is seven

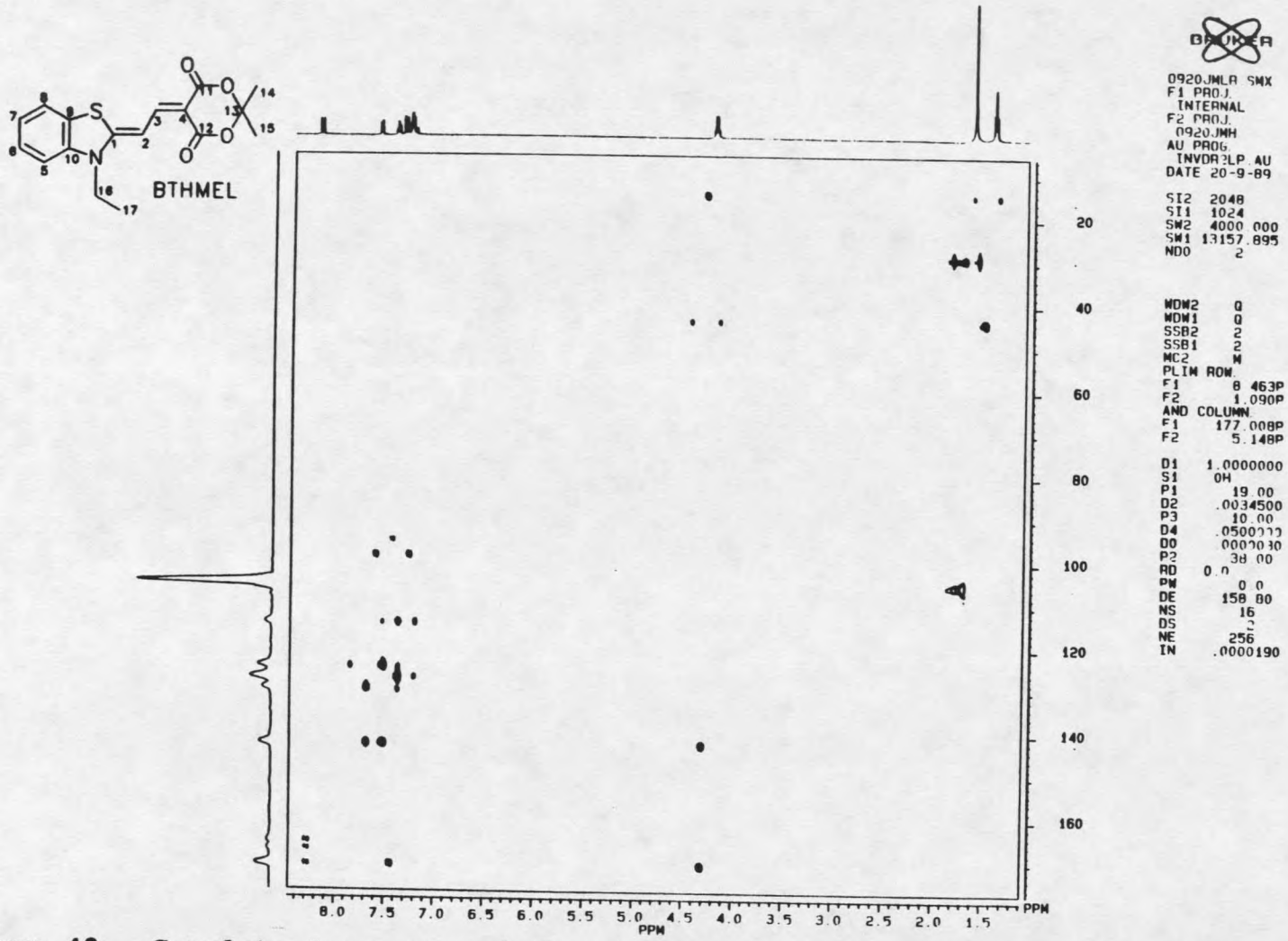

Figure 48. Complete long range information which shows through nitrogen coupling for BTHMEL.

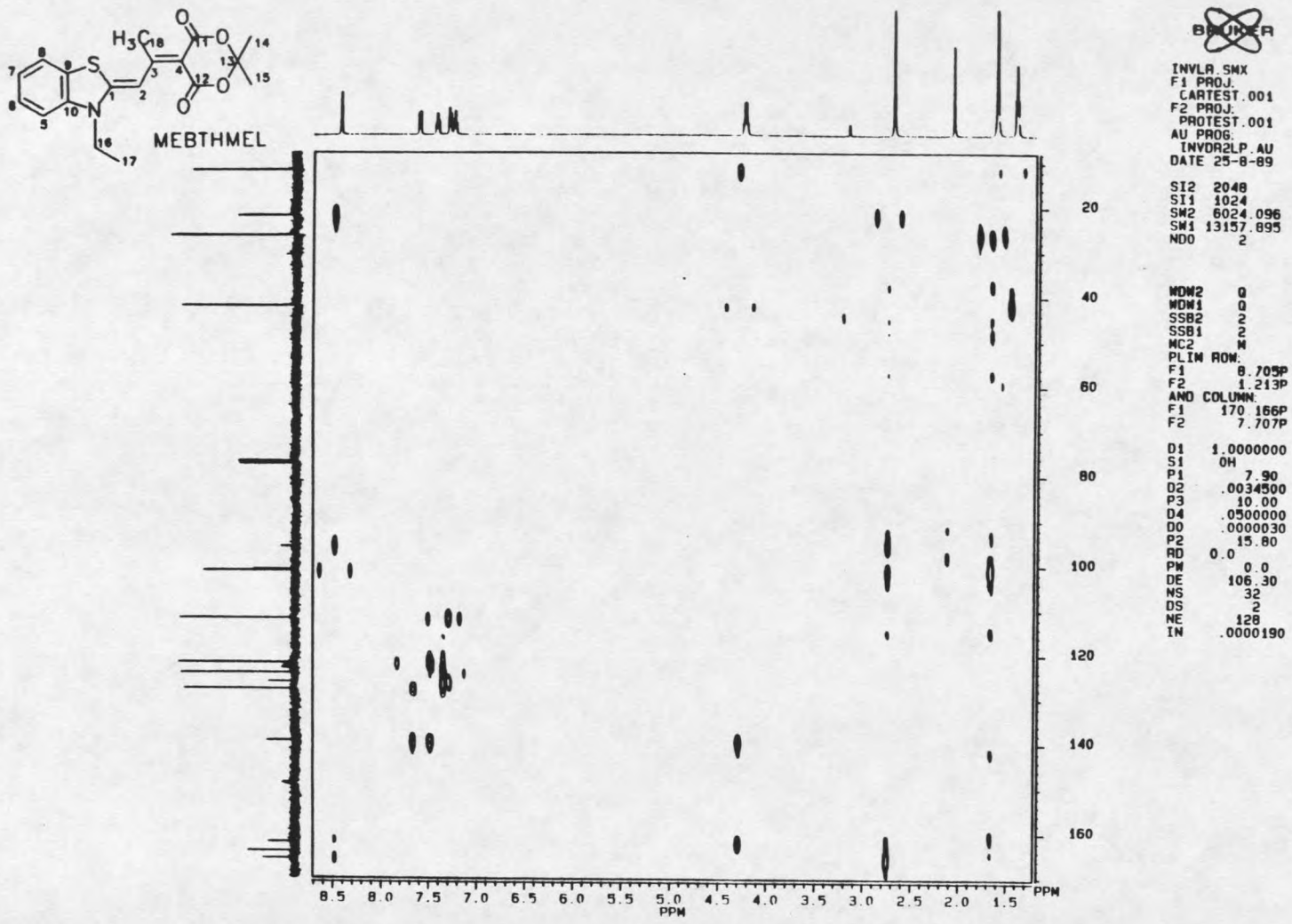

Figure 49. Complete long range information which shows through nitrogen coupling for MEBTHMEL.

carbon atoms). We would also expect to see some coupling to at least one other carbon atom in the chain (C1-C3). For these reasons the chemical shift at δ 162.2 has to be due to the C1 carbon atom and not C4.

Similarly, we believe C9 and C10 were also incorrectly assigned in the COLOC because of coupling from the C16 proton to δ 139.6. This coupling would be more likely for C10 than C9 because of distance and the lack of other supporting long range coupling that should occur at C5. This would also make earlier assignments more reasonable.

All of the stronger long range coupling seen previously along with these new assignments seem to favor a trend. For these conjugated systems, δ coupling will be stronger than β or γ coupling. This trend can be shown by looking at the intensities of the long range inverse experiments. For example, the proton on C2 in MEBTHMEL is coupled more strongly to C4 and C18 than to C1 and C3. Both of these stronger couplings are due to δ carbons. δ 4.300 (C16) is coupled to C1 and C10 more strongly δ (carbons) than C18. All of the aromatic ring long range signals are also δ coupled with the exception being C6 (δ 7.480). This proton shows coupling to C5 (δ 111.8) but this is weaker than the coupling to C10 and C8 which are again δ carbons. The same trend is seen in the BTHMEL dye. This trend should be considered when assigning

chemical shift correlations for these dye systems. Figures 50 and 51 show all of our chemical shift assignments for BTHMEL and MEBTHMEL respectively.

The merocyanines previously looked at all seem to have comparable shift data for the carbon spectra. Splitting patterns and chemical shift information obtained from the model study allows us to make assignments for similar merocyanines. The benzothiazole ring system remains fairly constant (see Table 10). This allows us to quickly assign this region from a more complex dye. Assignments for other aromatic ring systems can then be worked out. Electron donating and withdrawing groups still cause problems in the chain region but proton assignments are easily made from the COSY and coupling constants in the proton spectrum.

Table 10. ^{13}C NMR data for selected merocyanines.

DYE	CARBON CHEMICAL SHIFTS (ppm)					
	C5	C6	C7	C8	C9	C10
BTHMEL	112.1	127.8	125.0	122.5	125.6	140.8
BTHIND	111.5	127.4	124.5	122.3	125.5	140.1
MEBTHRHO	110.4	127.4	122.3	121.7	125.6	140.4
MEBTHMEL	111.8	127.9	124.3	122.0	126.4	139.6
MEBTHIND	111.4	127.7	123.8	122.0	126.7	139.9
MEBTHTBA	112.6	128.4	123.8	122.4	125.4	139.5

Model compound: BTHMEL

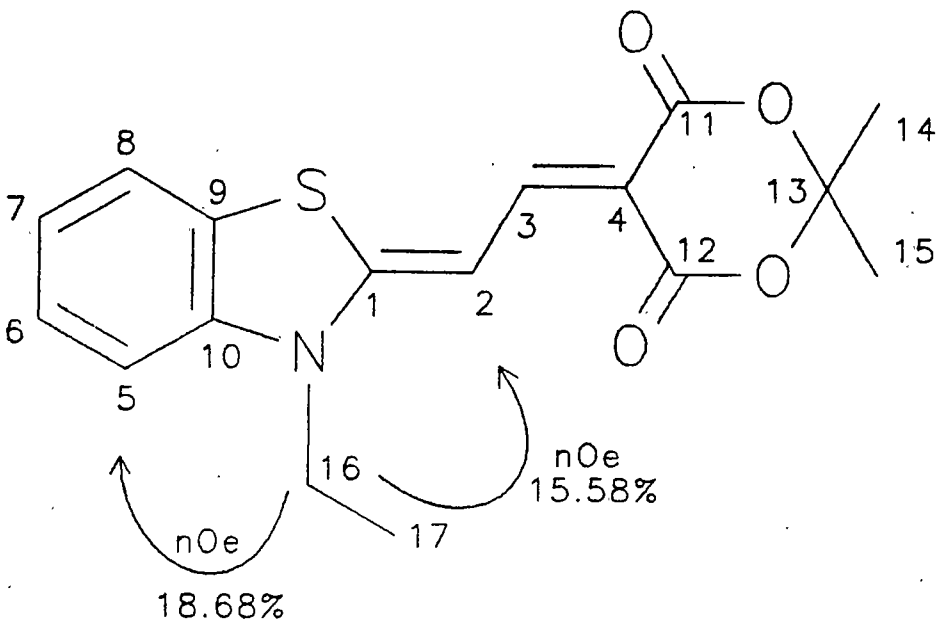

C_1= 163.7 (s)
C_2= 96.5 (d, J=166.6)
7.413 (d, J=13.7)
C_3= 150.5 (d, J=148.3)
8.283 (d, J=13.7)
C_4= 93.6 (s)
C_5= 112.1 (d, J=163.9)
7.292 (d, J=8.30)
C_6= 127.8 (d, J=164.2)
7.460 (brt, J=7.77)
C_7= 125.0 (d, J=170.5)
7.317 (brt, J=7.72)
C_8= 122.5 (d, J=165.4)
7.631 (d, J=7.85)
C_9= 125.6 (s)

C_{10}= 140.8 (s)
C_{11}= 167.0 or 165.0 (s)
C_{12}= 167.0 or 165.0 (s)
C_{13}= 103.1 (s)
C_{14}= 27.1 (q, J=128.2)
1.693 (s)
C_{15}= 27.1 (q, J=128.2)
1.693 (s)
C_{16}= 41.8 (t, J=144.3)
4.259 (q, J=7.27)
C_{17}= 12.4 (q, J=128.6)
1.464 (t, J=7.23)

Figure 50. Complete NMR assignments for BTHMEL.

Model compound: MEBTHMEL

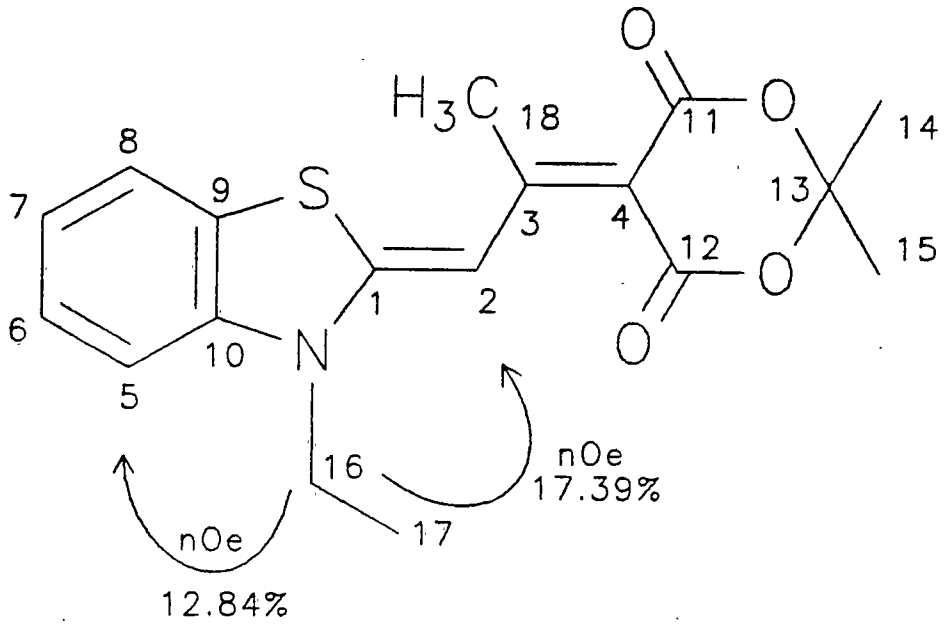

C_1= 162.2 (s)
C_2= 101.3 (d, J=158.0)
8.482 (d, brs)
C_3= 166.0 (s)
C_4= 96.0 (s)
C_5= 111.8 (d, J=166.0)
7.316 (d, J=9.40)
C_6= 127.9 (d, J=162.1)
7.480 (t, J=7.84)
C_7= 124.3 (d, J=163.3)
7.300 (t, J=8.12)
C_8= 122.0 (d, J=165.7)
7.651 (d, J=8.07)
C_9= 126.4 (s)

C_{10}= 139.6 (s)
C_{11}= 164.3 (s)
C_{12}= 164.3 (s)
C_{13}= 101.1 (s)
C_{14}= 26.5 (q, J=128.4)
1.678 (s)
C_{15}= 26.5 (q, J=128.4)
1.678 (s)
C_{16}= 42.1 (t, J=140.9)
4.300 (q, J=7.25)
C_{17}= 11.8 (q, J=129.0)
1.483 (t, J=7.24)
C_{18}= 22.0 (q, J=128.8)
2.756 (s)

Figure 51. Complete NMR assignments for MEBTHMEL.

Table 11. Proton chemical shifts for selected merocyanines.

DYE	PROTON CHEMICAL SHIFTS (ppm)	
	C2	C3
BTHRHO	5.293	7.581
BOXIND	6.991	8.222
BTHMEL	7.413	8.283
BTHIND	7.468	7.710
BTHTBA	7.874	8.427
MEBTHRHO	8.074	
MEBTHMEL	8.482	
MEBTHIND	8.720	
MEBTHTBA	8.840	

NMR spectroscopy of all of the dyes in our study revealed another trend. The C2 proton chemical shift varies depending on the polarity of the dye molecule. When we make a dye the polarity can be rated using the deviation data shown earlier. Table 11 shows a series of uncrowded and chain methyl crowded dyes in their increasing order of polarity. The polar dyes have the C2 proton signal further downfield from less polar dyes. This gives us another way to look at the polarity of new dye systems where the basicity or acidity of incorporated heterocycles hasn't been determined.

CONCLUSIONS

X-ray crystallography was the perfect tool for observing the physical properties of our series of merocyanines. The technique allowed us to look at the actual bond lengths and torsion angles and other characteristics of the merocyanines at the molecular level. One thing must be considered however. The bond lengths from a crystallographic point of view may not be as different as we might think. Some of the bonds of interest vary by very small amounts. To show that one bond distance is different from another would require the bonds to be different by at least three standard deviations. For some of our dyes this was observed, in others it was not.

When the series was considered as a whole, the trend can be clearly shown. Both the crowded and non-crowded merocyanines show that Brooker was right. The deviation of a merocyanine dye's wavelength was due to the electron donating and withdrawing abilities of the heterocycles incorporated in the dye molecule. Dyes that we predicted to be polar from his list of deviations do show the expected

bonding characteristics of a charge separated dipolar amidic system. Likewise, the predicted non-polar dyes resembled the charge neutral dipolar amidic system.

Crowded merocyanines also showed some interesting structural features. These dyes did have steric interactions between the carbonyl oxygen and chain methyl groups. This was seen by comparing the two merocyanines that incorporated a rhodanine as one of the heterocyclic end groups (BTHRHO with MEBTHRHO). When there were only protons in the chain (BTHRHO) the dye preferred to be in the Z conformation with respect to the sulfur atom on the benzothiazole ring. A chain methyl group caused enough of an interaction with the carbonyl group of the rhodanine ring that the E conformation was the only one observed by x-ray crystallography.

When we expanded this crowding study to include an indandione ring instead of a rhodanine an interesting observation was made. The indandione heterocycle won't allow the same type of release from steric interactions as the rhodanine ring due to the two carbonyl groups which wouldn't have two different planar conformations. This dye was expected to show some twisting due to crowding by the chain methyl group. This was not observed in the crystal structure. The data showed that the chain methyl crowded merocyanine (MEBTHIND) lengthened it's bond distances to accommodate the

chain methyl group into the plane of the chromophore. This leads us to believe that the π bonding interactions of the chromophore would require much greater energy to twist than that required for bond lengthening of the chain carbon atoms.

Further crystallographic study lead us to look at a BAA allopolar-like molecule. This model revealed some important information. Like merocyanines, the molecule showed that the chromophore remained planar as expected for the meropolar conformation if Brooker's notion about allopolar conformations is right. The out of plane carbonyl was not perpendicular to the chromophore as previously believed. This could be due to the difference in our model versus a real allopolar dye. Normal meropolar conformations would have an additional pair of carbon atoms in the meropolar chromophore's chain length that would make more room for the out of plane heterocycle to fit into a position perpendicular to the chromophore.

Now that we had a good representation of our dyes which were determined by crystallography we expanded our study to include the area of NMR spectroscopy. Using NMR techniques we rigorously assigned all of the chemical shifts for two model merocyanines. This was the first time that these dye systems had been experimentally assigned. All previous work involved chemical shift arguments instead of interrelated evidence for making NMR assignments. We used a battery of

experiments to assign chemical shift information experimentally. We did this because there have been incorrect assignments of molecules when only chemical shift arguments have been used.

Accurate chemical shift data were obtained from the proton and carbon NMR spectra. We needed the extra experimental evidence to correlate the chemical shifts for each atom with the actual numbers given by the carbon and proton spectra. We found some proton-proton correlations by coupling constants but most of the confirmation was shown by the COSY experiments. Carbon-proton correlations were made using the XHCORR experiment and backed up with the BIRDPH data. Long range couplings were observed with the COLOC experiment but the long range inverse experiments gave better data and helped assign chemical shifts previously misassigned due to incomplete data from the COLOC experiments. The nOe experiments were invaluable for observing C2 and C5 protons. These made assignments for the ring system possible and made us take a second look at the unusual chemical shifts observed from the C2 protons.

Once the model system was unequivocally assigned, we expanded upon the experimental evidence to include the other less soluble merocyanines. When this was done we found that carbon chemical shift correlations were nearly identical for

similar ring groups. When the benzothiazole dyes were looked at, all of the carbon chemical shifts varied by less than five parts per million. This helped us assign other carbon signals after disregarding the signals from the benzothiazole ring. The chain carbons didn't vary much for each merocyanine. These carbon chemical shifts differed by less than ten parts per million which would depend upon the polarity of the merocyanine.

The merocyanines and chain methyl merocyanines are both planar in the solid state which was shown by x-ray crystallography. This should also be true in the solution state. We believe this because there were nearly no differences between the absorption or ε values when BTHRHO was compared to MEBTHRHO or when BTHIND was compared to MEBTHIND.

Since this is true we looked at the bond lengthening by proton NMR to see if it could be detected in the solution state. Comparison of the C2 protons for both of the merocyanine dye systems (crowded and non-crowded) studied by crystallography showed that when a methyl group is added to the chain, the C2 proton moves downfield by approximately one part per million. We believe that this is due to shielding from the carbonyl oxygen (or sulfur in the case of rhodanine) when the merocyanine was not crowded. Incorporation of a methyl group must move the carbonyl away from the C2 proton

by lengthening the chain methyl bond lengths if our argument for both dyes being planar in the solution state is viable. Bond lengthening would remove most of the shielding caused by the carbonyl oxygen electrons and allow us to observe the relatively unperturbed chemical shift of the C2 proton. We believe the same thing is happening in merocyanines where the electron withdrawing group was changed to a six membered ring system.

We attempted to look at crowding by a carbonyl on a six membered ring by x-ray crystallography. This didn't work out as expected. MEBTHMEL and MEBTHTBA both readily formed crystals but were twinned. Crystallographic data for MEBTHMEL showed that the dye crystallized with an orthorhombic unit cell. Inconsistencies with the data suggested that the dye really crystallized in a monoclinic unit cell. This unit cell packed in two different orientations which confused the program. The twinning observed couldn't be modeled and so the crystal structure wasn't determined.

We did get a gross determination for MEBTHTBA. There was some sort of disorder observed for the molecule which made a good refinement impossible. The only information obtained was the crude structure which had to be supported by mass

spectrometry and NMR data. We were able to speculate on the structure of these dyes. This can be done by looking at the proton NMR information.

One assumption needs to be made. The non-crowded merocyanines (BTHMEL and BTHTBA) cannot be twisting out of the plane. This is a valid assumption because none of the other merocyanines previously studied by x-ray crystallography show twisting of the chromophore. We can now speculate upon the steric interactions that would arise when a chain methyl group is incorporated into the merocyanines. The absorptions for both the crowded and non-crowded dyes (BTHMEL versus MEBTHMEL, and BTHTBA versus MEBTHTBA) are nearly identical. The ε values are also very similar. This supports the earlier argument that chain methyl crowding doesn't affect the chromophore and therefore the chromophore wouldn't be twisted in the solution state for six membered ring systems. Six membered ring dyes are similar to previously mentioned five membered ring systems.

When these dyes were compared by proton NMR (shown previously in Table 11) we observed that the C2 protons again shifted downfield when a methyl group was incorporated into the chromophore chain. This suggests that the same type of bond lengthening is occurring for a merocyanine when the electron withdrawing group is a six membered ring.

We have shown that Brooker could be correct in thinking that an allopolar dye would be planar with respect to two of the heterocyclic rings. This can be suggested because crowding merocyanines (which would resemble the meropolar conformation of an allopolar dye) doesn't cause twisting of the chromophore. Again this must be due to the amount of energy needed to weaken the chromophore versus the amount needed to lengthen carbon-carbon bond distances. This was also shown to be true using our BAA allopolar model molecule. There are still some unanswered questions as to the conformation of the heterocycle out of the plane of the other two heterocycles that make up the chromophore of an allopolar dye.

We have provided a base from which to expand upon these systems. Our new approach to the synthesis of chain methyl merocyanines allows further study of different dyes. We are no longer confined to only methyl crowded merocyanines that contain a benzothiazole ring. This was shown by the synthesis of MEINDOLIND. We can also synthesize these dyes in better yields than the method used by Schelz.

Our synthetic approach also shows promise for the first trinuclear allopolar dyes. We will soon be able to expand to BB'A allopolar dyes using the scheme shown in Figure 52. Dye intermediates with leaving groups in the two position have

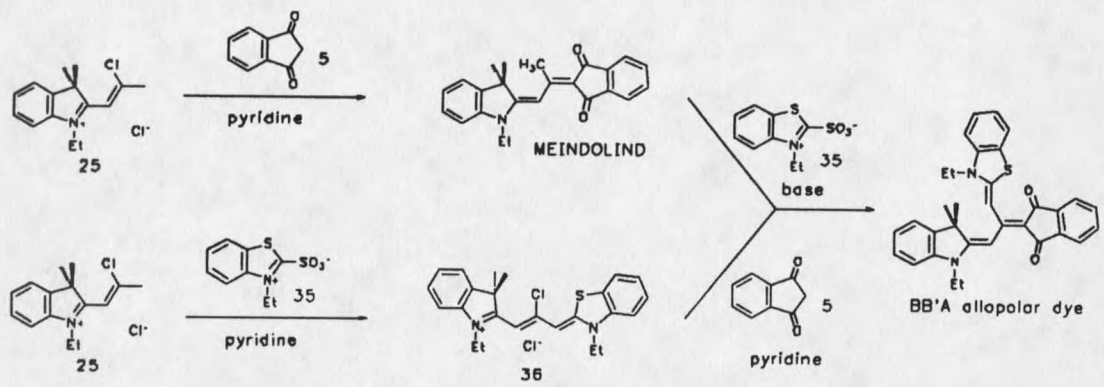

Figure 52. Proposed synthesis of a trinuclear allopolar dye.

been reported in the literature (81-83). The problem with reproducing these reactions is that the references have been patented. The patents give the general idea how to make the intermediates but don't report the procedures.

EXPERIMENTAL

Instrumentation

NMR spectra were obtained with Bruker AC-300 and AM-500 spectrometers using $CDCl_3$ as solvent and internal standard. The AC-300 ^{1}H data were taken at 300.130 MHz and the ^{13}C data at 75.470 MHz. AM-500 ^{1}H data were taken at 500.130 MHz the ^{13}C data at 125.759 MHz. All of the NMR experiments were done at room temperature except for the inverse detection experiments which were done at 300 °K. Chemical shifts are reported in ppm (δ units) relative to tetramethylsilane (δ = 0). X-ray data was collected on a Nicolet R3mE four cycle diffractometer and solved using SHELXTL (a structure refinement program) revision 4 (August 1983). UV/Vis spectra were obtained using Varian 634 and Carey model 14 spectrophotometers. Mass spectral analyses were done on VG Instruments MM-16F, 70E-HF, or TRIO-2 mass spectrometers. Melting points were taken on an Electrothermal apparatus and are uncorrected.

Crystallization

Single crystals used for x-ray crystallography were grown by three different techniques. One was the addition of methanol and/or ethanol to a saturated pyridine solution and then allowing the solution to sit at room temperature for approximately two weeks. By this time large enough crystals were formed. This technique was also carried out in the refrigerator with similar results.

To avoid water in the crystal lattice for BTHIND, an alternate technique was adopted. The dye was added to hot ethanol until a saturated solution was reached. This was poured into a stoppered vial and sealed for a year. The crystal obtained was devoid of water.

By far the most often used and possibly the best technique was diffusion of methanol into a saturated pyridine solution. This was accomplished by placing the dye solution into a desiccator containing methanol. Methanol diffused into the pyridine over a one to two week period giving bar crystals that were single in most cases.

Reactions and Data

2-[2-(3-Ethyl-2-benzothiazolinylidene)ethylidene]-1,3-indandione (BTHIND). 2-(2-Acetanilidovinyl)-3-ethylbenzothiazolium iodide (450 mg, 1.0 x 10^{-3} mol) and 1,3-indandione (160 mg, 8.9 x 10^{-4} mol) were combined in a 50 ml round bottom flask. Pyridine (10 ml) was then added followed by triethylamine (10 dp). The reaction mixture was brought to reflux and heating continued for thirty minutes. The solution was a deep purple-red color after heating. The reaction mixture was cooled to room temperature and methanol (25 ml) added to induce crystallization. The solution was kept in a refrigerator for five days. The purple crystalline dye was filtered from the reaction mixture to yield 266 mg which is 79.6% of the theoretical yield. mp. 256-60 °C; $\lambda_{max.}^{MeOH}$ = 504 nm.; ε_{504} = 1.27 x10^5; ^{1}H-NMR ($CDCl_3$) δ 1.49 (3H,t,J=7.212), 4.25 (2H,q,J=7.212), 7.25 (1H,brt,J=7.15), 7.42 (1H,ddd,J=8.30, 6.39, 1.14), 7.57 (2H,m), 7.73 (1H,brdd, J=5.22, 3.08), 7.86 (1H,d, J=13.37); ^{13}C-NMR ($CDCl_3$) δ 12.28 (q, J=131.3), 41.50 (t, J=135.6), 94.82 (d, J=165.1), 111.47 (d, J=163.5), 114.75 (s), 120.75 (d, J=160.7), 121.41 (d, J=169.5), 122.34 (d, J=165.9), 124.49 (d, J=165.4), 125.51 (s), 127.44 (d, J=159.8), 132.77 (d, J=162.5), 132.93 (d, J=155.3), 140.09 (s), 140.85 (2C,d, J=147.9), 141.47 (s),

166.83 (s), 191.04 (s), 192.40 (s); Low Resolution DIP EIMS: m/e 333 (100), 319 (20), 304 (18), 247 (17), 188 (47), 149 (52); High Resolution DIP EIMS: m/e 333.0819, $C_{20}H_{15}N_1O_2S_1$, MMU 0.4.

3-Ethyl-5-[2-(3-ethyl-2-benzothiazolinylidene)-ethylidene]rhodanine (BTHRHO). 2-(2-Acetanilidovinyl)-3-ethylbenzothiazolium iodide (1.0 g, 2.2 x 10^{-3} mol) and 3-ethylrhodanine (0.53 g, 3.3 x 10^{-3} mol) were combined in a 50 ml round bottom flask. Pyridine (20 ml) and triethylamine (2 dp) were added and the reaction mixture brought to reflux for one hour. The reaction mixture was poured into a 250 ml beaker and methanol (100 ml) added to promote crystallization. The solution was placed in the refrigerator overnight. The purple crystals were filtered to yield 83% of the dye. mp. 262-263 °C; $\lambda_{max.}^{MeOH}$ = 525 nm.; ε_{525} = 8.76 x10^4; ^{1}H-NMR ($CDCl_3$) δ 1.25 (3H,t,J=7.12), 1.38 (3H,t,J=7.25), 4.00 (2H,q,J=7.26), 4.14 (2H,q, J=7.12), 5.29 (1H,brd,J=12.92), 7.04 (1H,brd, J=8.17), 7.15 (1H,brt,J=7.64), 7.33 (1H,dt,J=7.83, 1.06), 7.46 (1H,dd,J=7.68, 1.08), 7.58 (1H,brd,J=10.45); ^{13}C-NMR ($CDCl_3$) δ 11.81 (q,J=130.8), 12.30 (q,J=128.1), 39.56 (t,J=142.4), 40.49 (t,J=141.6), 89.43 (d,J=158.1), 109.47 (s), 110.29 (d,J=160.3), 122.14 (d,J=172.7), 123.47 (d,J=166.8), 124.683 (s), 127.158 (d,J=161.6), 132.453 (d,J=153.7), 141.27 (s), 159.39 (s), 166.45 (s), 190.86 (s); Low Resolution DIP EIMS:

m/e 348 (94.8), 334 (10.3), 233 (100), 218 (17.1), 204 (53.7), 186 (7.5), 173 (38.8), 160 (9.5), 116.5 (21.5), 85 (14.3), 69 (31.2); High Resolution DIP EIMS: m/e 348.0405, $C_{16}H_{16}N_2O_1S_3$, MMU 2.0.

2-[2-(3-Ethyl-2-benzoxazolinylidene)ethylidene]-1,3-indandione (BOXIND). 2-[2-Acetanilidovinyl]-3-ethyl-benzoxazolium iodide (500 mg, 1.2 x 10^{-3} mol) was combined with 1,3-indandione (130 mg, 9.2 x 10^{-4} mol) in a 25 ml round bottom flask. Pyridine (10 ml) was added followed by triethylamine (5 dp) and acetic anhydride (10 dp). The reaction mixture was stirred at reflux for two hours. After cooling to room temperature, the reaction mixture was rinsed into a 250 ml beaker with methanol (100 ml). This solution was placed in an ice bath for three hours. The solution was vacuum filtered and the resulting red dye washed with cold methanol. We isolated 290 mg of the dye for a 62% yield. Cooling of the reaction mixture for longer periods (14 hours) yields the desired dye along with starting indandione. mp. 282-283 °C; $\lambda_{max.}^{MeOH}$ = 468, ε_{468} = 1.36 x 10^5; ^{1}H-NMR ($CDCl_3$) δ 1.489 (3H,t,J=7.26), 4.094 (2H,q,J=7.28), 6.991 (1H,d, J=13.46), 7.141 (1H,dd,-J=7.18,0.91), 7.279 (2H,m), 7.423 (1H,dd,J=7.48,1.51), 7.568 (2H,m), 7.733 (2H,brs), 8.222 (1H,d,J=13.47); ^{13}C-NMR ($CDCl_3$) δ 9.57 (q,J=128.9), 35.99 (t,J=144.9), 78.37 (d,J=166.6), 106.00 (d,J=165.8), 107.71

(d,J=170.0), 111.67 (2C,s), 118.15 (2C,d,J=162.2), 121.38 (d,J=162.9), 122.30 (d,J=164.5), 127.99 (s), 129.75 (2C,d,J=158.2), 137.92 (d,J=162.7), 143.91 (s), 160.37 (2C,s); Low Resolution DIP EIMS: m/e 317 (100), 303 (17.4), 288 (15.1), 274 (15.7), 260 (14.0), 244 (11.7), 232 (5.2), 204 (5.5), 184 (9.4), 172 (40.1), 159 (11.1), 146 (7.1), 133 (33.5); High Resolution DIP EIMS: m/e 317.1049, $C_{20}H_{15}N_1O_3$, MMU 0.3.

2-[2-Chloro-1-propenyl]-3-ethylbenzothiazolium Chloride (22). Phosgene (0.30 ml, 4.2 x 10^{-3} mol) was trapped in an ice bath in a 10 ml round bottom flask. Chloroform (1 ml) was then added and the phosgene dissolved. 1-[3-ethylbenzothiazolinyidene]-2-propanone (63.0 mg, 2.8 x 10^{-4} mol) was dissolved in chloroform (1.5 ml) and that solution injected into the phosgene solution. A precipitate formed immediately. The reaction was allowed to sit for two hours and then stirred overnight. The precipitate had dissolved and the clear reaction mixture was evaporated under nitrogen. Light brown to clear crystals were washed with cold acetone and air dried to give 57.3 mg or 73.3%. mp 157-158 °C.

2-[2-(3-Ethyl-2-benzothiazolinylidene)-1-methylethylidene]-1,3-indandione (MEBTHIND). 3-Ethyl-2-methylbenzothiazolium Iodide (3.4 g, 1.1 x 10^{-2} mol) was combined with 1,3-indandione (1.8 g, 1.2 x 10^{-2} mol) and 1,4-diaza-

bicyclo[2.2.2]octane (4.10 g, 3.7 x 10^{-2} mol) in a 50 ml round bottom flask and cooled in an ice bath. Acetic anhydride (16 ml, 1.7 x 10^{-1} mol) was slowly added and the reaction mixture was stirred for ten minutes. The reaction mixture was brought to room temperature and stirring continued for six hours. The solution was vacuum filtered and a brick-red precipitate collected. The precipitate was washed with cold methanol to yield 1.217 g or 31.6%. mp. 183 °C; $\lambda_{max.}^{MeOH}$ = 496 nm; ε_{496} = 1.40 x10^5; ^{1}H-NMR ($CDCl_3$) δ 1.55 (3H,t,J=7.22), 2.93 (3H,s), 4.34 (2H,q,J=7.23), 7.23 (1H,dt,J=7.78, 0.83), 7.24 (1H,brd, J=8.87), 7.42 (1H,dt,J=7.84, 1.28), 7.49 (2H,m), 7.58 (1H,brd,J=7.82), 7.64 (2H,m), 8.70 (1H,s); ^{13}C-NMR ($CDCl_3$) δ 11.84 (q,J=128.7), 17.53 (q,J=127.8), 41.88 (t,J=140.3), 98.77 (d,J=158.8), 111.36 (d,J=163.5), 114.42 (s), 120.72 (2C,d, J=162.4), 121.96 (d,J=164.1), 123.84 (d,J=163.6), 126.68 (s), 127.70 (d,J=163.3), 132.60 (2C,d, J=161.0), 139.94 (s), 140.37 (2C,s), 160.54 (s), 160.83 (s), 192.92 (2C,s); Low Resolution DIP EIMS: m/e 347 (100), 332 (43), 304 (15), 202 (36), 174 (14), 149 (46); High Resolution DIP EIMS: m/e 347.0967, $C_{21}H_{17}N_1O_2S_1$, MMU 1.3.

2-[3-(1-Indanonylidene)]-1,3-Indandione (6). 1,3-Indandione (2.80 g, 1.9 x 10^{-2} mol) was combined with acetone (2.1 mls) and chloroform (25 mls) in a 50 ml round bottom flask. The solution was yellow in color. After the addition

of triethylamine (1 ml), the reaction mixture immediately turned purple. It was allowed to stir overnight (approximately 16 hours). Vacuum filtration and wash with a small amount of chloroform yielded 1.061 g of a yellow-green solid. Total yield was 38.5%. mp 213-215 °C; ^{1}H-NMR ($CDCl_3$) δ 4.11 (3H,s), 7.71 (1H,t,J=6.53), 7.80 (2H,m), 7.82 (1H,dt,J=8.24, 1.00), 7.91 (1H,brd,J=7.63), 7.93 (1H,m), 7.98 (1H,m), 9.63 (1H,brd,J=8.08); ^{13}C-NMR ($CDCl_3$) δ 43.40 (t,J=135.2), 123.03 (d,J=), 123.37 (d,J=), 123.47 (d,J=), 125.85 (s), 131.66 (d,J=), 134.13 (d,J=), 135.30 (2C,d, J=163.4), 135.35 (d,J=163.4), 140.41 (s), 141.26 (s), 141.65 (s), 145.87 (s), 155.35 (s), 189.29 (s), 190.98 (s), 200.89 (s); Low Resolution GC EIMS: m/e 274 (64), 273 (93), 246 (100), 218 (33), 189 (94), 76 (40); High Resolution GC EIMS: m/e 274.0633, $C_{18}H_{10}O_3$, MMU -0.3.

2-Isopropylidene-1,3-indandione (8). 1,3-Indandione (1.0 g, 6.9 x 10^{-3} mol) and acetone (12 mls, 1.6 x 10^{-1} mol) were combined in a 25 ml round bottom flask and cooled in an ice bath with stirring. Ammonium hydroxide (1 ml conc.) was slowly added and the reaction mixture continued to stir for five minutes. It was then brought to room temperature and stirred for an additional hour and a half. The brown powder was collected by vacuum filtration and washed with acetone. Total yield was 534.6 mg or 41.9%. mp 122-123 °C Reported 145

°C. ^{1}H-NMR ($CDCl_3$) δ 2.59 (6H,s), 7.72 (2H,m), 7.89 (2H,m); ^{13}C-NMR ($CDCl_3$) δ 19.09 (q,J=129.2), 108.87 (s), 122.42 (d,J=165.1), 122.67 (d,J=165.1), 133.99 (d,J=162.0), 134.89 (d,J=161.8), 138.11 (s), 140.77 (s), 183.65 (s), 188.42 (s), 196.73 (s); Low Resolution DIP EIMS: m/e 188 (62.8), 173 (100), 105 (13.2), 89 (14.5), 77 (12.4); High Resolution GC EIMS: m/e 188.0474, $C_{11}H_8O_3$, MMU 0.0.

2,2-dimethyl-5-[2-(3-Ethyl-2-benzothiazolinylidene)-ethylidene]-1,3-dioxane-4,6-dione (BTHMEL). 2-(2-Acetanilidovinyl)-3-ethylbenzothiazolium iodide (500 mg, 1.1 x 10^{-3} mol) and 2,2-dimethyl-1,3-dioxane-4,6-dione (170 mg, 1.2 x 10^{-3} mol) were combined in a 10 ml round bottom flask. To the reaction was added pyridine (5 ml) and the mixture refluxed for one and a half hours. Cold methanol (20 ml) was added and the mixture transferred into a 50 ml beaker. This solution was kept in the refrigerator overnight. The yellow dye was filtered and washed with cold methanol. Total weight of the dye was 0.3210 grams or 87.0% of the theoretical yield. mp 227-229 °C; $\lambda_{max.}^{MeOH}$ = 456 nm; ε_{456} = 1.66 x 10^4; ^{1}H-NMR ($CDCl_3$) δ 1.46 (3H,t,J=7.23), 1.69 (6H,s), 4.26 (2H,q,J=7.27), 7.29 (1H,brd,J=8.30), 7.32 (1H,dt,J=7.72, 0.60), 7.41 (1H,d, J=13.75), 7.46 (1H,dt,J=7.77, 1.01), 7.63 (1H,dd,J=7.85, 0.63), 8.28 (1H,d,J=13.66); ^{13}C-NMR ($CDCl_3$) δ 12.37 (q,J=128.6), 27.05 (q,J=128.2), 41.78 (t,J=144.3), 93.58 (s),

96.56 (d,J=166.6), 103.08 (s), 112.06 (d,J=163.9), 122.55 (d,J=165.4), 125.09 (d,J=170.5), 125.65 (s), 127.76 (d,J=164.2), 140.81 (s), 150.50 (d,J=148.3), 163.66 (s), 165.17 (s), 168.70 (s); Low Resolution EIMS: m/e 331 (11.5), 274 (4.3), 245 (2.8), 228 (3.0), 203 (10.0), 186 (26.9), 173 (8.6), 162 (3.3), 149 (17.5), 108 (4.5), 58 (38.2); High Resolution DIP EIMS: m/e 331.0872, $C_{17}H_{17}N_1O_4S_1$, MMU 0.6.

2,2-dimethyl-5-[2-(3-Ethyl-2-benzothiazolinylidene)-1-methylethylidene]-1,3-dioxane-4,6-dione (MEBTHMEL). 2-Methyl-3-ethylbenzothiazolium iodide (1.50 g, 5.0 x 10^{-3} mol) and 2,2-dimethyl-1,3-dioxane-4,6-dione (710 mg, 5.0 x 10^{-3} mol) were combined in a 10 ml round bottom flask. Acetic anhydride (18 ml, 1.9 x 10^{-1} mol) was added and the mixture stirred for a couple of minutes. 1,4-Diazabicyclo[2.2.2]octane (1.164 g, 1.0 x 10^{-2} mol) was added to the reaction mixture and stirring continued for eight hours at room temperature. The reaction mixture was vacuum filtered and washed with cold methanol to yield 730.3 mg of yellow dye. This is 46.5% of the theoretical yield. mp 211 °C; $\lambda_{max.}^{MeOH}$ = 454 nm; ε_{454} = 7.15 x10^4; ^{1}H-NMR ($CDCl_3$) δ 1.48 (3H,t,J=7.24), 1.68 (6H,s), 2.76 (3H,s), 4.30 (2H,q,J=7.25), 7.30 (1H,t, J=8.12), 7.32 (1H,d,J=9.40), 7.48 (1H,t,J=7.84), 7.65 (1H,d,J=8.07), 8.48 (1H,brs); ^{13}C-NMR ($CDCl_3$) δ 11.78 (q,J=129.0), 22.03 (q,J=128.8), 26.47 (2C,q,J=128.4), 42.12 (t,J=140.9), 96.05 (s), 101.14 (s),

101.28 (d,J=158.0), 111.81 (d,J=166.0), 122.03 (d,J=165.7), 124.31 (d,J=163.3), 126.36 (s), 127.93 (d,J=162.1), 139.63 (s), 162.19 (s), 164.32 (2C,s), 166.04 (s); Low Resolution DIP EIMS: m/e 347 (100), 332 (43), 304 (15), 202 (36), 174 (14), 149 (46); High Resolution DIP EIMS: m/e 345.1015, $C_{18}H_{19}N_1O_4S_1$, MMU 1.9.

3-Ethyl-5-[2-(3-ethyl-2-benzothiazolinylidene)-1-methylethylidene]rhodanine (MEBTHRHO). 3-Ethyl-2-methyl-benzothiazolium iodide (0.82 g, 2.7 x 10^{-2} mol) was combined with 3-ethylrhodanine (0.55 g, 3.4 x 10^{-2} mol) and 1,4-diazabicyclo[2.2.2]octane (1.0 g, 9.2 x 10^{-3} mol) in a 25 ml round bottom flask. Acetic anhydride (10 ml, 1.1 x 10^{-1} mol) was added and the reaction mixture stirred for 18 hours at room temperature. The precipitate was filtered and rinsed with cold methanol. This purple powder was then recrystallized from ethanol to get rid of a white impurity assumed to be starting material. The yield after crystallization was 105 mg which is 12% of theoretical. mp. 207-208 °C; $\lambda_{max.}^{MeOH}$ = 503 nm; ε_{530} = 1.00 x 10^5; ^{1}H-NMR ($CDCl_3$) δ 1.25 (3H,t,J=7.15), 1.44 (3H,t,J=7.16), 2.28 (3H,brs), 4.13 (4H,m), 7.08 (1H,brd,J=8.21), 7.13 (1H,brt,J=7.56), 7.35 (1H,brt, J=7.46), 7.47 (1H,brd,J=7.72), 8.07 (1H,brs); ^{13}C-NMR ($CDCl_3$) δ 11.39 (q,J=128.5), 12.33 (q,J=127.1), 22.70 (q,J=126.7), 39.39 (t,J=140.9), 41.07 (t,J=132.9), 95.35

(d,J=159.9), 108.98 (s), 110.39 (d,J=164.5), 121.65 (d,J=163.7), 122.90 (d,J=162.7), 125.56 (s), 127.38 (d,J=161.9), 140.41 (s), 146.52 (s), 154.97 (s), 164.18 (s), 189.16 (s); Low Resolution DIP EIMS: m/e 362 (100), 247 (61), 232 (24), 218 (48), 187 (40), 174 (17), 149 (9), 124 (24); High Resolution DIP EIMS: m/e 362.0583, $C_{17}H_{18}N_2O_1S_3$, MMU -0.2.

1,3-Diethyl-5-[2-(3-ethyl-2-benzothiazolinylidene)-1-methylethylidene]-2-thiobarbituric Acid (MEBTHTBA). 1,3-Diethyl-2-thiobarbituric acid (71.0 mg, 3.6 x 10^{-4} mol) was combined with 3-ethyl-2-methylbenzothiazolium iodide (150 mg, 5.0 x 10^{-4} mol) and 1,4-diazabicyclo[2.2.2]octane (120 mg, 1.0 x 10^{-3} mol) in a 10 ml round bottom flask. Acetic anhydride (1.80 ml, 1.8 x 10^{-2} mol) was added and the reaction mixture stirred at room temperature for 48 hours. The solution was vacuum filtered and washed with cold methanol. The bright yellow dye weighed 44.3 mg which was 25.9% of the theoretical value. mp 211-213 °C; $\lambda_{max.}^{MeOH}$ = 492 nm; ε_{492} = 3.29 x 10^4; ^{1}H-NMR ($CDCl_3$) δ 1.29 (6H,t,J=6.97), 1.54 (3H,t, J=7.22), 2.76 (3H,brs), 4.45 (2H,q,J=7.22), 4.57 (4H,q, J=6.91), 7.41 (1H,brt,J=7.59), 7.45 (1H,brd, J=11.64), 7.57 (1H,t,J=7.68), 7.75 (1H,d,J=7.91), 8.84 (1H,brs); ^{13}C-NMR ($CDCl_3$) δ 12.39 (q,J=130.1), 12.70 (2C,q,J=126.4), 22.15 (q,J=128.5), 42.85 (t,J=143.0), 43.14 (2C,t,J=143.6), 105.75 (s), 112.62 (d,J=165.4), 122.45 (d,J=163.7), 123.82 (d,J=157.4), 125.36

(d,J=162.2), 128.42 (d,J=165.2), 136.33 (s), 139.47 (s), 149.37 (2C,s), 161.34 (s), 167.29 (s), 177.22 (s); Low Resolution DIP EIMS: m/e 401 (91), 387 (8), 368 (100), 313 (35), 200 (28), 186 (18), 173 (11), 149 (17); High REsolution DIP EIMS: m/e 401.1227, $C_{20}H_{23}N_3O_2S_2$, MMU 0.5.

1,3-Diethyl-5-[2-(3-ethyl-2-benzothiazolinylidene)-ethylidene]-2-thiobarbituric Acid (BTHTBA). 1,3-Diethyl-2-thiobarbituric acid (65.0 mg, 3.3×10^{-4} mol) was combined with 2-(2-acetanilidovinyl)-3-ethylbenzothiazolium iodide (130 mg, 3.0×10^{-4} mol) and pyridine (7 ml) in a 15 ml round bottom flask. The mixture was stirred to dissolve the reactants and then 3 drops of triethylamine added as a catalyst. The reaction mixture was refluxed for 45 minutes and the dye crystallized out of solution upon addition of cold methanol. The solution was placed in the refrigerator overnight and then the orange crystals were collected by vacuum filtration. The crystals were washed with cold methanol and weighed 105 mg or a 90.6% yield. mp 321-323 °C; $\lambda_{max.}^{MeOH}$ = 495 nm; $\varepsilon_{495} = 1.20 \times 10^5$; ^{1}H-NMR ($CDCl_3$) δ 1.30 (3H,t,J=6.79), 1.32 (3H,t, J=6.67), 1.51 (3H,t,J=7.40), 4.34 (2H,q,J=7.38), 4.58 (4H,q,J=6.97), 7.35 (1H,d,J=7.18), 7.37 (1H,t,J=7.84), 7.51 (1H,t,J=7.62), 7.69 (1H,d,J=7.37), 7.87 (1H,d, J=13.87), 8.43 (1H,d,J=14.08); Low

Resolution DIP EIMS: m/e 387 (100), 373 (13), 354 (72), 299 (46), 258 (15), 186 (39), 173 (14), 128 (17); High Resolution DIP EIMS: m/e 387.1085, $C_{19}H_{21}N_3O_2S_2$, MMU -1.0.

3-Ethyl-2-methylbenzothiazolium iodide (1). Iodoethane (25 ml, 3.1 x 10^{-1} mol) and 2-methylbenzothiazole (25 ml, 2.0 x 10^{-1} mol) were combined in a 250 ml round bottom flask and heated at reflux for 6 hours. The reaction mixture was cooled and the resulting precipitate was vacuum filtered. The filtrate was again refluxed for twelve hours. After cooling, the precipitate was filtered and the filtrate heated for a final twelve hours. After a final filtration the combined white crops of the white crystalline salt were washed with acetone and dried. A combined yield of 53% was obtained. mp. 195-196 °C; ^{1}H-NMR ($CDCl_3$) δ 1.62 (3H,t,J=7.39), 3.45, (3H,s), 4.95 (2H,q,J=7.42), 7.70 (1H,t,J=7.36), 7.81 (1H,t,J=8.47), 8.09 (1H,d, J=8.35), 8.32 (1H,d,J=8.03); ^{13}C-NMR ($CDCl_3$) δ 14.15 (q,J=128.4), 19.49 (q,J=134.2), 46.82 (t,J=145.4), 116.55 (d,J=166.5), 124.72 (d,J=171.0), 128.76 (d,J=172.7), 129.31 (s), 130.12 (d,J=164.5), 140.65 (s), 174.95 (s).

3-Ethyl-2-methylbenzoxazolium iodide. (2). Iodoethane (15 ml, 1.9 x 10^{-1} mol) and 2-methylbenzoxazole (20 ml, 1.7 x 10^{-1} mol) were combined in a 100 ml round bottom flask. The mixture was heated at reflux for twenty four hours. The resulting white crystals were filtered and washed with

acetone. The filtrate was again heated and the precipitate collected over a period of one week. The combined yield was 65%. mp. 198-200 °C; ^{1}H-NMR ($CDCl_3$) δ 1.63 (3H,t,J=7.45), 3.35 (3H,s), 4.74 (2H,q,J=7.41), 7.66 (2H,m), 7.78 (1H,m), 7.96 1H,m); ^{13}C-NMR ($CDCl_3$) δ 13.97 (q,J=129.9), 16.70 (q,J=134.6), 113.25 (d,J=168.1), 114.60 (d,J=172.3), 128.39 (d,J=166.1), 129.19 (s), 129.26 (d,J=167.0), 147.87 (s), 167.11 (s).

1-Ethyl-2,3,3-trimethylindolenium iodide (23). 2,3,3-Trimethylindolenine (20 ml, 1.3 x 10^{-1} mol) and iodoethane (20 ml, 2.5 x 10^{-1} mol) were combined in a 50 ml flask and refluxed for six hours. The resulting salt was vacuum filtered from the reaction mixture and washed with acetone. The reaction yielded 53% of the desired intermediate. mp. 231-2 °C; ^{1}H-NMR ($CDCl_3$) δ 1.59 (3H,t,J=7.55), 1.62 (6H,s), 3.12 (3H,s), 4.72 (2H,q,J=7.50), 7.55 (2H,m), 7.70 (2H,m); ^{13}C-NMR ($CDCl_3$) δ 13.46 (q,J=129.7), 16.79 (q,J=131.8), 22.90 (2C,q,J=131.8), 45.18 (t,J=145.1), 54.46 (s), 115.19 (d,J=162.7), 123.26 (d,J=166.4), 129.35 (d, J=163.6), 129.95 (d,J=163.9), 140.32 (s), 141.48 (s), 195.20 (s).

2-[1,3-(bis-1-ethyl-2-naphtho[1,2-d]thiazolenylidene)-isopropylidene]-1,3-indandione (ABMF). 9-Phenylthio-3,3-diethyl-β-naphthocarbocyanine ethylsulfate (590.0 mg, 8.4 x 10^{-4} mol) was dissolved in pyridine (15 ml) and triethylamine

(2 ml) added as a catalyst. 1,3-Indandione (240.0 mg, 1.6 x 10^{-3} mol) was then added and the reaction mixture brought to reflux for two and a half hours. The pyridine and triethylamine were evaporated to leave a sticky sludge. Methanol (150 ml) was added to the sludge and placed in the refrigerator for sixteen hours. The solution was then vacuum filtered and the resulting dye washed with cold methanol to yield 437.8 mg which is 87.2% of the theoretical value. mp. 302-3 °C; $\lambda_{max.}^{MeOH}$ = 602, 492; Low Resolution DIP FABMS (thioglycerol): m/e 609 (2), 530 (1), 488 (2), 471 (2), 455 (1), 446 (2), 430 (3), 413 (3), 397 (3), 380 (3), 364 (3), 347 (3), 338 (3), 322 (7), 307 (8).

3-Ethyl-2-benzoxazolinone (10). Sodium methoxide (11 g, 2.0 x 10^{-1} mol) was stirred into methanol (45 ml) in a 100 ml round bottom flask. The solution was stirred for ten minutes to dissolve as much of the sodium methoxide as possible. 2-Benzoxazolinone (25.0 g, 1.9 x 10^{-1} mol) and diethyl oxalate (30 ml, 2.2 x 10^{-1} mol) were then added and the reaction mixture refluxed for fifteen hours. 3-Ethyl-2-benzoxazolinone was isolated by vacuum distillation. The vacuum source was water aspiration. The distillation resulted in pure 3-ethyl-2-benzoxazolinone distilling at 165 °C. The compound is colorless and the yield was 21.32 g which was 70.5% of theoretical. ^{1}H-NMR ($CDCl_3$) δ 1.36 (3H,t,J=), 4.87 (2H,q,J=),

6.97 (1H,dd,J=7.61, 1.19), 7.09 (1H,dt,J=7.66, 1.40), 7.19 (2H,m); ^{13}C-NMR ($CDCl_3$) δ 12.82 (q,J=127.5), 36.97 (t,J=140.6), 108.02 (d,J=162.6), 109.78 (d,J=166.5), 122.10 (d,J=163.9), 123.60 (d,J=161.2), 130.68 (s), 142.56 (s), 154.09 (s); Low Resolution DIP EIMS: m/e 163 (100), 148 (57), 135 (67), 91 (21), 79 (27), 77 (27); High Resolution DIP EIMS: m/e 163.0645, $C_9H_9N_1O_2$, MMU -1.1.

o-Ethylaminophenol (20). 3-ethyl-2-benzoxazolinone (12.0 g, 7.4 x 10^{-2} mol) was dissolved in a sodium hydroxide solution (30 g NaOH/ 60 ml H_2O) and the reaction mixture refluxed for one hour. An additional 20 ml of water was added and refluxing continued for four more hours. The solution was cooled to room temperature and washed with diethyl ether (50 ml). The ether layer was discarded. Ice (25 g) was then added to the reaction mixture and then made acidic with concentrated hydrochloric acid. The reaction mixture was filtered and then made basic with sodium carbonate (powder). Once basic, orthoethylaminophenol readily crystallized out of solution. The crystals were filtered using vacuum filtration and washed with cold water. The crystals were allowed to dry at room temperature which resulted in 1.790 g for a 18.5% yield (82). mp. 105-110 °C; ^{1}H-NMR ($CDCl_3$) δ 1.26 (3H,brt,J=6.93), 3.12 (2H,brm), 3.97 (1H,brs), 6.69 (3H,brs),

6.84 (1H,brs); Low Resolution DIP EIMS: m/e 137 (59), 122 (99), 120 (100), 108 (8), 95 (18), 77 (20), 65 (29); High Resolution DIP EIMS: m/e 137.0845, $C_8H_{11}N_1O_1$, MMU -0.4.

1-(3,3-Dimethyl-1-Ethylindolinylidene)-2-propanone (24). 3-Ethyl-2,3,3-trimethylindolinium iodide (5.0 g, 1.6 x 10^{-2} mol) was combined with acetic anhydride (5 ml, 5.3 x 10^{-2} mol) in pyridine (20 ml) and triethylamine (5 ml) in a 50 ml round bottom flask. The reaction mixture was refluxed for three hours and then brought back to room temperature. The solution was roto-vapped near dryness and then 40 ml water was added. The mixture sat for twenty four hours and then the resulting white crystals collected by vacuum filtration and washed with cold water. We isolated 1.7 g for a 47.0% yield. mp. 78-79 °C; ^{1}H-NMR ($CDCl_3$) δ 1.23 (3H,t,J=7.23), 1.67 (6H,brs), 2.16 (3H,s), 3.70 (2H,brs), 5.31 (1H,brs), 6.71 (1H,brd,J=7.65), 6.95 (1H,t,J=7.39), 7.15 (2H,m); ^{13}C-NMR ($CDCl_3$) δ 10.81 (q,J=127.1), 23.07 (2C,q,J=122.1), 31.99 (q,J=125.8), 37.10 (t,J=134.2), 48.05 (s), 93.09 (d,J=147.4), 107.28 (d,J=154.9), 121.78 (2C,d,J=157.9), 127.34 (d,J=159.3), 140.11 (s), 142.47 (s), 169.36 (s), 193.20 (s); Low Resolution GC EIMS: m/e 229 (88), 214 (100), 199 (22), 186 (36), 170 (22), 158 (15), 144 (16), 115 (12), 91 (4), 77 (6); High Resolution DIP EIMS: m/e 229.1469, $C_{15}H_{19}N_1O_1$, MMU -0.2.

2-[2-(3,3-Dimethyl-1-ethyl-2-indolinylidene)-1-methylethylidene]-1,3-indandione (MEINDOLIND). 1-(3,3-dimethyl-1-ethylindolinylidene)-2-propanone (100 mg, 4.0 x 10^{-4} mol) was dissolved in freshly distilled toluene (2 ml). Triphosgene (39 mg, 1.5 x 10^{-4} mol) was then added and the reaction stirred at room temperature for half an hour after the final gas evolution. Triethylamine (0.5 ml) was added to the reaction mixture followed by 1,3-indandione (66 mg, 4.5 x 10^{-4} mol). The reaction mixture was refluxed for three hours and then cooled to room temperature. The solvents were evaporated off and the resulting tar taken up in diethyl ether (200 ml). The ether was filtered and then dried with anhydrous sodium sulfate. The ether was then evaporated off leaving the crude dye. Scraping the dye from the flask yielded 160 mg of crude dye which is 100% of theoretical. ^{1}H-NMR and low resolution DIP EIMS showed the crude mixture to be 75-80% of the pure dye. $\lambda_{max.}^{MeOH}$ = 496 nm; Low Resolution DIP EIMS: m/e 357 (100), 342 (71), 328 (26), 212 (90), 186 (78), 172 (74), 158 (44), 144 (17), 115 (16), 77 (21); High Resolution DIP EIMS: m/e 357.1719, $C_{24}H_{23}N_1O_2$, MMU 1.0.

1-(3-Ethylbenzothiazolinylidene)-2-propanone (22). 3-Ethyl-2-methylbenzothiazolium p-toluenesulfonate (0.75 g, 2.4 x 10^{-3} mol) was dissolved in pyridine (7 ml) and acetyl chloride slowly added (0.5 ml, 7.0 x 10^{-3} mol). The reaction

mixture was heated and stirred at 90 °C for ten minutes. The pyridine was taken off by rotary evaporation. Water was then added to the tar and allowed to sit at room temperature overnight. The lightly purple crystals were collected by vacuum filtration. The yield was 455 mg or 34% of the theoretical value. mp. 105-7 °C; ^{1}H-NMR ($CDCl_3$) δ 1.35 (3H,t,J=7.31), 2.22 (3H,s), 4.04 (2H,q,J=7.28), 5.85 (1H,brs), 7.09 (1H,d,J=8.18), 7.14 (1H,t,J=7.64), 7.32 (1H,t,J=8.42), 7.55 (1H,d,J=7.72); ^{13}C-NMR ($CDCl_3$) δ 11.56 (q,J=127.8), 28.85 (q,J=126.6), 40.55 (t,J=143.7), 89.78 (d,J=160.3), 109.49 (d,J=152.9), 122.39 (d,J=163.9), 122.60 (d,J=161.6), 126.35 (d,J=159.8), 127.36 (s), 139.02 (s), 159.84 (s), 190.97 (s); Low Resolution DIP EIMS: m/e 219 (100), 204 (98), 176 (50), 149 (75); High Resolution DIP EIMS: m/e 219.0732, $C_{12}H_{13}N_1O_1S_1$, MMU -1.5.

3-Ethyl-2-(methylthio)benzothiazolium triflouromethanesulfonate. 2-(Methylthio)benzothiazole (2.0 g, 1.0 x 10^{-2} mol) was dissolved in freshly distilled tetrahydrofuran (20 ml). Ethyl triflouromethanesulfonate (2.1 g, 1.1 x 10^{-2} mol, ethyl triflate), was slowly added and the reaction mixture stirred at room temperature for forty eight hours. This resulted in a white pasty sludge. Diethyl ether (50 ml) was then added to help precipitate the desired salt. The solution was vacuum filtered and washed with diethyl ether to yield

1.68 g of the salt. This is 40.3% of the theoretical yield. mp. 146-48 °C; ^{1}H-NMR ($CDCl_3$) δ 1.60 (3H,brs), 3.04 (3H,s), 3.40 (2H,brs), 7.59 (1H,t, J=7.94), 7.69 (1H,t,J=8.24), 7.88 (1H,d,J=8.12), 8.20 (1H,d,J=8.37); ^{13}C-NMR ($CDCl_3$) δ 17.94 (q,J=144.6), 26.46 (q,J=123.68), 70.61 (t,J=138.1), 117.94 (d, J=170.8), 119.01 (s), 121.98 (d,J=160.2), 127.75 (d,J=157.7), 129.92 (d,J=165.5), 141.70 (s), 179.81 (s).

REFERENCES CITED

REFERENCES CITED

1. L.G.S. Brooker, P.W. Vittum, The Journal of Photographic Science, 1957, **5**, p. 71-88.

2. F.M. Hamer, **The Chemistry of Heterocyclic Compounds, Vol. 18,** The Cyanine Dyes and Related Compounds, 1964, p. 441-587.

3. L.G.S. Brooker, P.W. Vittum, The Journal of Photographic Science, 1957, **5**, p. 71-88.

4. F.M. Hamer, **The Chemistry of Heterocyclic Compounds, Vol. 18,** The Cyanine Dyes and Related Compounds, 1964, p. 441-587.

5. L.G.S. Brooker, P.W. Vittum, The Journal of Photographic Science, 1957, **5**, p. 71-88.

6. D.M. Sturmer, D.W. Hazeltine, **The Theory of the Photographic Process, Fourth Edition,** T.H. James Ed., Sensitizing and Desensitizing Dyes, Chapter 8, 1977, pp. 194-234.

7. F.M. Hamer, **The Chemistry of Heterocyclic Compounds, Vol. 18,** The Cyanine Dyes and Related Compounds, 1964, p. 441-587.

8. D.M. Sturmer, D.W. Hazeltine, **The Theory of the Photographic Process, Fourth Edition,** T.H. James, Ed., Sensitizing and Desensitizing Dyes, Chapter 8, 1977, pp. 194-234.

9. D.M. Sturmer, **The Chemistry of Heterocyclic Compounds, Vol. 30,** Special topics in Heterocyclic Chemistry, 1977, A. Weissberger, E.C. Taylor , Eds., pp. 441-587.

10. I.J. Fox, L.G.S. Brooker, The American Journal of Physiology, 1956, **187(3)**, p. 599.

11. B. Seligmann, G.I. Gallin, Federation Proceedings, Federation of American Societies for Experimental Biology, 1981, **40(2)**, pp. 211-212.

12. H.D. Britt, W.B. Monig, Applied Spectroscopy, 1977, **31(2)**, pp. 104-9.

13. J.Y. Tsao, Optics Communications, 1986, **60(4)**, pp. 225-228.

14. B. Zhau, H. Xu, Huaxue Tongbau, 1983, **8**, pp. 22-26.

15. G.A. Chamberlain, Solar Cells, 1983, **10(3)**, pp. 199-210.

16. H. Oba, T. Sato, M. Umehara, Japan Kokai Tokkyo Koho JP 60,179,292 [85,179,292], 13 Sept. 1985, 8 pp.

17. K.K. Cannon, Japan Kokai Tokkyo Koho JP 58,219,091 [83,219,091], 20 Dec. 1983, 8 pp.

18. F.M. Hamer, **The Chemistry of Heterocyclic Compounds, Vol. 18**, The Cyanine Dyes and Related Compounds, 1964.

19. L.G.S. Brooker, P.W. Vittum, The Journal of Photographic Science, 1957, **5**, p. 71-88.

20. L.G.S. Brooker, G.H. Keyes, et. al., Journal of the American Chemical Society, 1951, **73**, pp. 5326-55.

21. G.E. Ficken, **The Chemistry of Synthetic Dyes, Vol. 4**, K. Venkataraman, Ed., 1971.

22. A.I. Kiprianov, Uspekhi Khimii, 1960, **29**, p. 1336.

23. A.I. Kiprianov, Ukrainskii Khimicheskii Zhurnal, 1952, **18**, p. 339.

24. A.I. Kiprianov, L.M. Yagupol'skii, Zhurnal Obshchei Khimii, 1950, **20**, p. 2111.

25. A.I. Kiprianov, Uspekhi Khimii, 1971, **40**, p. 594.

26. D.M. Sturmer, **The Chemistry of Heterocyclic Compounds, Vol. 30**, Special Topics in Heterocyclic Chemistry, 1977, A. Weissberger, E.C. Taylor , Eds., pp. 441-587.

27. D.M. Sturmer, D.W. Hazeltine, **The Theory of the Photographic Process, Fourth Edition**, T.H. James, ed., 1977.

28. L.G.S. Brooker, R.H Sprague, C.P. Smyth, G,L. Lewis, Journal of the American Chemical Society, 1940, **62**, p. 1116.

29. L.G.S. Brooker, **XIVth International Congress of Pure and Applied Chemistry**, Zurich, 1955, July 21-27, pp. 229-257.

30. L.G.S. Brooker, P.W. Vittum, The Journal of Photographic Science, 1957, 5, pp. 71-88.

31. C.L. Enwall, **Temperature Studies on Allopolar Isomerism**, Master of Science Thesis, Montana State University, 1968, p. 21.

32. L.G.S. Brooker, **XIVth International Congress of Pure and Applied Chemistry**, Zurich, 1955, July 21-27, pp. 229-257.

33. D.M. Sturmer, **The Chemistry of Heterocyclic Compounds, Vol. 30**, Special Topics in Heterocyclic Chemistry, 1977, A. Weissberger, E.C. Taylor , Eds., pp. 441-587.

34. D.M. Sturmer, D.W. Hazeltine, **The Theory of the Photographic Process, Fourth Edition**, T.H. James, ed., 1977, p. 198.

35. D.M. Sturmer, D.W. Hazeltine, **The Theory of the Photographic Process, Fourth Edition**, T.H. James, ed., 1977, p. 199.

36. D.M. Sturmer, **The Chemistry of Heterocyclic Compounds, Vol. 30**, Special Topics in Heterocyclic Chemistry, 1977, A. Weissberger, E.C. Taylor , Eds., p. 457.

37. D.M. Sturmer, D.W. Hazeltine, **The Theory of the Photographic Process, Fourth Edition**, T.H. James, ed., 1977, p. 198.

38. L.G.S. Brooker, P.W. Vittum, The Journal of Photographic Science, 1957, 5, pp. 71-88.

39. A.M. Bowler, **Determination of the Relative Steric Sizes of Alkyl Groups Using a Calculational Approach**, Master of Science Thesis, Montana State University, 1986.

40. L.G.S. Brooker, **The Theory of the Photographic Process**, C.E.K. Mees and T.H. James, Eds., 1966, p. 198.

41. M.M. Kul'chitskii, A. Il'chenko, L.M. Yagulpol'skii, Zhurnal Organicheskoj Khimii, 1973, **9**, p. 827.

42. D. Schelz, Helvetica Chimica Acta, 1975, **58**, pp. 1207-1216.

43. Junek, Fischer-Colbrie, Aigner, Braun, Helvetica Chemica Acta, 1972, **55(5)**, pp. 1459-1456.

44. **Aldrich**, 1988-1989, p. 340.

45. L.B. Kilgore, J.H. Ford, W.C. Wolfe, Industrial and Engineering Chemistry, 1942, **34(4)**, pp. 494-497.

46. N.N. Sveshnikov, I.I. Levkoev, N.I. Shirokova, N.A. Damir, Doklady Akademii Nauk SSSR, 1962, **148(5)**, pp. 1091-1094.

47. L. Oliveros, H. Wahl, Bulletin de le Societe Chimique de France, 1979, **9**, pp. 3204-3209.

48. N.N. Sveshnikov, I.I. Levkoev, N.I. Shirokova, N.A. Damir, Doklady Akademii Nauk SSSR, 1962, **148(5)**, pp. 1091-1094.

49. A. Whitaker, Zeitschrift fur Kristallographie, Bd., 1975, **142**, pp. 442-446.

50. D.L. Smith, Photographic Science and Engineering, 1974, **18(3)**, pp. 309-322.

51. K. Nakao, K. Yakeno, H. Yoshioka, K. Nakatsu, Acta Crystallogr., Sect. B, 1979, **B35(2)**, pp. 415-419.

52. K. Nakatsu, H. Yoshioka, S. Nishigaki, Nippon Shashin Gakkaishi, 1983, **46(2)**, pp. 89-98.

53. S. Lu, Z. Cai, Y. Chang, X. Jin, S. Zhou, R. Qian, Huaxue Xuebao, 1982, **40(7)**, pp. 657-665.

54. R. Larsen, M. Ellerd, Personal Communication, 1989, Montana State University.

55. C. Bai, Y. Chang, X. Xu, Kexue Tongbao, 1982, **27(15)**, pp. 922-924.

56. R. Radgelia, S. Dahne, Journal of Molecular Structure, 1970, 5, pp. 399-411.

57. R. Radeglia, A. Weber, Journal fur Praktische Chemie, 1972, **314(5-6)**, pp. 884-890.

58. E. Kleinpeter, R. Borsdorf, G. Bach, J.V. Grossmann, Journal fur Praktische Chemie, 1973, **315(4)**, pp. 587-599.

59. E. Kleinpeter, R. Borsdorf, G. Bach, J.V. Grossmann, Zeitschrift fuer Chemie, 1974, **5**, pp. 194-195.

60. R. Radeglia, E. Gey, T. Steiger, S. Kulpe, R. Luck, M. Ruthenberg, M. Sterl, S. Dahne, Journal fur Praktische Chime, 1974, **316(5)**, pp. 766-772.

61. W. Grahn, Tetrahedron, 1976, **32**, pp. 1931-1939.

62. P. Scheibe, S. Schneider, F. Dorr, E. Daltrozzo, Berichte der Bunsen-Gesellschaft, 1976, **80(7)**, pp.630-638.

63. A. Mehlhorn, J. Sauer, Zeitschrift fuer Chemie, 1978, **18**, pp. 339-340.

64. R. Bohme, E. Breitmaier, Liebigs Annalen der Chemie, 1985, pp. 1288-1296.

65. A.E. Derome, **Modern NMR Techniques for Chemistry Research**, 1987, Pergamon Press, p. 9.

66. A.E. Derome, **Modern NMR Techniques for Chemistry Research**, 1987, Pergamon Press, p. 227.

67. K. Nagayama, et. al., Journal of Magnetic Resonance, 1980, **40**, pp. 321.

68. D.H. Williams, I. Fleming, **Spectroscopic Methods in Organic Chemistry, Third Edition**, 1980, McGraw-Hill, p. 145.

69. A.E. Derome, **Modern NMR Techniques for Chemistry Research**, 1987, Pergamon Press, pp. 97-127.

70. M. Kinns, J.K.M. Sanders, Journal of Magnetic Resonance, 1984, **56**, p. 518.

71. A.E. Derome, **Modern NMR Techniques for Chemistry Research**, 1987, Pergamon Press, p. 106.

72. N. Chandrakumar, S. Subramanian, **Modern Techniques in High-Resolution FT-NMR**, 1987, Springer-Verlag, pp. 365-369.

73. R. Freeman, **A Handbook of Nuclear Magnetic Resonance**, 1987, Longman Scientific & Technical, pp. 142-147.

74. A.E. Derome, **Modern NMR Techniques for Chemistry Research**, 1987, Pergamon Press, p. 245-258.

75. A. Bax, G. Morris, Journal of Magnetic Resonance, 1981, **42**, p. 501.

76. R. Bohme, E. Breitmaier, Liebigs Annalen der Chemie, 1985, pp. 1288-1296.

77. A. Bax, S. Subramanian, Journal of Magnetic Reesonance, 1986, **67**, pp. 565-569.

78. A.E. Derome, **Modern NMR Techniques for Chemistry Research**, 1987, Pergamon Press, p. 254.

79. H. Kessler, et. al., Journal of Magnetic Resonance, 1984, **57**, p. 331.

80. A. Bax, M.F. Summers, Journal of the American Chemical Society, 1986, **108**, pp. 2093-2094.

81. D.M. Sturmer, D.W. Hazeltine, **The Theory of the Photographic Process, Fourth Edition**, T.H. James, ed., 1977, p. 209.

82. H. Larive, R.J. Dennilauer, Kodak-Pathe, FR. 1,274,963, Feb. 28, 1962, 3 pp.

83. H. Larive, R.J. Dennilauer, Eastman Kodak Company, U.S. 3,149,105 (Cl.260-240.7), Sept. 15, 1964, 5 pp.

84. G.W. Anderson, F. Bell, **Beilstein Handbuch der Organischen Chemie, 6**, p. 763.

APPENDICES

APPENDIX A

ATOMIC COORDINATES

Table 12. Atomic coordinates (x 10^4) and isotropic thermal parameters ($Å^2$ x 10^3) for BTHIND with water in the crystal lattice.

	x	y	z	U
C(1)	8335 (5)	3890 (4)	5932 (4)	46 (2)*
S(1)	9397 (2)	4740 (1)	7402 (1)	63 (1)*
N(1)	8456 (5)	2638 (3)	5944 (3)	50 (2)*
C(2)	7503 (6)	4440 (4)	4872 (4)	52 (2)*
C(3)	7268 (6)	5685 (4)	4914 (4)	52 (2)*
C(4)	6480 (6)	6297 (4)	3902 (4)	50 (2)*
C(5)	9673 (6)	1082 (4)	7386 (5)	65 (2)*
C(6)	10597 (7)	963 (5)	8604 (5)	78 (3)*
C(7)	11204 (7)	1992 (5)	9520 (5)	81 (3)*
C(8)	10922 (6)	3211 (5)	9247 (5)	73 (2)*
C(9)	9974 (6)	3356 (4)	8018 (4)	57 (2)*
C(10)	9374 (6)	2302 (4)	7105 (4)	55 (2)*
C(11)	6247 (6)	7620 (4)	4034 (4)	51 (2)*
C(12)	5693 (6)	5753 (4)	2604 (4)	56 (2)*
C(13)	4750 (6)	8981 (4)	2329 (5)	59 (2)*
C(14)	3938 (7)	8989 (5)	1062 (5)	69 (3)*
C(15)	3678 (7)	7925 (5)	209 (5)	74 (3)*
C(16)	4203 (6)	6798 (5)	610 (4)	68 (2)*
C(17)	5008 (6)	6797 (4)	1887 (4)	52 (2)*
C(18)	5303 (6)	7884 (4)	2740 (4)	50 (2)*
C(19)	7613 (6)	1676 (4)	4867 (4)	61 (2)*
C(20)	8761 (7)	1657 (5)	3926 (5)	97 (3)*
O(1)	6694 (4)	8386 (3)	4986 (3)	67 (1)*
O(2)	5553 (4)	4649 (3)	2131 (3)	76 (2)*
O(3a)	6147 (26)	8008 (16)	7518 (16)	100 (5)*
O(3b)	6760 (36)	7796 (35)	7545 (29)	148 (13)*

* Equivalent isotropic U defined as one third of the trace of the orthogonalised U_{ij} tensor.

Table 13. Atomic coordinates (x 10^4) and isotropic thermal parameters ($Å^2$ x 10^3) for BOXIND.

	x	y	z	U
C(1)	3406 (4)	-566 (2)	5638 (2)	50 (1)*
O(1)	3997 (2)	257 (1)	6143 (1)	57 (1)*
N(1)	4097 (3)	-1369 (2)	6115 (2)	52 (1)*
C(2)	2298 (4)	-505 (2)	4788 (2)	52 (1)*
C(3)	1655 (3)	400 (2)	4432 (2)	51 (1)*
C(4)	519 (3)	585 (2)	3601 (2)	48 (1)*
C(5)	6254 (4)	-1590 (3)	7632 (2)	67 (1)*
C(6)	7198 (4)	-1018 (3)	8336 (2)	79 (2)*
C(7)	7103 (4)	-1 (3)	8337 (2)	77 (1)*
C(8)	6052 (4)	519 (3)	7628 (2)	70 (1)*
C(9)	5132 (4)	-51 (2)	6935 (2)	53 (1)*
C(10)	5211 (4)	-1072 (2)	6922 (2)	51 (1)*
C(11)	-68 (4)	1582 (2)	3324 (2)	52 (1)*
C(12)	-284 (4)	-106 (2)	2882 (2)	51 (1)*
C(13)	-2185 (4)	2221 (2)	1851 (2)	61 (1)*
C(14)	-3210 (4)	1935 (2)	1015 (2)	68 (1)*
C(15)	-3329 (4)	946 (3)	746 (2)	71 (1)*
C(16)	-2434 (4)	215 (2)	1311 (2)	65 (1)*
C(17)	-1398 (3)	499 (2)	2140 (2)	50 (1)*
C(18)	-1266 (3)	1498 (2)	2400 (2)	49 (1)*
C(19)	3803 (4)	-2405 (2)	5819 (2)	63 (1)*
C(20)	5143 (5)	-2747 (3)	5338 (3)	96 (2)*
O(2)	308 (3)	2367 (1)	3750 (2)	74 (1)*
O(3)	-115 (3)	-1012 (1)	2863 (2)	73 (1)*

* Equivalent isotropic U defined as one third of the trace of the orthogonalised U_{ij} tensor.

Table 14. Atomic coordinates (x 10^4) and isotropic thermal parameters ($Å^2$ x 10^3) for BTHHRO.

	x	y	z	U
C(1)	2360 (5)	5425 (3)	4555 (3)	43 (1)*
S(1)	2080 (1)	4503 (1)	3070 (1)	51 (1)*
N(1)	2387 (4)	6675 (2)	4417 (3)	43 (1)*
C(2)	2542 (5)	4940 (3)	5686 (4)	47 (2)*
C(3)	2483 (5)	3634 (4)	5757 (4)	47 (2)*
C(4)	2649 (5)	3070 (3)	6839 (3)	43 (1)*
C(5)	2342 (5)	8140 (4)	2774 (4)	55 (2)*
C(6)	2252 (5)	8197 (4)	1502 (4)	63 (2)*
C(7)	2132 (5)	7127 (4)	664 (4)	63 (2)*
C(8)	2071 (5)	5948 (4)	1057 (4)	55 (2)*
C(9)	2141 (5)	5855 (3)	2323 (3)	44 (1)*
C(10)	2294 (4)	6952 (3)	3173 (3)	42 (1)*
C(11)	2576 (5)	1718 (3)	6840 (4)	47 (2)*
C(12)	3004 (5)	2448 (3)	9035 (4)	49 (2)*
C(13)	2763 (5)	7702 (3)	5513 (3)	52 (2)*
C(14)	4934 (6)	8296 (4)	6148 (4)	74 (2)*
O	2392 (4)	893 (2)	5940 (3)	61 (1)*
N(2)	2748 (4)	1443 (3)	8101 (3)	47 (1)*
S(2)	2998 (1)	3865 (1)	8395 (1)	52 (1)*
S(3)	3312 (2)	2409 (1)	10585 (1)	74 (1)*
C(15)	2666 (6)	114 (4)	8343 (4)	60 (2)*
C(16	608 (6)	-733 (4)	7915 (5)	82 (2)*

* Equivalent isotropic U defined as one third of the trace of the orthogonalised U_{ij} tensor.

Table 15. Atomic coordinates (x 10^4) and isotropic thermal parameters ($Å^2$ x 10^3) for BTHIND.

	x	y	z	U
C(1)	8331 (1)	2594 (3)	5740 (1)	34 (1)*
S(1)	8966 (1)	1917 (1)	5123 (1)	43 (1)*
N(1)	7585 (1)	1216 (3)	5675 (1)	36 (1)*
C(2)	8535 (1)	4332 (3)	6215 (1)	37 (1)*
C(3)	9365 (2)	5556 (3)	6322 (1)	37 (1)*
C(4)	9621 (1)	7338 (3)	6772 (1)	35 (1)*
C(5)	6822 (2)	-1996 (4)	4956 (1)	43 (1)*
C(6)	6885 (2)	-3457 (4)	4419 (1)	47 (1)*
C(7)	7619 (2)	-3349 (3)	4087 (1)	47 (1)*
C(8)	8300 (2)	-1760 (3)	4273 (1)	41 (1)*
C(9)	8232 (1)	-279 (3)	4801 (1)	35 (1)*
C(10)	7511 (1)	-395 (3)	5150 (1)	34 (1)*
C(11)	10548 (2)	8455 (3)	6910 (1)	37 (1)*
O(1)	11239 (1)	8014 (3)	6693 (1)	55 (1)*
C(12)	9052 (1)	8372 (3)	7182 (1)	35 (1)*
O(2)	8238 (1)	7877 (3)	7226 (1)	48 (1)*
C(13)	11196 (2)	11903 (3)	7668 (1)	44 (1)*
C(14)	10971 (2)	13435 (4)	8115 (1)	51 (1)*
C(15)	10098 (2)	13375 (4)	8276 (1)	54 (1)*
C(16)	9413 (2)	11773 (3)	8001 (1)	46 (1)*
C(17)	9637 (2)	10244 (3)	7560 (1)	36 (1)*
C(18)	10516 (2)	10306 (3)	7396 (1)	36 (1)*
C(19)	6904 (2)	1441 (4)	6113 (1)	42 (1)*
C(20)	5986 (2)	2660 (4)	5654 (2)	60 (1)*

* Equivalent isotropic U defined as one third of the trace of the orthogonalised U_{ij} tensor.

Table 16. Atomic coordinates (x 10^4) and isotropic thermal parameters ($Å^2$ x 10^3) for MEBTHRHO.

	x	y	z	U
C(1)	-3245 (2)	339 (2)	5851 (2)	38 (1)*
S(1)	-3364 (1)	-1354 (1)	5796 (1)	46 (1)*
N(1)	-4253 (1)	769 (1)	6943 (1)	39 (1)*
C(2)	-2320 (2)	1190 (2)	4960 (2)	41 (1)*
C(3)	-1218 (2)	888 (2)	3818 (2)	38 (1)*
C(4)	-423 (2)	1909 (2)	3018 (2)	40 (1)*
C(5)	-6273 (2)	0 (2)	8836 (2)	51 (1)*
C(6)	-7031 (2)	-1090 (2)	9447 (2)	60 (1)*
C(7)	-6687 (2)	-2324 (2)	8954 (2)	61 (1)*
C(8)	-5591 (2)	-2490 (2)	7843 (2)	56 (1)*
C(9)	-4809 (2)	-1414 (2)	7214 (2)	44 (1)*
C(10)	-5147 (2)	-179 (2)	7704 (2)	41 (1)*
S(2)	925 (1)	1636 (1)	1558 (1)	48 (1)*
C(11)	1288 (2)	3319 (2)	1216 (2)	44 (1)*
N(2)	420 (2)	4048 (2)	2158 (1)	45 (1)*
C(12)	-564 (2)	3324 (2)	3214 (2)	44 (1)*
S(3)	2528 (1)	3897 (1)	-116 (1)	62 (1)*
O	-1359 (2)	3890 (1)	4095 (1)	59 (1)*
C(13)	-880 (2)	-527 (2)	3424 (2)	50 (1)*
C(14)	-4434 (2)	2153 (2)	7255 (2)	52 (1)*
C(15)	-5497 (3)	3397 (2)	6462 (3)	83 (1)*
C(16)	432 (2)	5532 (2)	2111 (2)	57 (1)*
C(17)	1631 (3)	5522 (3)	2785 (3)	84 (1)*

* Equivalent isotropic U defined as one third of the trace of the orthogonalised U_{ij} tensor.

Table 17. Atomic coordinates (x 10^4) and isotropic thermal parameters ($Å^2$ x 10^3) for MEBTHIND.

	x	y	z	U
C(1)	2716 (5)	3387 (3)	5520 (2)	45 (1)*
S(1)	3436 (1)	3447 (1)	6429 (1)	51 (1)*
N(1)	2428 (5)	2318 (2)	5322 (2)	61 (1)*
C(2)	2441 (5)	4245 (3)	5039 (2)	46 (1)*
C(3)	2660 (4)	5358 (3)	5166 (2)	42 (1)*
C(4)	2316 (4)	6096 (2)	4591 (2)	42 (1)*
C(5)	2743 (6)	416 (3)	5796 (2)	68 (2)*
C(6)	3175 (6)	-196 (3)	6407 (2)	72 (2)*
C(7)	3669 (6)	293 (3)	7062 (2)	69 (2)*
C(8)	3803 (5)	1410 (3)	7121 (2)	63 (1)*
C(9)	3384 (5)	2035 (3)	6516 (2)	48 (1)*
C(10)	2830 (5)	1548 (3)	5856 (2)	54 (1)*
C(11)	2485 (5)	7287 (3)	4622 (2)	48 (1)*
O(1)	2937 (4)	7899 (2)	5127 (1)	71 (1)*
C(12)	1685 (5)	5813 (3)	3855 (2)	46 (1)*
O(2)	1359 (4)	4903 (2)	3589 (1)	66 (1)*
C(13)	1873 (5)	8765 (3)	3626 (2)	61 (1)*
C(14)	1287 (6)	8936 (3)	2913 (2)	70 (2)*
C(15)	826 (5)	8072 (3)	2469 (2)	67 (1)*
C(16)	915 (5)	7006 (3)	2719 (2)	60 (1)*
C(17)	1473 (5)	6843 (3)	3434 (2)	47 (1)*
C(18)	1942 (4)	7708 (3)	3882 (2)	46 (1)*
C(19)	3256 (5)	5776 (3)	5898 (2)	58 (1)*
C(20)	1430 (7)	1987 (4)	4575 (2)	83 (2)*
C(21)	2842 (7)	1853 (4)	4120 (3)	107 (2)*

* Equivalent isotropic U defined as one third of the trace of the orthogonalised U_{ij} tensor.

Table 18. Atomic coordinates (x 10^4) and isotropic thermal parameters ($Å^2$ x 10^3) for 1-(3-ethyl-2-benzothiazolylidene)-2-propanone.

	x	y	z	U
C(1)	6988 (2)	4470 (2)	4700 (1)	29 (1)*
C(2)	5793 (2)	3995 (2)	3487 (1)	33 (1)*
C(3)	5445 (2)	4962 (2)	2714 (1)	33 (1)*
C(4)	4216 (3)	4381 (2)	1436 (2)	45 (1)*
S(1)	8174 (1)	6339 (1)	5392 (1)	33 (1)*
N(1)	7335 (2)	3500 (1)	5452 (1)	31 (1)*
C(5)	9282 (2)	3467 (2)	7540 (2)	40 (1)*
C(6)	10532 (3)	4378 (3)	8609 (2)	47 (1)*
C(7)	11084 (3)	5970 (3)	8741 (2)	47 (1)*
C(8)	10433 (2)	6686 (2)	7806 (2)	40 (1)*
C(9)	9191 (2)	5771 (2)	6718 (1)	32 (1)*
C(10)	8614 (2)	4194 (2)	6599 (1)	31 (1)*
O(1)	6207 (2)	6447 (2)	3095 (1)	44 (1)*
C(11)	6525 (2)	1828 (2)	5116 (2)	37 (1)*
C(12)	7748 (3)	808 (2)	4586 (3)	62 (1)*
CL	2641 (1)	10243 (1)	2056 (1)	57 (1)*
O(2)	8207 (3)	9264 (2)	706 (2)	74 (1)*
O(3)	5460 (2)	8004 (2)	1489 (2)	59 (1)*

* Equivalent isotropic U defined as one third of the trace of the orthogonalised U_{ij} tensor.

Table 19. Atomic coordinates (x 10^4) and isotropic thermal parameters ($Å^2$ x 10^3) for ABMF.

	x	y	z	U
C(1)	5248 (3)	2789 (3)	6742 (2)	44 (1)*
S(1)	5954 (1)	2065 (1)	5843 (1)	52 (1)*
N(1)	5649 (3)	4513 (2)	6778 (1)	45 (1)*
C(2)	4344 (3)	1660 (3)	7307 (2)	47 (1)*
C(3)	3820 (3)	-144 (3)	7075 (2)	53 (1)*
C(4)	2913 (3)	-1404 (3)	7673 (2)	48 (1)*
C(5)	4130 (3)	2288 (3)	8206 (2)	49 (1)*
C(6)	2321 (3)	1924 (3)	8376 (2)	48 (1)*
C(7)	7115 (3)	7039 (3)	5981 (2)	57 (1)*
C(8)	7991 (4)	7560 (4)	5286 (2)	65 (1)*
C(9)	8311 (4)	6395 (4)	4734 (2)	65 (1)*
C(10)	7753 (3)	4698 (4)	4864 (2)	57 (1)*
C(11)	6877 (3)	4150 (3)	5567 (2)	48 (1)*
O(1)	4106 (3)	-754 (2)	6380 (1)	77 (1)*
C(12)	6565 (3)	5315 (3)	6118 (2)	47 (1)*
O(2)	5444 (2)	3099 (3)	8796 (1)	63 (1)*
C(13)	5089 (3)	5545 (3)	7375 (2)	53 (1)*
C(14)	6603 (4)	6636 (4)	8153 (2)	70 (1)*
C(15)	1357 (3)	-2836 (3)	7289 (2)	56 (1)*
C(16)	535 (4)	-4073 (4)	7798 (2)	68 (1)*
C(17)	1260 (4)	-3919 (4)	8706 (2)	72 (1)*
C(18)	2795 (4)	-2542 (4)	9087 (2)	68 (1)*
C(19)	3617 (4)	-1282 (3)	8578 (2)	58 (1)*
C(20)	2110 (4)	2146 (4)	9253 (2)	64 (1)*
C(21)	479 (5)	1885 (4)	9431 (2)	80 (2)*
C(22)	-957 (4)	1445 (4)	8746 (3)	83 (2)*
C(23)	-816 (4)	1201 (4)	7861 (2)	75 (1)*
C(24)	831 (3)	1423 (3)	7674 (2)	58 (1)*

* Equivalent isotropic U defined as one third of the trace of the orthogonalised U_{ij} tensor.

APPENDIX B

BOND LENGTHS

Table 20. Bond lengths (Å) for BTHIND with disordered water.

C(1)-S(1)	1.740	(4)	C(1)-N(1)	1.349	(5)
C(1)-C(2)	1.400	(6)	S(1)-C(9)	1.737	(5)
N(1)-C(10)	1.403	(5)	N(1)-C(19)	1.457	(5)
C(2)-C(3)	1.372	(6)	C(3)-C(4)	1.386	(6)
C(4)-C(11)	1.459	(6)	C(4)-C(12)	1.445	(6)
C(5)-C(6)	1.381	(7)	C(5)-C(10)	1.393	(7)
C(6)-C(7)	1.374	(7)	C(7)-C(8)	1.386	(8)
C(8)-C(9)	1.405	(6)	C(9)-C(10)	1.391	(6)
C(11)-C(18)	1.497	(6)	C(11)-O(1)	1.223	(5)
C(12)-C(17)	1.499	(7)	C(12)-O(2)	1.232	(5)
C(13)-C(14)	1.376	(7)	C(13)-C(18)	1.382	(7)
C(14)-C(15)	1.381	(8)	C(15)-C(16)	1.399	(8)
C(16)-C(17)	1.383	(6)	C(17)-C(18)	1.394	(6)
C(19)-C(20)	1.487	(8)	O(3a)-H(3a)	0.960	(35)
O(3a)-H(3b)	0.960	(31)	O(3b)-H(3a)	0.960	(42)
O(3b)-H(3b)	0.960	(52)			

Table 21. Bond lengths (Å) for BOXIND.

C(1)-O(1)	1.361	(3)	C(1)-N(1)	1.343	(3)
C(1)-C(2)	1.375	(4)	O(1)-C(9)	1.383	(3)
N(1)-C(10)	1.386	(3)	N(1)-C(19)	1.464	(3)
C(2)-C(3)	1.382	(4)	C(3)-C(4)	1.385	(4)
C(4)-C(11)	1.451	(4)	C(4)-C(12)	1.451	(4)
C(5)-C(6)	1.381	(5)	C(5)-C(10)	1.383	(4)
C(6)-C(7)	1.371	(6)	C(7)-C(8)	1.386	(4)
C(8)-C(9)	1.361	(4)	C(9)-C(10)	1.376	(4)
C(11)-C(18)	1.492	(4)	C(11)-O(2)	1.232	(3)
C(12)-C(17)	1.498	(4)	C(12)-O(3)	1.227	(3)
C(13)-C(14)	1.380	(4)	C(13)-C(18)	1.377	(4)
C(14)-C(15)	1.385	(5)	C(15)-C(16)	1.388	(4)
C(16)-C(17)	1.375	(4)	C(17)-C(18)	1.395	(4)
C(19)-C(20)	1.475	(5)			

Table 22. Bond lengths (Å) for BTHRHO.

C(1)-S(1)	1.751	(4)	C(1)-N(1)	1.362	(4)
C(1)-C(2)	1.371	(5)	S(1)-C(9)	1.732	(4)
N(1)-C(10)	1.407	(5)	N(1)-C(13)	1.464	(4)
C(2)-C(3)	1.404	(5)	C(3)-C(4)	1.367	(5)
C(4)-C(11)	1.442	(5)	C(4)-S2	1.749	(4)
C(5)-C(6)	1.382	(6)	C(5)-C(10)	1.384	(5)
C(6)-C(7)	1.369	(6)	C(7)-C(8)	1.372	(6)
C(8)-C(9)	1.386	(6)	C(9)-C(10)	1.392	(5)
C(11)-O	1.214	(5)	C(11)-N(2)	1.415	(5)
C(12)-N(2)	1.352	(5)	C(12)-S(2)	1.736	(4)
C(12)-S(3)	1.649	(4)	C(13)-C(14)	1.505	(5)
N(2)-C(15)	1.469	(5)	C(15)-C(16)	1.495	(5)

Table 23. Bond lengths (Å) for BTHIND.

C(1)-S(1)	1.733	(3)	C(1)-N(1)	1.365	(3)
C(1)-C(2)	1.386	(3)	S(1)-C(9)	1.744	(2)
N(1)-C(10)	1.394	(3)	N(1)-C(19)	1.468	(3)
C(2)-C(3)	1.384	(3)	C(3)-C(4)	1.388	(3)
C(4)-C(11)	1.452	(3)	C(4)-C(12)	1.450	(3)
C(5)-C(6)	1.386	(3)	C(5)-C(10)	1.389	(3)
C(6)-C(7)	1.385	(4)	C(7)-C(8)	1.376	(3)
C(8)-C(9)	1.384	(3)	C(9)-C(10)	1.391	(3)
C(11)-C(18)	1.502	(3)	C(11)-O(1)	1.222	(3)
C(12)-C(17)	1.496	(3)	C(12)-O(2)	1.236	(3)
C(13)-C(14)	1.393	(4)	C(13)-C(18)	1.386	(3)
C(14)-C(15)	1.381	(4)	C(15)-C(16)	1.393	(3)
C(16)-C(17)	1.383	(3)	C(17)-C(18)	1.393	(3)
C(19)-C(20)	1.499	(3)			

Table 24. Bond lengths (Å) for MEBTHRHO.

C(1)-C(2)	1.383	(2)	C(1)-N(1)	1.374	(2)
C(1)-S(1)	1.745	(2)	S(1)-C(9)	1.741	(2)
N(1)-C(10)	1.391	(2)	C(2)-C(3)	1.412	(2)
C(3)-C(4)	1.389	(2)	C(3)-C(13)	1.507	(3)
C(4)-S(2)	1.755	(2)	C(4)-C(12)	1.447	(3)
N(1)-C(14)	1.464	(3)	C(5)-C(6)	1.389	(3)
C(5)-C(10)	1.391	(2)	C(6)-C(7)	1.393	(4)
C(7)-C(8)	1.360	(3)	C(8)-C(9)	1.394	(3)
C(9)-C(10)	1.393	(3)	S(2)-C(11)	1.727	(2)
C(11)-N(2)	1.353	(2)	C(11)-S(3)	1.655	(2)
N(2)-C(12)	1.417	(2)	N(2)-C(16)	1.466	(3)
C(12)-O	1.199	(2)	C(14)-C(15)	1.488	(3)
C(16)-C(17)	1.478	(4)			

Table 25. Bond lengths (Å) for MEBTHIND.

C(1)-C(2)	1.387	(4)	C(1)-S(1)	1.738	(3)
C(1)-N(1)	1.370	(4)	C(2)-C(3)	1.389	(4)
C(3)-C(4)	1.411	(4)	C(3)-C(19)	1.492	(4)
C(4)-C(11)	1.464	(4)	C(4)-C(12)	1.456	(4)
S(1)-C(9)	1.737	(3)	N(1)-C(10)	1.386	(4)
N(1)-C(20)	1.568	(5)	C(5)-C(6)	1.382	(6)
C(5)-C(10)	1.391	(5)	C(6)-C(7)	1.383	(6)
C(7)-C(8)	1.374	(6)	C(8)-C(9)	1.379	(5)
C(9)-C(10)	1.399	(5)	C(11)-O(1)	1.227	(4)
C(11)-C(18)	1.499	(5)	C(12)-O(2)	1.234	(4)
C(12)-C(17)	1.488	(5)	C(13)-C(14)	1.380	(6)
C(13)-C(18)	1.380	(5)	C(14)-C(15)	1.368	(6)
C(15)-C(16)	1.386	(5)	C(16)-C(17)	1.378	(5)
C(17)-C(18)	1.375	(5)	C(20)-C(21)	1.419	(8)

Table 26. Bond lengths (Å) for 1-(3-ethyl-2-benzothiazolylidene)-2-propanone.

C(1)-C(2)	1.416 (2)	C(1)-S(1)	1.727 (1)
C(1)-N(1)	1.346 (2)	C(2)-C(3)	1.362 (3)
C(3)-C(4)	1.489 (2)	C(3)-O(1)	1.319 (2)
S(1)-C(9)	1.734 (2)	N(1)-C(10)	1.403 (2)
N(1)-C(11)	1.477 (2)	C(5)-C(6)	1.385 (2)
C(5)-C(10)	1.391 (3)	C(6)-C(7)	1.397 (3)
C(7)-C(8)	1.377 (3)	C(8)-C(9)	1.398 (2)
C(9)-C(10)	1.390 (2)	O(1)-H(1)	0.860 (23)
C(11)-C(12)	1.504 (3)	O(2)-H(2a)	0.860 (15)
O(2)-H(2b)	0.860 (9)	O(3)-H(3a)	0.860 (23)
O(3)-H(3b)	0.860 (23)		

Table 27. Bond lengths (Å) for ABMF.

C(1)-C(2)	1.401 (3)	C(1)-N(1)	1.361 (3)
C(1)-S(1)	1.746 (3)	C(2)-C(3)	1.423 (4)
C(2)-C(5)	1.503 (4)	C(3)-C(4)	1.497 (4)
C(3)-O(1)	1.249 (4)	C(4)-C(15)	1.395 (3)
C(4)-C(19)	1.377 (3)	C(5)-C(6)	1.485 (4)
C(5)-O(2)	1.221 (3)	C(6)-C(20)	1.384 (4)
C(6)-C(24)	1.394 (3)	S(1)-C(11)	1.738 (3)
N(1)-C(12)	1.405 (3)	N(1)-C(13)	1.476 (4)
C(7)-C(8)	1.378 (4)	C(7)-C(12)	1.389 (4)
C(8)-C(9)	1.392 (5)	C(9)-C(10)	1.365 (4)
C(10)-C(11)	1.392 (4)	C(11)-C(12)	1.389 (4)
C(13)-C(14)	1.521 (3)	C(15)-C(16)	1.368 (4)
C(16)-C(17)	1.383 (4)	C(17)-C(18)	1.362 (4)
C(18)-C(19)	1.380 (4)	C(20)-C(21)	1.363 (5)
C(21)-C(22)	1.354 (5)	C(22)-C(23)	1.379 (5)
C(23)-C(24)	1.389 (4)		

APPENDIX C

BOND ANGLES

Table 28. Bond angles (°) for BTHIND with water.

S(1)-C(1)-N(1)	110.8 (3)	S(1)-C(1)-C(2)	124.5 (3)
N(1)-C(1)-C(2)	124.7 (4)	C(1)-S(1)-C(9)	91.4 (2)
C(1)-N(1)-C(10)	115.0 (3)	C(1)-N(1)-C(19)	123.2 (3)
C(10)-N(1)-C(19)	121.7 (3)	C(1)-C(2)-C(3)	123.6 (4)
C(2)-C(3)-C(4)	126.7 (4)	C(3)-C(4)-C(11)	123.2 (4)
C(3)-C(4)-C(12)	127.5 (4)	C(11)-C(4)-C(12)	109.2 (4)
C(6)-C(5)-C(10)	117.4 (4)	C(5)-C(6)-C(7)	122.3 (5)
C(6)-C(7)-C(8)	120.7 (5)	C(7)-C(8)-C(9)	118.1 (4)
S(1)-C(9)-C(8)	128.7 (4)	S(1)-C(9)-C(10)	111.1 (3)
C(8)-C(9)-C(10)	120.2 (4)	N(1)-C(10)-C(5)	127.0 (4)
N(1)-C(10)-C(9)	111.7 (4)	C(5)-C(10)-C(9)	121.3 (4)
C(4)-C(11)-C(18)	106.0 (3)	C(4)-C(11)-O(1)	128.9 (4)
C(18)-C(11)-O(1)	125.1 (4)	C(4)-C(12)-C(17)	106.9 (4)
C(4)-C(12)-O(2)	128.9 (4)	C(17)-C(12)-O(2)	124.2 (4)
C(14)-C(13)-C(18)	118.9 (4)	C(13)-C(14)-C(15)	120.9 (5)
C(14)-C(15)-C(16)	121.0 (5)	C(15)-C(16)-C(17)	117.6 (5)
C(12)-C(17)-C(16)	130.3 (4)	C(12)-C(17)-C(18)	108.4 (4)
C(16)-C(17)-C(18)	121.3 (4)	C(11)-C(18)-C(13)	130.3 (4)
C(11)-C(18)-C(17)	109.4 (4)	C(13)-C(18)-C(17)	120.3 (4)
N(1)-C(19)-C(20)	112.5 (4)	H(3a)-O(3a)-H(3b)	108.8 (49)
H(3a)-O(3b)-H(3b)	108.8 (47)		

Table 29. Bond angles (°) for BOXIND.

O(1)-C(1)-N(1)	108.2 (2)	O(1)-C(1)-C(2)	122.0 (2)
N(1)-C(1)-C(2)	129.8 (3)	C(1)-O(1)-C(9)	107.8 (2)
C(1)-N(1)-C(10)	109.6 (2)	C(1)-N(1)-C(19)	126.1 (2)
C(10)-N(1)-C(19)	124.3 (2)	C(1)-C(2)-C(3)	121.1 (3)
C(2)-C(3)-C(4)	128.2 (3)	C(3)-C(4)-C(11)	122.0 (2)
C(3)-C(4)-C(12)	129.3 (2)	C(11)-C(4)-C(12)	108.6 (2)
C(6)-C(5)-C(10)	115.7 (3)	C(5)-C(6)-C(7)	122.4 (3)
C(6)-C(7)-C(8)	121.9 (3)	C(7)-C(8)-C(9)	115.3 (3)
O(1)-C(9)-C(8)	128.2 (3)	O(1)-C(9)-C(10)	108.2 (2)
C(8)-C(9)-C(10)	123.6 (3)	N(1)-C(10)-C(5)	132.8 (3)
N(1)-C(10)-C(9)	106.1 (2)	C(5)-C(10)-C(9)	121.1 (3)
C(4)-C(11)-C(18)	107.2 (2)	C(4)-C(11)-O(2)	128.2 (2)
C(18)-C(11)-O(2)	124.5 (2)	C(4)-C(12)-C(17)	106.6 (2)
C(4)-C(12)-O(3)	128.2 (2)	C(17)-C(12)-O(3)	125.2 (2)
C(14)-C(13)-C(18)	118.0 (3)	C(13)-C(14)-C(15)	120.9 (3)
C(14)-C(15)-C(16)	121.0 (3)	C(15)-C(16)-C(17)	118.2 (3)
C(12)-C(17)-C(16)	130.6 (3)	C(12)-C(17)-C(18)	109.0 (2)
C(16)-C(17)-C(18)	120.4 (2)	C(11)-C(18)-C(13)	130.1 (2)
C(11)-C(18)-C(17)	108.5 (2)	C(13)-C(18)-C(17)	121.4 (2)
N(1)-C(19)-C(20)	110.3 (3)		

Table 30. Bond angles (°) for BTHRHO.

S(1)-C(1)-N(1)	110.3	(3)	S(1)-C(1)-C(2)	123.9	(3)
N(1)-C(1)-C(2)	125.8	(3)	C(1)-S(1)-C(9)	91.5	(2)
C(1)-N(1)-C(10)	114.9	(3)	C(1)-N(1)-C(13)	122.9	(3)
C(10)-N(1)-C(13)	121.6	(3)	C(1)-C(2)-C(3)	122.8	(3)
C(2)-C(3)-C(4)	126.7	(4)	C(3)-C(4)-C(11)	123.6	(3)
C(3)-C(4)-S(2)	125.6	(3)	C(11)-C(4)-S(2)	110.8	(3)
C(6)-C(5)-C(10)	117.4	(4)	C(5)-C(6)-C(7)	121.7	(4)
C(6)-C(7)-C(8)	120.9	(4)	C(7)-C(8)-C(9)	118.9	(4)
S(1)-C(9)-C(8)	128.6	(3)	S(1)-C(9)-C(10)	111.6	(3)
C(8)-C(9)-C(10)	119.8	(3)	N(1)-C(10)-C(5)	127.1	(3)
N(1)-C(10)-C(9)	111.6	(3)	C(5)-C(10)-C(9)	121.3	(4)
C(4)-C(11)-O	128.4	(4)	C(4)-C(11)-N(2)	109.3	(3)
O-C(11)-N(2)	122.3	(3)	N(2)-C(12)-S(2)	110.6	(3)
N(2)-C(12)-S(3)	127.0	(3)	S(2)-C(12)-S(3)	122.4	(2)
N(1)-C(13)-C(14)	109.8	(4)	C(11)-N(2)-C(12)	117.0	(3)
C(11)-N(2)-C(15)	119.6	(3)	C(12)-N(2)-C(15)	123.3	(3)
C(4)-S(2)-C(12)	92.2	(2)	N(2)-C(15)-C(16)	111.9	(3)

Table 31. Bond angles (°) for BTHIND.

C(2)-C(1)-S(1)	124.4	(2)	C(2)-C(1)-N(1)	124.9	(2)
S(1)-C(1)-N(1)	110.6	(2)	C(1)-C(2)-C(3)	122.3	(2)
C(2)-C(3)-C(4)	126.5	(2)	C(3)-C(4)-C(11)	123.3	(2)
C(3)-C(4)-C(12)	127.6	(2)	C(11)-C(4)-C(12)	109.0	(2)
C(1)-S(1)-C(9)	91.8	(1)	C(1)-N(1)-C(10)	114.7	(2)
C(1)-N(1)-C(19)	122.6	(2)	C(10)-N(1)-C(19)	122.8	(2)
C(6)-C(5)-C(10)	118.1	(2)	C(5)-C(6)-C(7)	121.4	(2)
C(6)-C(7)-C(8)	120.8	(2)	C(7)-C(8)-C(9)	118.2	(2)
S(1)-C(9)-C(8)	128.1	(2)	S(1)-C(9)-C(10)	110.4	(2)
C(8)-C(9)-C(10)	121.5	(2)	N(1)-C(10)-C(5)	127.5	(2)
N(1)-C(10)-C(9)	112.5	(2)	C(5)-C(10)-C(9)	120.0	(2)
C(4)-C(11)-O(1)	128.4	(2)	C(4)-C(11)-C(18)	106.4	(2)
O(1)-C(11)-C(18)	125.2	(2)	C(4)-C(12)-O(2)	128.8	(2)
C(4)-C(12)-C(17)	106.7	(2)	O(2)-C(12)-C(17)	124.5	(2)
C(14)-C(13)-C(18)	117.6	(2)	C(13)-C(14)-C(15)	121.3	(2)
C(14)-C(15)-C(16)	121.1	(2)	C(15-C(16)-C(17)	117.8	(2)
C(12)-C(17)-C(16)	129.9	(2)	C(12)-C(17)-C(18)	108.9	(2)
C(16)-C(17)-C(18)	121.1	(2)	C(11)-C(18)-C(13)	130.1	(2)
C(11)-C(18)-C(17)	108.8	(2)	C(13)-C(18)-C(17)	121.1	(2)
N(1)-C(19)-C(20)	111.9	(2)			

Table 32. Bond angles (°) for MEBTHRHO.

C(2)-C(1)-S(1)	127.9	(1)	C(2)-C(1)-N(1)	122.2	(2)
S(1)-C(1)-N(1)	109.9	(1)	C(1)-C(2)-C(3)	128.7	(2)
C(2)-C(3)-C(4)	120.2	(2)	C(2)-C(3)-C(13)	121.6	(1)
C(4)-C(3)-C(13)	118.2	(1)	C(3)-C(4)-S(2)	122.9	(1)
C(3)-C(4)-C(12)	127.3	(1)	S(2)-C(4)-C(12)	109.8	(1)
C(1)-S(1)-C(9)	91.8	(1)	C(1)-N(1)-C(10)	115.0	(2)
C(1)-N(1)-C(14)	123.0	(1)	C(10)-N(1)-C(14)	121.9	(1)
C(6)-C(5)-C(10)	117.5	(2)	C(5)-C(6)-C(7)	121.7	(2)
C(6)-C(7)-C(8)	120.5	(2)	C(7)-C(8)-C(9)	119.0	(2)
S(1)-C(9)-C(8)	128.5	(2)	S(1)-C(9)-C(10)	110.8	(1)
C(8)-C(9)-C(10)	120.8	(2)	N(1)-C(10)-C(5)	127.1	(2)
N(1)-C(10)-C(9)	112.4	(1)	C(5)-C(10)-C(9)	120.5	(2)
C(4)-S(2)-C(11)	92.9	(1)	S(2)-C(11)-N(2)	110.7	(1)
S(2)-C(11)-S(3)	122.2	(1)	N(2)-C(11)-S(3)	127.1	(2)
C(11)-N(2)-C(12)	116.8	(2)	C(11)-N(2)-C(16)	123.4	(1)
C(12)-N(2)-C(16)	119.8	(1)	C(4)-C(12)-N(2)	109.9	(1)
C(4)-C(12)-O	129.3	(2)	N(2)-C(12)-O	120.9	(2)
N(1)-C(14)-C(15)	111.9	(2)	N(2)-C(16)-C(17)	112.2	(2)

Table 33. Bond angles (°) for MEBTHIND.

C(2)-C(1)-S(1)	128.2	(2)	C(2)-C(1)-N(1)	122.6	(3)
S(1)-C(1)-N(1)	109.2	(2)	C(1)-C(2)-C(3)	128.6	(3)
C(2)-C(3)-C(4)	119.2	(3)	C(2)-C(3)-C(19)	120.8	(3)
C(4)-C(3)-C(19)	119.9	(3)	C(3)-C(4)-C(11)	126.9	(3)
C(3)-C(4)-C(12)	126.2	(3)	C(11)-C(4)-C(12)	106.9	(3)
C(1)-S(1)-C(9)	92.5	(2)	C(1)-N(1)-C(10)	116.0	(3)
C(1)-N(1)-C(20)	122.3	(3)	C(10)-N(1)-C(20)	121.1	(3)
C(6)-C(5)-C(10)	117.9	(3)	C(5)-C(6)-C(7)	121.5	(4)
C(6)-C(7)-C(8)	120.9	(4)	C(7)-C(8)-C(9)	118.5	(4)
S(1)-C(9)-C(8)	128.7	(3)	S(1)-C(9)-C(10)	110.3	(2)
C(8)-C(9)-C(10)	121.0	(3)	N(1)-C(10)-C(5)	127.9	(3)
N(1)-C(10)-C(9)	111.9	(3)	C(5)-C(10)-C(9)	120.2	(3)
C(4)-C(11)-O(1)	130.7	(3)	C(4)-C(11)-C(18)	107.0	(3)
O(1)-C(11)-C(18)	122.2	(3)	C(4)-C(12)-O(2)	129.0	(3)
C(4)-C(12)-C(17)	108.1	(3)	O(2)-C(12)-C(17)	122.9	(3)
C(14)-C(13)-C(18)	118.6	(3)	C(13)-C(14)-C(15)	120.4	(4)
C(14)-C(15)-C(16)	121.4	(4)	C(15)-C(16)-C(17)	117.7	(3)
C(12)-C(17)-C(16)	130.2	(3)	C(12)-C(17)-C(18)	108.7	(3)
C(16)-C(17)-C(18)	121.1	(3)	C(11)-C(18)-C(13)	130.1	(3)
C(11)-C(18)-C(17)	109.3	(3)	C(13)-C(18)-C(17)	120.7	(3)
N(1)-C(20)-C(21)	105.8	(4)			

Table 34. Bond angles (°) for 1-(3-ethyl-2-benzothiazolylidene)-2-propanone.

C(2)-C1)-S(1)	124.7	(1)	C(2)-C(1)-N(1)	123.4	(1)
S(1)-C(1)-N(1)	111.9	(1)	C(1)-C(2)-C(3)	124.0	(1)
C(2)-C(3)-C(4)	121.4	(1)	C(2)-C(3)-O(1)	119.8	(1)
C(4)-C(3)-O(1)	118.7	(2)	C(1)-S(1)-C(9)	91.0	(1)
C(1)-N(1)-C(10)	114.2	(1)	C(1)-N(1)-C(11)	124.4	(1)
C(10)-N(1)-C(11)	121.4	(1)	C(6)-C(5)-C(10)	117.5	(2)
C(5)-C(6)-C(7)	121.2	(2)	C(6)-C(7)-C(8)	121.3	(1)
C(7)-C(8)-C(9)	117.9	(2)	S(1)-C(9)-C(8)	128.2	(1)
S(1)-C(9)-C(10)	111.2	(1)	C(8)-C(9)-C(10)	120.7	(2)
N(1)-C(10)-C(5)	126.9	(1)	N(1)-C(10)-C(9)	111.6	(1)
C(5)-C(10)-C(9)	121.4	(1)	C(3)-O(1)-H(1)	115.8	(13)
N(1)-C(11)-C(12)	111.7	(2)	H(2a)-O(2)-H(2b)	116.4	(25)
H(3a)-O(3)-H(3b)	113.1	(23)			

Table 35. Bond angles (°) for ABMF.

C(2)-C(1)-S(1)	121.7	(2)	C(2)-C(1)-N(1)	127.3	(2)
S(1)-C(1)-N(1)	110.9	(2)	C(1)-C(2)-C(3)	118.5	(2)
C(1)-C(2)-C(5)	122.3	(2)	C(3)-C(2)-C(5)	118.7	(2)
C(2)-C(3)-C(4)	120.7	(2)	C(3)-C(4)-O(1)	122.5	(2)
C(4)-C(3)-O(1)	116.8	(2)	C(3)-C(4)-C(15)	118.8	(2)
C(3)-C(4)-C(19)	122.8	(2)	C(15)-C(4)-C(19)	118.2	(2)
C(2)-C(5)-C(6)	120.0	(2)	C(2)-C(5)-O(2)	120.0	(2)
C(6)-C(5)-O(2)	120.0	(2)	C(5)-C(6)-C(20)	119.4	(2)
C(5)-C(6)-C(24)	121.8	(2)	C(20)-C(6)-C(24)	118.8	(3)
C(1)-S(1)-C(11)	91.0	(1)	C(1)-N(1)-C(12)	114.6	(2)
C(1)-N(1)-C(13)	126.7	(2)	C(12)-N(1)-C(13)	118.5	(2)
C(8)-C(7)-C(12)	118.0	(3)	C(7)-C(8)-C(9)	121.1	(3)
C(8)-C(9)-C(10)	120.7	(3)	C(9)-C(10)-C(11)	119.0	(3)
S(1)-C(11)-C(10)	128.0	(2)	S(1)-C(11)-C(12)	111.7	(2)
C(10)-C(11)-C(12)	120.2	(2)	N(1)-C(12)-C(7)	127.4	(3)
N(1)-C(12)-C(11)	111.6	(2)	C(7)-C(12)-C(11)	120.9	(2)
N(1)-C(13)-C(14)	112.0	(2)	C(4)-C(15)-C(16)	121.0	(2)
C(15)-C(16)-C(17)	119.8	(2)	C(16)-C(17)-C(18)	119.8	(3)
C(17)-C(18)-C(19)	120.5	(3)	C(4)-C(19)-C(18)	120.6	(2)
C(6)-C(20)-C(21)	120.9	(3)	C(20)-C(21)-C(22)	120.2	(4)
C(21)-C(22)-C(23)	121.0	(4)	C(22)-C(23)-C(24)	119.2	(3)
C(6)-C(24)-C(23)	119.8	(3)			

APPENDIX D

ANISOTROPIC THERMAL PARAMETERS

Table 36. Anisotropic thermal parameters ($Å^2 \times 10^3$) for BTHIND with water.

	U_{11}	U_{22}	U_{33}	U_{23}	U_{13}	U_{12}
C(1)	44 (3)	41 (3)	54 (3)	6 (2)	16 (2)	9 (2)
S(1)	81 (1)	50 (1)	57 (1)	5 (1)	15 (1)	13 (1)
N(1)	60 (3)	36 (2)	56 (2)	8 (2)	10 (2)	15 (2)
C(2)	59 (3)	46 (3)	55 (3)	9 (2)	14 (3)	19 (3)
C(3)	54 (3)	42 (3)	63 (3)	8 (2)	22 (3)	9 (2)
C(4)	62 (3)	43 (3)	54 (3)	12 (2)	16 (3)	23 (2)
C(5)	70 (4)	63 (3)	73 (4)	26 (3)	18 (3)	33 (3)
C(6)	76 (4)	88 (4)	81 (4)	39 (3)	20 (3)	40 (3)
C(7)	73 (4)	111 (5)	63 (4)	39 (3)	12 (3)	29 (4)
C(8)	66 (4)	85 (4)	62 (4)	19 (3)	13 (3)	5 (3)
C(9)	57 (3)	57 (3)	60 (3)	13 (2)	16 (3)	13 (3)
C(10)	53 (3)	55 (3)	61 (3)	22 (2)	17 (3)	13 (2)
C(11)	52 (3)	50 (3)	56 (3)	15 (2)	16 (3)	18 (2)
C(12)	61 (3)	47 (3)	65 (3)	17 (2)	20 (3)	18 (2)
C(13)	57 (3)	56 (3)	69 (4)	15 (3)	15 (3)	20 (3)
C(14)	69 (4)	67 (4)	82 (4)	28 (3)	20 (3)	30 (3)
C(15)	67 (4)	89 (4)	68 (4)	29 (3)	11 (3)	24 (3)
C(16)	73 (4)	68 (4)	63 (4)	8 (3)	17 (3)	11 (3)
C(17)	51 (3)	53 (3)	54 (3)	8 (2)	13 (3)	15 (2)
C(18)	50 (3)	45 (3)	61 (3)	18 (2)	21 (3)	15 (2)
C(19)	71 (4)	51 (3)	65 (3)	5 (2)	11 (3)	26 (3)
C(20)	91 (4)	82 (4)	110 (5)	-25 (4)	8 (4)	21 (3)
O(1)	94 (3)	49 (2)	60 (2)	-1 (2)	7 (2)	28 (2)
O(2)	113 (3)	44 (2)	73 (2)	-1 (2)	15 (2)	24 (2)
O(3a)	162 (9)	67 (7)	65 (6)	8 (4)	4 (6)	31 (6)
O(3b)	233 (29)	84 (14)	80 (14)	18 (11)	-2 (16)	-26 (20)

The anisotropic temperature factor exponent takes the form:

$-2\pi^2(h^2a^{*2}U_{11} + \ldots + 2hka^*b^*U_{12})$.

Table 37. Anisotropic thermal parameters ($Å^2$ x 10^3) for BOXIND.

	U_{11}	U_{22}	U_{33}	U_{23}	U_{13}	U_{12}
C(1)	58 (2)	41 (2)	53 (2)	2 (1)	17 (1)	1 (1)
O(1)	62 (1)	45 (1)	62 (1)	-0 (1)	10 (1)	2 (1)
N(1)	62 (2)	44 (1)	48 (1)	5 (1)	8 (1)	2 (1)
C(2)	59 (2)	47 (2)	50 (2)	7 (1)	10 (1)	3 (1)
C(3)	54 (2)	49 (2)	53 (2)	2 (1)	15 (1)	-1 (1)
C(4)	51 (2)	46 (2)	49 (2)	3 (1)	12 (1)	-1 (1)
C(5)	69 (2)	74 (2)	56 (2)	15 (2)	8 (2)	-3 (2)
C(6)	71 (2)	106 (3)	57 (2)	13 (2)	3 (2)	-8 (2)
C(7)	69 (2)	100 (3)	61 (2)	-14 (2)	9 (2)	-19 (2)
C(8)	70 (2)	68 (2)	73 (2)	-11 (2)	15 (2)	-8 (2)
C(9)	51 (2)	57 (2)	53 (2)	1 (2)	13 (2)	-2 (2)
C(10)	52 (2)	54 (2)	46 (2)	6 (2)	13 (2)	-2 (2)
C(11)	58 (2)	44 (2)	52 (2)	3 (1)	7 (1)	-1 (1)
C(12)	53 (2)	43 (2)	58 (2)	1 (1)	13 (1)	-4 (1)
C(13)	63 (2)	56 (2)	60 (2)	5 (2)	2 (2)	3 (2)
C(14)	65 (2)	75 (2)	59 (2)	13 (2)	3 (2)	4 (2)
C(15)	63 (2)	91 (2)	51 (2)	-5 (2)	-4 (2)	-3 (2)
C(16)	63 (2)	65 (2)	65 (2)	-15 (2)	6 (2)	-6 (2)
C(17)	48 (2)	50 (2)	54 (2)	-1 (1)	11 (1)	-3 (1)
C(18)	48 (2)	49 (2)	51 (2)	3 (1)	11 (1)	-1 (1)
C(19)	76 (2)	42 (2)	67 (2)	0 (1)	7 (2)	3 (2)
C(20)	96 (3)	79 (2)	102 (3)	-22 (2)	-5 (2)	7 (2)
O(2)	98 (2)	46 (1)	67 (1)	-8 (1)	-14 (1)	3 (1)
O(3)	83 (2)	42 (1)	88 (2)	-2 (1)	7 (1)	-1 (1)

The anisotropic temperature factor exponent takes the form:

$-2\pi^2(h^2a^{*2}U_{11} + \ldots + 2hka^*b^*U_{12})$.

Table 38. Anisotropic thermal parameters ($Å^2$ x 10^3) for BTHRHO.

	U_{11}	U_{22}	U_{33}	U_{23}	U_{13}	U_{12}
C(1)	41 (2)	37 (2)	53 (2)	6 (2)	17 (2)	11 (2)
S(1)	59 (1)	38 (1)	51 (1)	1 (1)	16 (1)	13 (1)
N(1)	51 (2)	32 (1)	48 (2)	4 (1)	20 (1)	12 (1)
C(2)	52 (2)	42 (2)	53 (2)	8 (2)	24 (2)	14 (2)
C(3)	41 (2)	43 (2)	55 (2)	8 (2)	17 (2)	8 (2)
C(4)	41 (2)	38 (2)	50 (2)	6 (2)	19 (2)	8 (2)
C(5)	54 (2)	42 (2)	64 (3)	9 (2)	16 (2)	10 (2)
C(6)	58 (3)	66 (3)	67 (3)	33 (2)	17 (2)	14 (2)
C(7)	60 (3)	79 (3)	49 (3)	18 (2)	17 (2)	18 (2)
C(8)	47 (2)	67 (3)	50 (2)	1 (2)	14 (2)	17 (2)
C(9)	35 (2)	47 (2)	46 (2)	2 (2)	11 (2)	9 (2)
C(10)	34 (2)	42 (2)	48 (2)	9 (2)	12 (2)	9 (2)
C(11)	46 (2)	44 (2)	50 (2)	11 (2)	17 (2)	10 (2)
C(12)	44 (2)	52 (2)	55 (2)	9 (2)	21 (2)	13 (2)
C(13)	71 (3)	39 (2)	53 (2)	4 (2)	30 (2)	16 (2)
C(14)	81 (3)	65 (3)	68 (3)	-9 (2)	28 (3)	9 (2)
O	87 (2)	44 (1)	54 (2)	5 (1)	27 (2)	19 (1)
N(2)	54 (2)	40 (2)	51 (2)	10 (1)	21 (2)	13 (1)
S(2)	58 (1)	45 (1)	55 (1)	4 (1)	23 (1)	13 (1)
S(3)	93 (1)	84 (1)	51 (1)	15 (1)	31 (1)	22 (1)
C(15)	79 (3)	52 (2)	62 (3)	20 (2)	29 (2)	28 (2)
C(16)	89 (4)	47 (2)	111 (4)	28 (3)	40 (3)	8 (2)

The anisotropic temperature factor exponent takes the form:

$-2\pi^2(h^2a^{*2}U_{11} + \ldots + 2hka^*b^*U_{12})$.

Table 39. Anisotropic thermal parameters ($Å^2$ x 10^3) for BTHIND.

	U_{11}	U_{22}	U_{33}	U_{23}	U_{13}	U_{12}
C(1)	32 (1)	35 (1)	35 (1)	1 (1)	12 (1)	-1 (1)
S(1)	41 (1)	42 (1)	52 (1)	-12 (1)	25 (1)	-12 (1)
N(1)	35 (1)	35 (1)	37 (1)	-1 (1)	15 (1)	-4 (1)
C(2)	37 (1)	36 (1)	38 (1)	-3 (1)	14 (1)	-2 (1)
C(3)	40 (1)	35 (1)	35 (1)	-0 (1)	13 (1)	2 (1)
C(4)	36 (1)	31 (1)	36 (1)	0 (1)	13 (1)	-1 (1)
C(5)	38 (1)	43 (1)	46 (1)	1 (1)	13 (1)	-7 (1)
C(6)	48 (1)	37 (1)	50 (1)	-4 (1)	9 (1)	-12 (1)
C(7)	54 (1)	39 (1)	43 (1)	-8 (1)	12 (1)	-2 (1)
C(8)	41 (1)	40 (1)	43 (1)	-6 (1)	14 (1)	-2 (1)
C(9)	30 (1)	33 (1)	37 (1)	-0 (1)	7 (1)	-2 (1)
C(10)	32 (1)	33 (1)	35 (1)	1 (1)	8 (1)	-1 (1)
C(11)	40 (1)	36 (1)	38 (1)	1 (1)	16 (1)	-2 (1)
O(1)	50 (1)	55 (1)	69 (1)	-11 (1)	35 (1)	-6 (1)
C(12)	37 (1)	35 (1)	32 (1)	2 (1)	11 (1)	1 (1)
O(2)	43 (1)	51 (1)	56 (1)	-4 (1)	26 (1)	-4 (1)
C(13)	46 (1)	40 (1)	41 (1)	3 (1)	9 (1)	-4 (1)
C(14)	61 (1)	36 (1)	44 (1)	-5 (1)	2 (1)	-8 (1)
C(15)	72 (2)	41 (1)	46 (1)	-9 (1)	16 (1)	4 (1)
C(16)	52 (1)	43 (1)	44 (1)	-3 (1)	18 (1)	5 (1)
C(17)	41 (1)	34 (1)	31 (1)	2 (1)	10 (1)	3 (1)
C(18)	38 (1)	32 (1)	32 (1)	3 (1)	7 (1)	-2 (1)
C(19)	42 (1)	44 (1)	47 (1)	1 (1)	24 (1)	-3 (1)
C(20)	50 (1)	68 (2)	70 (2)	4 (1)	28 (1)	8 (1)

The anisotropic temperature factor exponent takes the form:

$-2\pi^2(h^2a^{*2}U_{11} + \ldots + 2hka^*b^*U_{12})$.

Table 40. Anisotropic thermal parameters ($Å^2$ x 10^3) for MEBTHRHO.

	U_{11}	U_{22}	U_{33}	U_{23}	U_{13}	U_{12}
C(1)	37 (1)	37 (1)	39 (1)	-8 (1)	-5 (1)	-13 (1)
S(1)	47 (1)	38 (1)	52 (1)	-13 (1)	1 (1)	-17 (1)
N(1)	41 (1)	38 (1)	40 (1)	-10 (1)	1 (1)	-18 (1)
C(2)	40 (1)	40 (1)	43 (1)	-9 (1)	0 (1)	-17 (1)
C(3)	37 (1)	38 (1)	40 (1)	-10 (1)	-3 (1)	-12 (1)
C(4)	39 (1)	42 (1)	39 (1)	-11 (1)	0 (1)	-14 (1)
C(5)	51 (1)	58 (1)	43 (1)	-10 (1)	4 (1)	-25 (1)
C(6)	59 (1)	70 (1)	50 (1)	-9 (1)	7 (1)	-34 (1)
C(7)	62 (1)	62 (1)	60 (1)	-0 (1)	-1 (1)	-39 (1)
C(8)	58 (1)	46 (1)	66 (1)	-9 (1)	-6 (1)	-26 (1)
C(9)	43 (1)	41 (1)	46 (1)	-3 (1)	-5 (1)	-18 (1)
C(10)	41 (1)	42 (1)	38 (1)	-4 (1)	-4 (1)	-19 (1)
S(2)	50 (1)	50 (1)	45 (1)	-18 (1)	7 (1)	-21 (1)
C(11)	43 (1)	48 (1)	41 (1)	-9 (1)	-1 (1)	-18 (1)
N(2)	46 (1)	43 (1)	45 (1)	-10 (1)	3 (1)	-19 (1)
C(12)	41 (1)	44 (1)	43 (1)	-6 (1)	0 (1)	-16 (1)
S(3)	65 (1)	69 (1)	51 (1)	-17 (1)	16 (1)	-36 (1)
O	70 (1)	45 (1)	61 (1)	-19 (1)	11 (1)	-24 (1)
C(13)	54 (1)	45 (1)	53 (1)	-19 (1)	4 (1)	-19 (1)
C(14)	61 (1)	53 (1)	49 (1)	-21 (1)	12 (1)	-32 (1)
C(15)	100 (2)	44 (1)	76 (2)	-11 (1)	14 (1)	-8 (1)
C(16)	58 (1)	47 (1)	64 (1)	-14 (1)	3 (1)	-20 (1)
C(17)	101 (2)	72 (1)	99 (2)	-36 (1)	-15 (2)	-37 (1)

The anisotropic temperature factor exponent takes the form:

$-2\pi^2(h^2a^{*2}U_{11} + \ldots + 2hka^*b^*U_{12})$.

Table 41. Anisotropic thermal parameters ($Å^2 \times 10^3$) for MEBTHIND.

	U_{11}	U_{22}	U_{33}	U_{23}	U_{13}	U_{12}
C(1)	58 (2)	37 (2)	39 (2)	-2 (1)	3 (1)	-4 (2)
S(1)	63 (1)	45 (1)	44 (1)	0 (1)	3 (1)	-2 (1)
N(1)	105 (3)	39 (1)	38 (1)	0 (1)	2 (2)	-5 (2)
C(2)	58 (2)	38 (2)	42 (2)	2 (1)	1 (2)	-3 (1)
C(3)	48 (2)	37 (2)	40 (2)	-2 (1)	5 (1)	-4 (1)
C(4)	47 (2)	33 (1)	44 (2)	-2 (1)	3 (1)	0 (1)
C(5)	107 (3)	44 (2)	55 (2)	5 (2)	16 (2)	1 (2)
C(6)	97 (3)	48 (2)	74 (3)	15 (2)	23 (2)	12 (2)
C(7)	83 (3)	56 (2)	68 (3)	23 (2)	14 (2)	12 (2)
C(8)	75 (3)	60 (2)	54 (2)	11 (2)	5 (2)	6 (2)
C(9)	54 (2)	43 (2)	49 (2)	4 (1)	9 (2)	2 (2)
C(10)	75 (3)	40 (2)	48 (2)	10 (2)	12 (2)	3 (2)
C(11)	52 (2)	35 (2)	56 (2)	-5 (2)	5 (2)	0 (2)
O(1)	103 (2)	41 (1)	65 (2)	-10 (1)	-6 (2)	-8 (1)
C(12)	50 (2)	40 (2)	47 (2)	0 (1)	1 (1)	-3 (1)
O(2)	108 (2)	39 (1)	47 (1)	-4 (1)	-10 (1)	-9 (1)
C(13)	75 (3)	36 (2)	71 (3)	3 (2)	8 (2)	1 (2)
C(14)	81 (3)	47 (2)	81 (3)	21 (2)	9 (2)	9 (2)
C(15)	75 (3)	60 (2)	62 (2)	18 (2)	-3 (2)	2 (2)
C(16)	70 (3)	54 (2)	54 (2)	6 (2)	-1 (2)	1 (2)
C(17)	48 (2)	40 (2)	52 (2)	4 (1)	3 (2)	3 (1)
C(18)	48 (2)	37 (2)	52 (2)	-0 (1)	5 (2)	0 (2)
C(19)	81 (3)	43 (2)	49 (2)	-3 (2)	3 (2)	-7 (2)
C(20)	108 (4)	55 (2)	89 (3)	20 (2)	28 (3)	8 (2)
C(21)	107 (4)	70 (3)	143 (5)	-4 (3)	8 (4)	-4 (3)

The anisotropic temperature factor exponent takes the form:

$-2\pi^2(h^2a^{*2}U_{11} + \ldots + 2hka^*b^*U_{12})$.

Table 42. Anisotropic thermal parameters ($Å^2$ x 10^3) for 1-(3-ethyl-2-benzothiazolylidene)-2-propanone.

	U_{11}	U_{22}	U_{33}	U_{23}	U_{13}	U_{12}
C(1)	27 (1)	30 (1)	30 (1)	9 (1)	9 (1)	4 (1)
C(2)	30 (1)	35 (1)	32 (1)	8 (1)	6 (1)	2 (1)
C(3)	29 (1)	40 (1)	31 (1)	10 (1)	9 (1)	5 (1)
C(4)	42 (1)	55 (1)	33 (1)	12 (1)	4 (1)	4 (1)
S(1)	33 (1)	30 (1)	34 (1)	10 (1)	7 (1)	1 (1)
N(1)	29 (1)	30 (1)	32 (1)	10 (1)	5 (1)	3 (1)
C(5)	40 (1)	46 (1)	37 (1)	18 (1)	8 (1)	10 (1)
C(6)	44 (1)	62 (1)	35 (1)	18 (1)	6 (1)	16 (1)
C(7)	38 (1)	62 (1)	33 (1)	5 (1)	1 (1)	5 (1)
C(8)	35 (1)	42 (1)	36 (1)	3 (1)	5 (1)	1 (1)
C(9)	29 (1)	35 (1)	31 (1)	8 (1)	7 (1)	4 (1)
C(10)	28 (1)	36 (1)	30 (1)	11 (1)	7 (1)	5 (1)
O(1)	53 (1)	40 (1)	37 (1)	16 (1)	7 (1)	3 (1)
C(11)	35 (1)	30 (1)	46 (1)	14 (1)	8 (1)	-0 (1)
C(12)	57 (1)	34 (1)	94 (1)	4 (1)	27 (1)	5 (1)
CL	50 (1)	49 (1)	67 (1)	21 (1)	5 (1)	1 (1)
O(2)	59 (1)	92 (1)	68 (1)	33 (1)	8 (1)	-13 (1)
O(3)	72 (1)	57 (1)	64 (1)	34 (1)	27 (1)	18 (1)

The anisotropic temperature factor exponent takes the form:

$-2\pi^2(h^2a^{*2}U_{11} + \ldots + 2hka^*b^*U_{12})$.

Table 43. Anisotropic thermal parameters ($Å^2 \times 10^3$) for ABMF.

	U_{11}	U_{22}	U_{33}	U_{23}	U_{13}	U_{12}
C(1)	45 (1)	50 (1)	40 (1)	5 (1)	8 (1)	22 (1)
S(1)	64 (1)	56 (1)	44 (1)	8 (1)	19 (1)	29 (1)
N(1)	49 (1)	49 (1)	42 (1)	8 (1)	13 (1)	22 (1)
C(2)	51 (1)	53 (1)	40 (1)	7 (1)	12 (1)	23 (1)
C(3)	62 (1)	52 (1)	48 (2)	7 (1)	19 (1)	24 (1)
C(4)	53 (1)	50 (1)	51 (1)	9 (1)	17 (1)	27 (1)
C(5)	57 (1)	51 (1)	43 (1)	11 (1)	11 (1)	26 (1)
C(6)	54 (1)	47 (1)	49 (1)	12 (1)	17 (1)	24 (1)
C(7)	55 (2)	56 (2)	59 (2)	10 (1)	11 (1)	20 (1)
C(8)	59 (2)	65 (2)	67 (2)	28 (1)	13 (1)	18 (1)
C(9)	58 (2)	83 (2)	50 (2)	21 (1)	16 (1)	21 (1)
C(10)	57 (2)	73 (2)	44 (1)	12 (1)	15 (1)	26 (1)
C(11)	47 (1)	58 (1)	38 (1)	7 (1)	7 (1)	20 (1)
O(1)	115 (2)	56 (1)	69 (1)	10 (1)	49 (1)	32 (1)
C(12)	45 (1)	53 (1)	43 (1)	9 (1)	7 (1)	20 (1)
O(2)	59 (1)	77 (1)	48 (1)	1 (1)	3 (1)	26 (1)
C(13)	61 (2)	55 (1)	53 (2)	5 (1)	19 (1)	31 (1)
C(14)	80 (2)	60 (2)	70 (2)	-4 (1)	22 (2)	27 (1)
C(15)	58 (2)	56 (2)	57 (2)	7 (1)	14 (1)	26 (1)
C(16)	59 (2)	60 (2)	83 (2)	14 (2)	19 (2)	20 (1)
C(17)	83 (2)	62 (2)	84 (2)	33 (2)	36 (2)	32 (2)
C(18)	83 (2)	77 (2)	55 (2)	24 (1)	16 (2)	41 (2)
C(19)	60 (2)	57 (2)	58 (2)	10 (1)	11 (1)	26 (1)
C(20)	73 (2)	73 (2)	57 (2)	12 (1)	27 (1)	34 (1)
C(21)	95 (2)	79 (2)	82 (2)	18 (2)	48 (2)	38 (2)
C(22)	64 (2)	65 (2)	127 (3)	13 (2)	52 (2)	21 (2)
C(23)	50 (2)	55 (2)	114 (3)	10 (2)	10 (2)	18 (1)
C(24)	56 (2)	51 (1)	67 (2)	9 (1)	13 (1)	22 (1)

The anisotropic temperature factor exponent takes the form:

$-2\pi^2(h^2a^{*2}U_{11} + \ldots + 2hka^*b^*U_{12})$.

APPENDIX E

H-ATOM COORDINATES
AND
ISOTROPIC THERMAL PARAMETERS

Table 44. H-Atom coordinates (x 10^4) and isotropic thermal parameters ($Å^2$ x 10^3) for BTHIND with water.

	x	y	z	U
H(2)	7020	3853	3973	97
H(3)	7746	6245	5828	97
H(5)	9199	262	6680	97
H(6)	10853	29	8845	97
H(7)	11907	1850	10464	97
H(8)	11418	4026	9959	97
H(13)	4952	9818	2991	97
H(14)	3498	9841	731	97
H(15)	3059	7962	-784	97
H(16)	3989	5960	-52	97
H(19a)	7323	725	5230	97
H(19b)	6387	1900	4386	97
H(20a)	8079	927	3152	97
H(20b)	9991	1431	4395	97
H(20c)	9049	2601	3547	97
H(3a)	6462	8071	6696	97
H(3b)	5800	7105	7671	97

Table 45. H-Atom coordinates (x 10^4) and isotropic thermal parameters ($Å^2$ x 10^3) for BOXIND.

	x	y	z	U
H(2)	1924	-1175	4391	84
H(3)	2095	1043	4855	84
H(5)	6326	-2392	7636	84
H(6)	8042	-1385	8906	84
H(7)	7869	407	8908	84
H(8)	5968	1320	7625	84
H(13)	-2106	2990	2068	84
H(14)	-3927	2488	565	84
H(15)	-4132	740	87	84
H(16)	-2547	-558	1106	84
H(19a)	3807	-2864	6428	84
H(19b)	2590	-2464	5345	84
H(20a)	4910	-3512	5124	84
H(20b)	6358	-2690	5810	84
H(20c)	5141	-2291	4728	84

Table 46. H-Atom coordinates (x 10^4) and isotropic thermal parameters ($Å^2$ x 10^3) for BTHRHO.

	x	y	z	U
H(2)	2739	5589	6560	63
H(3)	2286	3012	4866	63
H(5)	2447	8989	3431	63
H(6)	2276	9109	1160	63
H(7)	2084	7214	-319	63
H(8)	1971	5107	392	63
H(13a)	2083	8444	5166	73
H(13b)	2156	7294	6214	73
H(14a)	5204	9027	6978	127
H(14b)	5533	8737	5459	127
H(14c)	5623	7548	6464	127
H(15a)	3465	-299	7816	73
H(15b)	3338	149	9372	73
H(16a)	-76	-799	6885	127
H(16b)	-201	-334	8443	127
H(16c)	615	-1700	8107	127

Table 47. H-Atom coordinates (x 10^4) and isotropic thermal parameters ($Å^2$ x 10^3) for BTHIND.

	x	y	z	U
H(2)	8028	4745	6512	61
H(3)	9863	5077	6027	61
H(5)	6253	-2099	5216	61
H(6)	6532	-4706	4255	61
H(7)	7657	-4526	3678	61
H(8)	8871	-1670	4015	61
H(13)	11877	11957	7539	61
H(14)	11489	14693	8340	61
H(15)	9943	14590	8622	61
H(16)	8731	11726	8126	61
H(19a)	6674	-65	6230	61
H(19b)	7298	2212	6669	61
H(20a)	5507	2788	5996	61
H(20b)	5583	1897	5098	61
H(20c)	6207	4174	5536	61

Table 48. H-Atom coordinates (x 10^4) and isotropic thermal parameters ($Å^2$ x 10^3) for MEBTHRHO.

	x	y	z	U
H(2)	-2459	2226	5164	82
H(5)	-6546	952	9226	82
H(6)	-7911	-979	10326	82
H(7)	-7295	-3154	9458	82
H(8)	-5332	-3440	7455	82
H(13a)	-498	-1440	4256	73
H(13b)	-6	-534	2528	69
H(13c)	-1894	-621	3204	77
H(14a)	-4868	2043	8332	82
H(14b)	-3341	2384	7010	82
H(15a)	-5601	4392	6726	82
H(15b)	-6595	3178	6702	82
H(15c)	-5067	3523	5382	82
H(16a)	619	6143	1056	82
H(16b)	-654	6059	2621	82
H(17a)	1596	6635	2723	82
H(17b)	2724	5001	2280	82
H(17c)	1449	4921	3844	82

Table 49. H-Atom coordinates (x 10^4) and isotropic thermal parameters ($Å^2$ x 10^3) for MEBTHIND.

	x	y	z	U
H(2)	1996	4018	4494	84
H(5)	2349	28	5287	84
H(6)	3126	-1077	6374	84
H(7)	3952	-209	7532	84
H(8)	4227	1789	7630	84
H(13)	2269	9443	3975	84
H(14)	1191	9758	2704	84
H(15)	384	8223	1912	84
H(16)	558	6326	2366	84
H(19a)	3347	6657	5885	84
H(19b)	4586	5439	6085	84
H(19c)	2266	5536	6256	84
H(20a)	489	2621	4373	84
H(20b)	686	1231	4615	84
H(21a)	2240	1624	3592	84
H(21b)	3777	1221	4332	84
H(21c)	3584	2611	4090	84

Table 50. H-Atom coordinates (x 10^4) and isotropic thermal parameters (Å^2 x 10^3) for 1-(3-ethyl-2-benzothiazolylidene)-2-propanone.

	x		y		z		U	
H(2)	5117		2793		3155			72(32)
H(4a)	3713		3150		1270			72(32)
H(4b)	5005		4555		819			72(32)
H(4c)	3038		5018		1294			72(32)
H(5)	8842		2239		7441			72(32)
H(6)	11091		3847		9354			72(32)
H(7)	12039		6652		9592			72(32)
H(8)	10869		7917		7910			72(32)
H(1)	6133	(316)	6977	(296)	2502	(253)		72(32)
H(11a)	6375		1490		5920			72(32)
H(11b)	5164		1665		4452			72(32)
H(12a)	7110		-402		4351			72(32)
H(12b)	9110		956		5247			72(32)
H(12c)	7902		1135		3779			72(32)
H(2a)	7847	(316)	9450	(308)	-65	(233)		72(32)
H(2b)	9446	(238)	9590	(314)	1140	(305)		72(32)
H(3a)	6465	(278)	8471	(303)	1312	(282)		72(32)
H(3b)	4665	(280)	8689	(277)	1675	(305)		72(32)

Table 51. H-Atom coordinates (x 10^4) and isotropic thermal parameters (Å^2 x 10^3) for ABMF.

	x	y	z	U
H(7)	6864	7944	6406	76
H(8)	8437	8895	5168	76
H(9)	9009	6840	4197	76
H(10)	7987	3796	4429	76
H(13a)	4640	6388	6985	76
H(13b)	4006	4682	7647	76
H(14a)	6136	7367	8571	76
H(14b)	7692	7510	7889	76
H(14c)	7056	5805	8551	76
H(15)	793	-2971	6578	76
H(16)	-677	-5167	7492	76
H(17)	611	-4887	9112	76
H(18)	3374	-2436	9793	76
H(19)	4825	-189	8891	76
H(20)	3254	2532	9803	76
H(21)	333	2029	10120	76
H(22)	-2234	1283	8895	76
H(23)	-1973	843	7321	76
H(24)	957	1207	6986	76

APPENDIX F

NON-BONDED DISTANCES

Table 52. Non-bonded distances for BTHIND with water.

Second atoms generated by transformation:
0.00000 + X 0.00000 + Y 0.00000 + Z

H3B -H3A	1.561	H20C-H20B	1.764	H20C-H20A	1.764
H20B-H20A	1.764	H19B-H19A	1.764	H3A -O1	1.903
H19A-H5	2.068	H19B-N1	2.073	H19A-N1	2.073
H3 -C2	2.092	H19B-H2	2.093	C20 -H19B	2.100
C20 -H19A	2.100	C4 -H3	2.105	H20C-C19	2.109
H20B-C19	2.109	H20A-C19	2.109	C3 -H2	2.109
C7 -H6	2.119	H6 -C5	2.124	H7 -C6	2.127
H14 -C13	2.128	H15 -C14	2.131	C15 -H14	2.132
H2 -C1	2.134	C8 -H7	2.137	C14 -H13	2.138
C18 -H13	2.143	C16 -H15	2.147	C6 -H5	2.150
C17 -H16	2.151	H8 -C7	2.151	C10 -H5	2.161
H16 -C15	2.165	C9 -H8	2.168	C9 -N1	2.311
C10 -C1	2.321	C18 -C12	2.348	O2 -H2	2.352
C17 -C11	2.361	C18 -C4	2.361	C17 -C4	2.365
C12 -C11	2.367	C10 -C6	2.370	C18 -C14	2.375
C17 -C15	2.379	C9 -C7	2.393	C15 -C13	2.399
C8 -C6	2.399	C17 -C13	2.407	C7 -C5	2.413
O1 -C18	2.417	O2 -C4	2.417	O2 -C17	2.418
C16 -C14	2.419	C18 -C16	2.420	O1 -C4	2.422
C10 -C8	2.423	C9 -C5	2.426	C2 -N1	2.435
C3 -C1	2.442	C20 -N1	2.447	C4 -C2	2.465
C19 -C1	2.469	C9 -C1	2.488	C19 -C10	2.498
C5 -N1	2.502	C11 -C3	2.503	C12 -C3	2.539
N1 -S1	2.553	C10 -S1	2.586	H19A-C10	2.588
H19A-C5	2.607	C13 -C11	2.613	H19B-C1	2.615
C16 -C12	2.616	C19 -H2	2.619	H19B-C2	2.633
H3 -C1	2.638	C11 -H3	2.683	H2 -N1	2.685
H20B-N1	2.692	H3 -S1	2.695	H20C-N1	2.696
O1 -H3	2.700	C4 -H2	2.715	C17 -C14	2.750
C9 -C6	2.751	C19 -H5	2.753	C18 -C15	2.754
C10 -C7	2.757	C2 -S1	2.783	C16 -C13	2.809
O3B -O1	2.814	C8 -C5	2.820	C8 -S1	2.836
O3A -O1	2.849	C19 -C2	2.945	O1 -C3	2.994
C19 -C5	3.010	O2 -C2	3.059	O2 -C3	3.066
H8 -S1	3.077	C12 -C2	3.085	O2 -C16	3.088
O1 -C13	3.094	C3 -S1	3.160		

Table 52. (continued)

Second atoms generated by transformation:
0.00000 + X 1.00000 + Y 0.00000 + Z

O1 -H19A 2.406

Second atoms generated by transformation:
2.00000 - X 1.00000 - Y 1.00000 - Z

O1 -H20B 2.528 H20C-S1 3.088

Second atoms generated by transformation:
2.00000 - X 1.00000 - Y 2.00000 - Z

O3B -H7 2.155 O3A -H7 2.360

Second atoms generated by transformation:
1.00000 - X 2.00000 - Y 1.00000 - Z

O3A -H13 2.669

Second atoms generated by transformation:
1.00000 - X 1.00000 - Y 0.00000 - Z

O2 -H16 2.415

Second atoms generated by transformation:
1.00000 - X 1.00000 - Y 1.00000 - Z

H3B -O2	1.960	H3a -H19B	2.320	O3A -H19B	2.569
O1 -H19B	2.608	O3B -O2	2.881	O3A -O2	2.896

Table 53. Non-bonded distances for BOXIND.

Second atoms generated by transformation:
0.00000 + X 0.00000 + Y 0.00000 + Z

H20C-H20B	1.764	H20C-H20A	1.764	H20B-H20A	1.764
H19B-H19A	1.764	H19B-N1	2.086	H19A-N1	2.086
H3 -C2	2.093	C4 -H3	2.095	C20 -H19B	2.096
C20 -H19A	2.096	H20C-C19	2.098	H20B-C19	2.098
H20A-C19	2.098	C7 -H6	2.115	H7 -C6	2.117
H6 -C5	2.124	H2 -C1	2.125	H14 -C13	2.131
C8 -H7	2.131	C3 -H2	2.132	H15 -C14	2.135
C15 -H14	2.136	C16 -H15	2.137	C17 -H16	2.140
C18 -H13	2.143	C9 -H8	2.143	C14 -H13	2.146
H16 -C15	2.152	C6 -H5	2.159	C10 -H5	2.160
H8 -C7	2.165	N1 -O1	2.191	C9 -N1	2.206
C9 -C1	2.218	H19B-H2	2.220	C10 -C1	2.230
C10 -O1	2.235	C9 -C7	2.321	C10 -C6	2.341
C17 -C11	2.344	C18 -C12	2.357	C12 -C11	2.357
C18 -C14	2.364	C17 -C4	2.366	C18 -C4	2.370
C17 -C15	2.371	C2 -O1	2.393	C3 -C1	2.401
C9 -C5	2.402	C18 -C16	2.404	C15 -C13	2.405
C8 -C6	2.410	C7 -C5	2.411	O3 -C4	2.411
C20 -N1	2.411	C10 -C8	2.412	H3 -O1	2.413
O2 -C18	2.414	C16 -C14	2.414	O2 -C4	2.416
C17 -C13	2.418	O3 -C17	2.423	C2 -N1	2.461
C8 -O1	2.469	C11 -C3	2.481	C4 -C2	2.489
O3 -H2	2.495	C19 -C1	2.502	C19 -C10	2.519
C5 -N1	2.537	C12 -C3	2.564	H3 -C1	2.572
C13 -C11	2.602	C16 -C12	2.611	O2 -H3	2.627
C11 -H3	2.639	H20C-N1	2.647	H20B-N1	2.647
H19B-C1	2.651	C9 -C6	2.694	H19A-C10	2.700
C10 -C7	2.717	C18 -C15	2.738	C17 -C14	2.753
H19B- C2	2.755	C4 -H2	2.773	C16 -C13	2.808
C3 -O1	2.811	C8 -C5	2.843	O2 -C3	2.956
O2 -C13	3.078	C19 -C2	3.087	O3 -C3	3.089
O3 -C16	3.100	C19 -C5	3.156	C12 -C2	3.160

Table 53. (continued)

Second atoms generated by transformation:
1.00000 - X 0.00000 - Y 1.00000 - Z

O2 -H20B 2.671

Second atoms generated by transformation:
-0.50000 - X -0.50000 + Y 0.50000 - Z

O3 -H13 2.632

Second atoms generated by transformation:
-0.50000 + X -0.50000 - Y -0.50000 + Z

H20A-H6 2.087 O3 -H5 2.496 O3 -H19A 2.583
C20 -H6 2.675

Second atoms generated by transformation:
-0.500000 + X 0.50000 - Y -0.50000 + Z

O2 -H8 2.538

Second atoms generated by transformation:
0.50000 + X 0.50000 - Y 0.50000 + Z

O2 -H14 2.596

Table 54. Non-bonded distances for BTHRHO.

Second atoms generated by transformation:
0.00000 + X 0.00000 + Y 0.00000 + Z

H16C-H16B	1.764	H16C-H16A	1.764	H16B-H16A	1.764
H15B-H15A	1.764	H14C-H14B	1.764	H14C-H14A	1.764
H14B-H14A	1.764	H13B-H13A	1.764	H13B-H2	2.023
H15B-N2	2.086	H15A-N2	2.086	C4 -H3	2.088
H13B-N1	2.088	H13A-N1	2.088	C16 -H15B	2.108
C16 -H15A	2.108	H2 -C1	2.113	H13A-H5	2.115
H16C-C15	2.116	H16B-C15	2.116	H16A-C15	2.116
C7 -H6	2.117	H3 -C2	2.121	H7 -C6	2.122
C14 -H13B	2.124	C14 -H13A	2.124	C8 -H7	2.124
H14C-C13	2.125	H14B-C13	2.125	H14A-C13	2.125
H6 -C5	2.128	H8 -C7	2.134	C3 -H2	2.142
C9 -H8	2.147	C6 -H5	2.151	C10 -H5	2.153
N2 -O	2.304	C9 -N1	2.316	N2 -C4	2.330
C10 -C1	2.335	C12 -C11	2.359	C10 -C6	2.363
C9 -C7	2.374	C8 -C6	2.384	O -C4	2.393
C10 -C8	2.403	C7 -C5	2.403	C9 -C5	2.420
C14 -N1	2.429	C2 -N1	2.433	C3 -C1	2.436
C16 -N2	2.456	C11 -C3	2.476	C4 -C2	2.477
C13 -C1	2.483	C15 -C12	2.484	C15 -C11	2.493
C9 -C1	2.495	C5 -N1	2.498	C13 -C10	2.507
C12 -C4	2.511	H15A-O	2.547	S2 -N2	2.549
N1 -S1	2.565	H15B-C12	2.590	C10 -S1	2.590
H13B-C1	2.643	H14C-N1	2.649	H13A-C10	2.651
C11 -H3	2.661	H15B-S3	2.664	O -H3	2.667
H13A-C5	2.680	H14B-N1	2.683	H2 -N1	2.689
S3 -N2	2.690	H16A-N2	2.697	H16B-N2	2.700
C10 -C7	2.740	C4 -H2	2.742	C9 -C6	2.744
C13 -H5	2.756	C2 -S1	2.762	S2 -C3	2.777
C15 -O	2.800	C8 -C5	2.800	C8 -S1	2.814
S2 -H2	2.854	O -C3	2.959	C13 -C2	2.963
S3 -S2	2.967	C13 -C5	3.015	H8 -S1	3.046
C3 -S1	3.121	C15 -S3	3.154	S2 -C2	3.237

Table 54. (continued)

Second atoms generated by transformation:
0.00000 + X 0.00000 + Y 1.00000 + Z

S2 -H8 2.844 S3 -S1 3.826

Second atoms generated by transformation:
0.00000 + X -1.00000 + Y 1.00000 + Z

H16C-H7 2.319

Second atoms generated by transformation:
0.00000 + X -1.00000 + Y 0.00000 + Z

H15A-H14A 2.019 O -H13A 2.624

Second atoms generated by transformation:
1.00000 - X 1.00000 - Y 1.00000 - Z

O -H14B 2.480 H14C-S1 3.083 S2 -C8 3.494

Second atoms generated by transformation:
0.00000 - X 0.00000 - Y 1.00000 - Z

H16C-S1 3.108

Second atoms generated by transformation:
0.00000 - X 1.00000 - Y 1.00000 - Z

H16B-H6 2.359

Second atoms generated by transformation:
1.00000 - X 1.00000 - Y 2.00000 - Z

S3 -H14C 3.081

Table 55. Non-bonded distances for BTHIND.

Second atoms generated by transformation:
0.00000 + X 0.00000 + Y 0.00000 + Z

H20C-H20B	1.764	H20C-H20A	1.764	H20B-H20A	1.764
H19B-H19A	1.764	H19B-H2	2.028	H19B-N1	2.084
H19A-N1	2.084	H3 -C2	2.104	C4 -H3	2.108
C20 -H19B	2.112	C20 -H19A	2.112	H20C-C19	2.119
H20B-C19	2.119	H20A-C19	2.119	C3 -H2	2.126
H2 -C1	2.128	C8 -H7	2.129	C15 -H14	2.130
H15 -C14	2.131	C7 -H6	2.134	H6 -C5	2.134
H7 -C6	2.137	H14 -C13	2.141	C16 -H15	2.142
H8 -C7	2.142	C9 -H8	2.149	C17 -H16	2.150
C6 -H5	2.151	C18 -H13	2.154	C10 -H5	2.154
H16 -C15	2.159	C14 -H13	2.160	H19A-H5	2.160
C9 -N1	2.315	C10 -C1	2.323	C18 -C12	2.352
C17 -C11	2.355	C12 -C11	2.363	C17 -C4	2.364
C18 -C4	2.366	C9 -C7	2.369	O2 -H2	2.374
C17 -C15	2.377	C18 -C14	2.377	C10 -C6	2.380
C8 -C6	2.401	C9 -C5	2.408	O1 -C4	2.409
C16 -C14	2.416	C7 -C5	2.416	C18 -C16	2.417
C15 -C13	2.418	C17 -C13	2.420	C17 -O2	2.421
C18 -O1	2.422	C10 -C8	2.422	O2 -C4	2.424
C3 -C1	2.426	H20A-H19B	2.429	H20A-H19A	2.430
H20B-H19A	2.434	H20C-H19B	2.435	N1 -C2	2.439
H15 -H14	2.442	H7 -H6	2.448	C20 -N1	2.458
C4 -C2	2.475	C19 -C1	2.485	C5 -N1	2.496
C9 -C1	2.496	C11 -C3	2.500	C19 -C10	2.512
C12 -C3	2.547	N1 -S1	2.556	C10 -S1	2.583
H19B-C2	2.601	C16 -C12	2.609	H19B-C1	2.618
C13 -C11	2.619	H3 -C1	2.619	C19 -H2	2.626
H19A-C10	2.642	S1 -H3	2.651	C11 -H3	2.685
O1 -H3	2.693	H19A-C5	2.697	N1 -H2	2.697
H20C-N1	2.701	H20B-N1	2.702	C4 -H2	2.735
C9 -C6	2.739	C18 -C15	2.752	C17 -C14	2.752
C10 -C7	2.762	S1 -C2	2.763	C19 -H5	2.777
H5 -N1	2.798	C8 -C5	2.811	C12 -H2	2.812
C8 -S1	2.817	C16 -C13	2.824	C19 -C2	2.951
O1 -C3	2.980	C19 -C5	3.036	H8 -S1	3.048
O2 -C2	3.068	O2 -C3	3.075	C16 -O2	3.084
C12 -C2	3.097	C13 -O1	3.100	S1 -C3	3.122
C20 -C1	3.297				

Table 55. (continued)

Second atoms generated by transformation:
0.00000 + X -1.00000 + Y 0.00000 + Z

H19A-O2 2.665 C19 -O2 3.207

Second atoms generated by transformation:
2.00000 - X 0.00000 - Y 1.00000 - Z

H8 -S1 2.915

Second atoms generated by transformation:
2.00000 - X 1.00000 - Y 1.00000 - Z

O1 -H8 2.681 O1 -S1 3.184 O1 -C8 3.205

Second atoms generated by transformation:
2.50000 - X 0.50000 + Y 1.50000 - Z

H13 -O1 2.633

Second atoms generated by transformation:
1.50000 - X 0.50000 + Y 1.50000 - Z

H16 -O2 2.754

Second atoms generated by transformation:
1.50000 - X -0.50000 + Y 1.50000 - Z

H19B-O2 2.423 C19 -O2 3.219

Second atoms generated by transformation:
1.50000 - X -1.50000 + Y 1.50000 - Z

H20A-H15 2.357 H19A-H15 2.432

Second atoms generated by transformation:
0.50000 + X 0.50000 - Y 0.50000 + Z

C13 -H7 2.703

Second atoms generated by transformation:
0.50000 + X 1.50000 - Y 0.50000 + Z

H14 -C8 2.859

Table 56. Non-bonded distances for MEBTHRHO.

Second atoms generated by transformation:
0.00000 + X 0.00000 + Y 0.00000 + Z

H17C-H17B	1.764	H17C-H17A	1.764	H17B-H17A	1.764
H16B-H16A	1.764	H15C-H15B	1.764	H15C-H15A	1.764
H15B-H15A	1.764	H14B-H14A	1.764	H13C-H13B	1.764
H13C-H13A	1.764	H13B-H13A	1.764	H14B-H2	1.934
H14A-H5	2.069	H14B-N1	2.081	H14A-N1	2.081
H16B-N2	2.083	H16A-N2	2.083	H2 -C1	2.091
C17 -H16B	2.093	C17 -H16A	2.093	H17C-C16	2.101
H17B-C16	2.101	H17A-C16	2.101	C15 -H14B	2.102
C15 -H14A	2.102	O -H2	2.102	H15C-C14	2.110
H15B-C14	2.110	H15A-C14	2.110	C8 -H7	2.115
C3 -H2	2.117	H8 -C7	2.123	H13C-C3	2.127
H13B-C3	2.127	H13A-C3	2.127	H6 -C5	2.134
C7 -H6	2.138	H7 -C6	2.145	C9 -H8	2.154
C6 -H5	2.156	C10 -H5	2.159	O -N2	2.278
C9 -N1	2.313	C10 -C1	2.333	N2 -C4	2.344
C12 -C11	2.360	C9 -C7	2.372	C10 -C6	2.377
H15C-H2	2.380	C8 -C6	2.390	O -C4	2.393
H16B-O	2.404	H17A-H16A	2.409	H17A-H16B	2.410
H17C-H16B	2.414	N1 -C2	2.414	H17B-H16A	2.416
C9 -C5	2.418	H15A-H14A	2.419	H13B-S2	2.419
H15A-H14B	2.422	H15C-H14B	2.423	C10 -C8	2.423
H15B-H14A	2.426	C4 -C2	2.429	C7 -C5	2.430
C17 -N2	2.444	H8 -H7	2.444	C15 -N1	2.446
H7 -H6	2.455	C16 -C11	2.483	C14 -H2	2.486
C13 -C4	2.487	C5 -N1	2.491	C16 -C12	2.495
C14 -C10	2.495	C14 -C1	2.495	C9 -C1	2.504
C3 -C1	2.520	C11 -C4	2.524	H13B-C4	2.533
C12 -C3	2.542	N2 -S2	2.543	C13 -C2	2.548
C12 -H2	2.559	N1 -S1	2.563	H16B-C12	2.574
C10 -S1	2.587	C4 -H2	2.588	N1 -H2	2.589
H14B-C2	2.603	H14A-C10	2.607	H14A-C5	2.624
C12 -S2	2.625	H16A-C11	2.637	H14B-C1	2.650
H17B-N2	2.686	H15B-N1	2.687	H17C-N2	2.688
H15C-N1	2.691	S3 -N2	2.696	H13C-S1	2.702
C9 -C6	2.741	C14 -H5	2.746	C10 -C7	2.765
H13A-S1	2.767	S2 -C3	2.768	C16 -O	2.772
H16A-S3	2.790	H5 -N1	2.797	C8 -C5	2.813
S1 -C2	2.814	C8 -S1	2.827	H13A-C2	2.837
H13C-C2	2.838	C14 -C2	2.909	O -C2	2.913
S3 -S2	2.962	C12 -C2	2.978	C14 -C5	3.006
O -C3	3.053	C13 -S1	3.054	H8 -S1	3.056
C13 -S2	3.059	C13 -C1	3.074	H17B-S3	3.108
C16 -S3	3.160	C15 -C1	3.255	C17 -C11	3.261
S1 -C3	3.350				

Table 56. (continued)

Second atoms generated by transformation:
1.00000 + X 0.00000 + Y -1.00000 + Z

S2 -H5 3.027 S3 -H5 3.028 S2 -H6 3.036

Second atoms generated by transformation:
1.00000 + X 1.00000 + Y -1.00000 + Z

H16A-H7 2.375 S3 -H7 2.882

Second atoms generated by transformation:
-1.00000 + X 0.00000 + Y 1.00000 + Z

H14A-S3 3.008

Second atoms generated by transformation:
0.000000 - X 0.00000 - Y 1.00000 - Z

S2 -C1 3.559 S2 -S1 3.930

Second atoms generated by transformation:
-1.00000 - X 0.00000 - Y 1.00000 - Z

S1 -S1 3.752

Second atoms generated by transformation:
0.00000 - X 1.00000 - Y 1.00000 - Z

H17A-H14B 2.282 H17C-O 2.743

Second atoms generated by transformation:
-1.00000 - X 1.00000 - Y 1.00000 - Z

H16B-H15B 2.445

Table 57. Non-bonded distances for MEBTHIND.

Second atoms generated by transformation:
0.00000 + X 0.00000 + Y 0.00000 + Z

H21C-H21B	1.764	H21C-H21A	1.764	H21B-H21A	1.764
H20B-H20A	1.764	H19C-H19B	1.764	H19C-H19A	1.764
H19B-H19A	1.764	O2 -H2	2.031	H20A-H2	2.034
H21C-C20	2.050	H21B-C20	2.050	H21A-C20	2.050
C21 -H20B	2.061	C21 -H20A	2.061	H19A-O1	2.085
H2 -C1	2.095	C3 -H2	2.097	H19C-C3	2.114
H19B-C3	2.114	H19A-C3	2.114	H15 -C14	2.177
C15 -H14	2.123	C8 -H7	2.126	C7 -H6	2.130
H6 -C5	2.130	H14 -C13	2.133	C16 -H15	2.134
H7 -C6	2.134	H8 -C7	2.138	C18 -H13	2.143
C14 -H13	2.143	C9 -H8	2.143	C17 -H16	2.146
C6 -H5	2.149	H16 -C15	2.153	C10 -H5	2.157
H20B-N1	2.192	H20A-N1	2.192	H20B-H5	2.219
H21C-H2	2.253	C9 -N1	2.308	C18 -C12	2.327
C10 -C1	2.337	C17 -C11	2.344	C12 -C11	2.347
C17 -C15	2.366	C9 -C7	2.366	C18 -C14	2.373
C10 -C6	2.376	H21B-H20B	2.378	H21C-H20A	2.379
C18 -C4	2.382	C17 -C4	2.383	C21 -N1	2.384
H21A-H20A	2.385	C15 -C13	2.385	H21A-H20B	2.387
C18 -O1	2.390	C17 -C13	2.393	C17 -O2	2.395
C18 -C16	2.397	C8 -C6	2.398	C16 -C14	2.402
C7 -C5	2.412	C4 -C2	2.416	C10 -C8	2.418
C9 -C5	2.419	N1 -C2	2.419	O2 -C4	2.430
H15 -H14	2.433	H7 -H6	2.444	O1 -C4	2.448
H8 -H7	2.459	C5 -N1	2.495	C3 -C1	2.502
C12 -H2	2.503	C19 -C2	2.506	C9 -C1	2.510
C19 -C4	2.514	H19A-C11	2.515	C20 -H2	2.528
N1 -S1	2.542	C12 -C3	2.557	C4 -H2	2.559
H19A-C4	2.565	C11 -C3	2.572	C20 -C10	2.574
C20 -C1	2.575	H21C-N1	2.577	H21B-N1	2.579
C10 -S1	2.581	C16 -C12	2.600	N1 -H2	2.600
C13 -C11	2.610	H20A-C2	2.680	H19B-S1	2.681
H20B-C10	2.699	H19C-S1	2.705	H20A-C1	2.728
C18 -C15	2.734	H20B-C5	2.736	C17 -C14	2.742
C9 -C6	2.742	C10 -C7	2.755	C16 -C13	2.791
C20 -H5	2.794	H19B-C2	2.796	H19C-C2	2.797
H5 -N1	2.805	C8 -C5	2.810	C8 -S1	2.813
S1 -C2	2.815	C21 -H2	2.828	H21C-C2	2.865
O2 -C2	2.876	C12 -C2	2.949	C20 -C2	2.969
C19 -O1	2.974	C19 -S1	3.019	C19 -C1	3.027
C19 -C11	3.037	C13 -O1	3.041	H8 -S1	3.048
C16 -O2	3.049	C20 -C5	3.071	O2 -C3	3.071
O1 -C3	3.118	C21 -C1	3.245	C21 -C10	3.290
S1 -C3	3.341				

Table 57. (continued)

Second atoms generated by transformation:
0.00000 + X 1.00000 + Y 0.00000 + Z

O1 -H6 2.652 O1 -H5 2.664

Second atoms generated by transformation:
0.00000 - X 1.00000 - Y 1.00000 - Z

H19C-O2 2.751 C17 -S1 3.643

Second atoms generated by transformation:
1.00000 - X 1.00000 - Y 1.00000 - Z

H21C-H19A 2.412 H21B-O1 2.730

Second atoms generated by transformation:
1.000000 - X -0.50000 + Y 1.50000 - Z

H7 -S1 3.064

Second atoms generated by transformation:
0.00000 - X 0.50000 + Y 0.50000 - Z

H15 -O2 2.547

Second atoms generated by transformation:
0.00000 - X -0.50000 + Y 0.50000 - Z

H16 -H14 2.302

Table 58. Non-bonded distances for 1-(3-ethyl-2-benzothiazolylidene)-2-propanone.

Second atoms generated by transformation:
0.00000 + X 0.00000 + Y 0.00000 + Z

H3B -H3A	1.538	H2B -H2A	1.561	O3 -H1	1.581
H3A -O2	1.738	H12C-H12B	1.764	H12C-H12A	1.764
H12B-H12A	1.764	H11B-H11A	1.764	H4C -H4B	1.764
H4C -H4A	1.764	H4B -H4A	1.764	H1 -C3	1.897
H11B-H2	1.982	H11B-N1	2.094	H11A-N1	2.094
C3 -H2	2.099	H4C -C3	2.111	H4B -C3	2.111
H4A -C3	2.111	C12 -H11B	2.117	C12 -H11A	2.117
H12C-C11	2.124	H12B-C11	2.124	H12A-C11	2.124
C8 -H7	2.126	H6 -C5	2.134	H11A-H5	2.135
H8 -C7	2.144	C7 -H6	2.144	H7 -C6	2.144
H2 -C1	2.147	C6 -H5	2.153	H3A -H1	2.159
C10 -H5	2.159	C9 -H8	2.163	H3B -H1	2.180
H3B -CL	2.203	H4A -H2	2.280	O1 -C2	2.284
C10 -C1	2.309	C9 -N1	2.311	C10 -C6	2.373
C9 -C7	2.377	C8 -C6	2.418	C10 -C8	2.423
C7 -C5	2.423	C9 -C5	2.426	O1 -C4	2.429
N1 -C2	2.432	C3 -C1	2.452	C12 -N1	2.467
C9 -C1	2.470	H1 -C4	2.484	C4 -C2	2.488
C11 -C1	2.498	C5 -N1	2.500	C11 -C10	2.512
O3 -O1	2.518	N1 -S1	2.554	H4A -C2	2.564
C10 -S1	2.585	C11 -H2	2.608	H11B-C2	2.616
H11A-C10	2.640	H11B-C1	2.648	C4 -H2	2.666
N1 -H2	2.670	H11A-C5	2.674	O1 -S1	2.686
O3 -O2	2.690	H12C-N1	2.706	H12B-N1	2.708
C11 -H5	2.743	C10 -C7	2.751	C9 -C6	2.757
O1 -C1	2.763	S1 -C2	2.788	C8 -S1	2.821
C8 -C5	2.829	C11 -C12	2.960	C11 -C5	3.012
H8 -S1	3.058	O3 -CL	3.160	S1 -C3	3.173

Table 58. (continued)

Second atoms generated by transformation:
0.00000 + X 1.00000 + Y 0.00000 + Z

CL -H2 2.641 CL -H11B 2.886 CL -H4A 3.023

Second atoms generated by transformation:
1.00000 + X 0.00000 + Y 1.00000 + Z

H6 -H4C 2.315

Second atoms generated by transformation:
1.00000 + X 0.00000 + Y 0.00000 + Z

H2B -CL 2.310 O2 -CL 3.267

Second atoms generated by transformation:
1.00000 - X 1.00000 - Y 0.00000 - Z

H4B -H4B 2.226

Second atoms generated by transformation:
1.00000 - X 1.00000 - Y 1.00000 - Z

CL -H5 2.623 C5 -H4C 2.762 CL -H11A 3.049

Second atoms generated by transformation:
2.00000 - X 2.00000 - Y 1.00000 - Z

H2B -H8 2.318 O2 -H8 2.610

Second atoms generated by transformation:
2.00000 - X 0.00000 - Y 1.00000 - Z

H12B-H12B 2.317

Second atoms generated by transformation:
1.00000 - X 2.00000 - Y 0.00000 - Z

H2A -CL 2.346 O2 -CL 3.302

Table 59. Non-bonded distances for ABMF.

Second atoms generated by transformation:
0.00000 + X 0.00000 + Y 0.00000 + Z

H14C-H14B	1.764	H14C-H14A	1.764	H14B-H14A	1.764
H13B-H13A	1.764	H13B-N1	2.092	H13A-N1	2.092
H22 -C21	2.107	C22 -H21	2.112	C21 -H20	2.116
H18 -C17	2.117	C10 -H9	2.118	H21 -C20	2.120
C18 -H17	2.120	C16 -H15	2.120	H16 -C15	2.126
H8 -C7	2.127	H10 -C9	2.128	C23 -H22	2.130
H19 -C4	2.130	C14 -H13B	2.131	C14 -H13A	2.131
H19 -C18	2.132	C19 -H18	2.133	H20 -C6	2.134
H23 -C22	2.139	C17 -H16	2.139	H17 -C16	2.139
H14C-C13	2.139	H14B-C13	2.139	H14A-C13	2.139
C9 -H8	2.141	H9 -C8	2.143	C8 -H7	2.144
H15 -C4	2.144	H24 -C23	2.145	C24 -H23	2.148
H24 -C6	2.149	C11 -H10	2.152	C12 -H7	2.155
H13A-H7	2.173	H14C-O2	2.252	H13B-C5	2.264
C11 N1	2.311	H14B-H7	2.326	C12 -C1	2.328
O1 -C4	2.343	O1 -C2	2.345	O2 -C6	2.346
C22 -C20	2.355	O2 -C2	2.363	C12 -C8	2.372
C18 -C16	2.375	C11 -C9	2.375	C19 -C15	2.379
C23 -C21	2.380	C17 -C15	2.380	C19 -C17	2.381
C24 -C22	2.389	C21 -C6	2.390	C24 -C20	2.391
C18 -C4	2.395	C10 -C8	2.397	C16 -C4	2.405
C23 -C6	2.407	C12 -C10	2.410	C9 -C7	2.413
C11 -C7	2.417	C3 -C1	2.427	N1 -C2	2.475
C13 -C12	2.476	C20 -C5	2.477	C14 -N1	2.485
C11 -C1	2.485	C15 -C3	2.491	H20 -O2	2.497
C7 -N1	2.505	C24 -C5	2.515	C5 -C3	2.517
C19 -C3	2.525	C13 -C1	2.537	C4 -C2	2.538
C5 -C1	2.554	O1 -S1	2.554	N1 -S1	2.569
C6 -C2	2.588	C12 -S1	2.595	H19 -C5	2.596
H13A-C12	2.613	H13B-C6	2.628	H24 -C2	2.640
H19 -O2	2.644	H13B-O2	2.644	H13B-C1	2.656
H20 -C5	2.668	H13A-C7	2.673	H15 -C3	2.676
C13 -H7	2.683	H13B-C2	2.712	H14C-N1	2.728
H14B-N1	2.728	H24 -C5	2.738	C18 -C15	2.740
H19 -C3	2.744	C23 -C20	2.751	C19 -C16	2.751
C12 -C16	2.751	C11 -C8	2.751	S1 -C2	2.754
C22 -C6	2.755	C24 -C21	2.757	O1 -C1	2.768
C17 -C4	2.774	C20 -O2	2.792	C10 -C7	2.803
C10 -S1	2.817	C15 -O1	2.907	C5 -C4	2.912
C13 -C7	2.961	C13 -C5	2.968	C19 -C5	2.981
C24 -C2	2.996	S1 -C3	3.011	C14 -O2	3.038
H10 -S1	3.043	N1 -C5	3.057	O2 -C1	3.085
C13 -C2	3.095	C13 -O2	3.114	C19 -C2	3.161

Table 59. (continued)

Second atoms generated by transformation:
-1.00000 + X 0.00000 + Y 0.00000 + Z

H22 -H19 2.275 H23 -S1 3.051

Second atoms generated by transformation:
0.00000 + X -1.00000 + Y 0.00000 + Z

C19 -H14A 2.742

Second atoms generated by transformation:
0.00000 + X 1.00000 + Y 0.00000 + Z

C21 -H17 2.761

Second atoms generated by transformation:
1.000000 - X 0.00000 - Y 1.00000 - Z

H15 -H10 2.195 O1 -H10 2.583 S1 -S1 3.839

Second atoms generated by transformation:
1.00000 - X 0.00000 - Y 2.00000 - Z

H18 -O2 2.380

APPENDIX G

TORSION ANGLES

Table 60. Torsion angles for BTHIND with water.

N1	C1	S1	C9	-.5(.4)	C2	C1	S1	C9	-179.2(.4)
S1	C1	N1	C10	.3(.5)	S1	C1	N1	C19	176.8(.3)
C2	C1	N1	C10	179.0(.4)	C2	C1	N1	C19	-4.5(.7)
S1	C1	C2	H2	172.9(.2)	S1	C1	C2	C3	-7.1(.7)
N1	C1	C2	H2	-5.6(.5)	N1	C1	C2	C3	174.4(.4)
C1	S1	C9	C8	-179.8(.5)	C1	S1	C9	C10	.6(.4)
C1	N1	C10	C5	179.1(.5)	C1	N1	C10	C9	.1(.6)
C19	N1	C10	C5	2.5(.7)	C19	N1	C10	C9	-176.4(.4)
C1	N1	C19	H19A	-151.9(.3)	C1	N1	C19	H19B	-32.8(.4)
C1	N1	C19	C20	87.6(.5)	C10	N1	C19	H19A	24.3(.4)
C10	N1	C19	H19B	143.4(.3)	C10	N1	C19	C20	-96.2(.5)
C1	C2	C3	H3	-.9(.5)	C1	C2	C3	C4	179.1(.5)
H2	C2	C3	H3	179.1(.0)	H2	C2	C3	C4	-.9(.6)
C2	C3	C4	C11	178.6(.5)	C2	C3	C4	C12	2.0(.8)
H3	C3	C4	C11	-1.3(.5)	H3	C3	C4	C12	-178.0(.4)
C3	C4	C11	C18	-178.3(.4)	C3	C4	C11	O1	1.2(.8)
C12	C4	C11	C18	-1.1(.5)	C12	C4	C11	O1	178.3(.5)
C3	C4	C12	C17	179.3(.5)	C3	C4	C12	O2	.2(.8)
C11	C4	C12	C17	2.3(.5)	C11	C4	C12	O2	-176.8(.5)
H5	C5	C6	H6	.3(.4)	H5	C5	C6	C7	-179.7(.4)
C10	C5	C6	H6	-179.7(.3)	C10	C5	C6	C7	.3(.8)
H5	C5	C10	N1	.8(.6)	H5	C5	C10	C9	179.6(.3)
C6	C5	C10	N1	-179.2(.5)	C6	C5	C10	C9	-.4(.8)
C5	C6	C7	H7	179.3(.4)	C6	C5	C10	N1	-179.2(.5)
H6	C6	C7	H7	-.7(.4)	H6	C6	C7	C8	179.3(.4)
C6	C7	C8	H8	-178.9(.4)	C6	C7	C8	C9	1.1(.8)
H7	C7	C8	H8	1.1(.4)	H7	C7	C8	C9	-178.9(.3)
C7	C8	C9	S1	179.3(.4)	C7	C8	C9	C10	-1.2(.7)
H8	C8	C9	S1	-.8(.6)	H8	C8	C9	C10	178.8(.3)
S1	C9	C10	N1	-.5(.5)	S1	C9	C10	C5	-179.5(.4)
C8	C9	C10	N1	179.8(.4)	C8	C9	C10	C5	.8(.7)
C4	C11	C18	C13	179.8(.5)	C4	C11	C18	C17	-.6(.5)
O1	C11	C18	C13	.3(.8)	O1	C11	C18	C17	179.9(.4)
C4	C12	C17	C16	177.3(.5)	C4	C12	C17	C18	-2.7(.5)
O2	C12	C17	C16	-3.6(.8)	O2	C12	C17	C18	176.5(.5)
H13	C13	C14	H14	-.1(.4)	H13	C13	C14	C15	179.9(.4)
C18	C13	C14	H14	179.9(.3)	C18	C13	C14	C15	-.1(.8)
H13	C13	C18	C11	-1.6(.6)	H13	C13	C18	C17	178.7(.3)
C14	C13	C18	C11	178.4(.5)	C14	C13	C18	C17	-1.3(.7)
C13	C14	C15	H15	-178.9(.4)	C13	C14	C15	C16	1.1(.8)
H14	C14	C15	H15	1.1(.4)	H14	C14	C15	C16	-178.9(.4)
C14	C15	C16	H16	179.3(.4)	C14	C15	C16	C17	-.7(.8)
H15	C15	C16	H16	-.7(.3)	H15	C15	C16	C17	179.3(.3)
C15	C16	C17	C12	179.3(.5)	C15	C16	C17	C18	-.7(.7)
H16	C16	C17	C12	-.7(.6)	H16	C16	C17	C18	179.3(.3)
C12	C17	C18	C11	2.0(.5)	C12	C17	C18	C13	-178.3(.4)
C16	C17	C18	C11	-178.0(.4)	C16	C17	C18	C13	1.7(.7)
N1	C19	C20	H20A	179.8(.3)	N1	C19	C20	H20B	59.8(.4)
N1	C19	C20	H20C	-60.3(.4)	H19A	C19	C20	H20A	59.3(.2)
H19A	C19	C20	H20B	-60.7(.1)	H19A	C19	C20	H20C	179.3(.0)
H19B	C19	C20	H20A	-59.8(.2)	H19B	C19	C20	H20B	-179.8(.0)
H19B	C19	C20	H20C	60.2(.1)	HO3A	O3	O3′	HO3B	-116.8(4.6)
HO3B	O3	O3′	HO3A	116.8(4.6)	HO3B	O3	HO3A	O3′	-64.1(5.2)
HO3A	O3	HO3B	O3′	64.1(5.2)	HO3B	O3′	HO3A	O3	64.1(4.6)
HO3A	O3′	HO3B	O3	-64.1(5.2)					

Table 61. Torsion angles for BOXIND.

N1	C1	O1	C9	2.2(.3)	C2	C1	O1	C9	-177.4(.3)
O1	C1	N1	C10	-2.6(.3)	O1	C1	N1	C19	-179.8(.3)
C2	C1	N1	C10	177.0(.3)	C2	C1	N1	C19	-.2(.5)
O1	C1	C2	H2	176.8(.2)	O1	C1	C2	C3	-3.9(.5)
N1	C1	C2	H2	-2.7(.4)	N1	C1	C2	C3	176.6(.3)
C1	O1	C9	C8	178.7(.3)	C1	O1	C9	C10	-1.1(.3)
C1	N1	C10	C5	-178.6(.3)	C1	N1	C10	C9	1.9(.4)
C19	N1	C10	C5	-1.3(.5)	C19	N1	C10	C9	179.2(.3)
C1	N1	C19	H19A	-144.6(.3)	C1	N1	C19	H19B	-24.8(.3)
C1	N1	C19	C20	95.3(.3)	C10	N1	C19	H19A	38.5(.3)
C10	N1	C19	H19B	158.4(.2)	C10	N1	C19	C20	-81.5(.4)
C1	C2	C3	H3	1.9(.4)	C1	C2	C3	C4	-178.9(.3)
H2	C2	C3	H3	-178.7(.0)	H2	C2	C3	C4	.4(.4)
C2	C3	C4	C11	179.0(.3)	C2	C3	C4	C12	-.7(.5)
H3	C3	C4	C11	-1.9(.3)	H3	C3	C4	C12	178.4(.3)
C3	C4	C11	C18	180.0(.3)	C3	C4	C11	O2	-.5(.5)
C12	C4	C11	C18	-.3(.3)	C12	C4	C11	O2	179.3(.3)
C3	C4	C12	C17	179.8(.3)	C3	C4	C12	O3	-.1(.6)
C11	C4	C12	C17	.1(.3)	C11	C4	C12	O3	-179.8(.3)
H5	C5	C6	H6	1.9(.2)	H5	C5	C6	C7	-179.0(.3)
C10	C5	C6	H6	-178.7(.2)	C10	C5	C6	C7	.5(.5)
H5	C5	C10	N1	-.4(.5)	H5	C5	C10	C9	179.0(.2)
C6	C5	C10	N1	-179.9(.3)	C6	C5	C10	C9	-.5(.5)
C5	C6	C7	H7	179.4(.3)	C5	C6	C7	C8	-.2(.6)
H6	C6	C7	H7	-1.5(.2)	H6	C6	C7	C8	178.9(.3)
C6	C7	C8	H8	179.7(.3)	C6	C7	C8	C9	-.1(.5)
H7	C7	C8	H8	.2(.2)	H7	C7	C8	C9	-179.7(.2)
C7	C8	C9	O1	-179.6(.3)	C7	C8	C9	C10	.1(.5)
H8	C8	C9	O1	.6(.4)	H8	C8	C9	C10	-179.8(.2)
O1	C9	C10	N1	-.5(.3)	O1	C9	C10	C5	180.0(.3)
C8	C9	C10	N1	179.8(.3)	C8	C9	C10	C5	.2(.5)
C4	C11	C18	C13	178.7(.3)	C4	C11	C18	C17	.4(.3)
O2	C11	C18	C13	-.9(.5)	O2	C11	C18	C17	-179.2(.3)
C4	C12	C17	C16	-180.0(.3)	C4	C12	C17	C18	.1(.3)
O3	C12	C17	C16	-.1(.5)	O3	C12	C17	C18	-180.0(.3)
H13	C13	C14	H14	.6(.2)	H13	C13	C14	C15	-179.5(.2)
C18	C13	C14	H14	-178.8(.2)	C18	C13	C14	C15	1.1(.5)
H13	C13	C18	C11	.5(.4)	H13	C13	C18	C17	178.6(.2)
C14	C13	C18	C11	179.9(.3)	C14	C13	C18	C17	-1.9(.5)
C13	C14	C15	H15	179.9(.2)	C13	C14	C15	C16	.5(.5)
H14	C14	C15	H15	-.2(.2)	H14	C14	C15	C16	-179.7(.2)
C14	C15	C16	H16	179.2(.2)	C14	C15	C16	C17	-1.1(.5)
H15	C15	C16	H16	-.2(.2)	H15	C15	C16	C17	179.4(.2)
C15	C16	C17	C12	-179.6(.3)	C15	C16	C17	C18	.3(.5)
H16	C16	C17	C12	.0(.4)	H16	C16	C17	C18	179.9(.2)
C12	C17	C18	C11	-.3(.3)	C12	C17	C18	C13	-178.8(.3)
C16	C17	C18	C11	179.8(.3)	C16	C17	C18	C13	1.3(.5)
N1	C19	C20	H20A	180.0(.2)	N1	C19	C20	H20B	60.0(.2)
N1	C19	C20	H20C	-60.0(.2)	H19A	C19	C20	H20A	59.8(.1)
H19A	C19	C20	H20B	-60.2(.1)	H19A	C19	C20	H20C	179.9(.0)
H19B	C19	C20	H20A	-59.8(.1)	H19B	C19	C20	H20B	-179.9(.0)
H19B	C19	C20	H20C	60.2(.1)					

Table 62. Torsion angles for BTHRHO.

N1	C1	S1	C9	3.1(.3)	C2	C1	S1	C9	-176.4(.3)
S1	C1	N1	C10	-3.2(.3)	S1	C1	N1	C13	-174.8(.3)
C2	C1	N1	C10	176.2(.3)	C2	C1	N1	C13	4.6(.5)
S1	C1	C2	H2	178.7(.2)	S1	C1	C2	C3	-1.3(.5)
N1	C1	C2	H2	-.6(.4)	N1	C1	C2	C3	179.3(.4)
C1	S1	C9	C8	177.3(.3)	C1	S1	C9	C10	-2.2(.3)
C1	N1	C10	C5	-178.4(.3)	C1	N1	C10	C9	1.5(.4)
C13	N1	C10	C5	-6.6(.5)	C13	N1	C10	C9	173.3(.3)
C1	N1	C13	H13A	-154.0(.3)	C1	N1	C13	H13B	-34.1(.3)
C1	N1	C13	C14	86.0(.4)	C10	N1	C13	H13A	34.9(.3)
C10	N1	C13	H13B	154.8(.2)	C10	N1	C13	C14	-85.2(.4)
C1	C2	C3	H3	.1(.4)	C1	C2	C3	C4	-179.9(.3)
H2	C2	C3	H3	-179.9(.0)	H2	C2	C3	C4	.1(.4)
C2	C3	C4	C11	-179.9(.3)	C2	C3	C4	S2	-.6(.5)
H3	C3	C4	C11	.1(.4)	H3	C3	C4	S2	179.4(.2)
C3	C4	C11	O	1.0(.6)	C3	C4	C11	N2	-178.7(.3)
S2	C4	C11	O	-178.4(.3)	S2	C4	C11	N2	1.9(.4)
C3	C4	S2	C12	179.6(.3)	C11	C4	S2	C12	-1.1(.3)
H5	C5	C6	H6	-.4(.3)	H5	C5	C6	C7	179.6(.3)
C10	C5	C6	H6	179.6(.2)	C10	C5	C6	C7	-.4(.6)
H5	C5	C10	N1	-.7(.4)	H5	C5	C10	C9	179.4(.2)
C6	C5	C10	N1	179.3(.3)	C6	C5	C10	C9	-.6(.5)
C5	C6	C7	H7	-179.2(.3)	C5	C6	C7	C8	.8(.6)
H6	C6	C7	H7	.8(.3)	H6	C6	C7	C8	-179.2(.3)
C6	C7	C8	H8	179.8(.3)	C6	C7	C8	C9	-.2(.6)
H7	C7	C8	H8	-.2(.3)	H7	C7	C8	C9	179.8(.2)
C7	C8	C9	S1	179.7(.3)	C7	C8	C9	C10	-.8(.5)
H8	C8	C9	S1	-.3(.4)	H8	C8	C9	C10	179.2(.2)
S1	C9	C10	N1	.9(.4)	S1	C9	C10	C5	-179.2(.3)
C8	C9	C10	N1	-178.7(.3)	C8	C9	C10	C5	1.2(.5)
C4	C11	N2	C12	-2.2(.4)	C4	C11	N2	C15	178.5(.3)
O	C11	N2	C12	178.1(.3)	O	C11	N2	C15	-1.2(.5)
S2	C12	N2	C11	1.4(.4)	S2	C12	N2	C15	-179.3(.3)
S3	C12	N2	C11	-178.0(.3)	S3	C12	N2	C15	1.3(.5)
N2	C12	S2	C4	-.1(.3)	S3	C12	S2	C4	179.3(.3)
N1	C13	C14	H14A	-177.9(.2)	N1	C13	C14	H14B	62.1(.3)
N1	C13	C14	H14C	-57.9(.3)	H13A	C13	C14	H14A	62.1(.1)
H13A	C13	C14	H14B	-57.9(.1)	H13A	C13	C14	H14C	-177.9(.0)
H13B	C13	C14	H14A	-57.8(.1)	H13B	C13	C14	H14B	-177.8(.0)
H13B	C13	C14	H14C	62.2(.1)	C11	N2	C15	H15A	39.9(.3)
C11	N2	C15	H15B	159.2(.2)	C11	N2	C15	C16	-80.5(.5)
C12	N2	C15	H15A	-139.4(.3)	C12	N2	C15	H15B	-20.1(.4)
C12	N2	C15	C16	100.3(.4)	N2	C15	C16	H16A	59.9(.4)
N2	C15	C16	H16B	-60.1(.3)	N2	C15	C16	H16C	179.9(.2)
H15A	C15	C16	H16A	-60.5(.1)	H15A	C15	C16	H16B	179.5(.0)
H15A	C15	C16	H16C	29.5(.2)	H15B	C15	C16	H16A	-179.8(.0)
H15B	C15	C16	H16B	60.2(.1)	H15B	C15	C16	H16C	-59.8(.2)

Table 63. Torsion angles for BTHIND.

S1	C1	C2	H2	170.9(.1)	S1	C1	C2	C3	-9.1(.3)
N1	C1	C2	H2	-7.1(.2)	N1	C1	C2	C3	173.0(.2)
C2	C1	S1	C9	-179.7(.2)	N1	C1	S1	C9	-1.5(.1)
C2	C1	N1	C10	178.9(.2)	C2	C1	N1	C19	.1(.3)
S1	C1	N1	C10	.7(.2)	S1	C1	N1	C19	-178.1(.1)
C1	C2	C3	H3	-1.3(.2)	C1	C2	C3	C4	178.7(.2)
H2	C2	C3	H3	178.7(.0)	H2	C2	C3	C4	-1.2(.2)
C2	C3	C4	C11	174.8(.2)	C2	C3	C4	C12	-4.2(.3)
H3	C3	C4	C11	-5.1(.2)	H3	C3	C4	C12	175.8(.2)
C3	C4	C11	O1	-2.7(.3)	C3	C4	C11	C18	178.1(.2)
C12	C4	C11	O1	176.5(.2)	C12	C4	C11	C18	-2.7(.2)
C3	C4	C12	O2	1.1(.3)	C3	C4	C12	C17	-178.6(.2)
C11	C4	C12	O2	-178.1(.2)	C11	C4	C12	C17	2.3(.2)
C1	S1	C9	C8	-178.6(.2)	C1	S1	C9	C10	1.9(.1)
C1	N1	C10	C5	-179.0(.2)	C1	N1	C10	C9	.7(.2)
C19	N1	C10	C5	-.2(.3)	C19	N1	C10	C9	179.5(.2)
C1	N1	C19	H19A	-149.9(.1)	C1	N1	C19	H19B	-30.7(.2)
C1	N1	C19	C20	89.7(.2)	C10	N1	C19	H19A	31.4(.2)
C10	N1	C19	H19B	150.6(.1)	C10	N1	C19	C20	-89.0(.2)
H5	C5	C6	H6	.7(.1)	H5	C5	C6	C7	-179.3(.1)
C10	C5	C6	H6	-179.3(.1)	C10	C5	C6	C7	.6(.3)
H5	C5	C10	N1	.4(.2)	H5	C5	C10	C9	-179.3(.1)
C6	C5	C10	N1	-179.6(.2)	C6	C5	C10	C9	.7(.3)
C5	C6	C7	H7	178.9(.1)	C5	C6	C7	C8	-1.1(.3)
H6	C6	C7	H7	-1.1(.1)	H6	C6	C7	C8	178.9(.1)
C6	C7	C8	H8	-179.9(.1)	C6	C7	C8	C9	.1(.3)
H7	C7	C8	H8	.1(.1)	H7	C7	C8	C9	-179.9(.1)
C7	C8	C9	S1	-178.3(.2)	C7	C8	C9	C10	1.2(.3)
H8	C8	C9	S1	1.7(.2)	H8	C8	C9	C10	-178.8(.1)
S1	C9	C10	N1	-1.8(.2)	S1	C9	C10	C5	178.0(.1)
C8	C9	C10	N1	178.6(.2)	C8	C9	C10	C5	-1.6(.3)
C4	C11	C18	C13	-177.8(.2)	C4	C11	C18	C17	2.1(.2)
O1	C11	C18	C13	2.9(.3)	O1	C11	C18	C17	-177.2(.2)
C4	C12	C17	C16	178.2(.2)	C4	C12	C17	C18	-.9(.2)
O2	C12	C17	C16	-1.5(.3)	O2	C12	C17	C18	179.4(.2)
H13	C13	C14	H14	-.6(.1)	H13	C13	C14	C15	179.5(.2)
C18	C13	C14	H14	179.4(.1)	C18	C13	C14	C15	-.5(.3)
H13	C13	C18	C11	.3(.3)	H13	C13	C18	C17	-179.6(.1)
C14	C13	C18	C11	-179.8(.2)	C14	C13	C18	C17	.3(.3)
C13	C14	C15	H15	-179.6(.1)	C13	C14	C15	C16	.3(.3)
H14	C14	C15	H15	.4(.1)	H14	C14	C15	C16	-179.6(.1)
C14	C15	C16	H16	-180.0(.2)	C14	C15	C16	C17	.0(.3)
H15	C15	C16	H16	-.0(.1)	H15	C15	C16	C17	180.0(.1)
C15	C16	C17	C12	-179.2(.2)	C15	C16	C17	C18	-.2(.3)
H16	C16	C17	C12	.8(.3)	H16	C16	C17	C18	179.8(.1)
C12	C17	C18	C11	-.7(.2)	C12	C17	C18	C13	179.2(.2)
C16	C17	C18	C11	-179.9(.2)	C16	C17	C18	C13	.0(.3)
N1	C19	C20	H20A	-180.0(.1)	N1	C19	C20	H20B	60.0(.2)
N1	C19	C20	H20C	-60.0(.2)	H19A	C19	C20	H20A	59.7(.1)
H19A	C19	C20	H20B	-60.3(.1)	H19A	C19	C20	H20C	179.7(.0)
H19B	C19	C20	H20A	-59.6(.1)	H19B	C19	C20	H20B	-179.6(.0)
H19B	C19	C20	H20C	60.4(.1)					

Table 64. Torsion angles for MEBTHRHO.

S1	C1	C2	H2	178.5(.1)	S1	C1	C2	C3	-2.1(.3)
N1	C1	C2	H2	-.7(.2)	N1	C1	C2	C3	178.7(.2)
C2	C1	S1	C9	-177.6(.2)	N1	C1	S1	C9	1.7(.1)
C2	C1	N1	C10	177.2(.2)	C2	C1	N1	C14	-.0(.2)
S1	C1	N1	C10	-2.1(.2)	S1	C1	N1	C14	-179.3(.1)
C1	C2	C3	C4	178.3(.2)	C1	C2	C3	C13	-1.2(.3)
H2	C2	C3	C4	-2.3(.2)	H2	C2	C3	C13	178.2(.1)
C2	C3	C4	S2	-178.2(.1)	C2	C3	C4	C12	.8(.3)
C13	C3	C4	S2	1.2(.2)	C13	C3	C4	C12	-179.8(.2)
C2	C3	C13	H13A	-59.9(.2)	C2	C3	C13	H13B	-179.9(.1)
C2	C3	C13	H13C	60.1(.2)	C4	C3	C13	H13A	120.6(.1)
C4	C3	C13	H13B	.6(.2)	C4	C3	C13	H13C	-119.3(.1)
C3	C4	S2	C11	179.1(.2)	C12	C4	S2	C11	-.1(.1)
C3	C4	C12	N2	-178.6(.2)	C3	C4	C12	O	1.2(.3)
S2	C4	C12	N2	.5(.2)	S2	C4	C12	O	-179.6(.2)
C1	S1	C9	C8	178.8(.2)	C1	S1	C9	C10	-1.0(.1)
C1	N1	C10	C5	-178.6(.2)	C1	N1	C10	C9	1.4(.2)
C14	N1	C10	C5	-1.3(.3)	C14	N1	C10	C9	178.7(.2)
C1	N1	C14	H14A	-154.8(.1)	C1	N1	C14	H14B	-35.5(.2)
C1	N1	C14	C15	84.6(.2)	C10	N1	C14	C14A	28.2(.2)
C10	N1	C14	H14B	147.5(.1)	C10	N1	C14	C15	-92.4(.2)
H5	C5	C6	H6	.6(.1)	H5	C5	C6	C7	-179.6(.1)
C10	C5	C6	H6	-179.8(.1)	C10	C5	C6	C7	.1(.3)
H5	C5	C10	N1	-.3(.2)	H5	C5	C10	C9	179.7(.1)
C6	C5	C10	N1	-180.0(.2)	C6	C5	C10	C9	.1(.3)
C5	C6	C7	H7	179.9(.1)	C5	C6	C7	C8	-.4(.3)
H6	C6	C7	H7	-.2(.1)	H6	C6	C7	C8	179.4(.2)
C6	C7	C8	H8	-179.6(.1)	C6	C7	C8	C9	.6(.3)
H7	C7	C8	H8	.1(.1)	H7	C7	C8	C9	-179.7(.1)
C7	C8	C9	S1	179.7(.2)	C7	C8	C9	C10	-.5(.3)
H8	C8	C9	S1	-.1(.2)	H8	C8	C9	C10	179.7(.1)
S1	C9	C10	N1	.0(.2)	S1	C9	C10	C5	180.0(.1)
C8	C9	C10	N1	-179.8(.2)	C8	C9	C10	C5	.1(.3)
C4	S1	C11	N2	-.4(.1)	C4	S2	C11	S3	-179.6(.1)
S2	C11	N2	C12	.9(.2)	S2	C11	N2	C16	-177.6(.1)
S3	C11	N2	C12	180.0(.1)	S3	C11	N2	C16	1.5(.3)
C11	N2	C12	C4	-.9(.2)	C11	N2	C12	O	179.2(.2)
C16	N2	C12	C4	177.6(.2)	C16	N2	C12	O	-2.2(.3)
C11	N2	C16	H16A	33.7(.2)	C11	N2	C16	H16B	152.9(.1)
C11	N2	C16	C17	-86.5(.2)	C12	N2	C16	H16A	-144.7(.1)
C12	N2	C16	H16B	-25.5(.2)	C12	N2	C16	C17	95.0(.2)
N1	C14	C15	H15A	179.8(.1)	N1	C14	C15	H15B	59.8(.1)
N1	C14	C15	H15C	-60.0(.1)	H14A	C14	C15	H15A	59.2(.1)
H14A	C14	C15	H15B	-60.8(.1)	H14A	C14	C15	H15C	179.4(.0)
H14B	C14	C15	H15A	-60.1(.1)	H14B	C14	C15	H15B	179.9(.0)
H14B	C14	C15	H15C	60.1(.1)	N2	C16	C17	H17A	179.9(.1)
N2	C16	C17	H17B	59.8(.2)	N2	C16	C17	H17C	-60.2(.2)
H16A	C16	C17	H17A	59.6(.1)	H16A	C16	C17	H17B	-60.4(.1)
H16A	C16	C17	H17C	179.6(.0)	H16B	C16	C17	H17A	-59.6(.1)
H16B	C16	C17	H17B	-179.7(.0)	H16B	C16	C17	H17C	60.3(.1)

Table 65. Torsion angles for MEBTHIND.

S1	C1	C2	H2	179.6(.2)	S1	C1	C2	C3	-.4(.6)
N1	C1	C2	H2	-.7(.4)	N1	C1	C2	C3	179.3(.4)
C2	C1	S1	C9	-178.9(.3)	N1	C1	S1	C9	1.3(.3)
C2	C1	N1	C10	177.6(.3)	C2	C1	N1	C20	-11.3(.6)
S1	C1	N1	C10	-2.6(.4)	S1	C1	N1	C20	168.5(.3)
C1	C2	C3	C4	179.5(.3)	C1	C2	C3	C19	-.4(.6)
H2	C2	C3	C4	-.5(.4)	H2	C2	C3	C19	179.6(.2)
C2	C3	C4	C11	-179.6(.3)	C2	C3	C4	C12	1.7(.5)
C19	C3	C4	C11	.3(.5)	C19	C3	C4	C12	-178.3(.3)
C2	C3	C19	H19A	179.9(.3)	C2	C3	C19	H19B	59.9(.3)
C2	C3	C19	H19C	-60.1(.3)	C4	C3	C19	H19A	.0(.3)
C4	C3	C19	H19B	-120.0(.3)	C4	C3	C19	H19C	120.0(.3)
C3	C4	C11	O1	-.2(.6)	C3	C4	C11	C18	-179.0(.3)
C12	C4	C11	O1	178.6(.4)	C12	C4	C11	C18	-.1(.4)
C3	C4	C12	O2	-1.1(.6)	C3	C4	C12	C17	179.0(.3)
C11	C4	C12	O2	-180.0(.4)	C11	C4	C12	C17	.1(.4)
C1	S1	C9	C8	-179.9(.4)	C1	S1	C9	C10	.2(.3)
C1	N1	C10	C5	-176.9(.4)	C1	N1	C10	C9	2.9(.5)
C20	N1	C10	C5	11.8(.6)	C20	N1	C10	C9	-168.4(.4)
C1	N1	C20	H20A	-27.5(.4)	C1	N1	C20	H20B	-148.6(.3)
C1	N1	C20	C21	92.0(.4)	C10	N1	C20	H20A	143.2(.3)
C10	N1	C20	H20B	22.1(.4)	C10	N1	C20	C21	-97.4(.4)
H5	C5	C6	H6	.4(.3)	H5	C5	C6	C7	-179.6(.3)
C10	C5	C6	H6	-179.6(.3)	C10	C5	C6	C7	.4(.7)
H5	C5	C10	N1	1.3(.5)	H5	C5	C10	C9	-178.5(.2)
C6	C5	C10	N1	-178.7(.4)	C6	C5	C10	C9	1.5(.6)
C5	C6	C7	H7	177.9(.3)	C5	C6	C7	C8	-2.1(.7)
H6	C6	C7	H7	-2.1(.3)	H6	C6	C7	C8	177.9(.3)
C6	C7	C8	H8	-178.2(.3)	C6	C7	C8	C9	1.8(.6)
H7	C7	C8	H8	1.8(.3)	H7	C7	C8	C9	-178.2(.3)
C7	C8	C9	S1	-179.8(.3)	C7	C8	C9	C10	.2(.6)
H8	C8	C9	S1	.2(.4)	H8	C8	C9	C10	-179.9(.3)
S1	C9	C10	N1	-1.7(.4)	S1	C9	C10	C5	178.1(.3)
C8	C9	C10	N1	178.4(.4)	C8	C9	C10	C5	-1.8(.6)
C4	C11	C18	C13	-179.7(.4)	C4	C11	C18	C17	.1(.4)
O1	C11	C18	C13	1.5(.6)	O1	C11	C18	C17	-178.8(.3)
C4	C12	C17	C16	-180.0(.4)	C4	C12	C17	C18	-.0(.4)
O2	C12	C17	C16	.1(.6)	O2	C12	C17	C18	-180.0(.3)
H13	C13	C14	H14	-1.5(.3)	H13	C13	C14	C15	178.5(.3)
C18	C13	C14	H14	178.5(.2)	C18	C13	C14	C15	-1.5(.6)
H13	C13	C18	C11	1.1(.5)	H13	C13	C18	C17	-178.7(.2)
C14	C13	C18	C11	-178.9(.4)	C14	C13	C18	C17	1.3(.6)
C13	C14	C15	H15	-179.4(.3)	C13	C14	C15	C16	.6(.7)
H14	C14	C15	H15	.6(.3)	H14	C14	C15	C16	-179.4(.3)
C14	C15	C16	H16	-179.6(.3)	C14	C15	C16	C17	.4(.6)
H15	C15	C16	H16	.4(.3)	H15	C15	C16	C17	-179.6(.2)
C15	C16	C17	C12	179.4(.4)	C15	C16	C17	C18	-.6(.6)
H16	C16	C17	C12	-.6(.5)	H16	C16	C17	C18	179.4(.2)
C12	C17	C18	C11	-.0(.4)	C12	C17	C18	C13	179.7(.3)
C16	C17	C18	C11	179.9(.3)	C16	C17	C18	C13	-.3(.6)
N1	C20	C21	H21A	-179.9(.2)	N1	C20	C21	H21B	60.1(.3)
N1	C20	C21	H21C	-59.9(.3)	H20A	C20	C21	H21A	-60.5(.2)
H20A	C20	C21	H21B	179.5(.0)	H20A	C20	C21	H21C	59.5(.2)
H20B	C20	C21	H21A	60.7(.2)	H20B	C20	C21	H21B	-59.3(.2)
H20B	C20	C21	H21C	-179.3(.0)					

Table 66. Torsion angles for 1-(3-ethyl-2-benzothiazolylidene)-2-propanone.

S1	C1	C2	H2	-179.6(.1)	S1	C1	C2	C3	.4(.3)
N1	C2	C2	H2	.7(.2)	N1	C1	C2	C3	-179.3(.2)
C2	C1	S1	C9	-178.8(.2)	N1	S1	C1	C9	1.0(.1)
C2	C1	N1	C10	177.7(.2)	C2	C1	N1	C11	-.0(.3)
S1	C1	N1	C10	-2.1(.2)	S1	C1	N1	C11	-179.8(.1)
C1	C2	C3	C4	178.3(.2)	C1	C2	C3	O1	-1.7(.3)
H2	C2	C3	C4	-1.7(.2)	H2	C2	C3	O1	178.3(.1)
C2	C3	C4	H4A	-.2(.2)	C2	C3	C4	H4B	-120.2(.2)
C2	C3	C4	H4C	119.8(.2)	O1	C3	C4	H4A	179.8(.1)
O1	C3	C4	H4B	59.8(.2)	O1	C3	C4	H4C	-60.2(.2)
C2	C3	O1	H1	167.9(2.0)	C4	C3	O1	H1	-12.0(2.0)
C1	S1	C9	C8	-179.7(.2)	C1	S1	C9	C10	.2(.1)
C1	N1	C10	C5	-177.7(.2)	C1	N1	C10	C9	2.3(.2)
C11	N1	C10	C5	.1(.3)	C11	N1	C10	C9	-179.9(.2)
C1	N1	C11	H11A	-149.6(.1)	C1	N1	C11	H11B	-30.3(.2)
C1	N1	C11	C12	90.1(.2)	C10	N1	C11	H11A	32.8(.2)
C10	N1	C11	H11B	152.1(.1)	C10	N1	C11	C12	-87.5(.2)
H5	C5	C6	H6	.7(.1)	H5	C5	C6	C7	-179.3(.1)
C10	C5	C6	H6	-179.3(.1)	C10	C5	C6	C7	.7(.3)
H5	C5	C10	N1	.6(.2)	H5	C5	C10	C9	-179.4(.1)
C6	C5	C10	N1	-179.4(.2)	C6	C5	C10	C9	.6(.3)
C5	C6	C7	H7	178.8(.1)	C5	C6	C7	C8	-1.2(.3)
H6	C6	C7	H7	-1.2(.1)	H6	C6	C7	C8	178.8(.1)
C6	C7	C8	H8	-179.7(.1)	C6	C7	C8	C9	.3(.3)
H7	C7	C8	H8	.3(.1)	H7	C7	C8	C9	-179.7(.1)
C7	C8	C9	S1	-179.1(.2)	C7	C8	C9	C10	1.0(.3)
H8	C8	C9	S1	.9(.2)	H8	C8	C9	C10	-179.0(.1)
S1	C9	C10	N1	-1.4(.2)	S1	C9	C10	C5	178.6(.1)
C8	C9	C10	N1	178.5(.2)	C8	C9	C10	C5	-1.5(.3)
N1	C11	C12	H12A	-179.9(.1)	N1	C11	C12	H12B	60.1(.2)
N1	C11	C12	H12C	-59.9(.1)	H11A	C11	C12	H12A	59.8(.1)
H11A	C11	C12	H12B	-60.2(.1)	H11A	C11	C12	H12C	179.8(.0)
H11B	C11	C12	H12A	-59.5(.1)	H11B	C11	C12	H12B	-179.5(.0)
H11B	C11	C12	H12C	60.5(.1)					

Table 67. Torsion angles for ABMF.

S1	C1	C2	C3	-7.1(.3)	S1	C1	C2	C5	164.4(.2)
N1	C1	C2	C3	170.7(.2)	N1	C1	C2	C5	-17.9(.4)
C2	C1	S1	C11	-179.2(.20	N1	C1	S1	C11	2.7(.2)
C2	C1	N1	C12	-179.8(.2)	C2	C1	N1	C13	-5.3(.4)
S1	C1	N1	C12	-1.8(.2)	S1	C1	N1	C13	172.7(.2)
C1	C2	C3	C4	177.6(.2)	C1	C2	C3	O1	-1.4(.4)
C5	C2	C3	C4	5.8(.4)	C5	C2	C3	O1	-173.2(.3)
C1	C2	C5	C6	118.6(.3)	C1	C2	C5	O2	-61.4(.4)
C3	C2	C5	C6	-69.9(.3)	C3	C2	C5	O2	110.1(.3)
C2	C3	C4	C15	131.0(.3)	C2	C3	C4	C19	-53.9(.4)
O1	C3	C4	C15	-49.9(.4)	O1	C3	C4	C19	125.1(.3)
C3	C4	C15	H15	-3.7(.3)	C3	C4	C15	C16	176.3(.3)
C19	C4	C15	H15	-179.0(.2)	C19	C4	C15	C16	1.0(.5)
C3	C4	C19	C18	-175.4(.3)	C3	C4	C19	H19	4.6(.4)
C15	C4	C19	C18	-.3(.5)	C15	C4	C19	H19	179.7(.2)
C2	C5	C6	C20	165.2(.3)	C2	C5	C6	C24	-17.2(.4)
O2	C5	C6	C20	-14.8(.4)	O2	C5	C6	C24	162.8(.3)
C5	C6	C20	H20	-2.3(.3)	C5	C6	C20	C21	177.6(.3)
C24	C6	C20	H20	180.0(.2)	C24	C6	C20	C21	-.1(.4)
C5	C6	C24	C23	-175.9(.3)	C5	C6	C24	H24	4.1(.3)
C20	C6	C24	C23	1.7(.4)	C20	C6	C24	H24	-178.3(.2)
C1	S1	C11	C10	-179.4(.2)	C1	S1	C11	C12	-2.9(.2)
C1	N1	C12	C7	178.7(.2)	C1	N1	C12	C11	.4(.3)
C13	N1	C12	C7	3.8(.3)	C13	N1	C12	C11	-175.4(.2)
C1	N1	C13	H13A	-135.5(.2)	C1	N1	C13	H13B	-16.2(.2)
C1	N1	C13	C14	104.2(.3)	C12	N1	C13	H13A	38.8(.2)
C12	N1	C13	H13B	158.1(.1)	C12	N1	C13	C14	-81.5(.3)
H7	C7	C8	H8	.3(.2)	H7	C7	C8	C9	-179.7(.2)
C12	C7	C8	H8	-179.7(.2)	C12	C7	C8	C9	.3(.4)
H7	C7	C12	N1	.4(.3)	H7	C7	C12	C11	179.5(.2)
C8	C7	C12	N1	-179.6(.2)	C8	C7	C12	C11	-.5(.4)
C7	C8	C9	H9	-179.5(.2)	C7	C8	C9	C10	.4(.4)
H8	C8	C9	H9	.5(.2)	H8	C8	C9	C10	-179.6(.2)
C8	C9	C10	H10	170.9(.2)	C8	C9	C10	C11	-.9(.4)
H9	C9	C10	H10	-1.0(.2)	H9	C9	C10	C11	179.0(.2)
C9	C10	C11	S1	176.9(.2)	C9	C10	C11	C12	.7(.4)
H10	C10	C11	S1	-3.1(.3)	H10	C10	C11	C12	-179.3(.2)
S1	C11	C12	N1	2.5(.3)	S1	C11	C12	C7	-176.8(.2)
C10	C11	C12	N1	179.3(.2)	C10	C11	C12	C7	.0(.4)
N1	C13	C14	H14A	180.0(.1)	N1	C13	C14	H14B	59.9(.2)
N1	C13	C14	H14C	-60.0(.2)	H13A	C13	C14	H14A	59.6(.1)
H13A	C13	C14	H14B	-60.4(.1)	H13A	C13	C14	H14C	179.6(.0)
H13B	C13	C14	H14A	-59.6(.1)	H13B	C13	C14	H14B	-179.6(.0)
H13B	C13	C14	H14C	60.4(.1)	C4	C15	C16	H16	179.3(.2)
C4	C15	C16	C17	-.7(.5)	H15	C15	C16	H16	-.7(.2)
H15	C15	C16	C17	179.3(.3)	C15	C16	C17	H17	179.7(.2)
C15	C16	C17	C18	-.5(.6)	H16	C16	C17	H17	-.3(.3)
H16	C16	C17	C18	179.6(.3)	C16	C17	C18	H18	-179.9(.3)
C16	C17	C18	C19	1.2(.6)	H17	C17	C18	H18	1.0(.3)
H17	C17	C18	C19	-178.9(.3)	C17	C18	C19	C4	-.8(.6)
C17	C18	C19	H19	179.2(.3)	H18	C18	C19	C4	179.3(.2)
H18	C18	C19	H19	-.7(.2)	C6	C20	C21	H21	178.2(.2)
C6	C20	C21	C22	-1.7(.5)	H20	C20	C21	H21	-1.9(.2)
H20	C20	C21	C22	178.2(.2)	C20	C21	C22	H22	-178.0(.2)
C20	C21	C22	C23	2.0(.5)	H21	C21	C22	H22	2.0(.2)
H21	C21	C22	C23	-177.9(.2)	C21	C22	C23	H23	179.6(.2)
C21	C22	C23	C24	-.4(.5)	H22	C22	C23	H23	-.4(.2)
H22	C22	C23	C24	179.6(.2)	C22	C23	C24	C6	-1.5(.4)
C22	C23	C24	H24	178.6(.2)	H23	C23	C24	C6	178.5(.2)
H23	C23	24	H24	-1.5(.2)					

APPENDIX H

ATOM LISTS

Table 68. Atom list for BTHIND with water in the unit cell.

	A	B	C	ALPHA	BETA	GAMMA	VOLUME
CELL DIMENSIONS:	7.903	10.580	10.692	91.48	101.69	103.09	850.3

ATOM	NUMBER/ CELL	ATOMIC NUMBER	ATOMIC WEIGHT	WEIGHT (%)	ABSORPTION COEFF.
C	40.	6.	12.01	68.3	0.5
H	34.	1.	1.01	4.9	0.0
N	2.	7.	14.01	4.0	0.0
O	6.	8.	16.00	13.7	0.2
S	2.	16.	32.06	9.1	1.2

NUMBER OF ATOMS IN THE UNIT CELL =	84.	
UNIT CELL SCATTERING F(000) =	368.	ELECTRONS
UNIT CELL VOLUME =	850.3	$Å^3$
UNIT CELL MASS =	702.9	AMU
CALCULATED DENSITY =	1.37	G/CM^3
ABSORPTION COEFFICIENT =	2.0	CM^{-1} MO

Table 69. Atom list for BOXIND.

	A	B	C	ALPHA	BETA	GAMMA	VOLUME
CELL DIMENSIONS:	8.061	13.448	14.547	90.00	101.63	90.00	1544.6

ATOM	NUMBER/ CELL	ATOMIC NUMBER	ATOMIC WEIGHT	WEIGHT (%)	ABSORPTION COEFF.
C	80.	6.	12.01	75.7	0.6
H	60.	1.	1.01	4.8	0.0
N	4.	7.	14.01	4.4	0.0
O	12.	8.	16.00	15.1	0.2

NUMBER OF ATOMS IN THE UNIT CELL =	156.	
UNIT CELL SCATTERING F(000) =	664.	ELECTRONS
UNIT CELL VOLUME =	1544.6	$Å^3$
UNIT CELL MASS =	1269.4	AMU
CALCULATED DENSITY =	1.36	G/CM^3
ABSORPTION COEFFICIENT =	0.9	CM^{-1} MO

Table 70. Atom list for BTHRHO.

	A	B	C	ALPHA	BETA	GAMMA	VOLUME
CELL DIMENSIONS:	7.452	10.750	10.954	95.40	107.51	103.51	800.8

ATOM	NUMBER/ CELL	ATOMIC NUMBER	ATOMIC WEIGHT	WEIGHT (%)	ABSORPTION COEFF.
C	32.	6.	12.01	55.1	0.4
H	32.	1.	1.01	4.6	0.0
N	4.	7.	14.01	8.0	0.0
O	2.	8.	16.00	4.6	0.0
S	6.	16.	32.06	27.6	3.8

NUMBER OF ATOMS IN THE UNIT CELL =	76.	
UNIT CELL SCATTERING F(000) =	364.	ELECTRONS
UNIT CELL VOLUME =	800.8	$Å^3$
UNIT CELL MASS =	697.0	AMU
CALCULATED DENSITY =	1.45	G/CM^3
ABSORPTION COEFFICIENT =	4.5	CM^{-1} MO

Table 71. Atom list for BTHIND.

	A	B	C	ALPHA	BETA	GAMMA	VOLUME
CELL DIMENSIONS:	14.292	6.517	18.058	90.00	111.35	90.00	1566.5

ATOM	NUMBER/ CELL	ATOMIC NUMBER	ATOMIC WEIGHT	WEIGHT (%)	ABSORPTION COEFF.
C	80.	6.	12.01	72.0	0.5
H	60.	1.	1.01	4.5	0.0
N	4.	7.	14.01	4.2	0.0
O	8.	8.	16.00	9.6	0.2
S	4.	16.	32.06	9.6	1.3

NUMBER OF ATOMS IN THE UNIT CELL =	156.	
UNIT CELL SCATTERING F(000) =	696.	ELECTRONS
UNIT CELL VOLUME =	1566.5	$Å^3$
UNIT CELL MASS =	1333.7	AMU
CALCULATED DENSITY =	1.41	G/CM^3
ABSORPTION COEFFICIENT =	2.1	CM^{-1} MO

Table 72. Atom list for MEBTHRHO.

	A	B	C	ALPHA	BETA	GAMMA	VOLUME
CELL DIMENSIONS:	9.461	9.961	10.475	71.53	75.14	71.28	873.5

ATOM	NUMBER/ CELL	ATOMIC NUMBER	ATOMIC WEIGHT	WEIGHT (%)	ABSORPTION COEFF.
C	34.	6.	12.01	56.3	0.4
H	36.	1.	1.01	5.0	0.0
N	4.	7.	14.01	7.7	0.0
O	2.	8.	16.00	4.4	0.0
S	6.	16.	32.06	26.5	3.5

NUMBER OF ATOMS IN THE UNIT CELL =	82.	
UNIT CELL SCATTERING F(000) =	380.	ELECTRONS
UNIT CELL VOLUME =	873.5	$Å^3$
UNIT CELL MASS =	725.1	AMU
CALCULATED DENSITY =	1.38	G/CM^3
ABSORPTION COEFFICIENT =	4.1	CM^{-1} MO

Table 73. Atom list for MEBTHIND.

	A	B	C	ALPHA	BETA	GAMMA	VOLUME
CELL DIMENSIONS:	7.312	12.241	18.826	90.00	96.10	90.00	1675.5

ATOM	NUMBER/ CELL	ATOMIC NUMBER	ATOMIC WEIGHT	WEIGHT (%)	ABSORPTION COEFF.
C	84.	6.	12.01	72.6	0.5
H	68.	1.	1.01	4.9	0.0
N	4.	7.	14.01	4.0	0.0
O	8.	8.	16.00	9.2	0.1
S	4.	16.	32.06	9.2	1.2

NUMBER OF ATOMS IN THE UNIT CELL =	168.	
UNIT CELL SCATTERING F(000) =	728.	ELECTRONS
UNIT CELL VOLUME =	1675.5	$Å^3$
UNIT CELL MASS =	1389.8	AMU
CALCULATED DENSITY =	1.38	G/CM^3
ABSORPTION COEFFICIENT =	2.0	CM^{-1} MO

Table 74. Atom list for 1-(3-ethyl-2-benzothiazolylidene)-2-propanone.

	A	B	C	ALPHA	BETA	GAMMA	VOLUME
CELL DIMENSIONS:	7.496	8.835	11.766	101.95	105.84	94.83	725.2

ATOM	NUMBER/ CELL	ATOMIC NUMBER	ATOMIC WEIGHT	WEIGHT (%)	ABSORPTION COEFF.
C	24.	6.	12.01	49.4	0.4
H	36.	1.	1.01	6.2	0.0
N	2.	7.	14.01	4.8	0.1
O	6.	8.	16.00	16.4	0.3
S	2.	16.	32.06	11.0	1.4
CL	2.	17.	35.45	12.1	1.9

NUMBER OF ATOMS IN THE UNIT CELL =	72.	
UNIT CELL SCATTERING F(000) =	308.	ELECTRONS
UNIT CELL VOLUME =	725.2	$Å^3$
UNIT CELL MASS =	583.6	AMU
CALCULATED DENSITY =	1.34	G/CM^3
ABSORPTION COEFFICIENT =	4.0	CM^{-1} MO

Table 75. Atom list for ABMF.

	A	B	C	ALPHA	BETA	GAMMA	VOLUME
CELL DIMENSIONS:	8.302	8.459	15.169	92.80	99.97	112.55	961.2

ATOM	NUMBER/ CELL	ATOMIC NUMBER	ATOMIC WEIGHT	WEIGHT (%)	ABSORPTION COEFF.
C	48.	6.	12.01	74.8	4.2
H	38.	1.	1.01	5.0	0.0
N	2.	7.	14.01	3.6	0.3
O	4.	8.	16.00	8.3	1.2
S	2.	16.	32.06	8.3	10.2

NUMBER OF ATOMS IN THE UNIT CELL =	94.	
UNIT CELL SCATTERING F(000) =	404.	ELECTRONS
UNIT CELL VOLUME =	961.2	$Å^3$
UNIT CELL MASS =	771.0	AMU
CALCULATED DENSITY =	1.33	G/CM^3
ABSORPTION COEFFICIENT =	16.0	CM^{-1} MO

APPENDIX I

DATA ACQUISITION PARAMETERS

Table 76. Data acquisition parameters for BTHIND with water.

CELL DIMENSIONS[CD]:	A	B	C	ALPHA	BETA	GAMMA
	7.9027	10.5803	10.6917	91.475	101.693	103.093
	0.0016	0.0032	0.0020	0.021	0.015	0.020

WAVELENGTH[WL]:	<ALPHA>	ALPHA1	ALPHA2
	0.71069	0.70926	0.71354

ORIENTATION MATRIX[OM]:

-0.00555	-0.08484	-0.03999
-0.04022	-0.04735	-0.08693
0.12665	0.00543	-0.00431

ANGULAR DRIVE SPEEDS[AS]: 234.4 234.4 234.4 234.4

RECENTER[RC]:	FLAG	%DROP	INTERVAL
	0	0.	0

MAGNETIC TAPE PARAMS[TP]:	UNIT	RECORD LENGTH
	1	124

INDEX RESTRICTION[IR]:	TYPE	LATTICE	USER
	0	0	0

HKL FILE PARAMS[HK]:	START			END		
	0	0	0	0	0	0

COINCIDENCE CORRECTION[CC]:	DEAD TIME	LOW CUT	HIGH CUT	ATTENUATION
	0.0000022	2500.	50000.	25.346

MINMAX CUTOFFS[MM]:	MIN2TH	MAX2TH	MINIMUM HKL	MAXIMUM HKL	FRIEDEL +-HKL
	3.0	60.0	0 0 0	15 15 15	0 1

SCAN PARAMS[SR]:	SCAN RANGES	BG/SCAN	DISPERSION
	1.0 1.0	1.00	1.00

DIFFRACTION VECTOR[DV]:	PSI START	PSI END	DELTA PSI
	0.0	0.0	0.0

SCAN SPEED[SS]:	FIXED	VARIABLE - SLOW	FAST	LOW	HIGH
	0.00	14.65	60.00	150.	2500.

WYCKOFF OMEGA PARMS[WP]:	#STEPS	#CALC	#ADD'L	MIN INT
	3	3	6	100.

OUTPUT VARIABLES[OV]:	#CHECKS	INTERVAL	TOTAL	MT	PRINT	STEPS	#/PAGE
	0	50	5000	1	0	16	48

STARTING PARMS[SP]:	SEQ #	HKL	PAGE	EXPOSURE
	1	0 0 1	1	2.90

CHECK REFLECTIONS[CR]:

#	H	K	L	I(MIN)
1	-3	1	5	0.
2	1	-6	2	0.
3	2	5	-2	0.

Table 77. Data acquisition parameters for BOXIND.

CELL DIMENSIONS[CD]:	A	B	C	ALPHA	BETA	GAMMA
	8.0611	13.4478	14.5471	90.000	101.632	90.000
	0.0014	0.0025	0.0026	0.000	0.014	0.000

WAVELENGTH[WL]:	<ALPHA>	ALPHA1	ALPHA2
	0.71069	0.70926	0.71354

ORIENTATION MATRIX[OM]:

-0.00077	0.05342	-0.04791
-0.01634	-0.05134	-0.05076
-0.12559	0.00635	-0.00737

ANGULAR DRIVE SPEEDS[AS]: 234.4 234.4 234.4 234.4

RECENTER[RC]:	FLAG	%DROP	INTERVAL
	0	0.	0

MAGNETIC TAPE PARAMS[TP]:	UNIT	RECORD LENGTH
	1	124

INDEX RESTRICTION[IR]:	TYPE	LATTICE	USER
	0	0	0

HKL FILE PARAMS[HK]:	START			END		
	0	0	0	0	0	0

COINCIDENCE CORRECTION[CC]:	DEAD TIME	LOW CUT	HIGH CUT	ATTENUATION
	0.0000020	2500.	50000.	25.776

MINMAX CUTOFFS[MM]:	MIN2TH	MAX2TH	MINIMUM HKL			MAXIMUM HKL			FRIEDEL +-HKL
	3.0	55.0	-11	0	0	11	18	19	0	1

SCAN PARAMS[SR]:	SCAN RANGES		BG/SCAN	DISPERSION
	0.8	0.8	0.20	1.00

DIFFRACTION VECTOR[DV]:	PSI START	PSI END	DELTA PSI
	0.0	0.0	0.0

SCAN SPEED[SS]:	FIXED	VARIABLE - SLOW	FAST	LOW	HIGH
	0.00	15.00	60.00	150.	2500.

WYCKOFF OMEGA PARMS[WP]:	#STEPS	#CALC	#ADD'L	MIN INT
	3	3	6	100.

OUTPUT VARIABLES[OV]:	#CHECKS	INTERVAL	TOTAL	MT	PRINT	STEPS	#/PAGE
	3	97	6000	1	0	16	48

STARTING PARMS[SP]:	SEQ #	HKL			PAGE	EXPOSURE
	1	-11	0	0	1	1.00

CHECK REFLECTIONS[CR]:	#	H	K	L	I(MIN)
	1	-5	0	3	0.
	2	3	6	0	0.
	3	0	-4	-7	0.

Table 78. Data acquisition parameters for BTHRHO.

```
                          A       B       C      ALPHA   BETA   GAMMA
CELL DIMENSIONS[CD]: 7.4521 10.7495 10.9540 95.395 107.512 103.513
                     0.0010  0.0016  0.0017  0.012   0.011   0.011

                    <ALPHA>     ALPHA1     ALPHA2
WAVELENGTH[WL]:     0.71069     0.70926    0.71354

ORIENTATION MATRIX[OM]:    -0.02901   -0.09575   -0.00060
                            0.06778    0.01683    0.09623
                           -0.12648   -0.00007    0.01415

ANGULAR DRIVE SPEEDS[AS]:   234.4   234.4   234.4   234.4

RECENTER[RC]:  FLAG     %DROP     INTERVAL
                 0        0.         0

MAGNETIC TAPE PARAMS[TP]:  UNIT     RECORD LENGTH
                             1          124

INDEX RESTRICTION[IR]:    TYPE      LATTICE     USER
                            0          0          0

HKL FILE PARAMS[HK]:              START              END
                                0   0   0        0   0   0

COINCIDENCE CORRECTION[CC]: DEAD TIME   LOW CUT   HIGH CUT ATTENUATION
                            0.0000022    2500.      50000.     25.346

MINMAX CUTOFFS[MM]: MIN2TH MAX2TH MINIMUM HKL MAXIMUM HKL FRIEDEL +-HKL
                      3.0    50.0  -9 -13  0   9  13  14      0       1

SCAN PARAMS[SR]:  SCAN RANGES    BG/SCAN    DISPERSION
                   0.7  0.7        0.20         1.00

DIFFRACTION VECTOR[DV]:  PSI START     PSI END     DELTA PSI
                             0.0          0.0          0.0

SCAN SPEED[SS]:  FIXED   VARIABLE - SLOW   FAST   LOW   HIGH
                 0.00                14.65  60.00  150.  2500.

WYCKOFF OMEGA PARMS[WP]:  #STEPS  #CALC  #ADD'L   MIN INT
                            3       3       6       100.

OUTPUT VARIABLES[OV]:  #CHECKS  INTERVAL  TOTAL  MT  PRINT  STEPS  #/PAGE
                         3         97      6000   1    0      16     48

STARTING PARMS[SP]:  SEQ #        HKL         PAGE   EXPOSURE
                       1       -9 -13  0       1       1.25

CHECK REFLECTIONS[CR]:  #   H  K  L  I(MIN)
                        1  -3  1  5    0.
                        2   1 -6  2    0.
                        3   2  5 -2    0.
```

Table 79. Data acquisition parameters for BTHIND.

CELL DIMENSIONS[CD]:	A	B	C	ALPHA	BETA	GAMMA
	14.2922	6.5174	18.0582	90.000	111.350	90.000
	0.0016	0.0008	0.0022	0.000	0.009	0.000

WAVELENGTH[WL]:	<ALPHA>	ALPHA1	ALPHA2
	0.71069	0.70926	0.71354

ORIENTATION MATRIX[OM]:	-0.00616	0.15283	0.00015
	0.07357	0.01135	0.03164
	0.01392	0.00760	-0.05034

ANGULAR DRIVE SPEEDS[AS]: 234.4 234.4 234.4 234.4

RECENTER[RC]:	FLAG	%DROP	INTERVAL
	0	0.	0

MAGNETIC TAPE PARAMS[TP]:	UNIT	RECORD LENGTH
	1	124

INDEX RESTRICTION[IR]:	TYPE	LATTICE	USER
	0	0	0

HKL FILE PARAMS[HK]:	START			END		
	0	0	0	0	0	0

COINCIDENCE CORRECTION[CC]:	DEAD TIME			LOW CUT		HIGH CUT		ATTENUATION		
	0.0000018			2500.		50000.		25.185		
MINMAX CUTOFFS[MM]:	MIN2TH	MAX2TH	MINIMUM HKL			MAXIMUM HKL			FRIEDEL +-HKL	
	64.5	70.0	-24	0	0	24	11	30	0	1

SCAN PARAMS[SR]:	SCAN RANGES		BG/SCAN	DISPERSION
	0.6	0.6	0.50	1.00

DIFFRACTION VECTOR[DV]:	PSI START	PSI END	DELTA PSI
	0.0	0.0	0.0

SCAN SPEED[SS]:	FIXED	VARIABLE - SLOW	FAST	LOW	HIGH
	0.00	10.00	30.00	150.	2500.

WYCKOFF OMEGA PARMS[WP]:	#STEPS	#CALC	#ADD'L	MIN INT
	3	3	6	100.

OUTPUT VARIABLES[OV]:	#CHECKS	INTERVAL	TOTAL	MT	PRINT	STEPS	#/PAGE
	3	97	6000	1	0	16	48

STARTING PARMS[SP]:	SEQ #	HKL			PAGE	EXPOSURE
	1	-24	0	0	137	26.77

CHECK REFLECTIONS[CR]:	#	H	K	L	I(MIN)
	1	0	2	-8	0.
	2	1	0	9	0.
	3	-3	-3	0	0.

Table 80. Data acquisition parameters for MEBTHRHO.

CELL DIMENSIONS[CD]:	A	B	C	ALPHA	BETA	GAMMA
	9.4609	9.9613	10.4757	71.531	75.135	71.275
	0.0013	0.0013	0.0015	0.011	0.011	0.010

WAVELENGTH[WL]:	<ALPHA>	ALPHA1	ALPHA2
	0.71069	0.70926	0.71354

ORIENTATION MATRIX[OM]:

0.06230	-0.08359	-0.04040
-0.01353	0.06423	-0.09352
0.09366	0.03019	-0.00795

ANGULAR DRIVE SPEEDS[AS]: 234.4 234.4 234.4 234.4

RECENTER[RC]:	FLAG	%DROP	INTERVAL
	0	0.	0

MAGNETIC TAPE PARAMS[TP]:	UNIT	RECORD LENGTH
	1	124

INDEX RESTRICTION[IR]:	TYPE	LATTICE	USER
	0	0	0

HKL FILE PARAMS[HK]:	START			END		
	0	0	0	0	0	0

COINCIDENCE CORRECTION[CC]:	DEAD TIME	LOW CUT	HIGH CUT	ATTENUATION
	0.0000020	2500.	50000.	25.386

MINMAX CUTOFFS[MM]:	MIN2TH	MAX2TH	MINIMUM HKL			MAXIMUM HKL			FRIEDEL	+-HKL
	59.5	70.0	-16	-17	0	16	17	17	0	1

SCAN PARAMS[SR]:	SCAN RANGES		BG/SCAN	DISPERSION
	0.6	0.6	0.50	1.00

DIFFRACTION VECTOR[DV]:	PSI START	PSI END	DELTA PSI
	0.0	0.0	0.0

SCAN SPEED[SS]:	FIXED	VARIABLE - SLOW	FAST	LOW	HIGH
	5.00	5.00	30.00	150.	2500.

WYCKOFF OMEGA PARMS[WP]:	#STEPS	#CALC	#ADD'L	MIN INT
	3	3	6	100.

OUTPUT VARIABLES[OV]:	#CHECKS	INTERVAL	TOTAL	MT	PRINT	STEPS	#/PAGE
	3	97	6300	1	0	16	48

STARTING PARMS[SP]:	SEQ #	HKL			PAGE	EXPOSURE
	5509	-16	-17	0	117	33.57

CHECK REFLECTIONS[CR]:	#	H	K	L	I(MIN)
	1	-5	-6	0	0.
	2	0	6	4	0.
	3	6	0	1	0.

Table 81. Data acquisition parameters for MEBTHIND.

	A	B	C	ALPHA	BETA	GAMMA
CELL DIMENSIONS[CD]:	7.3120	12.2412	18.8255	90.000	96.096	90.000
	0.0011	0.0015	0.0023	0.000	0.011	0.000

	<ALPHA>	ALPHA1	ALPHA2
WAVELENGTH[WL]:	0.71069	0.70926	0.71354

ORIENTATION MATRIX[OM]:	-0.00944	-0.00801	0.05235
	-0.01488	-0.08076	-0.00620
	0.13641	-0.00936	0.00867

ANGULAR DRIVE SPEEDS[AS]: 234.4 234.4 234.4 234.4

RECENTER[RC]:	FLAG	%DROP	INTERVAL
	0	0.	0

MAGNETIC TAPE PARAMS[TP]:	UNIT	RECORD LENGTH
	1	124

INDEX RESTRICTION[IR]:	TYPE	LATTICE	USER
	0	0	0

HKL FILE PARAMS[HK]:	START			END		
	0	0	0	0	0	0

COINCIDENCE CORRECTION[CC]:	DEAD TIME	LOW CUT	HIGH CUT	ATTENUATION
	0.0000020	2500.	50000.	25.386

MINMAX CUTOFFS[MM]:	MIN2TH	MAX2TH	MINIMUM HKL			MAXIMUM HKL			FRIEDEL +-HKL	
	54.5	62.0	-11	0	0	11	18	28	0	1

SCAN PARAMS[SR]:	SCAN RANGES		BG/SCAN	DISPERSION
	0.6	0.6	0.20	1.00

DIFFRACTION VECTOR[DV]:	PSI START	PSI END	DELTA PSI
	0.0	0.0	0.0

SCAN SPEED[SS]:	FIXED	VARIABLE - SLOW	FAST	LOW	HIGH
	0.00	2.00	15.00	150.	2500.

WYCKOFF OMEGA PARMS[WP]:	#STEPS	#CALC	#ADD'L	MIN INT
	3	3	6	100.

OUTPUT VARIABLES[OV]:	#CHECKS	INTERVAL	TOTAL	MT	PRINT	STEPS	#/PAGE
	3	97	1712	1	0	16	48

STARTING PARMS[SP]:	SEQ #	HKL			PAGE	EXPOSURE
	4289	-11	0	0	92	11.78

CHECK REFLECTIONS[CR]:	#	H	K	L	I(MIN)
	1	1	3	5	0.
	2	4	1	-4	0.
	3	-1	-3	3	0.

Table 82. Data acquisition parameters for 1-(3-ethyl-2-benzothiazolylidene)-2-propanone.

CELL DIMENSIONS[CD]:	A	B	C	ALPHA	BETA	GAMMA
	7.4964	8.8351	11.7664	101.947	105.838	94.826
	0.0007	0.0007	0.0010	0.007	0.008	0.007

WAVELENGTH[WL]:	<ALPHA>	ALPHA1	ALPHA2
	0.71069	0.70926	0.71354

ORIENTATION MATRIX[OM]:

0.13304	-0.00868	0.00236
-0.04388	-0.06855	-0.08438
0.00634	0.09442	-0.03399

ANGULAR DRIVE SPEEDS[AS]: 234.4 234.4 234.4 234.4

RECENTER[RC]:	FLAG	%DROP	INTERVAL
	0	0.	0

MAGNETIC TAPE PARAMS[TP]:	UNIT	RECORD LENGTH
	1	124

INDEX RESTRICTION[IR]:	TYPE	LATTICE	USER
	0	0	0

HKL FILE PARAMS[HK]:	START			END		
	0	0	0	0	0	0

COINCIDENCE CORRECTION[CC]:	DEAD TIME	LOW CUT	HIGH CUT	ATTENUATION
	0.0000022	2500.	50000.	25.346

MINMAX CUTOFFS[MM]:	MIN2TH	MAX2TH	MINIMUM HKL			MAXIMUM HKL			FRIEDEL +-HKL	
	3.0	60.0	-11	-13	0	11	13	17	0	1

SCAN PARAMS[SR]:	SCAN RANGES		BG/SCAN	DISPERSION
	0.6	0.6	0.20	1.00

DIFFRACTION VECTOR[DV]:	PSI START	PSI END	DELTA PSI
	0.0	0.0	0.0

SCAN SPEED[SS]:	FIXED	VARIABLE - SLOW	FAST	LOW	HIGH
	0.00	14.65	60.00	150.	2500.

WYCKOFF OMEGA PARMS[WP]:	#STEPS	#CALC	#ADD'L	MIN INT
	3	3	6	100.

OUTPUT VARIABLES[OV]:	#CHECKS	INTERVAL	TOTAL	MT	PRINT	STEPS	#/PAGE
	3	97	6000	1	0	16	48

STARTING PARMS[SP]:	SEQ #	HKL	PAGE	EXPOSURE
	1	-11 -13 0	1	1.00

CHECK REFLECTIONS[CR]:

#	H	K	L	I(MIN)
1	0	3	4	0.
2	-4	0	3	0.
3	3	-4	-1	0.

Table 83. Data acquisition parameters for ABMF.

CELL DIMENSIONS[CD]:	A	B	C	ALPHA	BETA	GAMMA
	8.3023	8.4592	15.1692	92.801	99.974	112.548
	0.0008	0.0006	0.0014	0.007	0.007	0.006

WAVELENGTH[WL]:	<ALPHA>	ALPHA1	ALPHA2
	1.54178	1.54051	1.54433

ORIENTATION MATRIX[OM]:	-0.01068	-0.03659	0.06116
	-0.13274	-0.04287	-0.01791
	-0.00666	-0.11608	-0.02217

ANGULAR DRIVE SPEEDS[AS]:	234.4	234.4	234.4	234.4

RECENTER[RC]:	FLAG	%DROP	INTERVAL
	0	0.	0

MAGNETIC TAPE PARAMS[TP]:	UNIT	RECORD LENGTH
	1	124

INDEX RESTRICTION[IR]:	TYPE	LATTICE	USER
	0	0	0

HKL FILE PARAMS[HK]:	START			END		
	0	0	0	0	0	0

COINCIDENCE CORRECTION[CC]:	DEAD TIME	LOW CUT	HIGH CUT	ATTENUATION
	0.0000031	2500.	60000.	28.868

MINMAX CUTOFFS[MM]:	MIN2TH	MAX2TH	MINIMUM HKL			MAXIMUM HKL			FRIEDEL +-HKL	
	100.0	150.0	0	-11	-20	11	11	20	0	1

SCAN PARAMS[SR]:	SCAN RANGES		BG/SCAN	DISPERSION
	1.0	1.0	0.50	1.00

DIFFRACTION VECTOR[DV]:	PSI START	PSI END	DELTA PSI
	0.0	0.0	0.0

SCAN SPEED[SS]:	FIXED	VARIABLE - SLOW	FAST	LOW	HIGH	
	15.00	14.65	60.00	150.	2500.	

WYCKOFF OMEGA PARMS[WP]:	#STEPS	#CALC	#ADD'L	MIN INT	
	3	3	6	100.	

OUTPUT VARIABLES[OV]:	#CHECKS	INTERVAL	TOTAL	MT	PRINT	STEPS	#/PAGE
	0	97	1609	1	0	16	48

STARTING PARMS[SP]:	SEQ #	HKL			PAGE	EXPOSURE
	4009	12	-11	-20	109	21.20

CHECK REFLECTIONS[CR]:	#	H	K	L	I(MIN)
	1	0	2	-8	0.
	2	1	0	9	0.
	3	-3	-3	0	0.

APPENDIX J

FOFC TABLES

A complete listing of FOFC tables can be obtained by writing:

X-Ray Crystallographic Laboratory
Department of Chemistry
Gaines Hall
Montana State University
Bozeman, Montana 59717